THE PERFORMANCE OF
DESICCANT DEHUMIDIFIER AIR-CONDITIONING SYSTEMS
USING COOLED DEHUMIDIFIERS

by

KENNETH JOHN SCHULTZ

A thesis submitted in partial fulfillment of the
requirements for the degree of

MASTER OF SCIENCE

(Mechanical Engineering)

at the

UNIVERSITY OF WISCONSIN-MADISON

1983

ACKNOWLEDGEMENTS

The guidance and assistance provided by my advisors, Professors J.W. Mitchell, W.A. Beckman, and J.A. Duffie, was greatly appreciated. In particular, I thank Professor Mitchell for his special patience and encouragements. It has been a pleasure to work with the other graduate students and staff of the Solar Energy Laboratory, all have been friendly and helpful. Special thanks go to officemates Jeff Jurinak for all his help and guidance and Bob Howe for assisting me through those moments of frustration.

To my wife Debbie, "thanks Sweetie" for all of your patience, understanding, and support. This work is as much your accomplishment as it is mine.

To those who must read this work, Professors G.E. Myers, W.A. Beckman, and J.W. Mitchell, I appreciate your time and effort and sincerely apologize for the excessive length.

Financial assistance for this work was provided by the Solar Heating and Cooling Research and Development Branch, Office of Conservation and Solar Applications, U.S. Department of Energy. The assistance and cooperation of Dr. Z. Lavan and Dr. W. Worek was also appreciated.

TABLE OF CONTENTS

TABLE OF CONTENTS (continued)

TABLE OF CONTENTS (continued)

LIST OF FIGURES

LIST OF FIGURES (continued)

LIST OF FIGURES (continued)

LIST OF FIGURES (continued)

LIST OF FIGURES (continued)

LIST OF FIGURES (continued)

LIST OF TABLES

NOMENCLATURE

c	specific heat
C	heat capacity rate
COP_a, COP_e, COP_{th}	coefficient of performance, defined by eqs (6.2.5), (6.2.3), (6.2.2) respectively
CR	cost ratio, defined by eq (6.3.1)
f_{SOL}, FSOL	fraction of thermal energy supplied by solar system defined by eq (6.2.6)
F_i	characteristic potentials for heat and mass transfer, defined by eq (3.1.3)
h	enthalpy of air or vapor
h_{fg}, h°_{fg}	latent heat of vaporization of water, referenced to 0°C
h_s	heat of adsorption
H	enthalpy of desiccant matrix
ΔH_w	integral heat of wetting
L	length of desiccant channel
m	mass of desiccant
$\dot{m}$	mass flowrate of air
$\dot{m}_D$, $\dot{m}_R$	process side and regeneration side flowrates, respectively, through desiccant air-conditioning system
$\dot{m}_{inf}$	building infiltration rate

NOMENCLATURE (continued)

$\dot{m}_L$, $\dot{m}_{L,max}$	mass flowrate of air from air-conditioning system to the load
$(\dot{m}_R/\dot{m}_D)^*$	optimum flow ratio for ideal cooled dehumidifier, defined by eq (4.2.18)
P	Pressure
ΔP_i	pressure drop through component i
q	heat transfer per unit mass flowrate
q_c	dehumidifier process side cooling
$q_{cap,T}$, $q_{cap,S}$, $q_{cap,L}$	total, sensible, and latent specific cooling capacity respectively
q_{th}	specific thermal energy required
Q	energy quantity, integrated energy transfer
$\dot{Q}$	heat transfer rate, Q = mq
$\dot{Q}_{load,T}$, $\dot{Q}_{load,S}$, $\dot{Q}_{load,L}$	total, sensible, and latent cooling loads respectively
$\dot{Q}_{fan}$	electric power consumed to run the fan
r_c	cooled dehumidifier parameter defined by eq (4.3.3)
rh	relative humidity
t	temperature of an air stream or state
t_{SINK}	temperature of dehumidifier cooling stream
t_{WB}	wet-bulb temperature
T_H	temperature of desiccant matrix after preheating process in ideal cooled dehumidifier (eq (4.2.17))

NOMENCLATURE (continued)

u	speed of property wave propagation through the desiccant matrix
UA	building heat loss coefficient
v	velocity of through dehumidifier flow channel
w	specific humidity of air
W	water content of the desiccant per unit mass
W_{DRY}	water content of desiccant at end of regeneration process (eq (4.29))
W_{WET}	water content of desiccant at end of dehumidification process (eq (4.25))
x	axial distance along dehumidifier channel
α_i	slope of a characteristic F_i potential on a psychrometric chart, defined by eq (3.1.5)
γ_i	desiccant properties analogous to specific heats
ε_{EC}	evaporative cooler effectiveness, defined by eq (2.5.2)
ε_{HX}	heat exchanger effectiveness, defined by eq (2.5.1)
$\varepsilon_{F_1}, \varepsilon_{F_2}$	adiabatic dehumidifier effectivenesses, defined by eq (3.2.2)
$\varepsilon_t, \varepsilon_w$	cooled dehumidifier effectivenesses, defined by eqs (4.32) and (4.3.1) respectively
η_{fan}	fan efficiency
θ	time or period

NOMENCLATURE (continued)

θ_{BD}, θ_{BR}	ideal period lengths for optimum dehumidification and regeneration, respectively, of the cooled dehumdifier
θ_P	period length for purge processes (section 4.2.3)
μ	ratio of the mass of dry desiccant to the mass of dry air in a given control volume; ratio of air flowrate to "matrix flowrate", $\dot{m}_{air}\theta_D/m_{mat}$

subscripts

in, out	refers to an inlet or outlet condition
rm	refers to the room state or state of the conditioned space
amb	refers to the ambient condition
des	refers to the desiccant or desiccant matrix
design	value is at design condition
C,H	refers to matrix state in precooling or preheating process respectively (section 4.2.3)
D	refers to dehumidifier outlet state or process flow stream
mat	matrix, heat exchanger or dehumidifier base material
R	refers to regeneration state or regeneration flow stream

NOMENCLATURE (continued)

superscripts

*	refers to adiabatic saturation state, optimum flow ratio, or ideal dehumidifier outlet state
+	ideal outlet state of dehumidifier with flow ratio other than optimum
A	ideal dehumidifier outlet state if process were adiabatic

Abstract

Potential exists for improving desiccant dehumidifier performance by providing cooling during the dehumidification process. Several desiccant dehumidifier air-conditioning system cycles incorporating cooled dehumidifiers are derived from the adiabatic cycles. An idealized model of the cooled dehumidifier based on an equilibrium analysis is presented. This model is extended to non-ideal dehumidifiers by defining three semi-empirical parameters. The model provides an easily computed method for determining cooled dehumidifier performance for use in obtaining estimates of seasonal system performance.

The operating characteristics of the cooled dehumidifier cycles, in particular, the cooled Dunkle cycle, are determined. The effects of ambient condition, regeneration temperature, room state, and level of individual component performance are investigated. Estimates of long term performance of the cooled Dunkle cycle are obtained from computer models. Both gas-fired and solar-fired operation are considered. The results are compared with those of previously studied adiabatic cycles

It is concluded that well engineered components are required for satisfactory desiccant system performance. The adiabatic systems appear to have an advantage over the cooled Dunkle systems based on operating costs, but solar-fired cooled Dunkle systems may be competitive with the adiabatic systems in climates with moderate cooling loads.

CHAPTER 1

INTRODUCTION

The realization of our dependence on foreign sources of energy caused by the energy shortage of a decade ago spurred the investigation of various technologies which would use alternative energy sources. Technologies driven with solar energy were optimistically looked to to displace significant amounts of fossil fuels in the heating and cooling of residential and commercial buildings. In particular, open-cycle air-conditioning systems using a solid desiccant dehumidifier in combination with a regenerative evaporative cooling system were proposed as alternatives to the standard electrically driven vapor compression systems.

Even though current energy supplies appear to be sufficient, investigation of desiccant cooling systems continues because of economic motives. The natural gas industry is looking for new markets because of growing supplies [1]. Gas-fired or solar-fired with gas backup desiccant cooling systems could give the gas industry a share of the air-conditioning energy market now dominated by electric utilities. Electric utilities might also benefit if desiccant systems proved successful [2]. In many locations, electrically driven air-conditioning results in high demands for electricity. If some of this demand could be displaced by another energy source, the need for increased future generating capacity

could be diminished and present facilities could be operated more efficiently. From the consumer's point of view, while there are strong arguments to reduce the drain on non-renewable energy sources, the desire to lower the monthly utilities bill will decide the viability of desiccant cooling systems.

1.1 Adiabatic Systems[1]

Desiccant cooling systems which use adiabatic dehumidifiers have been studied extensively. Silica gel and molecular sieve are the desiccants most commonly used. A number of system configurations have been proposed with the ventilation and recirculation cycles [3] receiving the most interest. Another configuration of possible interest is the Dunkle cycle [4]. These systems are pictured and briefly described in section 2.2. Estimates of the seasonal performances of these systems have been determined by computer simulation [3,5,6,7].

The study of systems using adiabatic dehumidifiers has been aided significantly by the development of a theory that predicts dehumidifier performance through an analogy with heat transfer alone [8]. The nonlinear, coupled, partial differential equations that describe the combined heat and mass transfer processes in the dehumidifier are transformed into two equations of the same form as the describing equation for heat transfer alone. The

---

[1] Reference [6] contains a well documented history of the development of desiccant air-conditioning systems.

dehumidifier performance can then be determined using the known heat transfer solution. The analogy theory therefore provides an easily computed model of the adiabatic dehumidifier suitable for use in seasonal simulations of system performance. The alternative finite difference model is impractical for this purpose because it is time consuming and expensive to run.

1.2 Cooled Systems

Because of the dependence of the desiccant properties on temperature, there are potential benefits to system performance if cooling is provided during the dehumidification process. Typical desiccants can adsorb more moisture when at a lower temperature. This may allow the use of a smaller system to obtain the same cooling capacity as an adiabatic system. A cooled dehumidifier can be regenerated at a lower temperature than an adiabatic system and still produce the same capacity. This feature may be particularly important when the cooling system is coupled to a solar energy system.

A staged, adiabatic dehumidifier with intercooling was proposed by Lunde [9]. An experimental study of a water cooled bed has been carried out by Pryor [10]. Extensive work on a cross-cooled dehumidifier system has been done at the Illinois Institute of Technology (IIT) including the development of a cross-cooled dehumidifier prototype [11] and testing and modeling of its performance [12,13]. Although numerical solutions to cooled dehumidifier operation have been developed [14], this

method is again too time consuming and expensive for use in obtaining estimates of seasonal performance. Current estimates are based on computer simulations using a linear regression of dehumidifier performance data obtained from a finite difference solution as the dehumidifier model [15]. A drawback of this method is that the effects on system performance of design changes in the dehumidifier can not be assessed without redoing the finite difference solution for the changed dehumidifier.

1.3 Objectives

The main purpose of this work is to assess the potential performance of desiccant cooling systems using a cooled silica gel dehumidifier. Because of the limited nature of design point performance calculations, estimates of long term performance are required in order to make a full assessment. This was not feasible with the models available, so the first goal of this work is to develop an easily computed model of the cooled dehumidifier suitable for use in long term computer simulations. This occurs in two steps. First, a model of an idealized dehumidifier based on equilibrium processes is developed. The only information required are the inlet conditions and the desiccant properties. Second, a model of a non-ideal dehumidifier is obtained by defining three empirical parameters which describe the degree to which the non-ideal dehumidifier processes approach the ideal. The three parameters carry the effects of the dehumidifier design.

The second goal of this work is to determine the characteristics of a particular system configuration. The effects of individual component performance, room state, ambient condition, and regeneration temperature on overall system performance are investigated and compared with adiabatic systems. This information is useful in determining which components are most important and in explaining long term performance results.

This leads to the third and major goal of this work; to assess the long term performance of a cooled desiccant air-conditioning system. The assessment is made based on estimates of thermal performance and parasitic power consumption. Both gas-fired and solar/gas-fired options are investigated. Operation in three climates, Miami, FL (warm and humid), Phoneix, AZ (hot and dry), and Columbia, MO (moderate, with a substantial heating load), are included. The assessment is made through a comparison of the cooled system performance with that of the well-studied adiabatic systems.

In summary then, the objectives are:

A. Development of an easily computed model for the cooled dehumidifier (Chapter 4) through
   1. development of an idealized equilibrium model and
   2. definition of three empirical parameters to describe a non-ideal dehumidifier.

B. Investigate the characteristics of a particular system configuration (Chapter 5) by determining the effects on overall system performance of

1. ambient condition,
2. regeneration temperature,
3. room state, and
4. individual component performance.

C. Assess overall cooled desiccant system performance (Chapter 6) by looking at:

1. thermal performance and parasitic power consumption.
2. both gas-fired and solar/gas-fired operation.
3. a range of climates.
   a. Miami, FL (warm and humid)
   b. Phoenix, AZ (hot and dry)
   c. Columbia, MO (moderate, substantial heating load)
4. a comparison with adiabatic system performance.

CHAPTER 2

DESICCANT AIR-CONDITIONING SYSTEMS

The operation of desiccant air-conditioning systems is based on dehumidifying moist air and supplying this dry air to an evaporative cooling system. This chapter presents descriptions of the configuration and operation of two systems using adiabatic dehumidifiers, the ventilation cycle and Dunkle cycle. The recirculation cycle is not looked at because Jurinak [6] has shown it not to work as well as the other two.[2] A configuration appropriate to using a cooled dehumidifier is then constructed. The models used to describe the performance of the individual components are presented along with the properties of the silica gel desiccant used in this work.

Table 2.0.1 contains a listing of the code letters that are used in labeling the schematic diagrams of the various systems to be presented.

---

[2] For balance flow between the two sides of the dehumidifier, the only flow ratio considered in this work for the adiabatic systems. Jurinak [7] has shown that the recirculation cycle performance can be improved to match that of the ventilation cycle by using unbalanced flows in the dehumidifier.

Table 2.0.1

Component Codes for Labeling Figures

EC	evaporative cooler
HX	heat exchanger
DH	dehumidifier
HS	heat source (gas and/or solar)

2.1 Evaporative Cooling Systems

Under certain conditions, simple evaporative cooling can be used to meet the cooling load. Such a system is shown in figure 2.1.1. Ambient air is cooled by the adiabatic saturation process and introduced into the room. The cooling capacity of the system is given by the product of the mass flow of air delivered to the room and the enthalpy difference between the room and inlet states. Ambient conditions under which useful cooling can be produced are limited to those with a wet-bulb temperature less than the room wet-bulb temperature as shown in figure 2.1.1.

The range of ambient conditions under which useful cooling can be provided can be increased by adding another evaporative cooler and a heat exchanger as shown in figure 2.1.2. This is the regenerative evaporative cooling system. Room air (6) is evaporatively cooled (7) to provide a sink for the heat exchanger. Ambient air (1) is cooled in the heat exchanger (3) before being evaporatively cooled (4) and sent to the room. While useful cooling is extended to warmer ambient temperatures, it is still limited to conditions that are drier than the room state. At high temperatures, the cooling load may become larger than the capacity of the system which is limited by the allowable air flow rate.

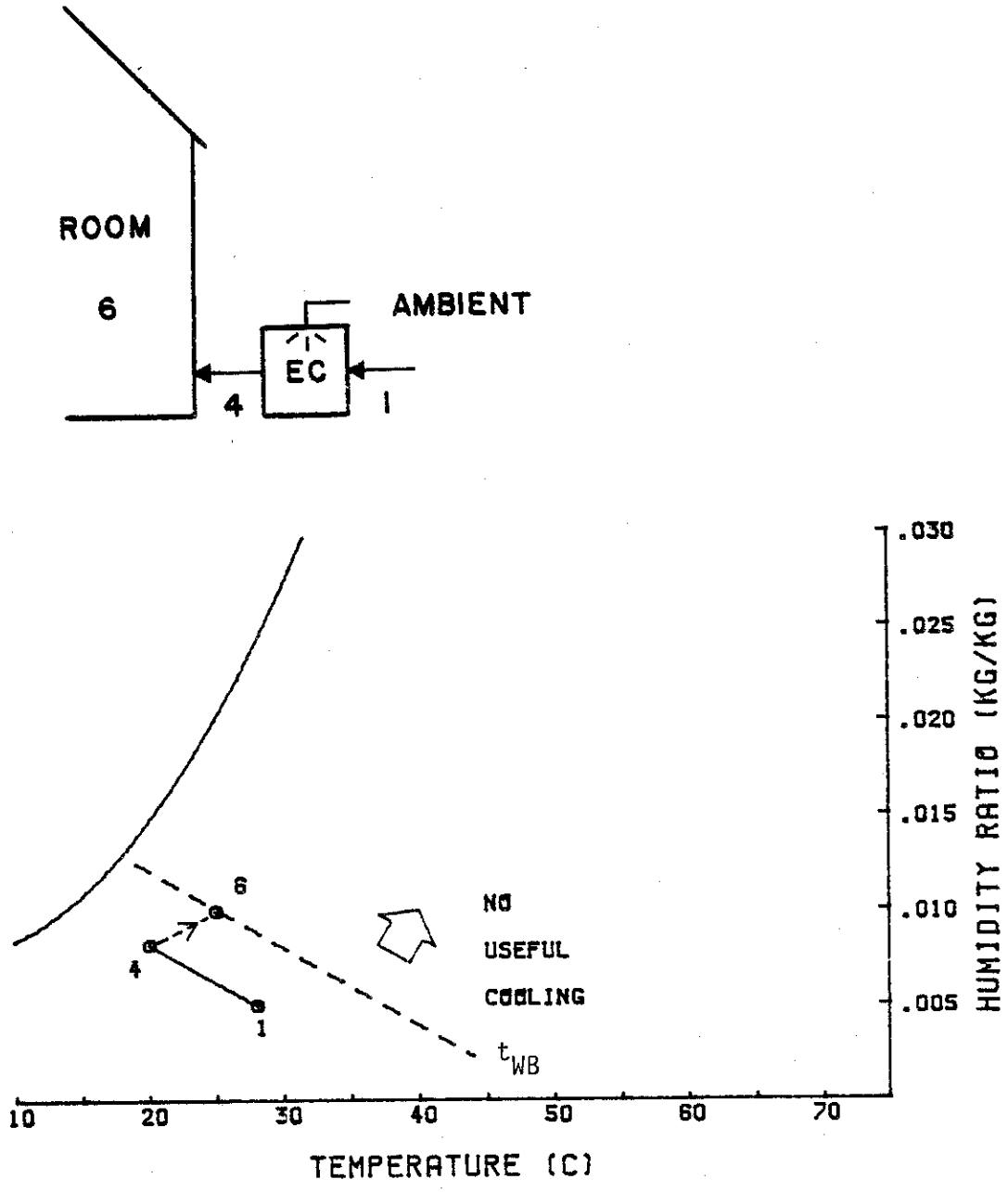

Figure 2.1.1 Simple evaporative cooling system.

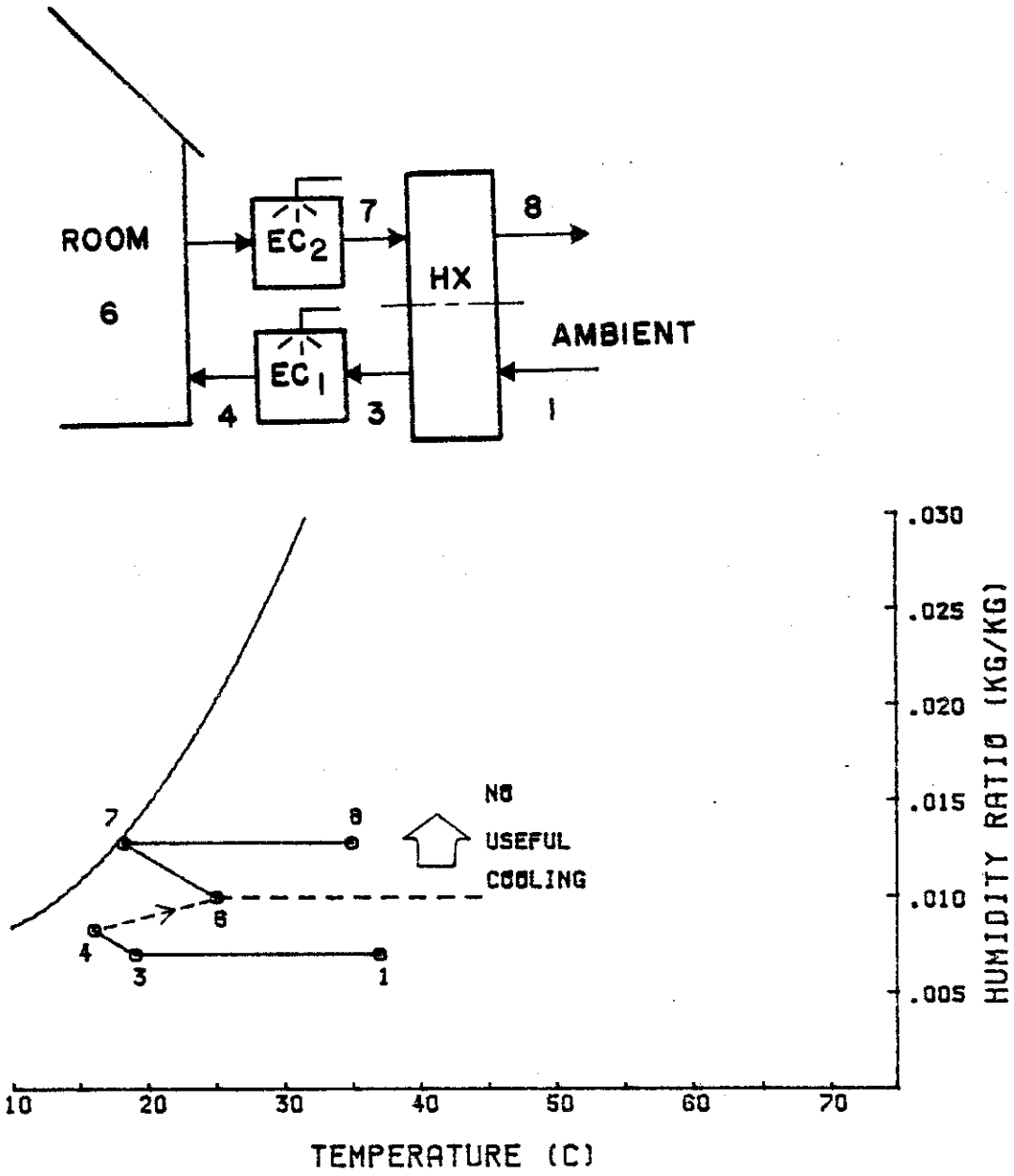

Figure 2.1.2 Regenerative evaporative cooling system.

2.2 Adiabatic Dehumidifier Desiccant Systems

In humid climates, a dehumidifier can be added to supply dry air to the regenerative evaporation cooling system. In hot climates with high cooling loads, the addition of a dehumidifier can help increase capacity by supplying drier air to the evaporator cooler. Perhaps the simplest way of doing this is shown in figure 2.2.1. This system, using an adiabatic dehumidifier, is called the ventilation cycle. A rotary type heat exchanger and dehumidifier are depicted. Ambient air (1) is dried in the dehumidifier (2) and then sent to the regenerative evaporative cooling section. For this system to work, the desiccant must be regenerated (dried out) so it can be used again. As will be shown in chapter 3, the adiabatic dehumidification process for the desiccant used in this work is approximately the reverse of the adiabatic saturation process. In cooling the process stream, the heat exchanger heats the regenerating stream (9), reclaiming much of the temperature rise due to the dehumidification process. Additional thermal energy (gas and/or solar) is needed to reach the required regeneration temperature (11). This is in contrast to the evaporative cooling systems which required energy only to move the air around. The regenerating stream removes moisture from the desiccant (12), again approximately following an adiabatic saturation line.

Other configurations of components are possible. The Dunkle cycle is pictured in figure 2.2.2. The Dunkle cycle conditions

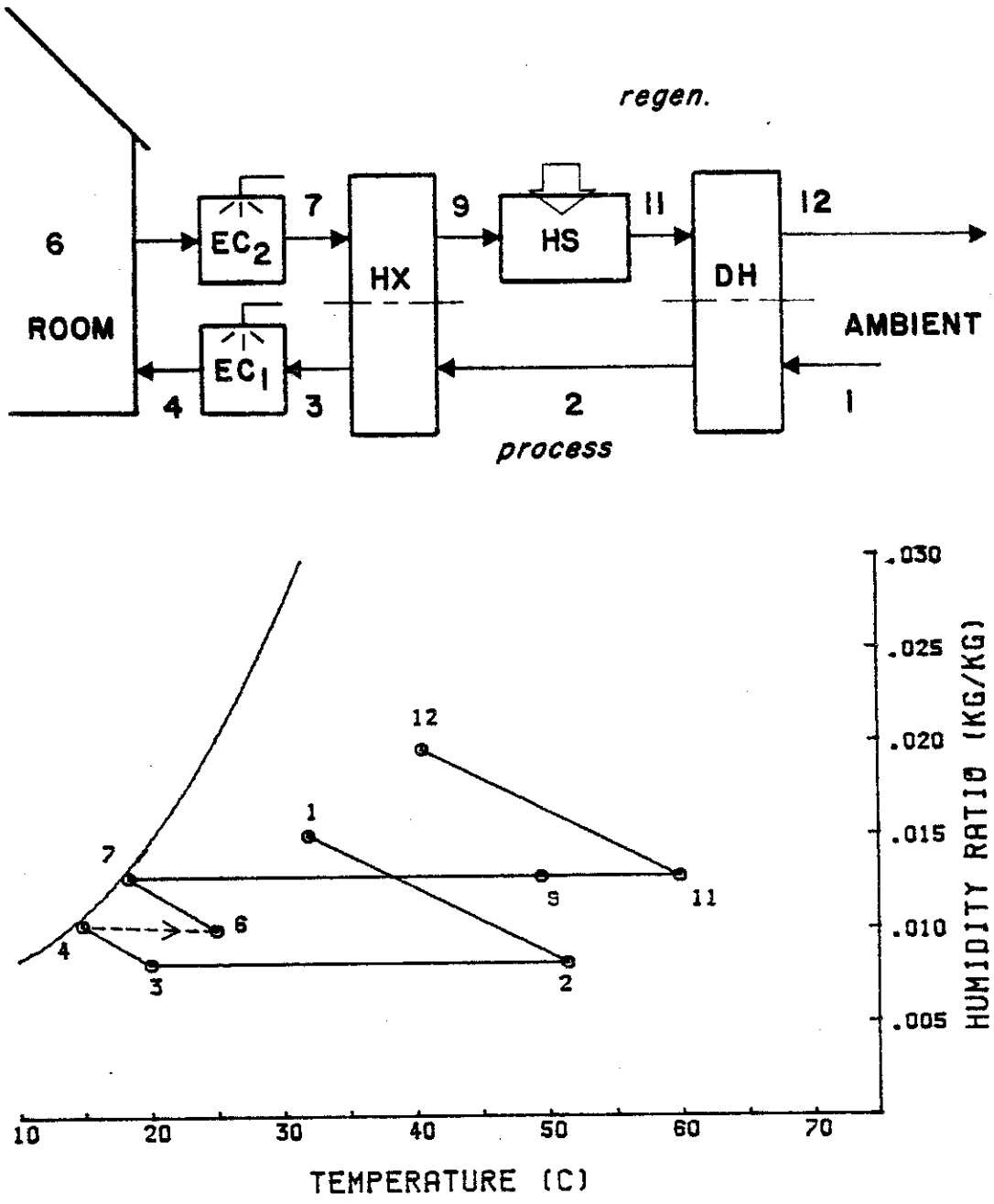

Figure 2.2.1 Ventilation cycle desiccant dehumidifier cooling system.

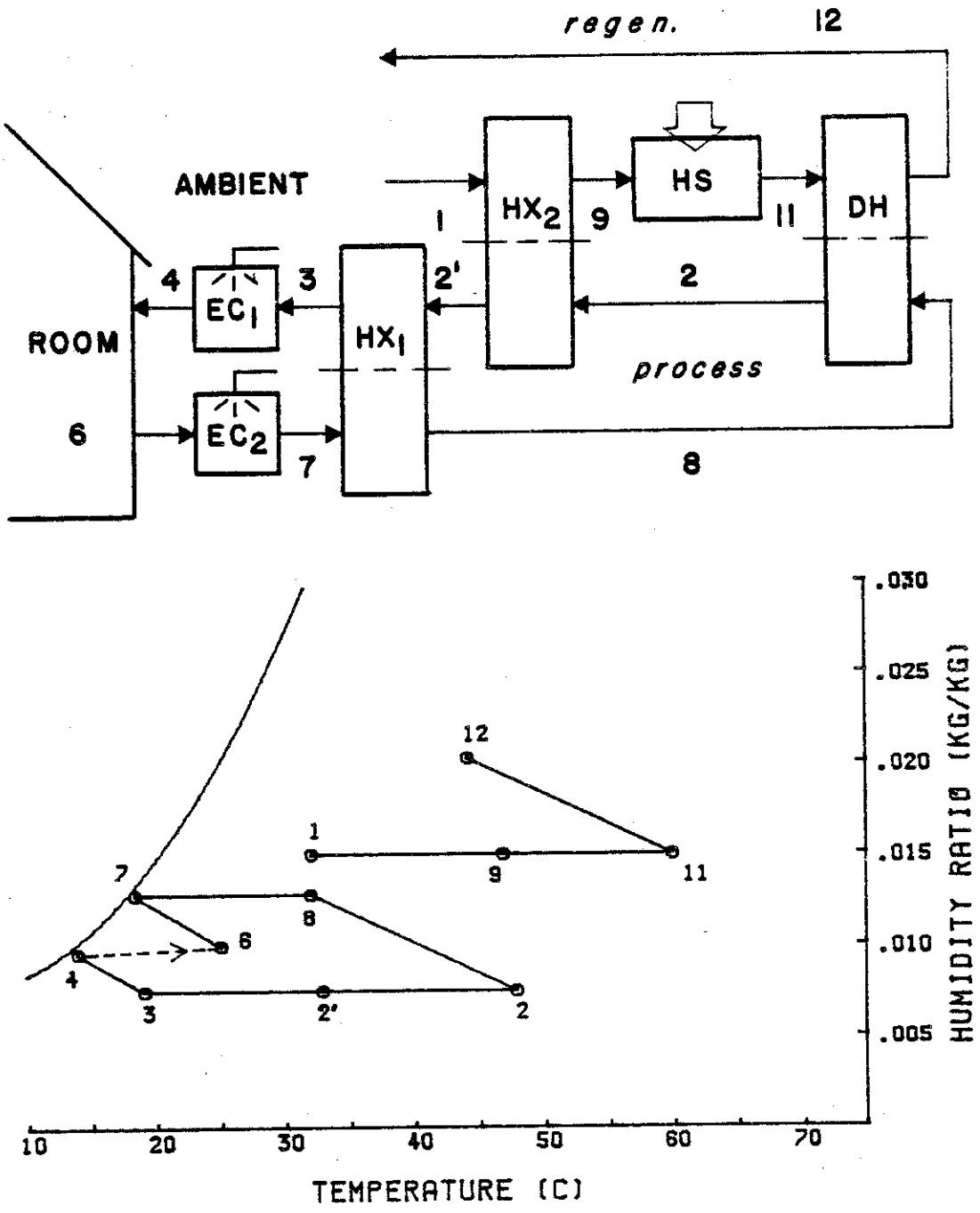

Figure 2.2.2 Dunkle cycle desiccant dehumidifier cooling system.

recirculated room air rather than supplying fresh air to the room as in the vent cycle. Ambient air is used for the regenerating stream. This cycle contains an additional heat exchanger (HX_2) which reclaims energy from the dehumidifier outlet state (2) and transfers it to the regenerating stream (9). Although the air flow paths are somewhat different than in the vent cycle, the Dunkle cycle is again essentially a dehumidifier (and an additional heat exchanger) attached to a regenerative evaporator cooling system.

A schematic diagram and psychrometric representation of the recirculation cycle is shown in figure A.1 of appendix A. The recirc cycle has the same configuration of components as the vent cycle, but with different flow streams. Instead of processing ambient air, the recirc cycle conditions room air and recirculates it. Ambient air is used for the regenerating stream rather than room air. This results in the sink for the heat exchanger being the wet-bulb temperature of the ambient rather than the room. This can result in a loss of cooling capacity compared with the vent cycle, but it is compensated for by sending drier air (not evaporatively cooled) to the dehumidifier.

2.3 Dehumidifier Processes: Adiabatic Versus Cooled

The cooling capacity of a desiccant system depends significantly on how dry the air leaving the dehumidifier can be made. Figure 2.3.1 shows that the drier air from the dehumidifier (w_2') will have a lower wet-bulb temperature after passing through the heat exchanger (3') and therefore has a greater potential for

cooling ($\Delta h' > \Delta h$).

The adiabatic dehumidification process for the desiccant used in this work is shown in chapter 3 to be approximately the reverse of the adiabatic saturation process. The outlet state of an ideal adiabatic dehumidifier is near the intersection of t_{WB} line through the inlet state and the rh line through the regeneration inlet state as shown in figure 2.3.2 and 2.3.3.

It is shown in chapter 4 that the outlet state of an idealized cooled dehumidifier lies near the intersection of the rh line through the regeneration inlet state with the temperature of the cooling stream, t_{SINK} as shown in figure 2.3.2 and 2.3.3.

Figure 2.3.2 shows that the cooled dehumidification process produces a drier outlet state than the adiabatic process when the desiccant is regenerated at the same temperature. Therefore, the cooled dehumidifier has the potential for producing a larger cooling capacity or requiring a lower flow rate to produce the same capacity as the adiabatic dehumidifier.

If the two dehumidifiers are compared based on producing the same potential cooling capacity (same w_{out}), figure 2.3.3 shows that the cooled system might be able to operate with a lower regeneration temperature. This may benefit the interaction with the solar energy collection system by requiring less auxiliary energy and/or lowering collector losses.

These arguments are based on the dehumidifier only. They are not directly applicable to the complete systems because the

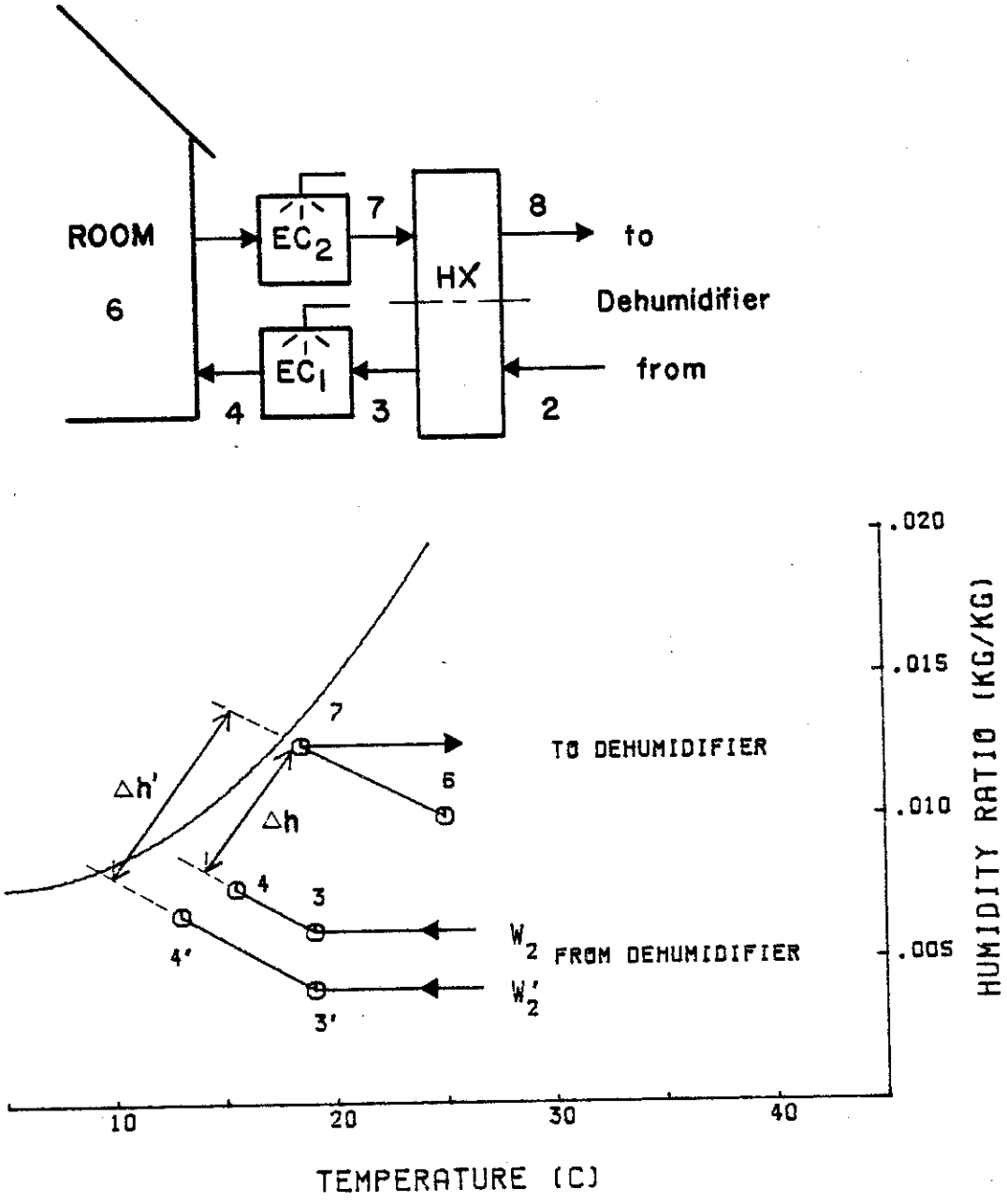

Figure 2.3.1 Increased cooling capacity from drier dehumidifier outlet state.

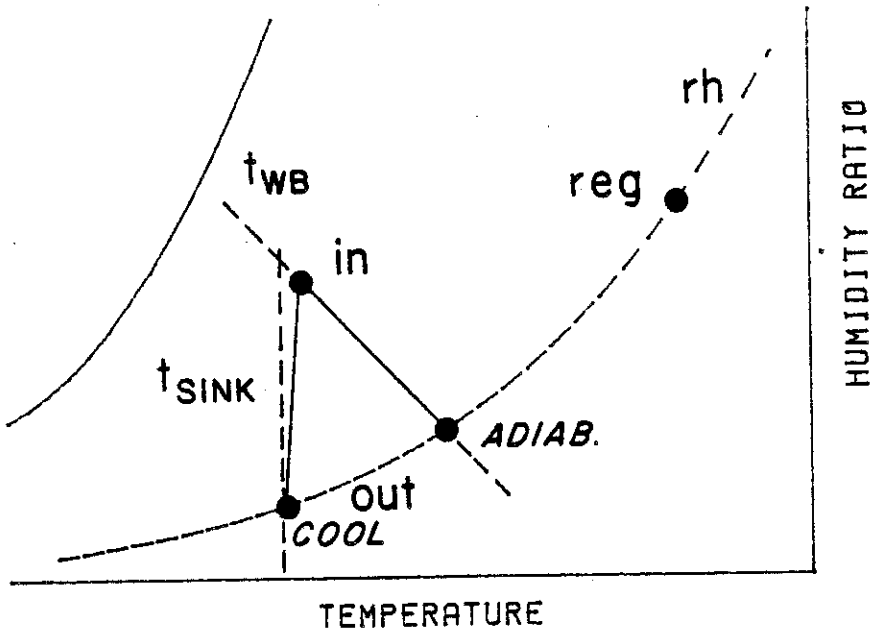

Figure 2.3.2 Cooled and adiabatic dehumidifier outlet states with same regeneration temperature.

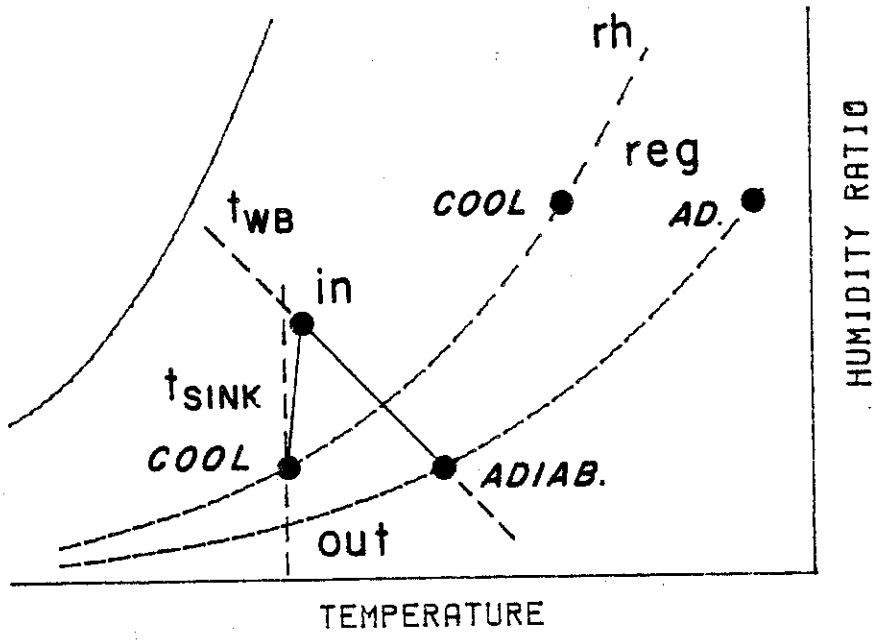

Figure 2.3.3 Regeneration temperatures required to obtain same outlet humidity ratio from cooled and adiabatic dehumidifiers.

flow paths of the air streams through the other components are not the same for each system. The trade-offs involved are pointed out in the next section.

2.4 Cooled Dehumidifier Desiccant Systems

The operation of cooled dehumidifier systems depends on a source of cooling for the dehumidification process. Extensive use of evaporative cooling is made in desiccant air-conditioning systems, so a logical choice for the dehumidifier cooling stream is to use evaporatively cooled ambient air.

A configuration of components suitable for use with a cooled dehumidifier can be constructed by considering the Dunkle cycle. The purpose of heat exchanger HX_2 is to reclaim energy from the warm dehumidifier outlet state (2) and transfer it to the regenerating stream (9). If a cooled dehumidifier were used in this configuration, much of this energy is carried away by the cooling stream and lost. The dehumidifier outlet state is cooler, but because of the temperature dependence of the desiccant properties, it is also drier. If heat exchanger HX_2 is removed from the process stream and placed in the regenerating stream, the loss of the energy in the dehumidifier outlet stream (2) can be compensated for by reclaiming energy from the regenerating outlet stream (12). This configuration, the cooled Dunkle cycle, is shown in figure 2.4.1.

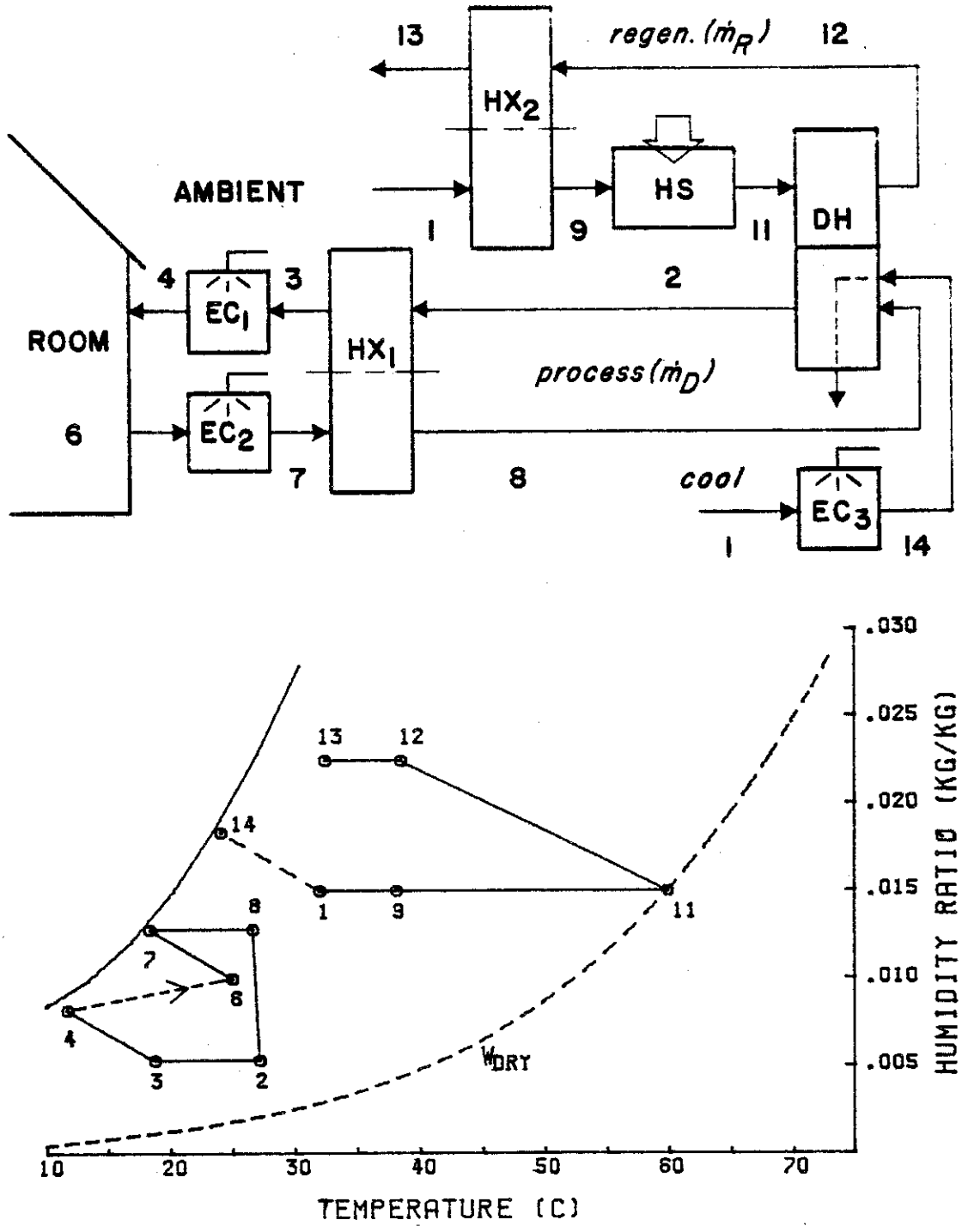

Figure 2.4.1 Cooled Dunkle cycle cooling system.

Because the outlet state of the dehumidifier (2) in the cooled system is drier than in the Dunkle system, the cooled system has a larger cooling capacity when operated at the same regeneration temperature. But the cooled cycle also requires a larger thermal energy input. In a different light, the cooled system requires a lower regeneration temperature to match the capacity of the adiabatic system. This will have an impact when the system is coupled with a solar energy system. The trade-off between the potential for increased cooling capacity and the requirement of additional thermal energy in the cooled system will be evaluated in chapters 5 and 6. The implications of using a cooled dehumidifier system on the desiccant system-solar system interaction will also be evaluated in chapter 6.

The ventilation and recirculation cycles can be modified to operate with a cooled dehumidifier also. The cooled recirc cycle is shown in figure A.2 of appendix A. An additional heat exchanger (HX_2) has been included to compensate for the loss of thermal energy from the dehumidifier outlet state (2) (carried away by the cooling stream) by reclaiming energy from the regeneration outlet state (12). Another modification that has been made is to use ambient air (1) directly for the regenerating stream rather than the evaporatively cooled ambient stream (8). The desiccant can be regenerated to a lower moisture content using the drier air and therefore the outlet state of the dehumidifier (2) will be drier. This is the system currently being investigated

at the Illinois Institute of Technology.

The cooled vent cycle is shown in figure A.3 of appendix A. An additional heat exchanger is again included. Two options are available for a choice of regenerating stream, either ambient air (1) or evaporatively cooled room air (8). In most cases, the drier air stream should be used because this will result in regeneration of the desiccant to a drier moisture content and subsequently increased dehumidification. This may not hold true for high ambient air temperatures ($t_1 > t_{12}$, therefore bypass HX_2) where using ambient air instead of room air may result in a decreased thermal energy requirement.

2.5 Component Models

2.5.1 Dehumidifiers

The adiabatic dehumidifiers in the vent and Dunkle cycles are modeled by the analogy method presented in chapter 3. The performance is given by two parameters, ε_{F_1} and ε_{F_2} (eqs. 3.2.2) which measure the actual dehumidifier performance relative to the ideal performance.

The model for the cooled dehumidifier is developed in chapter 4. Three parameters, ε_w (eq. 4.3.1), ε_t (4.3.2), and r_c (eq. 4.3.3), are defined to describe the performance of a non-ideal dehumidifier in terms of an ideal one.

2.5.2 Heat Exchangers

The heat exchangers in this work are modeled by a

temperature effectiveness

$$\varepsilon_{HX} = \frac{t_{1,out} - t_{1,in}}{t_{2,in} - t_{1,in}} \qquad (2.5.1)$$

where stream 1 is the stream with the minimum capacity rate, $\dot{m}c$ (the drier air stream for balanced flow through the heat exchanger), and $t_{2,in} - t_{1,in}$ represents the maximum possible temperature change of stream 1. The outlet temperature of stream 2 is then found from an energy balance.

2.5.3 Evaporator Coolers

The evaporative coolers are modeled by an effectiveness that represents the approach of the actual outlet state to the ideal saturated outlet state

$$\varepsilon_{EC} = \frac{t_{out} - t_{in}}{t^* - t_{in}} = \frac{w_{out} - w_{in}}{w^* - w_{in}} \qquad (2.5.2)$$

where the "*" designates the saturated outlet state of the adiabatic saturation process.

2.6 Properties

2.6.1 Moist Air Properties

Moist air is considered here to be an ideal gas mixture of air and water vapor. The enthalpy of moist air per unit mass of dry air is given by

$$h = c_{dry\ air}\, t + w(h^{\circ}_{fg} + c_{vapor}\, t) \qquad (2.6.1)$$

where the enthalpy of the dry air has been referenced to 0°C. The enthalpy of the water vapor is referenced to liquid water at 0°C where h°_{fg} is the heat of vaporization at the reference temperature. Table 2.6.1 lists the values used for $c_{dry\ air}$, c_{vapor}, and h°_{fg}.

The saturation humidity ratio, required in the evaporative cooler model, is given by

$$w^{*} = .62198 \frac{P_{SAT}}{P_{TOT} - P_{SAT}} \qquad (2.6.2)$$

where P_{SAT} is given by

$$\log_{10}\left(\frac{P_{SAT}}{218.167}\right) = -\frac{X}{T}\left(\frac{a + bX + cX^3}{1 + dX}\right) \qquad (2.6.3)\ [23]$$

with P_{SAT} = [atm]

$X = 647.27 - T$

T = [°K]

$a = 3.2437814$

$b = 5.86826 \times 10^{-3}$

$c = 1.1702379 \times 10^{-8}$

$d = 2.1878462 \times 10^{-3}$

The latent heat of vaporization of water is of interest in the development of the cooled dehumidifier in chapter 4. Its variation with temperature is approximated as a linear function

$$h_{fg} = h^{\circ}_{fg} + (c_{vapor} - c_{liq})t \qquad (2.6.4)$$

Table 2.6.1

Moist Air and Silica Gel Properties

$c_{dry\ air}$ = 1005 J/kg

c_{vapor} = 1859 J/kg

c_{liq} = 4187 J/kg

$c_{silica\ gel}$ = 921 J/kg (also c_{des}, $c_{dry\ des}$)

$h_{fg}^{\circ}(0°C)$ = 2.5014×10^{6} J/kg

P_{TOT} = 1 atm

where again 0°C has been used as the reference temperature at which h°_{fg} is evaluated.

2.6.2 Desiccant Properties

Silica gel is used as the desiccant in this work. The partial pressure of water vapor in equilibrium with the moist silica gel is given by

$$P_{vapor} = \frac{1}{29.91}\left[(29.91)\ (2.009\ W)P_{SAT}\right]^{h_s/h_{fg}} \qquad (2.6.5)\ [17]$$

where P_{vapor} and P_{SAT} are in atmospheres, W is the water content of the desiccant per unit mass of dry desiccant, and h_s/h_{fg} is the ratio of the heat of sorption of water on the silica gel to the latent heat of vaporization. Brandemuehl [24] has found the following expression to fit the published data,

$$\frac{h_s}{h_{fg}} = 1 + 0.2843\ \exp(-10.28\ W) \qquad (2.6.6)$$

An equation representing the equilibrium relationship between moist air and desiccant can be obtained from eq.(2.6.5) and the relation

$$w = .62198\ \frac{P_{vapor}}{P_{TOT} - P_{vapor}}$$

assuming $P_{vapor} << P_{TOT}$ and $P_{TOT} = 1$ atm,

$$w(t,W) = .02080 \left(60.09\ W\ P_{SAT}(t)\right)^{h_s/h_{fg}} \qquad (2.6.7)$$

This equation is implicit in W because h_s/h_{fg} is a function of W. The equilibrium relation W = W(t,w) is found numerically from eq(2.6.7) by applying Newton's method. Figure 2.6.1 shows the lines of constant W on a psychrometric chart overlayed on lines of constant relative humidity.

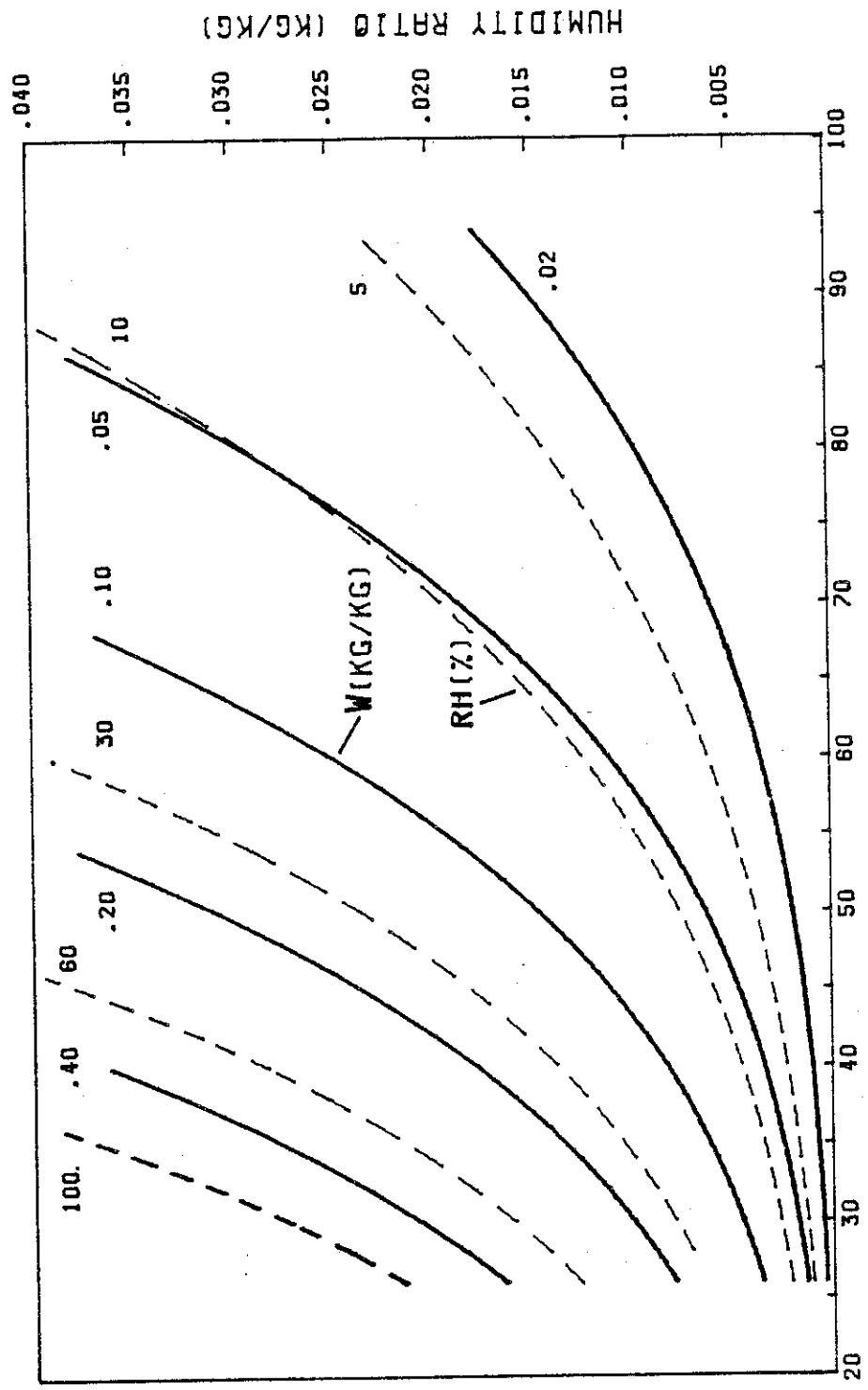

Figure 2.6.1 Psychrometric diagram of silica gel water content and relative humidity.

CHAPTER 3

THE ADIABATIC DEHUMIDIFIER AND THE ANALOGY METHOD

The study of desiccant air conditioning systems with adiabatic dehumidifiers has been aided significantly by the development of the analogy theory of Banks, Close, and Maclaine-cross [8,16,17] which provides an easily computed model for the adiabatic dehumidifier. This allows estimates of seasonal performance to be obtained using computer simulation.

In this chapter, an outline of the analogy model of the adiabatic dehumidifier is presented. This model is used later to obtain performance estimates of the adiabatic desiccant systems against which the cooled dehumidifier system performances will be compared. Also, it is used in the development of the idealized cooled dehumidifier in chapter 4.

The geometry of choice for the adiabatic dehumidifier has been the counterflow rotating wheel where one side of the wheel is dehumidifying an air stream while the other side is being regenerated (dried) by a heated air stream. The dehumidifier could also consist of two beds which are switched between the two air streams. These geometries are shown in figure 3.0.1.

3.1. Idealized Adiabatic Dehumidifier Model

The idealized adiabatic dehumidifier model presented here

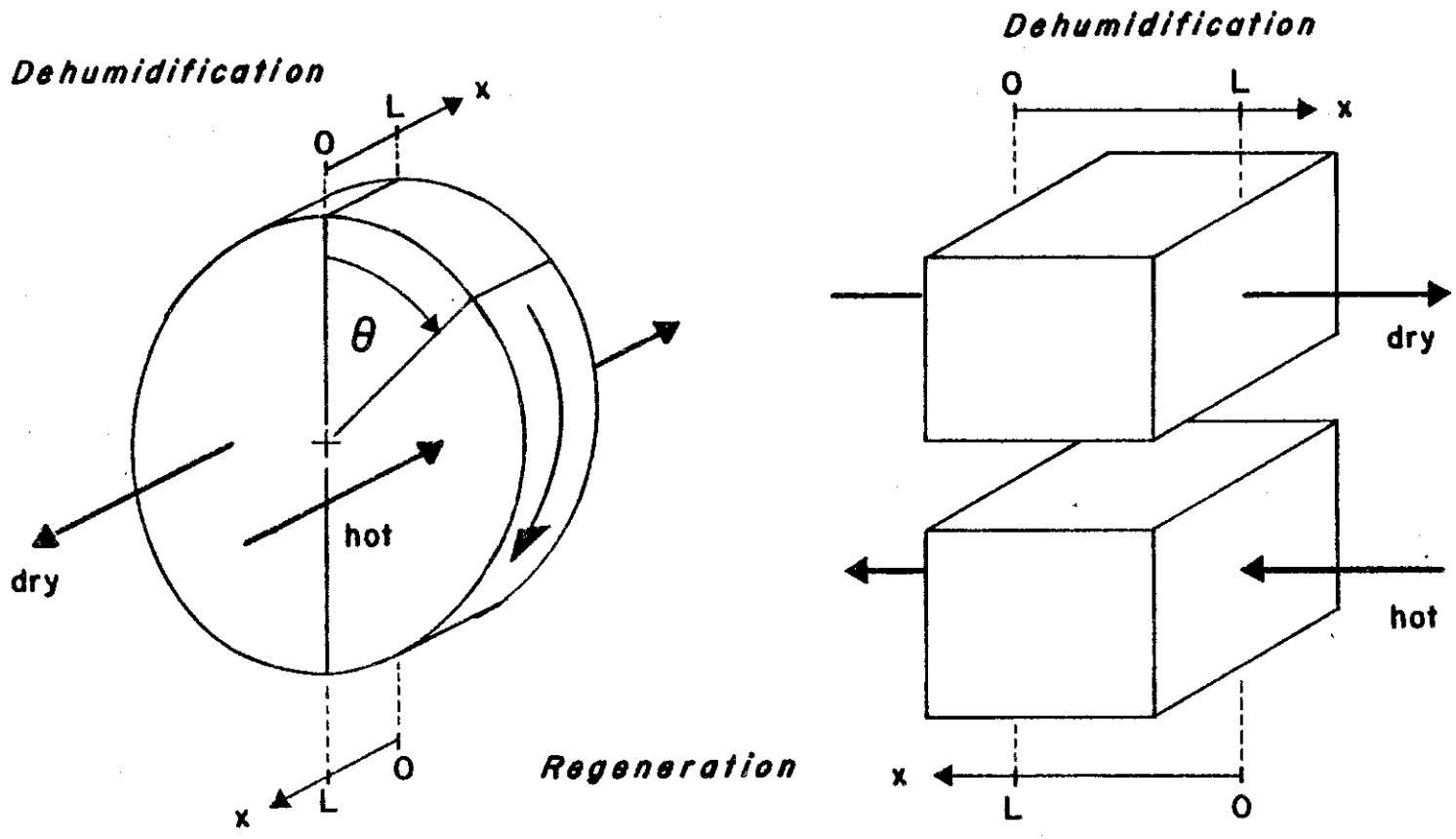

Figure 3.0.1 Rotary wheel and bed type adiabatic dehumidifiers.

is based on the assumption of equilibrium between the desiccant and air stream at all times and positions. This situation is obtained by assuming the coefficients describing the heat and mass transfer process are infinite. It is also assumed in the following development that the processes occur under steady-state operating conditions with uniform inlet conditions.

The differential equations describing the heat and mass transfer between the desiccant and the air stream are obtained by applying mass and energy balances to the control volume in figure 3.1.1. The results are

$$\frac{\partial w}{\partial \theta} + v \frac{\partial w}{\partial x} + \mu \frac{\partial W}{\partial \theta} = 0$$

$$\frac{\partial h}{\partial \theta} + v \frac{\partial h}{\partial x} + \mu \frac{\partial H}{\partial \theta} = 0 \qquad (3.1.1)$$

where v is the air velocity and μ is the ratio of the mass of dry desiccant to the mass of dry air in the control volume. These equations are nonlinear and coupled through the dependence of enthalpy on moisture content. Assuming equilibrium between the air and the desiccant given by

$$W = W(t,w)$$

$$H = H(t,w)$$

$$h = h(t,w)$$

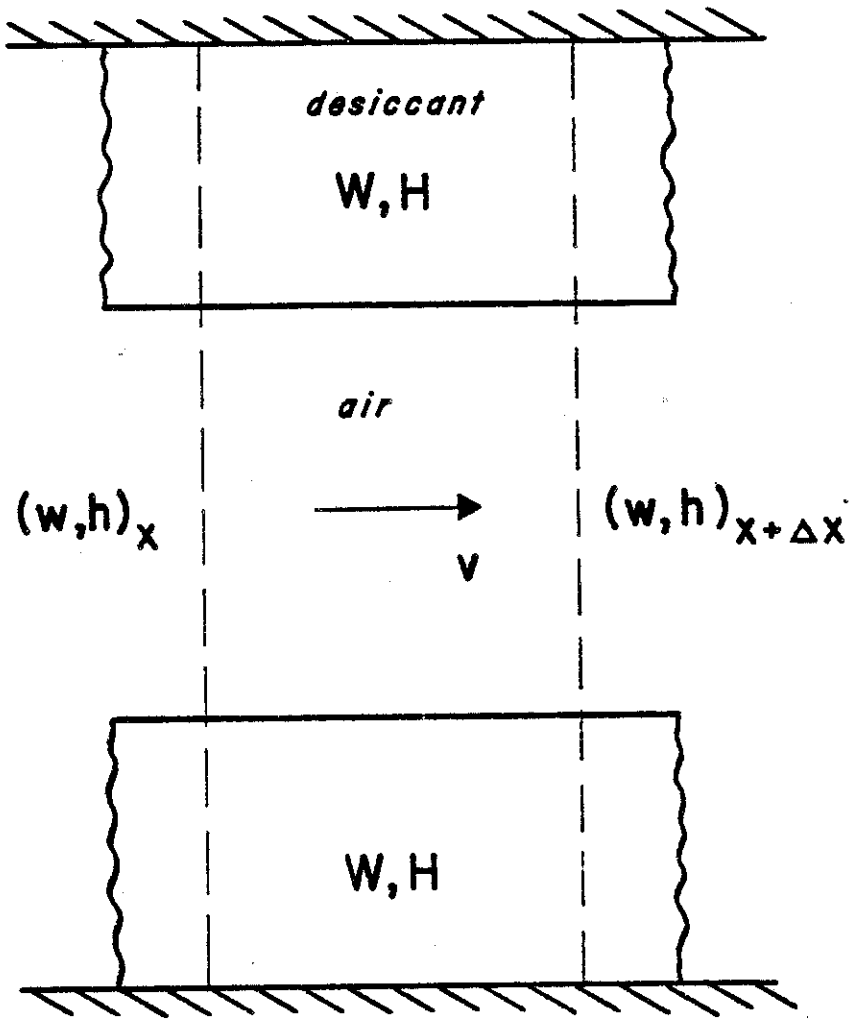

Figure 3.1.1 Adiabatic dehumidifier control volume idealized as a parallel passage channel.

eqs (3.1.1) can be manipulated into two equations of identical form [16],

$$\left(\frac{\partial t}{\partial \theta} + \alpha_i \frac{\partial w}{\partial \theta}\right) + u_i\left(\frac{\partial t}{\partial x} + \alpha_i \frac{\partial w}{\partial x}\right) = 0 \qquad i = 1,2 \tag{3.1.2a}$$

where

$$u_i = \frac{v}{1 + \mu\gamma_i} \tag{3.1.2b}$$

and the α_i and γ_i are functions of the desiccant and moist air properties [16,7]. If functions $F_i(t,w)$ are defined such that

$$\left.\frac{\partial F_i}{\partial w}\right)_t = \alpha_i \left.\frac{\partial F_i}{\partial t}\right)_w \tag{3.1.3}$$

eqs (3.1.2a) can be transformed [16] to

$$\frac{\partial F_i}{\partial \theta} + u_i \frac{\partial F_i}{\partial x} = 0 \qquad i = 1,2 \tag{3.1.4}$$

where the F_i are termed the characteristic potentials.

Eq (3.1.3) can be rearranged to

$$\alpha_i = \left.\frac{\partial F_i}{\partial w}\right) \Big/ \left.\frac{\partial F_i}{\partial t}\right)_w = -\left.\frac{\partial t}{\partial w}\right)_{F_i} \qquad i = 1,2 \tag{3.1.5}$$

The α_i are related to the slopes of lines of constant F_i when plotted on a psychrometric chart. Remembering that the α_i are functions of the desiccant and moist air properties, eq (3.1.5)

can be integrated to determine the paths of the constant F_i. This has been done [17] for the silica gel-moist air system being used in this work (section 2.5) and is shown in figure 3.1.2 superimposed on lines of constant t_{WB} and rh. Note the similarity between lines of constant F_1 and t_{WB} and lines of constant F_2 and rh.

Eqs (3.1.4) are of the same form as the equation for heat transfer only [8] with the F_i analogous to t and the γ_i analogous to σ, the ratio of the specific heat of the dry desiccant to that of dry air. With the appropriate assumptions and approximations [7,8], the combined heat and mass transfer problem can be solved by superimposing the two F_i solutions found from the analogous heat transfer only problem.

Eqs (3.1.4) (together with infinite transfer coefficients) are also of the form of a first order wave equation [7,8]. The solution of such an equation is a step change in F_i that travels through the desiccant with a velocity u_i. The wave velocity is dependent on the system properties through γ_i (eq(3.1.2b)) which are shown in figure 3.1.3. γ_1 is much less than γ_2 over the range shown. This means that changes in F_1 will travel through the desiccant much faster than changes in F_2.

These results can be conveniently represented on a wave diagram with bed (or wheel) position, x, and time (or wheel travel angle), θ, as the coordinates as shown in figure 3.1.4. Consider the dehumidification process for example. The left-hand axis represents the situation at the beginning of the dehumidification

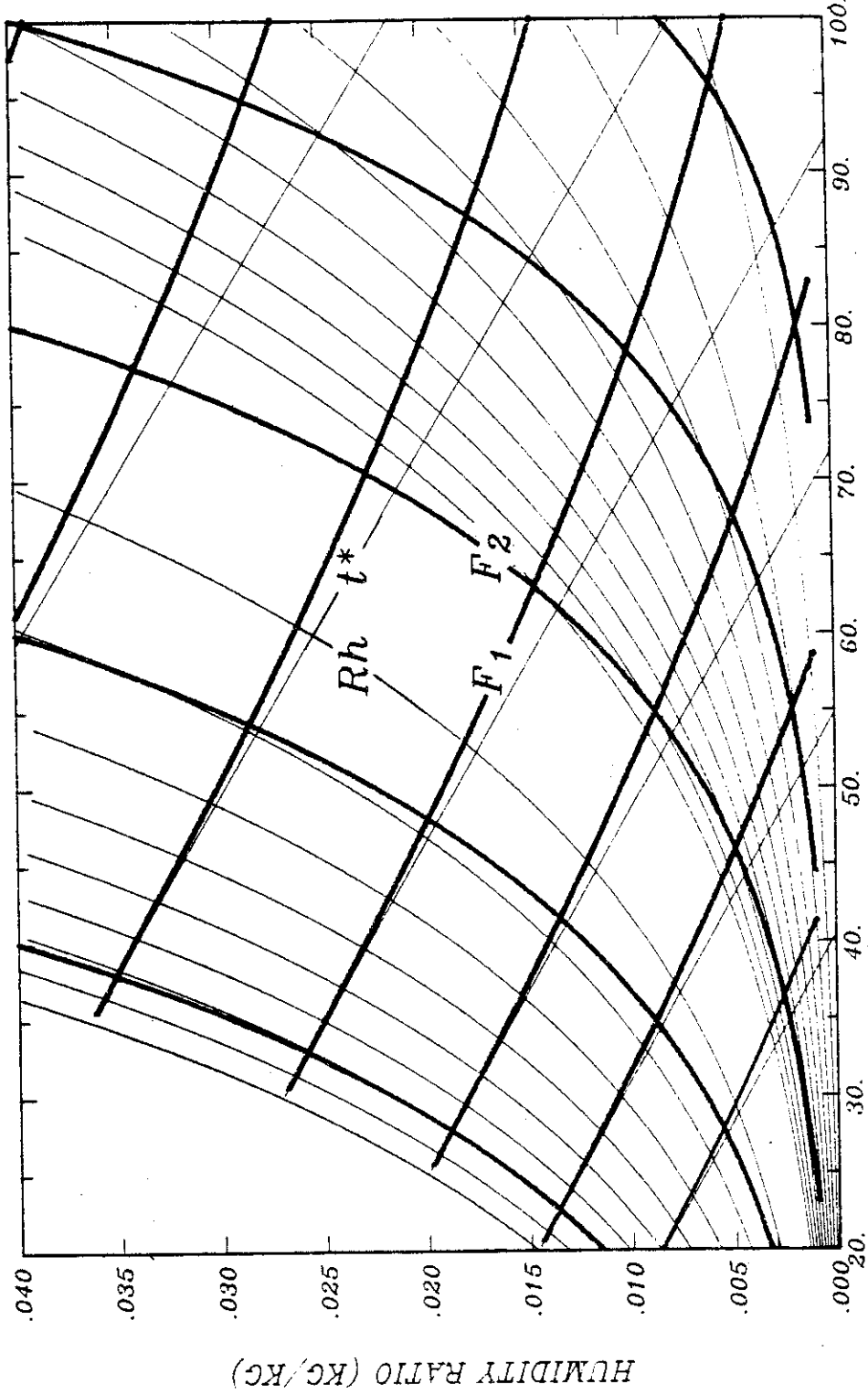

Figure 3.1.2 Characteristic potentials F_1 and F_2 for moist air-silica gel superimposed on wet bulb temperature (t^*) and relative humidity lines (Rh) (from ref [7]).

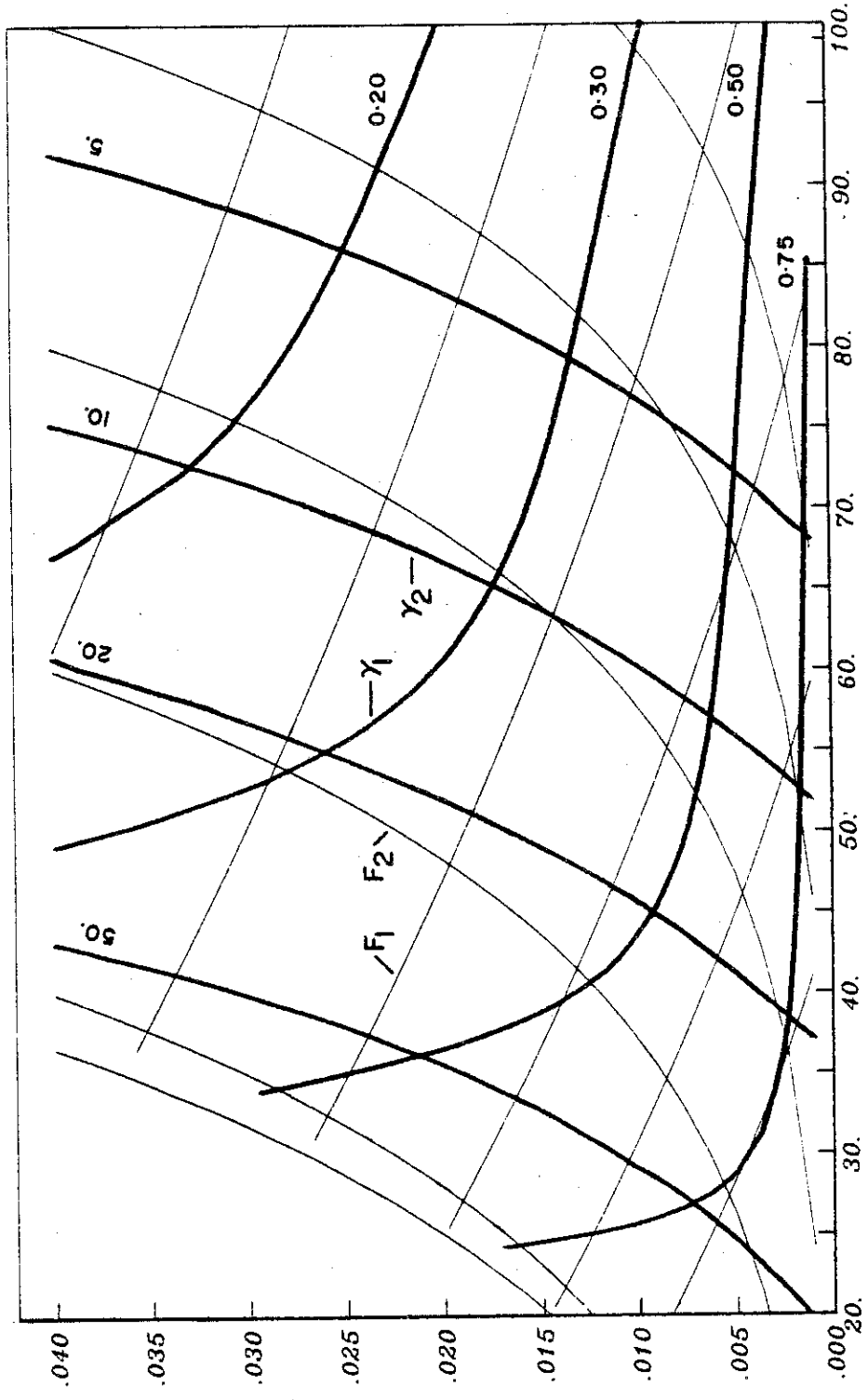

Figure 3.1.3 γ_1 and γ_2 superimposed on F_1 and F_2 for moist air-silica gel (from ref[7]).

period where the desiccant has just been regenerated. The desiccant is therefore in equilibrium with the regenerating air stream R. The desiccant state can be represented by

$$F_{iR} = F_i(t_{R,in}, w_{R,in}) \quad i = 1,2 \tag{3.1.6}$$

As the air stream to be dehumidified is blown through the bed, a step change in F_1 passes rapidly through the bed. The position of the wave front as it moves through the bed is given by the diagonal line. Ahead of the F_1 change wave, the air stream has come to equilibrium with the desiccant and leaves at state R. The outlet air is at state R for only a short time. In determining the idealized outlet state, this part will be neglected.

Behind the F_1 wave and ahead of the F_2 wave, the desiccant is at the intermediate state F_{1P}, F_{2R}. The air leaving the dehumidifier ahead of the F_2 wave is in equilibrium with this state given by D^* or

$$\begin{aligned} w^*_{D,out} &= w(F_{1P}, F_{2R}) \\ t^*_{D,out} &= t(F_{1P}, F_{2R}) \end{aligned} \tag{3.1.7}$$

Behind the F_2 front, the desiccant has come to equilibrium with the inlet state

$$F_{iP} = F_i(t_{D,in}, w_{D,in}) \quad i = 1 = 2 \tag{3.1.8}$$

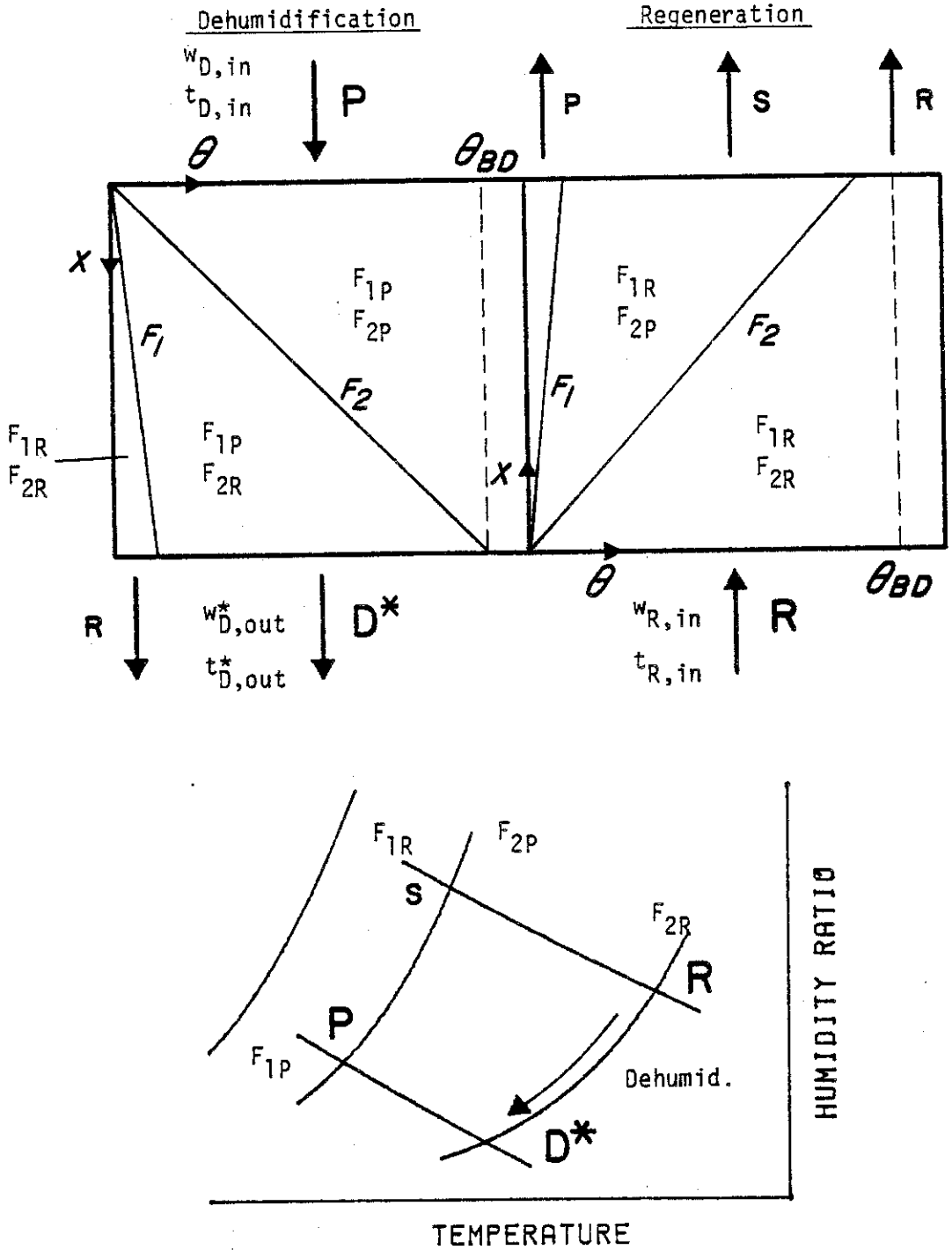

Figure 3.1.4 Wave diagram and psychrometric representation of idealized adiabatic dehumidifier processes.

and can therefore do no more dehumidifying. The maximum amount of dehumidification (and therefore the largest capacity) occurs when the dehumidification period is taken as the time for the F_2 wave to pass through the bed, θ_{BD}. For times shorter than this, the full capacity of the bed is not used. For periods greater than θ_{BD}, nondehumidified air with little potential for cooling is passed on to the rest of the system.

The same description applies to the regenerating period. Figure 3.1.3 shows that γ_{2R} is less than γ_{2P} which means the F_2 wave in the regenerating period travels faster than in the dehumidification period.[3] The easiest way to determine the average outlet state of the regenerating period is to do mass and energy balances on the whole dehumidifier.

3.2 Non-ideal Adiabatic Dehumidifier Model

The solution to the non-ideal heat transfer only problem can be presented in terms of a temperature effectiveness

$$\varepsilon = \frac{t_{A,out} - t_{A,in}}{t_{B,in} - t_{A,in}}$$

where stream A has the minimum capacity rate ratio

$$\frac{C_{air}}{C_{mat}} = \frac{(\dot{m}c)_{air}}{(mc)_{mat}/\theta_D} = \frac{1}{\mu\sigma} \qquad (3.2.1)$$

---

[3] For balanced mass flowrates, the only flow ratio used for the adiabatic systems in this work. See ref[7] for the effects of unbalanced flow.

and $t_{B,in} - t_{A,in}$ is the maximum possible temperature change for the heat exchanger. The temperature effectiveness is usually presented in terms of non-dimensional parameters describing the properties and geometry of the exchanger (see, for example, Kays and London [18]). The heat transfer only solution can be applied to the non-ideal heat and mass transfer problem by using the analogous parameters to determine effectiveness for the F_i potentials [19].

In the heat transfer only problem, the effectiveness is applied to the stream with the smaller capacity rate ratio. The analogous "capacity rate ratio" for the heat and mass exchanger is $1/\mu\gamma$. In section 3.2, it was noted that the γ_i for the dehumidification period are greater than for the regenerating period, implying that the F_i effectiveness should be applied to the dehumidifying period (the period with the slower F_i waves).

$$\varepsilon_{F_i} = \frac{F_{iD} - F_{iP}}{F_{iR} - F_{iP}} \qquad i = 1,2 \qquad (3.2.2)$$

These are shown in figure 3.2.1. The outlet air state of the regeneration stream is then found from mass and energy balances.

Rather than integrating eqs (3.1.5) each time to determine F_i, Jurinak [7] has determined curve fits for the F_i to which eqs (3.2.2) can be applied directly. For the silica gel used in this work, the F_i are fitted by

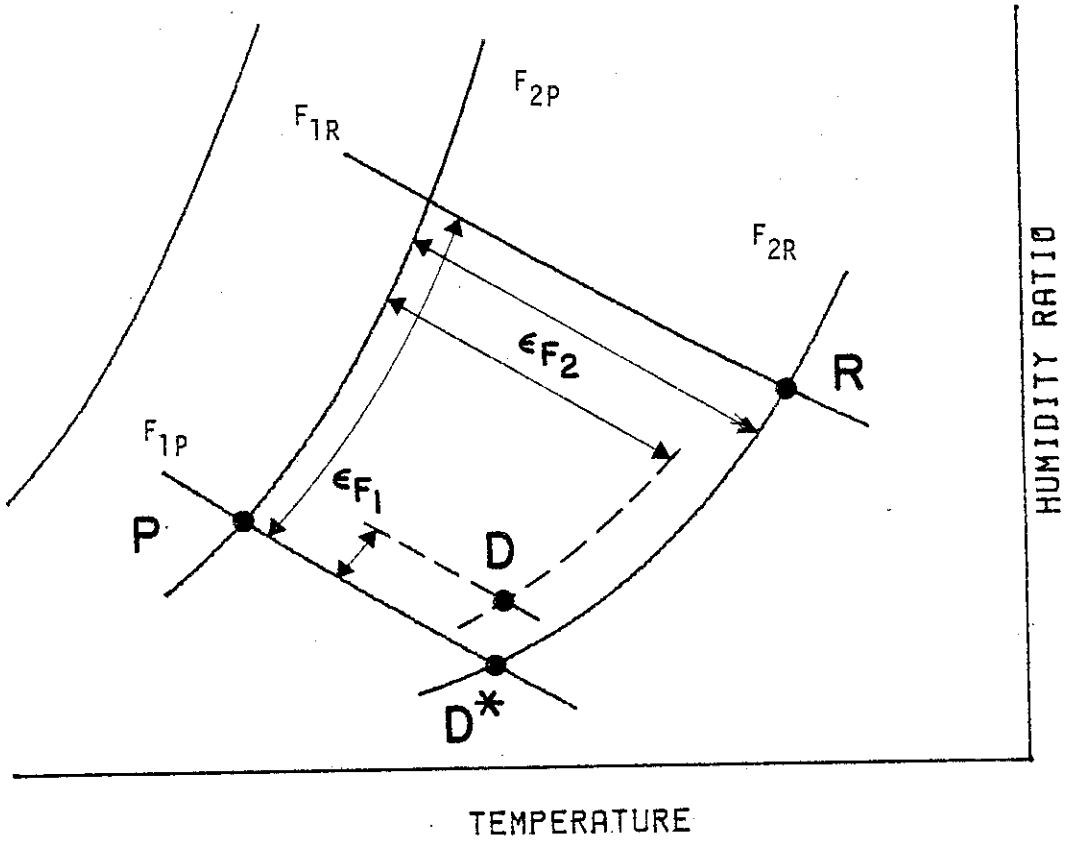

Figure 3.2.1 Adiabatic dehumidifier F_i effectivenesses.

$$F_1(t,w) = -\frac{2865}{t^{1.49}} + 4.344\ w^{.8624}$$

$$F_2(t,w) = \frac{t^{1.49}}{6360} - 1.127\ w^{.07969} \qquad (3.2.3)$$

where t is in °K and w is in unit mass of water per unit mass of dry air. The F_1 and F_2 equations cannot be solved explicitly for t and w, though. Temperature can be eliminated between the F_1 and F_2 equations leaving a function of w only. w can then be solved for by applying Newton's method. t can then be found from either of eqs (3.2.3).

CHAPTER 4

THE COOLED DEHUMIDIFIER MODEL

A theory similar to the analogy method for adiabatic dehumidifiers does not exist for cooled dehumidifiers. With only finite difference models available, evaluation of the seasonal performance of a cooled dehumidifier air-conditioning system is difficult and expensive. In this chapter, a model of a cooled dehumidifier suitable for long term computer simulations is developed. A description of the cyclic operation of a cooled dehumidifier is given. An idealized equilibrium model that depends only on the inlet conditions and desiccant properties is presented. This model is then extended to non-ideal dehumidifiers by defining three parameters which describe the degree to which the non-ideal dehumidifier processes approach the ideal.

4.1 Description of the Cooled Dehumidifier Cycle

The cooled dehumidifier prototype being investigated at IIT uses two cross-flow, parallel passage, fixed-bed dehumidifiers [11]. This geometry is used because of the simplicity in attaching the desiccant material to the supporting structure and in the ducting of the process and cooling air streams. The parallel passages are designed for laminar flow in order to keep the pressure drop to a minimum. Figure 4.1.1 shows this cross-cooled geometry with the addition of fins. Only the channels through which the air stream

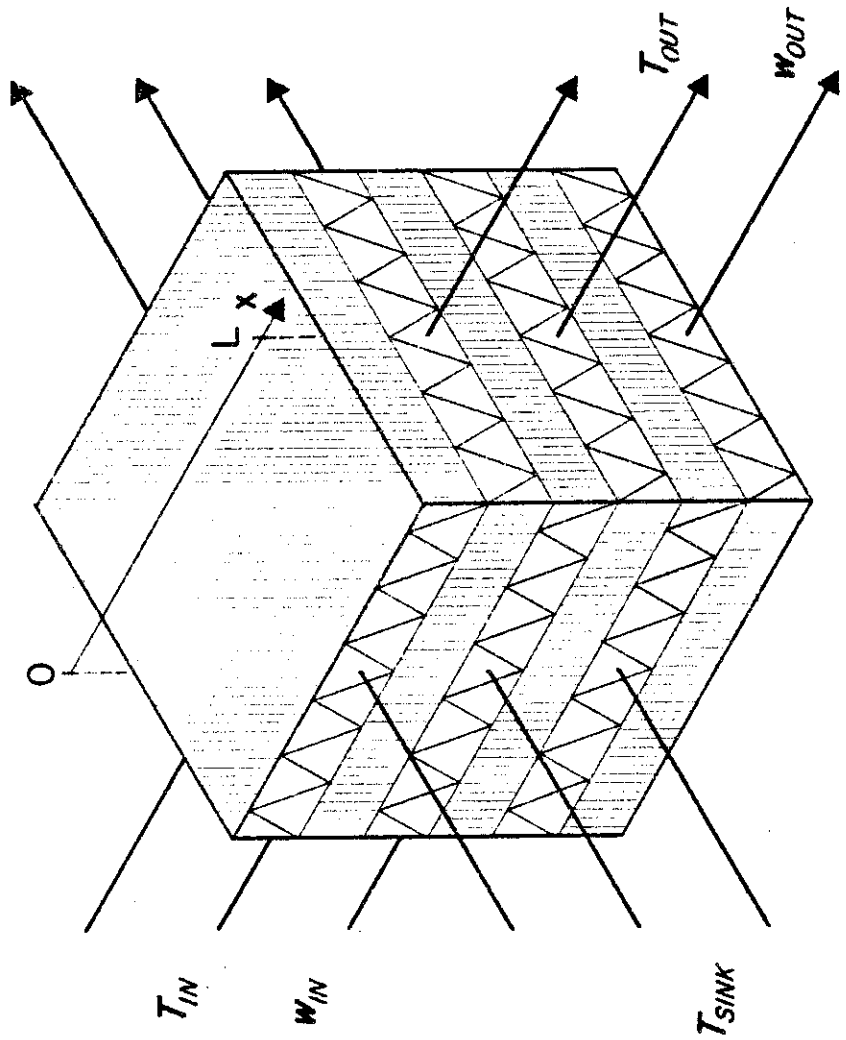

Figure 4.1.1 A cross-cooled desiccant dehumidifier geometry.

to be dehumidified flow contains desiccant material. A geometry suitable for continuous rotary operation has also been proposed [14].

Figure 4.1.2 shows a schematic diagram of the operating cycle of a cooled dehumidifier. The desiccant bed in (a) is being regenerated (dried out) with a heated air stream. When the bed is fully regenerated, it will be in equilibrium with the regenerating air stream and will therefore be hot.

A precooling process follows during which cool air is blown through the cooling channels to remove the heat from the regenerated bed in preparation for the dehumidification process (b). This process reduces the load on the dehumidification cooling stream.

After being precooled, the bed is ready to dehumidify the process air stream which is blown through the desiccant-lined channels (c). Cool air is blown through the cooling channels to remove the heat generated by the adsorption of moisture in the desiccant and to keep the bed at a lower temperature. The air humidity ratio in equilibrium with the desiccant at this temperature is drier than with no cooling (see figure 2.3.2).

When the desiccant becomes saturated, the bed is removed from the process air stream. At this point, the bed is cool but regeneration of the bed requires heating it to a relatively high temperature. The other bed has just finished being regenerated and is ready for precooling. The heat removed from the hot bed during precooling can be used to preheat the cool, saturated bed about to be regenerated (d).

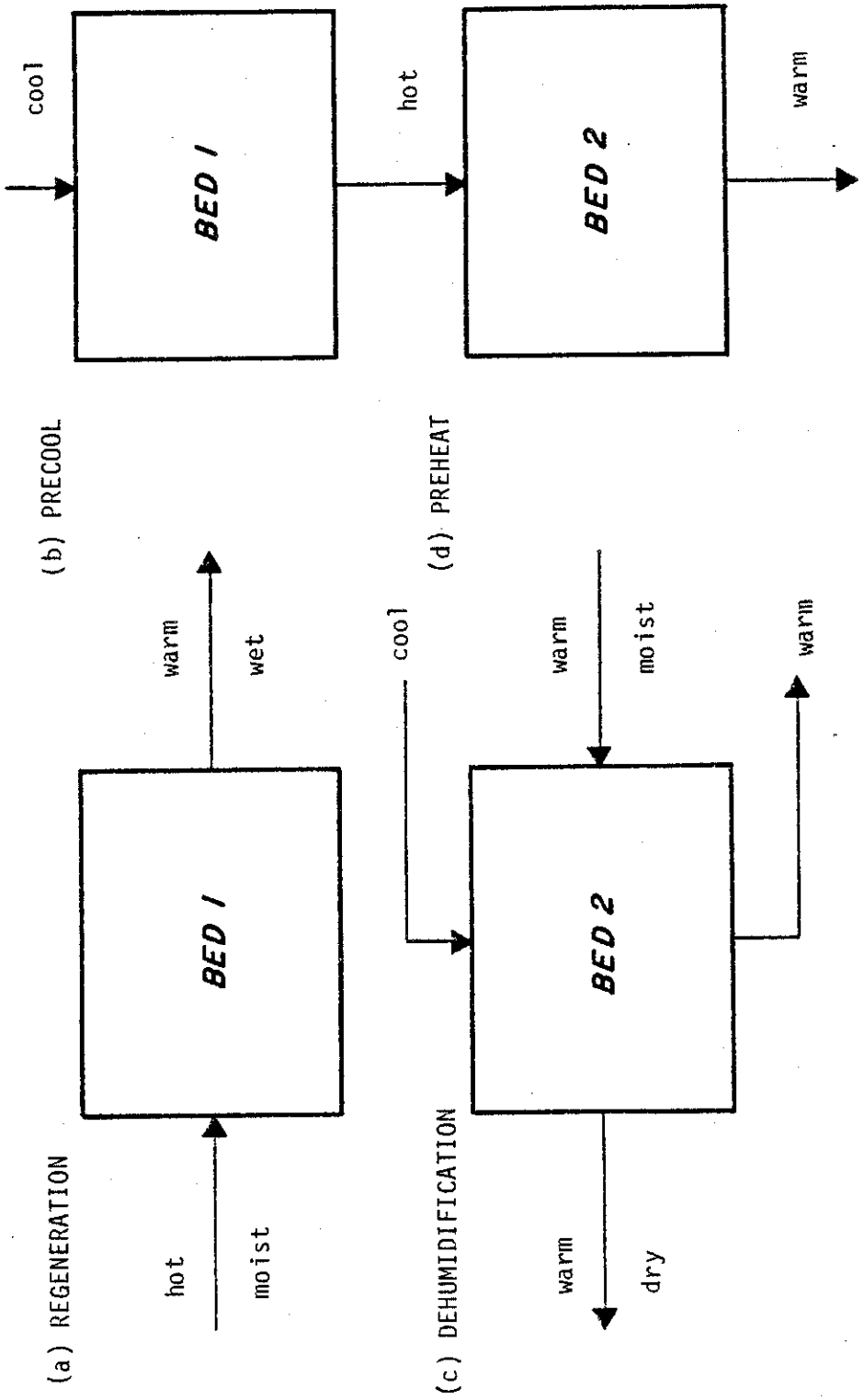

Figure 4.1.2 Cooled dehumidifier cycle.

After preheating, the bed is regenerated and the cycle repeated. While one bed is being regenerated, the other is dehumidifying, and while one bed is being precooled, the other is being preheated.

4.2 Idealized Cooled Dehumidifier Model

The model of the idealized cooled dehumidifier to be presented does not depend on any particular geometry but does follow the operating cycle described in section 4.1. An underlying assumption in the following model is that the processes occur under steady state operating conditions with uniform inlet states.

4.2.1 Cooled Dehumidification Process

The following assumptions are made in the idealized model of the cooled dehumidification process:

i) The desiccant bed has been uniformly precooled to some sink temperature.

ii) Sufficient cooling is supplied during the dehumidification process so that the bed is maintained at the sink temperature.

iii) Heat and mass transfer coefficients are infinite so that there is equilibrium between the air stream and the desiccant at all times and positions.

The first two assumptions reduce the problem to an isothermal mass transfer process. A water balance on the control volume in figure 4.2.1 shows the describing equation to be

$$\frac{\partial w}{\partial \theta} + v \frac{\partial w}{\partial x} + \mu \frac{\partial W}{\partial \theta} = 0 \qquad (4.2.1)$$

where v is the fluid velocity and μ is the ratio of the mass of dry desiccant to the mass of dry air in the dehumidifier. The equilibrium relationship $w = w(T,W)$ produces the identities

$$\frac{\partial w}{\partial \theta} = \left.\frac{\partial w}{\partial T}\right)_W \frac{\partial T}{\partial \theta} + \left.\frac{\partial w}{\partial W}\right)_T \frac{\partial W}{\partial \theta}$$

$$\frac{\partial w}{\partial x} = \left.\frac{\partial w}{\partial T}\right)_W \frac{\partial T}{\partial x} + \left.\frac{\partial w}{\partial W}\right)_T \frac{\partial W}{\partial x} \qquad (4.2.2)$$

The desiccant temperature T is constant by the second assumption above and so the first term in each of eqs (4.2.2) drops out. Substitution of eqs (4.2.2) into eq (4.2.1) gives

$$\frac{\partial W}{\partial \theta} + u \frac{\partial W}{\partial x} = 0 \qquad (4.2.3)$$

where

$$u = \frac{v}{1 + \mu \left.\frac{\partial W}{\partial w}\right)_T} \qquad (4.2.4)$$

Eq (4.2.3) is of the form of the first order kinetic wave equation that was discussed in section 3.1 while developing the adiabatic dehumidifier model. A step change in W will propagate through the desiccant bed with a velocity u.

Figure 4.2.2 presents the results in the form of a wave diagram. The left-hand axis represents the situation at the beginning of the dehumidification period when the whole bed has

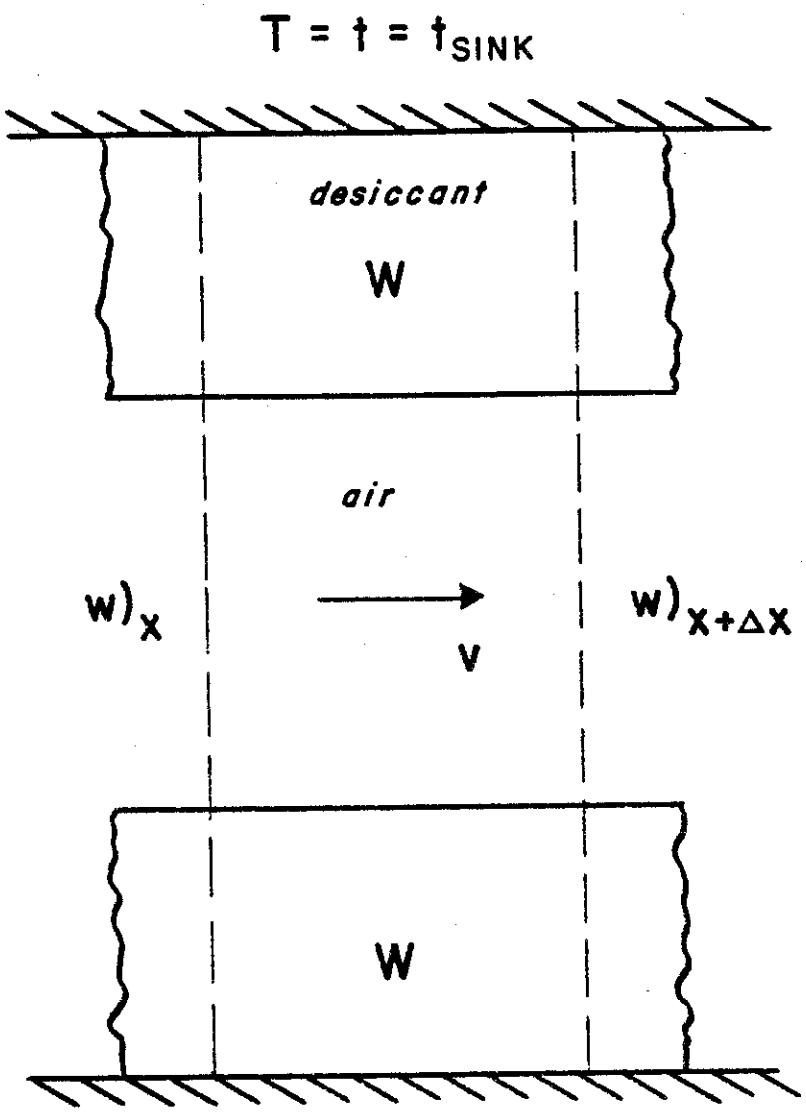

Figure 4.2.1 Cooled dehumidifier control volume idealized as a parallel passage channel.

just been regenerated to W_{DRY} and precooled to t_{SINK}. If moist air with humidity ratio $w_{D,in}$ is passed through the bed, a wave front moves through the bed with its position in the bed as a function of time shown by the diagonal line. Behind the wave front, the desiccant has adsorbed moisture from the air such that it is in equilibrium with the cooled inlet air stream,

$$W_{WET} = W(t_{SINK}, w_{D,in}) \tag{4.2.5}$$

Ahead of the wave, the air has been dehumidified and leaves the bed in equilibrium with the desiccant,

$$w^{*}_{D,out} = w(t_{SINK}, W_{DRY}) \tag{4.2.6}$$

After the wave front has passed through the bed, the desiccant can no longer adsorb any more moisture and the outlet humidity ratio will be the same as the inlet. The time it takes for the wave to break through is θ_{BD}. This period length produces the maximum amount of dehumidification. If the dehumidification period θ_D is less than θ_{BD}, some of the adsorbing capacity of the bed is wasted. If the period is greater than θ_{BD}, moist air with no potential for cooling is passed on to the rest of the system.

4.2.2 Adiabatic Regeneration Process

Regeneration of the desiccant occurs adiabatically. The analogy method presented in chapter 3 provides an efficient model

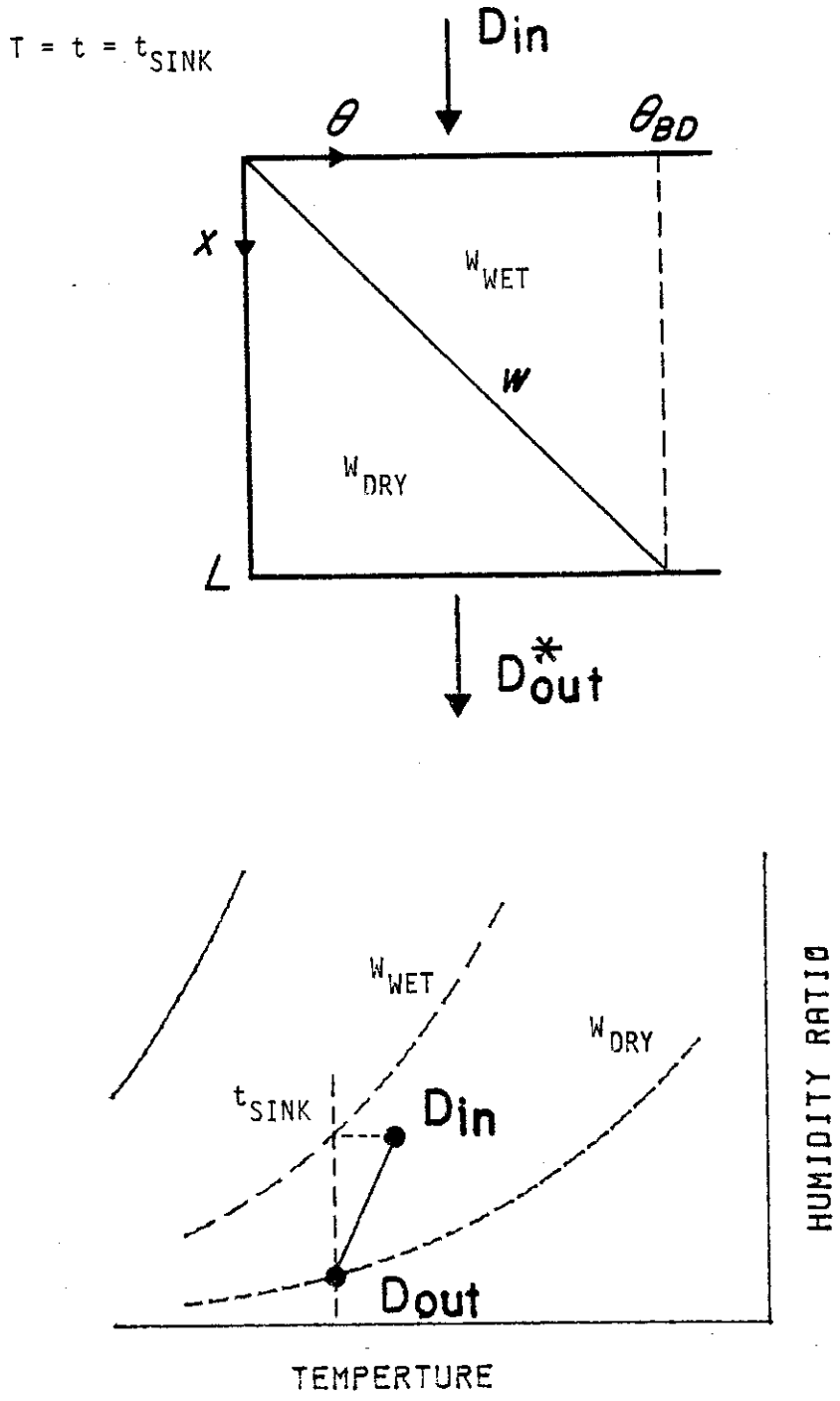

Figure 4.2.2 Wave diagram and psychrometric representation of idealized cooled dehumidification process.

for this period of the idealized dehumidifier cycle.

A desiccant bed that has gone through the cooled dehumidification period has a moisture content W_{WET} given by eq (4.2.5). Prior to being regenerated, it is preheated to some temperature T_H (given by eq (4.2.17)). This state is represented by the left-hand axis of figure 4.2.3 and labeled as A.

If a heated air stream at state R is blown through the bed, an F_1 wave moves rapidly through the bed followed by an F_2 wave sometime later as described in section 3.1. Again, because the F_1 wave travels so fast, the short time that the outlet air state is at A is neglected. Behind the F_1 wave, the desiccant is at the state given by

$$F_{1R} = F_1(t_{R,in}, w_{R,in})$$

$$F_{2A} = F_2(T_H, W_{WET}) \tag{4.2.7}$$

Ahead of the F_2 wave, the air is in equilibrium with the desiccant and therefore leaves at state RA,

$$t^*_{R,out} = t(F_{1R}, F_{2A})$$

$$w^*_{R,out} = w(F_{1R}, F_{2A}) \tag{4.2.8}$$

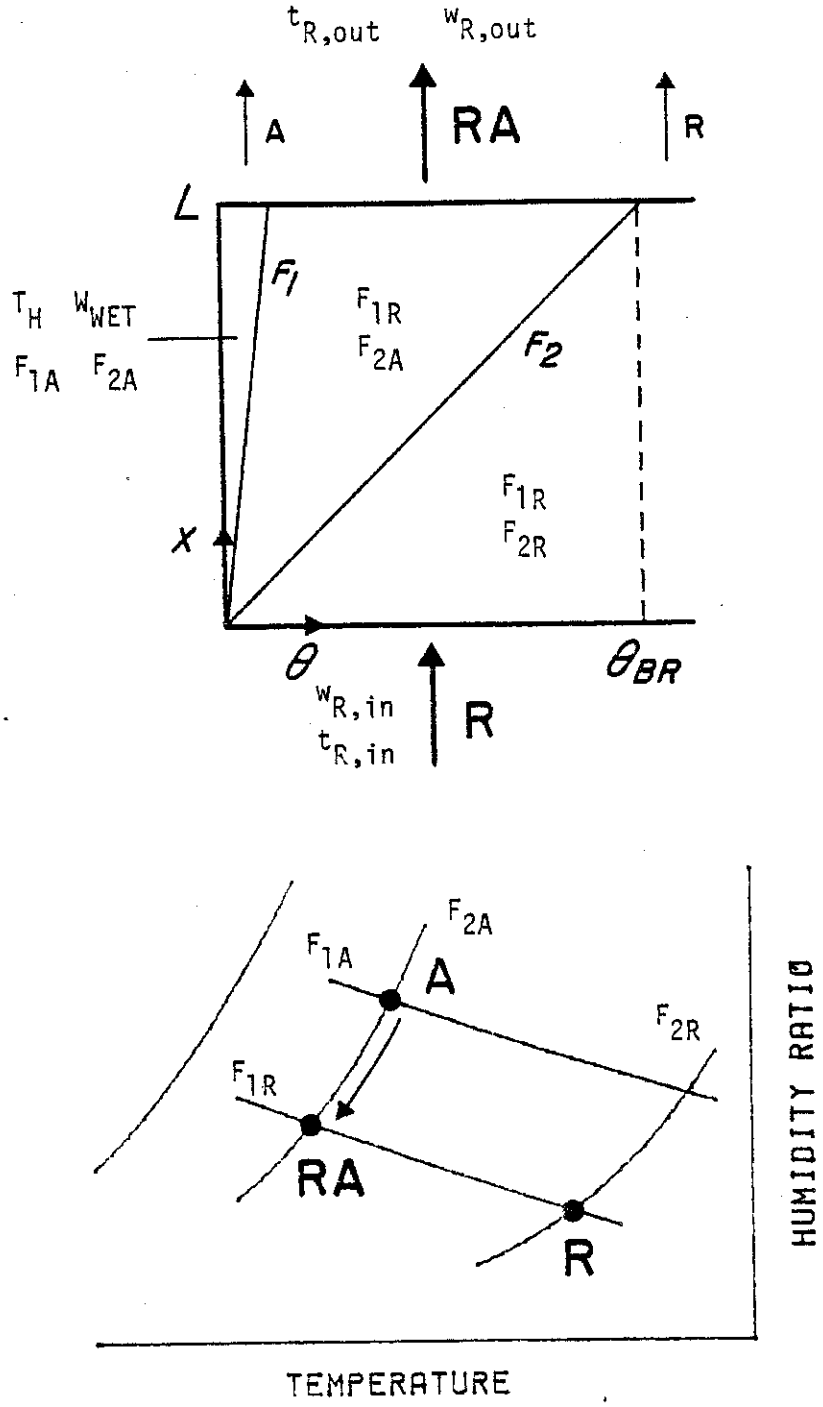

Figure 4.2.3 Wave diagram and psychrometric representation of idealized (adiabatic) dehumidification process in cooled dehumidifier cycle.

Behind the F_2 wave, the desiccant has come to equilibrium with the inlet air stream and its state is given by

$$F_{iR} = F_i(t_{R,in}, w_{R,in}) \qquad i = 1,2$$

or

$$T = t_{R,in} \tag{4.2.9}$$

$$W_{DRY} = W(t_{R,in}, w_{R,in})$$

The F_2 wave breaks through the bed after time θ_{BR}. This period length results in the maximum regeneration of the desiccant. If the regeneration period, θ_R, is less than θ_{BR}, the bed will not be fully regenerated and therefore will have less dehumidifying capacity. If the period is greater than θ_{BR}, the air heated at some expense will be blown through the bed and exhausted without doing anything.

To obtain optimum performance from the dehumidifier, the dehumidification period should be chosen as $\theta_D = \theta_{BD}$ and the regeneration period should be chosen as $\theta_R = \theta_{BR}$. Because the two processes occur at the same time, the periods must be equal, $\theta_D = \theta_R$. In general, θ_{BD} and θ_{BR} will not be equal because the wave speeds are not equal, so obtaining the optimum performance of the dehumidifier is not a simple matter. Operation of the dehumidifier to obtain $\theta_{BD} = \theta_{BR}$ and the consequences of $\theta_{BD} \neq \theta_{BR}$ are discussed in section 4.2.4.

4.2.3 Precooling and Preheating Processes

The precooling and preheating processes for the idealized dehumidifier are modeled as counter-current heat exchange processes with infinite heat transfer coefficients. The solution will be presented in terms of waves in order to remain consistent with the other periods.

The precooling and preheating processes occur at constant moisture content. A differential energy balance on a small control volume of the bed gives the following equation (neglecting the storage term of the air),

$$\frac{\partial T}{\partial \theta} + u \frac{\partial T}{\partial x} = 0 \qquad (4.2.10)$$

where

$$u = \frac{C_{air} L}{C_{des} \theta_P} \qquad (4.2.11)$$

and C_{air}/C_{des} is the capacity rate ratio for the process

$$\frac{C_{air}}{C_{des}} = \frac{\dot{m}_{air} c_{air}}{(m_{des} c_{des})/\theta_P} \qquad (4.2.12)$$

where θ_P is the period of the precool/preheat process. Eq (4.2.10) is again a kinetic wave equation describing a step change in bed temperature T propagating through the bed with velocity u.

If the specific heats of the individual species are assumed to be constants, the specific heat of moist air (per unit mass of dry air) is given by

$$c_{air} = c_{dry\ air} + wc_{vapor} \qquad (4.2.13)$$

The enthalpy of a moist desiccant (per unit mass of dry desiccant) is given by [17]

$$H = c_{dry\ des}(T - T'_{ref}) + c_{liq}\quad W(T - T''_{ref}) + \Delta H_w$$

where ΔH_w is the integral heat of wetting defined as

$$\Delta H_w = h_{fg} \int_0^W \left(1 - \frac{h_s}{h_{fg}}\right) dW$$

where h_{fg} is the latent heat of vaporization of water and h_s is the heat of adsorption of water by the desiccant. If it is assumed that h_s/h_{fg} is independent of temperature, the integral heat of wetting can be written as

$$\Delta H_w = [h^{\circ}_{fg} + (c_{vapor} - c_{liq}\quad)\ (T - T^{\circ}_{ref})]\quad \frac{\Delta H_w}{h_{fg}}$$

where h_{fg} has been approximated as a linear function of temperature (eq (2.6.4)) and where $\Delta H_w/h_{fg}$ is not a function of temperature. From the definition of specific heat, $c_{des} = \partial H/\partial t)_W$, the desiccant specific heat (per unit mass of dry desiccant) is found to be

$$c_{des} = c_{dry\ des} + c_{liq}\quad W + (c_{vapor} - c_{liq})\ \frac{\Delta H_w}{h_{fg}} \qquad (4.2.14)$$

Figure 4.2.4 shows a wave diagram representation of the precooling process. The bed is initially at $T = t_{R,in}$ as it has just completed regeneration. As air at t_{SINK} is blown through the cooling channels of the bed, a temperature wave passes through the bed. Ahead of the wave, the air is in equilibrium with the bed and leaves at $t_{R,in}$. The energy removed from the bed has been reclaimed at its highest possible temperature. Behind the wave, the bed has been cooled down to the temperature of the inlet air stream, t_{SINK}. This fulfills the first assumption made about the idealized cooled dehumidification process in section 4.2.1.

The period θ_P is chosen to be the minimum time required to completely cool the bed. From eq (4.2.11),

$$\theta_P = \frac{L}{u} = \frac{C_{des,C}}{C_{air}} \cdot \theta_P$$

which means that the capacity rate ratio is unity for the idealized precool process,

$$\frac{C_{des,C}}{C_{air}} = 1 \qquad (4.2.15)$$

For the preheat process, the desiccant bed is initially at t_{SINK} as it has just completed the dehumidification process. As the hot air stream from the precool process flows through the bed, a temperature wave passes through the bed as shown in figure 4.2.5. Ahead of the wave, the air is in equilibrium with the initial bed temperature and leaves at t_{SINK}. This is the same

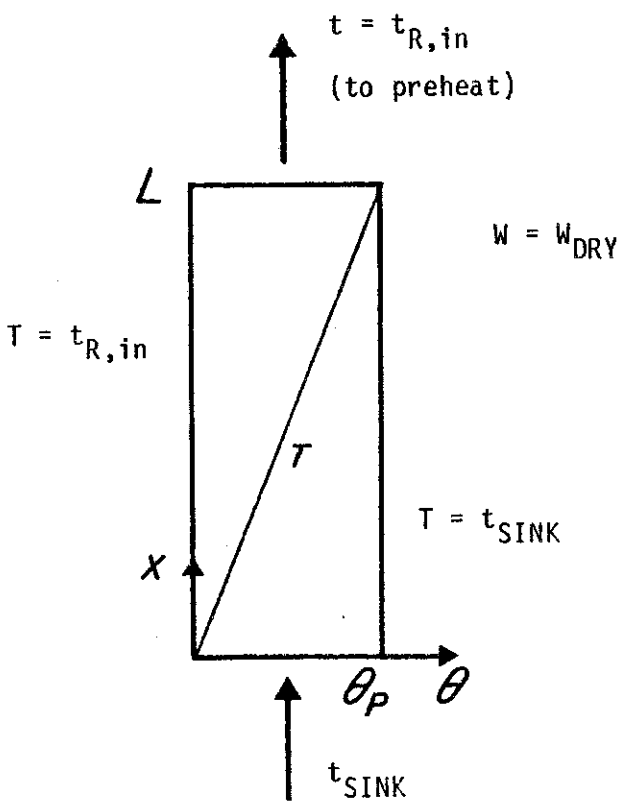

Figure 4.2.4 Wave diagram of idealized precooling process in cooled dehumidifier cycle.

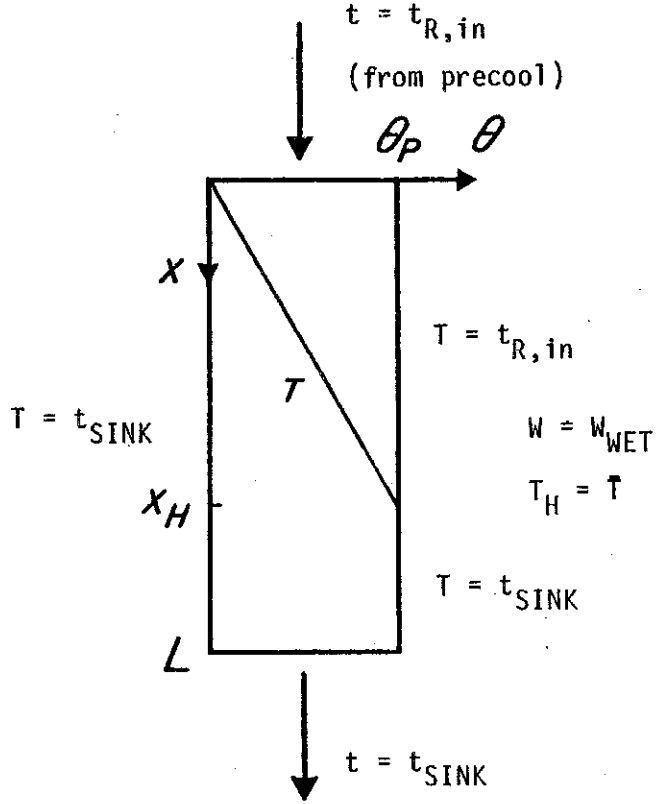

Figure 4.2.5 Wave diagram of idealized preheating process in cooled dehumidifier cycle.

temperature at which the air stream entered the cycle and therefore it carries no net energy into or away from the system. It does not enter into the overall energy balance.

Because the desiccant bed contains more water during the preheat process (after adsorption) than during precooling (after regeneration), its specific capacity and therefore capacity rate is higher during preheating. The temperature wave will propagate through the bed at a slower rate during preheating. At the end of the period, the wave will only have traveled a distance

$$x_H = u\theta_P = \frac{C_{air}}{C_{des,H}} L$$

Making used of eqs (4.2.12) and (4.2.15), this can be written as

$$\frac{x_H}{L} = \frac{C_{des,C}}{C_{des,C}} = \frac{c_{des,C}}{c_{des,H}} \qquad (4.2.16)$$

where

$$c_{des,C} = c_{des}(W_{DRY}) \ \& \ c_{des,H} = c_{des}(W_{WET})$$

From figure 4.2.5, the average temperature of the bed at the end of the preheat period is

$$\overline{T} = t_{R,in} \frac{c_{des,C}}{c_{des,H}} + t_{SINK}\left(1 - \frac{c_{des,C}}{c_{des,H}}\right) \qquad (4.2.17)$$

For simplicity, the bed is considered to be at a uniform state as it enters the regeneration period, i.e., $T_H = \overline{T}$.

4.2.4 Determination of the "Minimum Capacity Rate" Period

As with the adiabatic dehumidifier, determination of the appropriate outlet air states from the idealized cooled dehumidifier depends on knowing the "minimum capacity rate" stream or, in other words, the period with the slower wave. This was relatively easy to do for the adiabatic dehumidifier where the dehumidifying period was found to have the "minimum capacity rate". It is somewhat more difficult here, as the "minimum capacity rate" period is not limited to just one of the periods.

A complete idealized dehumidifier cycle is pictured in figure 4.2.6. The inlet and outlet states of the air streams are given above and below each period. The desiccant states at the end of one period and beginning of the next are given between the periods. The diagonal lines represent the passage of a step change in the appropriate bed property through the bed as a function of time. Figure 4.2.6 depicts a symmetric design where $\theta_D = \theta_R$ and the mass flow rates, $\dot{m}_D$ and $\dot{m}_R$, are controlled such that the W and F_2 wave speeds are equal. Maximum dehumidification and regeneration occur when

$$\theta^* = \theta_{BD} = \theta_{BR}$$

For the dehumidifying/regenerating period chosen as θ^*, the dehumidifier cycle can be represented by the control volume in figure 4.2.7. A water balance on the control volume shows the relationship between the ratio of the flowrates and the air

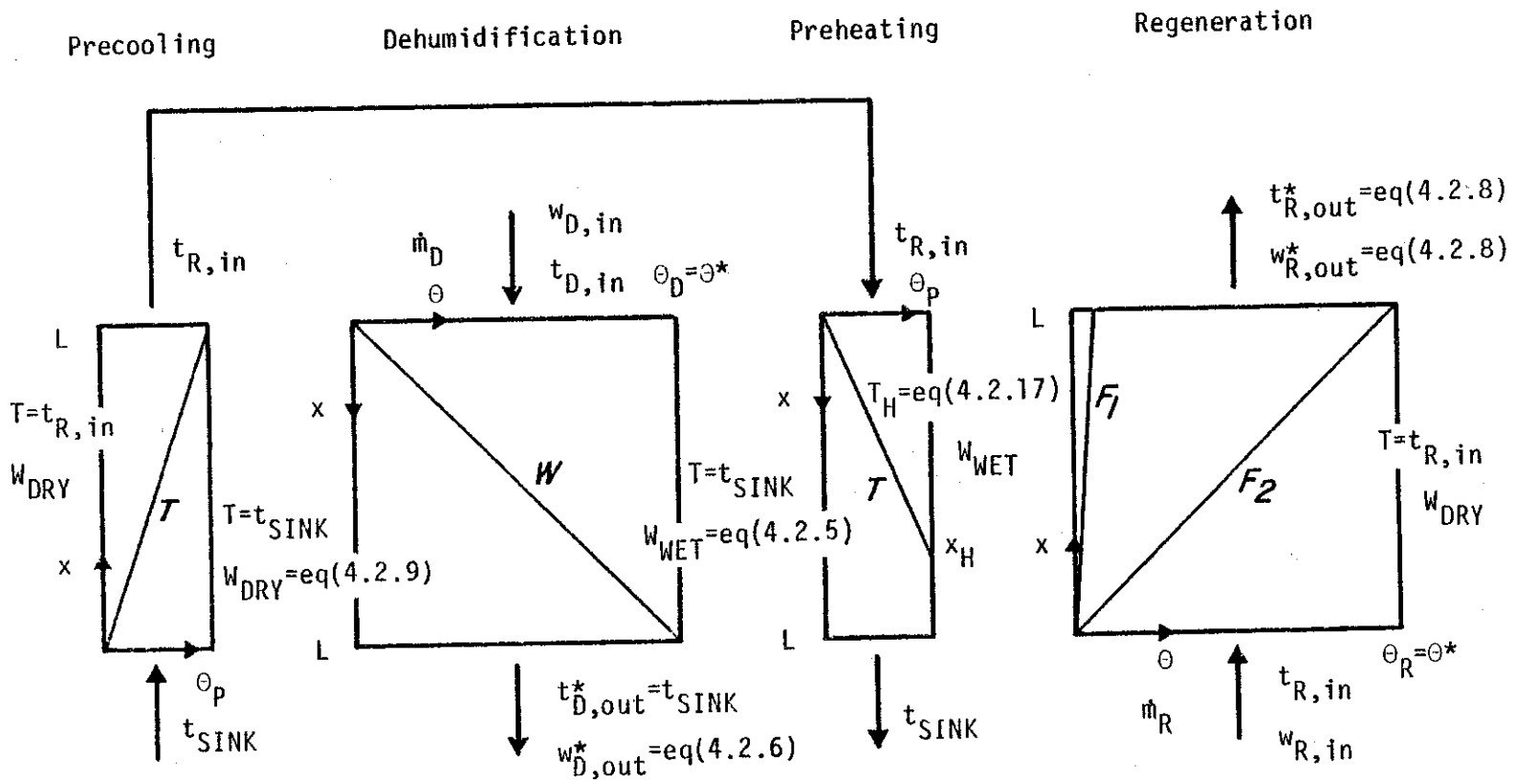

Figure 4.2.6 Wave diagram of complete idealized cooled dehumidifier cycle.

states to be

$$\frac{\dot{m}_R^*}{\dot{m}_D^*} = \left(\frac{\dot{m}_R}{\dot{m}_D}\right)^* = -\frac{w_{D,in} - w_{D,out}^*}{w_{R,in} - w_{R,out}^*} \qquad (4.2.18)$$

where the air states are either given or can be determined from the relations presented earlier. Since the wave speeds are equal, the dehumidifying and regenerating periods have the same "capacity rate".

The flowrate ratio given by eq (4.2.18) can be thought of in two ways. It is the flow ratio between the two periods required to obtain a "capacity rate ratio" of unity. This would require somehow controlling the flowrate depending on the inlet states. This would not be an easy task to accomplish.

In actuality, the flowrate ratio will probably be preset so that θ_{BD} and θ_{BR} will not in general be equal (i.e., "capacity rate ratio" not equal to unity). If the air stream through the bed with the faster wave was stopped after that wave had passed through and that bed was then kept idle until the other bed's wave passed through, the ratio of the average flowrates over the whole period (greater of θ_{BD} and θ_{BR}) would be given by eq (4.2.18). This can be stated another way, using an integrated water balance, as

$$\frac{\dot{m}_R \theta_{BR}}{\dot{m}_D \theta_{BD}} = -\frac{w_{D,in} - w_{D,out}^*}{w_{R,in} - w_{R,out}^*} = \left(\frac{\dot{m}_R}{\dot{m}_D}\right)^* \qquad (4.2.19)$$

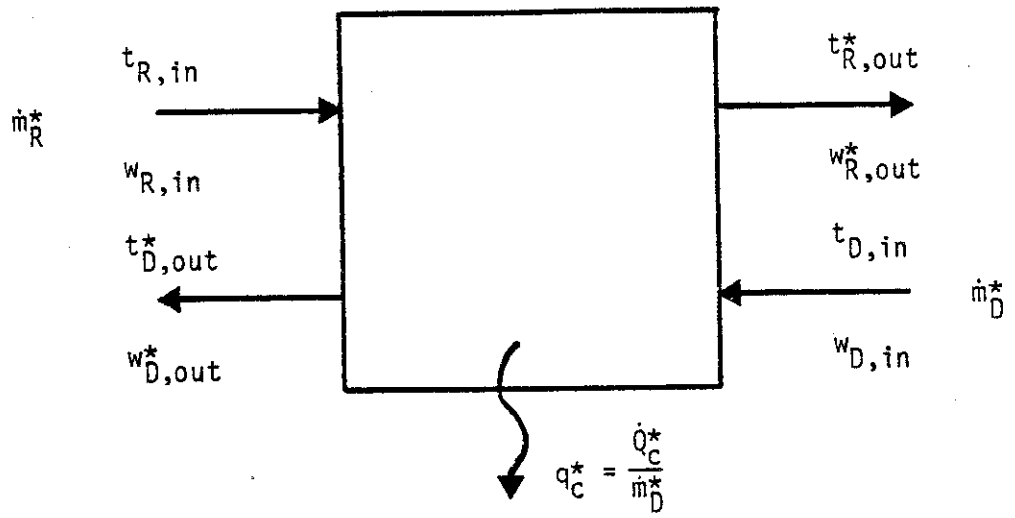

Figure 4.2.7 Control volume and air states for idealized cooled dehumidifier with flowrates set for maximum dehumidification and regeneration.

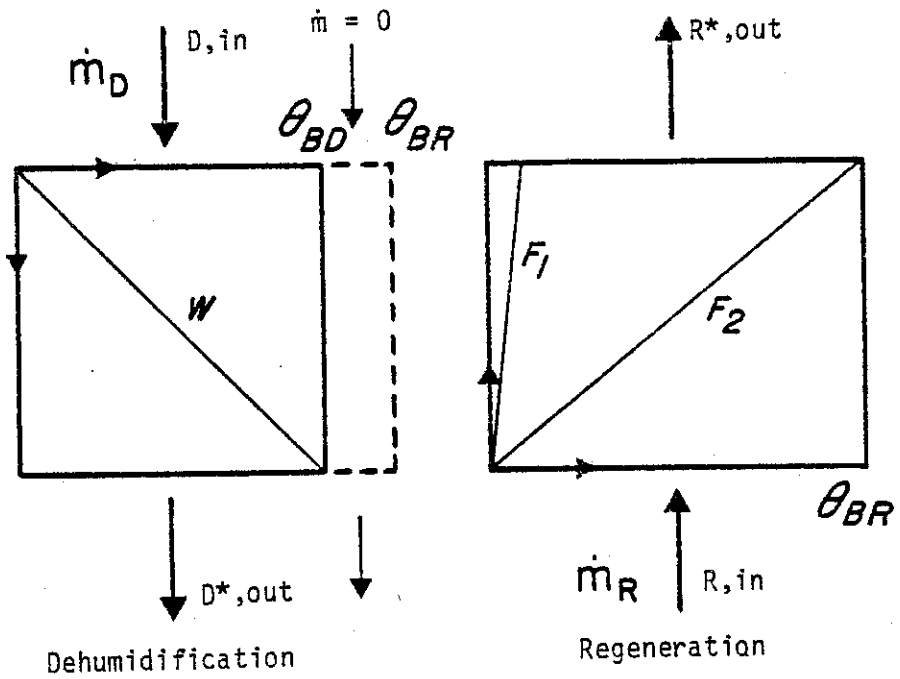

Figure 4.2.8 Wave diagram for idealized cooled dehumidifier cycle with fixed flowrates and variable period length for maximum dehumidification and regeneration.

A wave diagram for $\theta_{BR} > \theta_{BD}$ (regenerating period as "minimum capacity rate" period if θ_D is taken as θ_{BR} rather than θ_{BD}) is shown in figure 4.2.8.

A energy balance on the control volume in figure 4.2.7 shows the cooling required during the idealized dehumidification process with a flowrate ratio of $(\dot{m}_R/\dot{m}_D)^*$ to be

$$q_c^* = (h_{D,in} - h_{D,out}^*) + \left(\frac{\dot{m}_R}{\dot{m}_D}\right)^* (h_{R,in} - h_{R,out}^*) \qquad (4.2.20)$$

For flowrate ratios other than that given by eq (4.2.18), one of the periods will be the "minimum capacity rate" period. Two cases can occur:

i) $\dfrac{\dot{m}_R}{\dot{m}_D} > \left(\dfrac{\dot{m}_R}{\dot{m}_D}\right)^*$ or $\theta_{BR} < \theta_{BD}$

This situation is pictured in figure 4.2.9. The dehumidifying period is the "minimum capacity rate" period. The outlet air state from the dehumidification process is given by

$$t_{D,out}^+ = t_{D,out}^*$$

$$w_{D,out}^+ = w_{D,out}^* \qquad (4.2.21)$$

An energy balance on just the dehumidifying period shows the required cooling q_c^+ to be q_c^* (as given by eq (4.2.20)), as the initial and final desiccant states and the inlet and outlet air

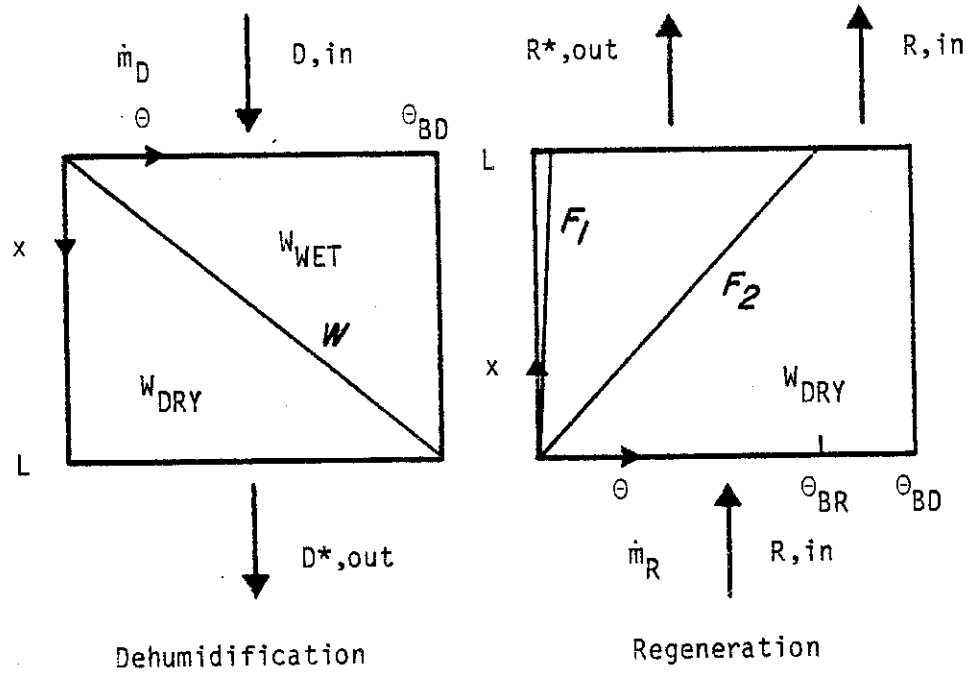

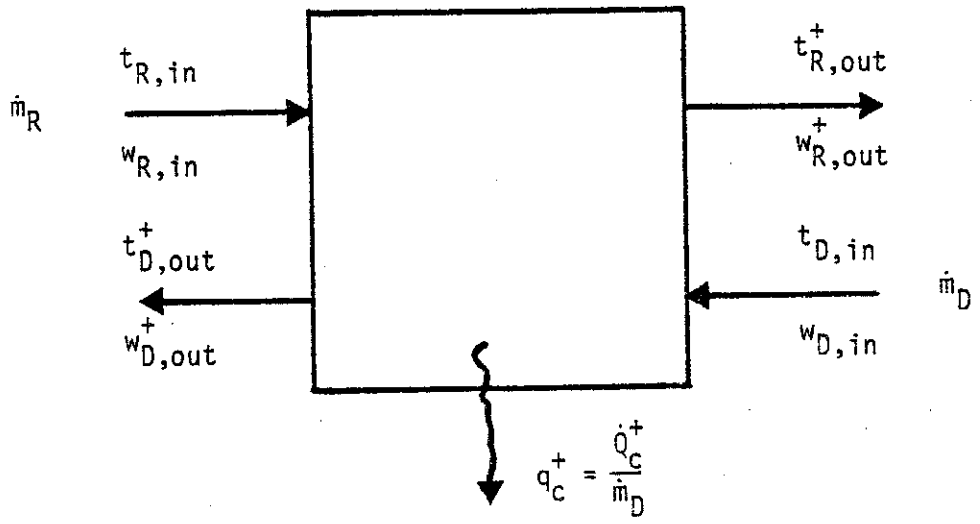

Figure 4.2.9 Wave diagram and control colume for idealized cooled dehumidifier cycle with a flow ratio greater than $(\dot{m}_R/\dot{m}_D)^*$.

states are the same for both cases. The outlet state of the regeneration stream can most easily be found from overall water and energy balances,

$$w^{+}_{R,out} = w_{R,in} - \frac{(\dot{m}_R/\dot{m}_D)^*}{(\dot{m}_R/\dot{m}_D)} (w_{R,in} - w^{*}_{R,out})$$

$$h^{+}_{R,out} = h_{R,in} - \frac{(\dot{m}_R/\dot{m}_D)^*}{(\dot{m}_R/\dot{m}_D)} (h_{R,in} - h^{*}_{R,out})$$

ii) $$\frac{\dot{m}_R}{\dot{m}_D} < \left(\frac{\dot{m}_R}{\dot{m}_D}\right)^* \quad \text{or} \quad \theta_{BD} < \theta_{BR}$$

This situation is pictured in figure 4.2.10. The regeneration period is the "minimum capacity rate" period. The outlet air state from the regenerating period is given by

$$t^{+}_{R,out} = t^{*}_{R,out}$$

$$w^{+}_{R,out} = w^{*}_{R,out}$$

A water balance on the control volume shows the average dehumidifier outlet humidity ratio to be

$$w^{+}_{D,out} = w_{D,in} - \frac{(\dot{m}_R/\dot{m}_D)}{(\dot{m}_R/\dot{m}_D)^*} (w_{D,in} - w^{*}_{D,out}) \qquad (4.2.22)$$

where eq (4.2.19) has been used to convert from θ's to $\dot{m}$'s. The outlet temperature is $t^{*}_{D,out}$ and the cooling required

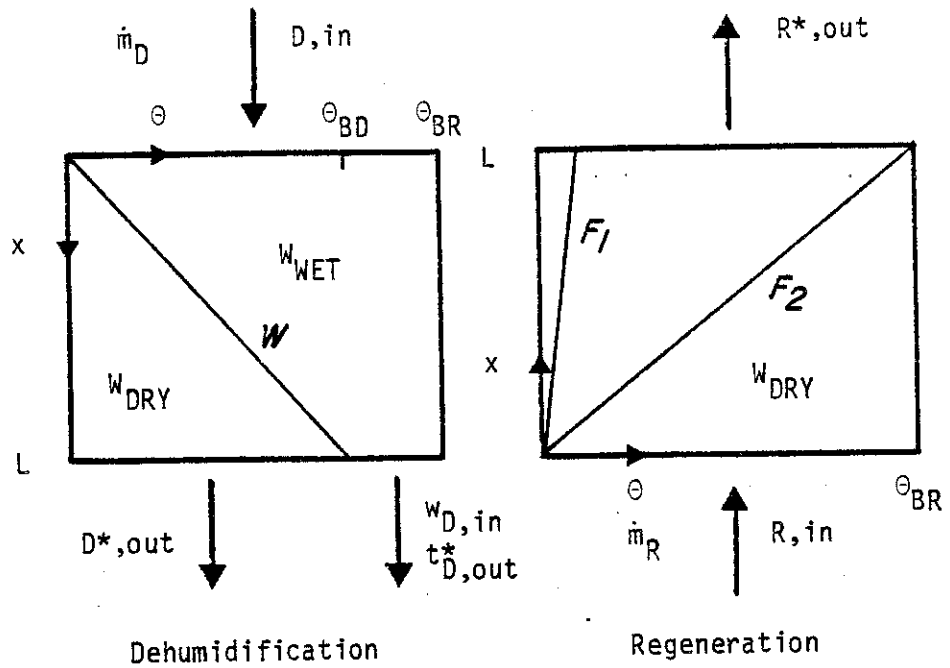

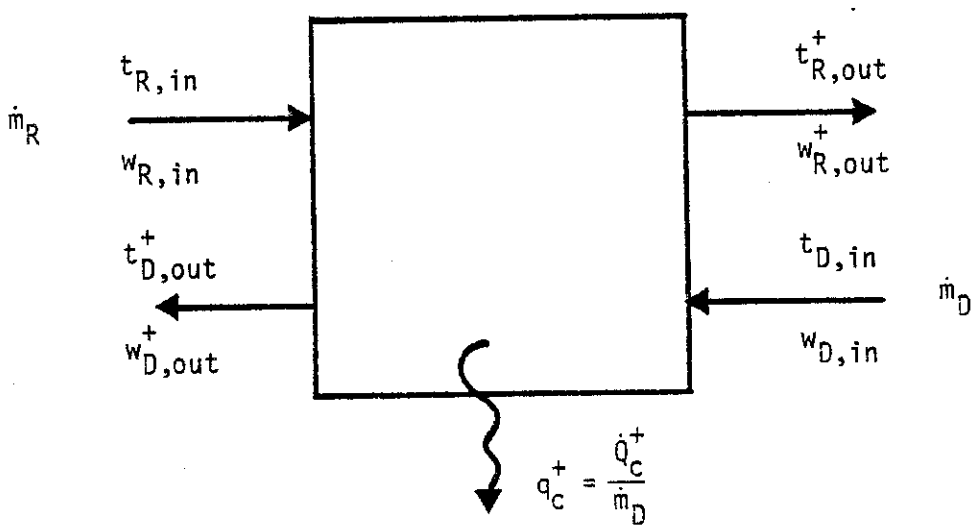

Figure 4.2.10 Wave diagram and control volume for idealized cooled dehumidifier cycle with a flow ratio less than $(\dot{m}_R/\dot{m}_D)^*$.

during dehumidification is determined from an energy balance,

$$q_c^+ = (h_{D,in}^+ - h_{D,out}^+) + \frac{\dot{m}_R}{\dot{m}_D} (h_{R,in} - h_{R,out}^*) \qquad (4.2.23)$$

The air states for these two situations in the idealized dehumidifier are shown on a psychrometric diagram in figure 4.2.11. For case i), figure 4.2.9 shows that for time greater than θ_{BR}, regeneration inlet air passes through the bed without doing anything. This air has been heated at some expense and is lost. System thermal performance is decreased by operating with a flowrate ratio greater than $(\dot{m}_R/\dot{m}_D)^*$. For case ii), figure 4.2.10 shows that moist air is passed on to the rest of the system. The average dehumidifier outlet state is wetter than optimum as shown in figure 4.2.11. Cooling capacity can therefore be significantly decreased by operating the dehumidifier with a flowrate ratio less than $(\dot{m}_R/\dot{m}_D)^*$.

4.3 Non-ideal Cooled Dehumidifier Model

A semi-empirical approach is taken to obtain a model of the non-ideal cooled dehumidifier. The non-idealities of the cooled dehumidifier are lumped into these processes:

i) mass transfer between the air stream and desiccant. This depends significantly on what happens in both the regeneration and dehumidification periods.

ii) heat transfer between the process air stream and the desiccant in the dehumidifying period.

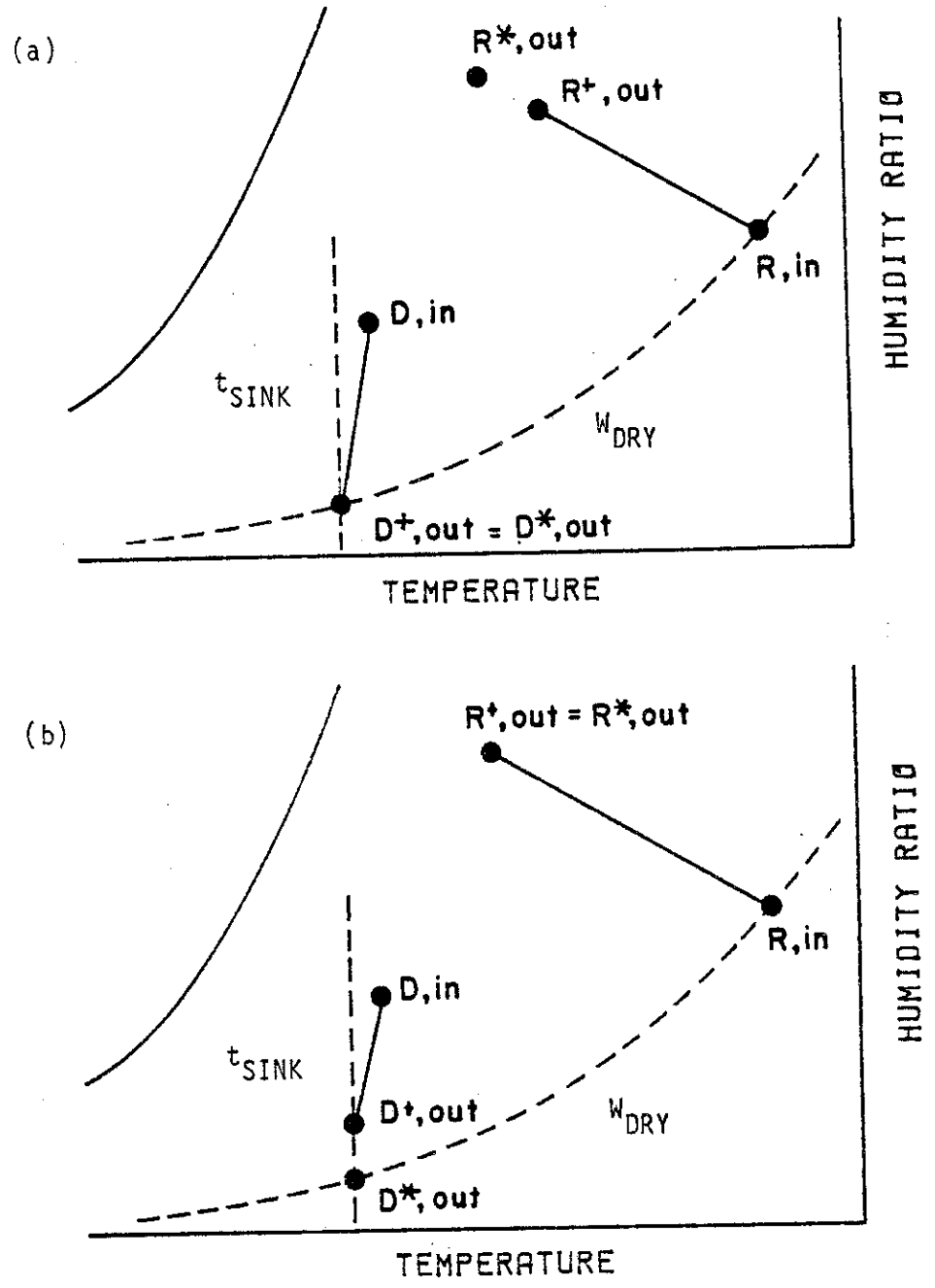

Figure 4.2.11 Psychrometric representation of idealized dehumidifier cycle for

(a) $\dot{m}_R/\dot{m}_D > (\dot{m}_R/\dot{m}_D)^*$ and

(b) $\dot{m}_R/\dot{m}_D < (\dot{m}_R/\dot{m}_D)^*$.

iii) Heat transfer between the bed and the cooling stream in the dehumidifying period. The effects of non-ideal precooling and preheating will also be accounted for here.

4.3.1 Humidity Effectiveness

The non-ideal mass transfer in the dehumidifier can be represented as the ratio of the moisture actually exchanged to the maximum possible. The maximum moisture exchanged is determined as the change in humidity ratio of the "minimum capacity rate" air stream of the idealized dehumidifier. It is convenient to perform the non-ideal calculations in terms of the dehumidifying period air states. The humidity effectiveness of the cooled dehumidifier is then defined as

$$\varepsilon_w = \frac{w_{D,in} - w_{D,out}}{w_{D,in} - w^+_{D,out}} \qquad 0 \leq \varepsilon_w \leq 1 \qquad (4.3.1)$$

where $w^+_{D,out}$ is obtained from eq (4.2.21) or eq (4.2.22) depending on which period is the "minimum capacity rate" period. Figure 4.3.1 shows this effectiveness on a psychrometric chart. The outlet humidity ratio of the regenerating air stream is determined from a water balance on the dehumidifier.

4.3.2 Temperature Effectiveness

The dehumidification process can range from adiabatic (no cooling) to ideal cooling (maintain bed at t_{SINK}). The cooling

process can be viewed as reducing the outlet air temperature from the adiabatic limit toward the sink temperature. The temperature effectiveness is then defined as

$$\varepsilon_t = \frac{t^A_{D,out} - t_{D,out}}{t^A_{D,out} - t_{SINK}} \qquad 0 \leq \varepsilon_t \leq 1 \tag{4.3.2}$$

where $t^A_{D,out}$ is the outlet temperature if the dehumidifier is operated adiabatically,

$$t^A_{D,out} = t(F_{1D}, F_{2R})$$

where

$$F_{1D} = F_1(t_{D,in}, w_{D,in})$$

$$F_{2R} = F_2(t_{R,in}, w_{R,in})$$

This effectiveness is also shown in figure 4.3.1.

4.3.3 Cooling Ratio

For the particular desiccant used in this work, the idealized adiabatic regeneration process is nearly isenthalpic due to the similarity of between F_1 and h lines (see figures 3.1.3 and 4.3.2). Figure 4.3.2 and eq (4.2.23) show that

$$q_c^+ \approx h^A_{D,out} - h^+_{D,out}$$

In section 4.2.3, it was noted that the precooling and preheating processes had no effect on the overall energy balance

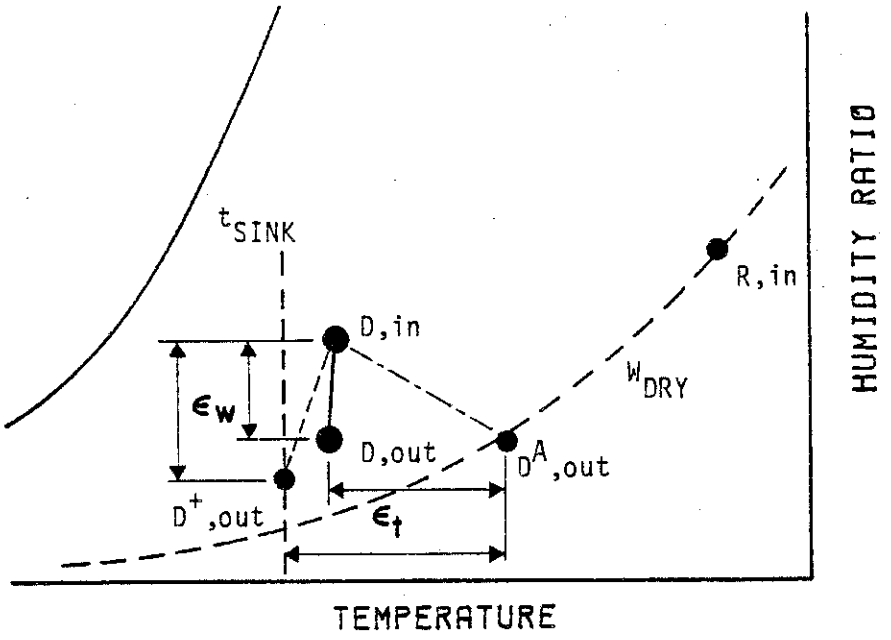

Figure 4.3.1 Cooled dehumidifier humidity and temperature effectiveness.

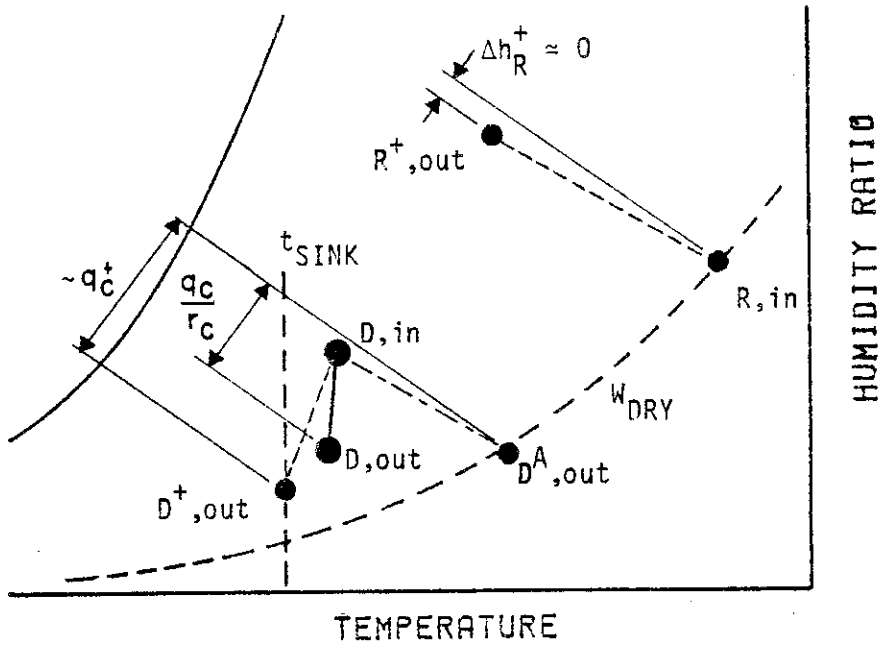

Figure 4.3.2 Cooled dehumidifier cooling ratio.

because the air stream entered and exited from the dehumidifier at the same temperature. In a non-ideal system, this will not be so. The air stream will exit at a higher temperature than it entered, therefore carrying net energy away from the system. The easiest way to handle this is to redefine q_c as the total cooling supplied to the dehumidifier cycle, i.e., the sum of the cooling provided during dehumidification and the cooling done by the precooling/preheating air stream.

A cooling ratio can then be defined as

$$r_c = \frac{q_c}{h^A_{D,out} - h_{D,out}} \qquad (4.3.3)$$

as shown in figure 4.3.2. This ratio contains the effects of non-idealities in the cooling process, the precooling and preheating processes, and the regeneration processes (deviations of the non-ideal outlet state from constant F_1 or h). The cooling ratio defined in this manner works well for dehumidifiers not too close to ideal. As the dehumidifier approaches the ideal, the cooling ratio approaches unity, but in the limit, eq (4.3.3) is not exact.[4]

---

[4] In retrospect, eq (4.3.3) is useful in obtaining a correlation for r_c from data. But a more satisfying definition for use in a model would have been

$$r_c' = \frac{q_c}{q_c^+}$$

The distinction is not that important here but would be when considering a desiccant whose F_1 was less similar to h than here.

4.3.4 Estimates of the Three Non-Ideal Cooled Dehumidifier Parameters

Worek [20] performed experiments on a prototype of a cross-cooled desiccant dehumidifier. The dehumidifier bed consisted of a silica gel-teflon matrix mounted on aluminum sheets put together to form parallel cross-flow channels. The bed was about 0.6 m on each side. The effects of variables such as flow rate, period length, and inlet states on the outlet states of the dehumidifier were investigated. The tests were run by switching a single bed through the cycle described in section 4.1 until periodic steady-state operation was obtained. The inlet and outlet states are reported as functions of time. Estimates are made of the performance of a complete desiccant system by assuming the performance of the other components. A total of 14 test runs are reported. This is a rather limited amount of data and, while it may suggest trends, it is not enough to obtain reasonable estimates of long-term performance.

To obtain estimates of the parameters defined above, the time-averaged inlet and outlet states for each of the runs were determined. Using property data found in ref [21] for the desiccant and a rough estimate of the F_i potentials [22], estimates of the ideal cooled and adiabatic outlet states were obtained and estimates of the parameters were made. The results are shown in table 4.3.1.

While the estimates obtained from the data are fairly rough, they are indicative of the current state-of-the-art

Table 4.3.1

Estimates of Non-Ideal Cooled Dehumidifier Parameters

	current	future	
	(prototype)†	better	best
ε_w	0.5(± .05)	.80	.90
ε_t	0.7(± .02)	.85	.95
r_c	1.2(± .07)	1.10	1.05

†Calculated from IIT data [20].

technology in cooled dehumidifiers. For desiccant systems in general to have any advantage over standard air-conditioning systems, high performance components will be required. For this reason, systems with dehumidifier parameters given by the last two columns of table 4.3.1 will be investigated here. They represent a rather significant improvement in moisture transfer and a moderate improvement in heat transfer.

CHAPTER 5

OPERATING CHARACTERISTICS OF COOLED DEHUMIDIFIER DESICCANT AIR-CONDITIONING SYSTEMS

This chapter presents a description of the steady state operating characteristics of the cooled dehumidifier desiccant air-conditioning systems constructed in chapter 2, with emphasis on the cooled Dunkle cycle. The effects of ambient condition, flow ratio, regeneration temperature, room state, and the level of individual component performance on the thermal performance of the overall system are investigated.

5.1 Measures of System Thermal Performance

The thermal performance of desiccant air-conditioning systems is measured by the amount of cooling that can be produced and the amount of thermal energy consumed in the process. In this chapter, energy quantities will be based on a unit mass flowrate of process stream air, i.e., "specific" quantities.

Figure 5.1.1 is a psychrometric diagram of the operating states of the cooled Dunkle cycle (duplicate of figure 2.4.1). The total specific cooling capacity is given by the enthalpy difference between the room state and the inlet state,

$$q_{cap,T} = h_6 - h_4$$

The thermal energy required to raise the process stream to the regeneration temperature is

$$q'_{th} = h_{11} - h_9 \quad \text{or} \quad q_{th} = \frac{\dot{m}_R}{\dot{m}_D}(h_{11} - h_9) \qquad (5.1.1)$$

where the possibility of unbalanced flow has been allowed for. The thermal coefficient of performance is defined as

$$COP = \frac{q_{cap,T}}{q_{th}}$$

The total cooling capacity has two components. The sensible capacity represents the system's potential for maintaining the room within a comfortable temperature region and is given by

$$q_{cap,S} = c_{air}(t_6 - t_4)$$

The latent capacity represents the system's potential for removing moisture from the room and maintaining a comfortable humidity level. It is given by

$$q_{cap,L} = h_v(w_6 - w_4)$$

where h_v is the enthalpy of the vapor referenced to water at 0°C.

The ratio between the sensible capacity and latent capacity can be controlled by varying the room inlet evaporative cooler (EC_1) outlet state. This can be done by controlling ε_{EC_1} or bypassing part of the air stream around EC_1. The evaporative cooler outlet state has very little effect on the total cooling capacity because the evaporative cooling process is nearly isenthalpic, therefore the sum of the sensible and latent capacities must remain constant as the outlet state of EC_1 is varied.

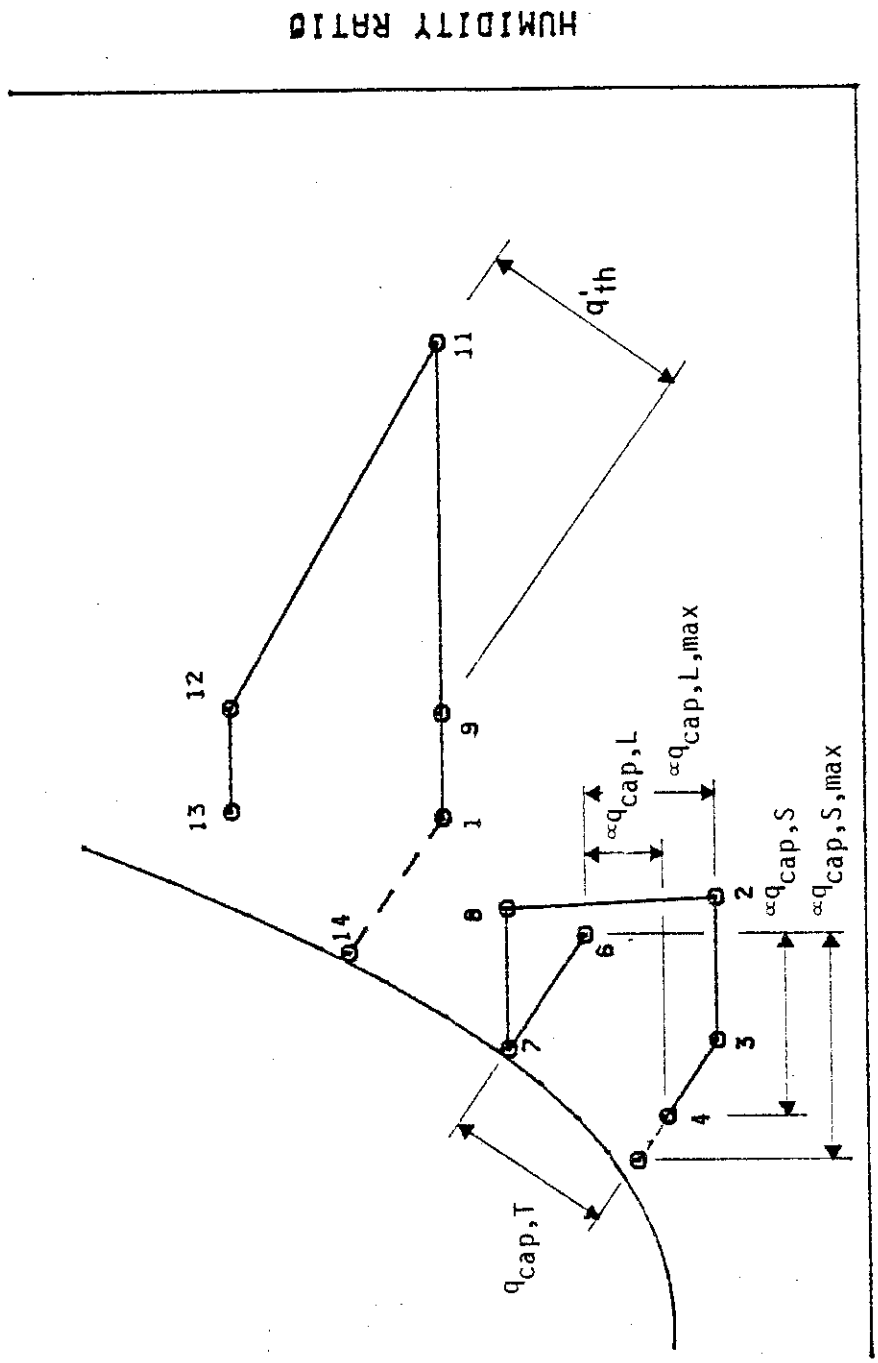

Figure 5.1.1 Measures of thermal performance of the cooled Dunkle cycle.

Control over the ratio of sensible to latent capacity is important in maintaining a comfortable room state. Maximum sensible capacity occurs when EC_1 is operated at its maximum effectiveness. Maximum latent capacity occurs when EC_1 is completely by-passed ($\varepsilon_{EC_1} = 0$)

Other quantities of interest are the energy transfers in the heat exchangers,

$$q_{HX_1} = h_2 - h_3$$

$$q_{HX_2} = \frac{\dot{m}_R}{\dot{m}_D} (h_9 - h_1)$$

Actual energy transfer rates are proportional to the mass flowrate of the process stream,

$$\dot{Q}_i = \dot{m}_D q_i \qquad (5.1.2)$$

Control of the process stream flowrate will then allow the "specific" capacities of the system to be matched to the cooling load. The quantities above are defined similarly for the other systems.

5.2 Characteristics of the Cooled Dunkle Cycle

5.2.1 Effect of Ambient Condition

The effect of ambient condition on the performance of desiccant systems can be conveniently represented on a

psychrometric chart. Figure 5.2.1a shows the effects of ambient condition on the total specific cooling capacity of the cooled Dunkle cycle. The cooling capacity is affected significantly by the level of the ambient humidity ratio and moderately by the temperature. Cooling capacity depends mainly on how much dehumidification is done. Figure 5.2.2a shows that as ambient temperature (1) increases, the sink temperature (14) for the dehumidifier increases, and the dehumidifier outlet state (2) becomes slightly warmer and wetter. Increasing ambient humidity ratio also results in a higher sink temperature, but the increase in regeneration humidity has a larger effect as shown in figure 5.2.2b. The regenerated desiccant moisture content, W_{DRY}, is higher so less dehumidification can be done.

The thermal COP of the cooled Dunkle cycle as a function of ambient condition is shown in figure 5.2.1b. The characteristics depend strongly on the ambient state. In the upper left region of the chart (warm and humid conditions), COP is almost unaffected by the ambient condition. Figures 5.2.1c and 5.2.2 show that the required thermal energy input varies with ambient condition in the same manner and degree as cooling capacity. In this region, HX_2 reduces the thermal energy requirement significantly by reclaiming energy from the regeneration outlet state (12).

In the lower right region of the chart (hot and dry), COP varies strongly with changes in ambient condition. In this region,

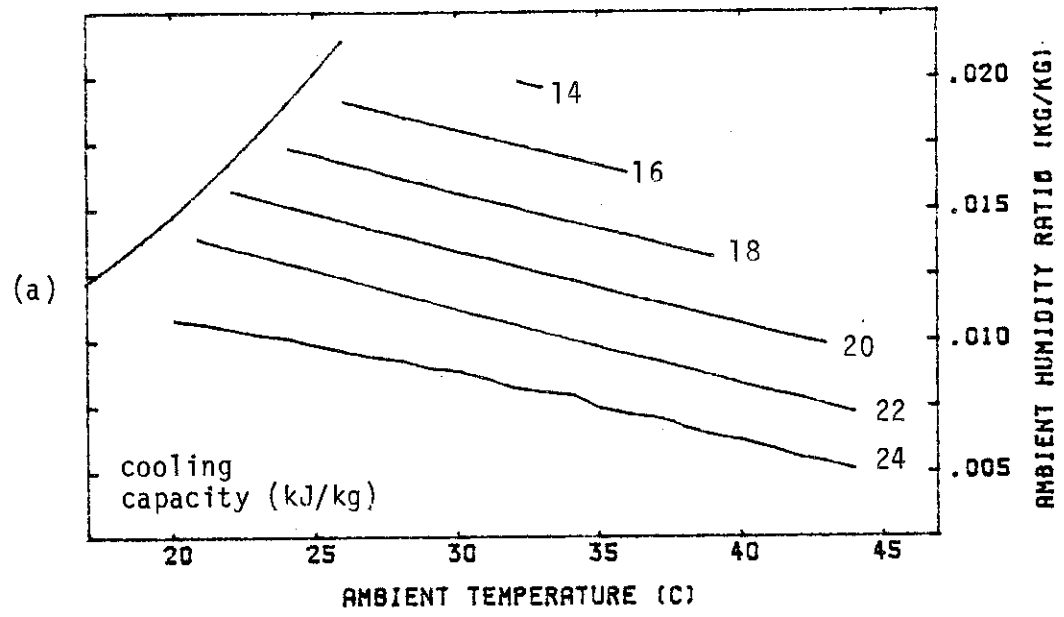

Figure 5.2.1 Effect of ambient condition on cooled Dunkle cycle performance.

$\varepsilon_w = .80$ $\varepsilon_t = .85$ $r_c = 1.10$

$\varepsilon_{EC} = .96$ $\varepsilon_{HX} = .95$ $T_{REG} = 60°C$

$t_{RM} = 25°C$ $w_{RM} = .010$ $\dot{m}_R/\dot{m}_D = 1.0$

(a) total cooling capacity.

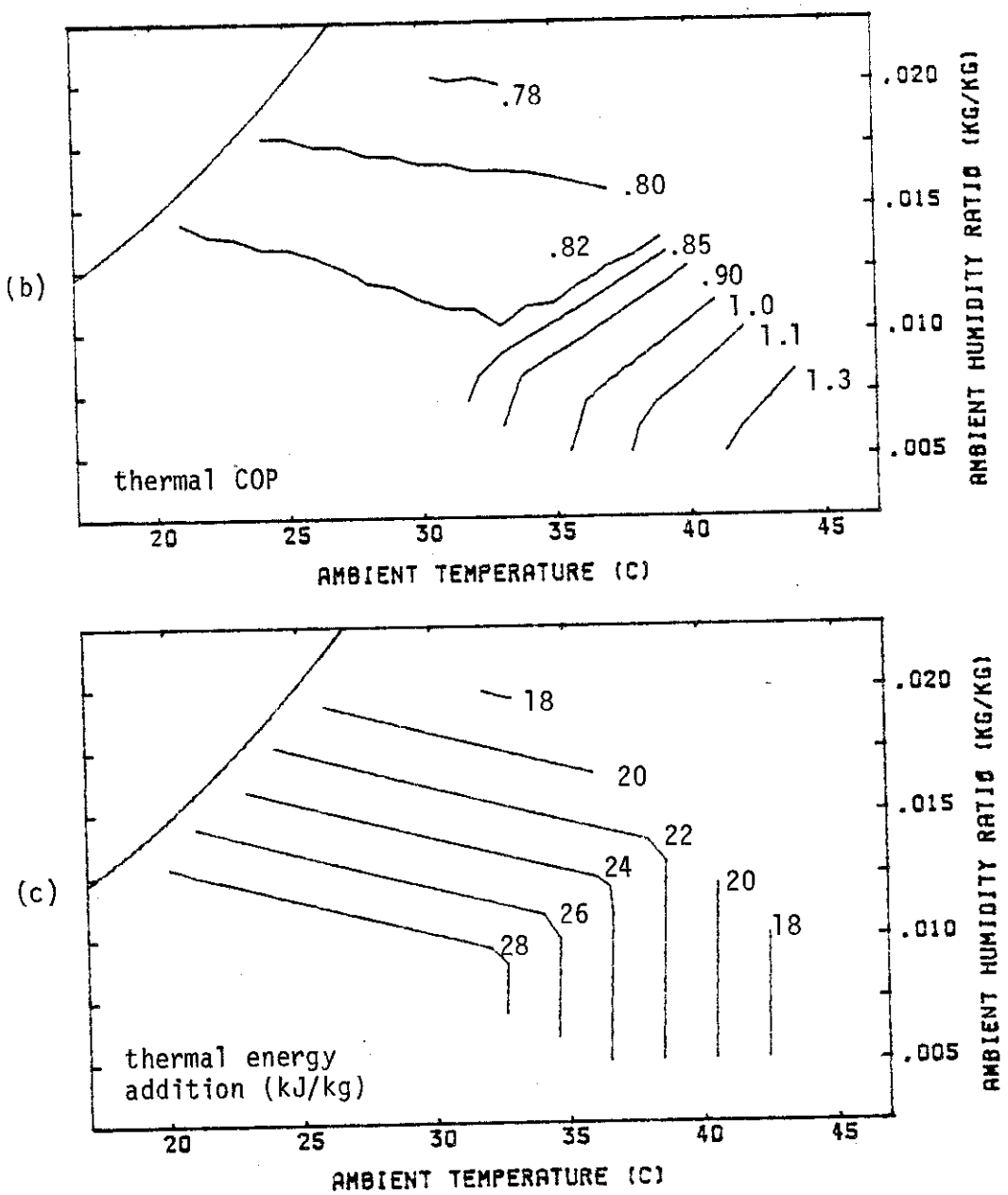

Figure 5.2.1 (cont) (b) thermal coefficient of performance.
(c) required thermal energy addition.

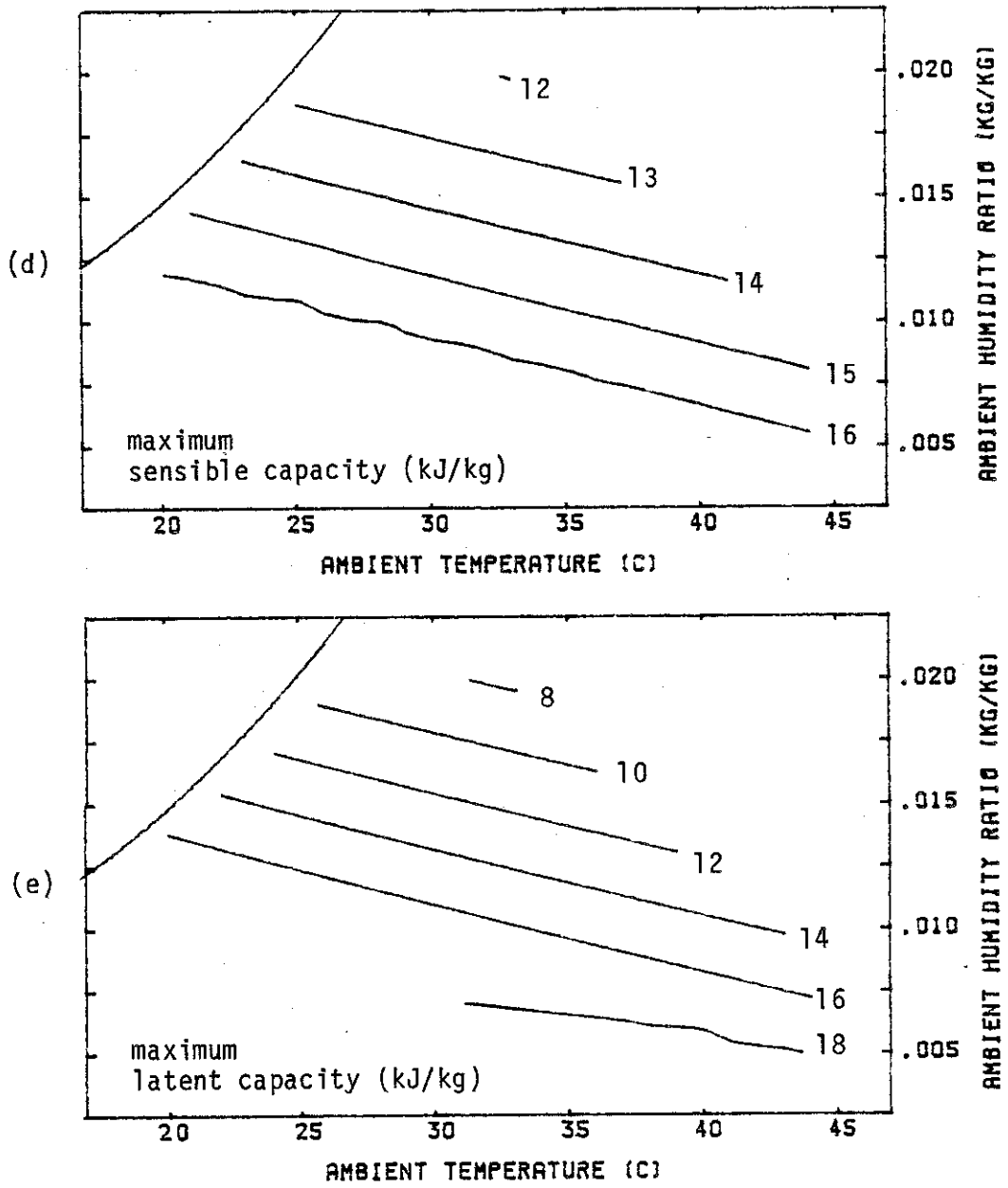

Figure 5.2.1 (cont) (d) maximum sensible cooling capacity.
(e) maximum latent cooling capacity.

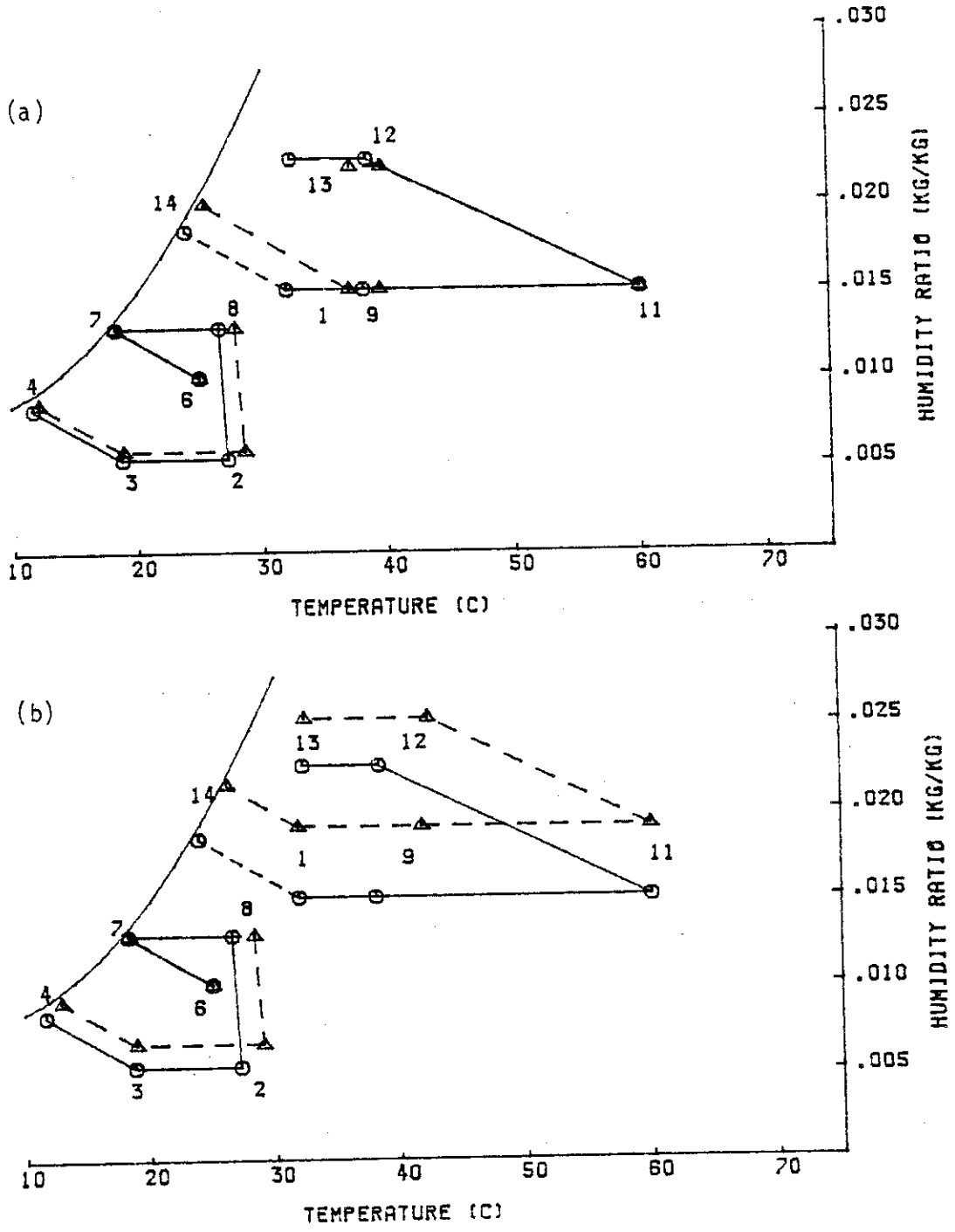

Figure 5.2.2 Cooled Dunkle cycle psychrometric diagram showing effects of (a) ambient temperature and (b) ambient humidity ratio.

the ambient temperature (1) is higher than the regeneration outlet temperature and so HX_2 can not reclaim any useful energy (it is bypassed). The thermal energy input is then given by

$$q_{th} = \frac{\dot{m}_R}{\dot{m}_D} c_{air} (t_{11} - t_1)$$

The change in thermal energy input with ambient temperature is

$$\frac{\Delta q_{th}}{\Delta t_1} = - \frac{\dot{m}_R}{\dot{m}_D} c_{air} \doteq - 1.0 \frac{kJ}{kg - °C}$$

for balanced flow. From figure 5.2.1a, the change in cooling capacity with ambient temperature is found to be

$$\frac{\Delta q_{cap,T}}{\Delta t_1} \doteq - .26 \frac{kJ}{kg - °C}$$

COP increases rapidly as ambient temperature increases because the required thermal energy decreases much more rapidly than cooling capacity. The thermal energy input in this region is only very slightly dependent on ambient humidity, so the variation of COP is due mainly to the humidity effect on cooling capacity.

The effect of ambient condition on the maximum sensible and maximum latent capacities are shown in figure 5.2.1d-e. The variation is the same as total cooling capacity for the same reasons.

5.2.2 Effect of Regeneration/Process Stream Flow Ratio

In the development of the idealized dehumidifier in chapter 4, the flow ratio $(\dot{m}_R/\dot{m}_D)^*$ was defined by eq (4.2.18) to provide equal periods for complete dehumidification and regeneration,

$$\left(\frac{\dot{m}_R}{\dot{m}_D}\right)^* = \frac{w_8 - w_2^*}{w_{12}^* - w_{11}} \qquad (5.2.1)$$

where the subscripts have been changed to those appropriate for the cooled Dunkle cycle. The variation of $(\dot{m}_R/\dot{m}_D)^*$ with ambient conditions is shown in figure 5.2.3a. Figure 5.2.3b shows that as the sink temperature (14) increases with ambient temperature, the idealized dehumidifier outlet state (2^*) becomes slightly wetter as it moves up along W_{DRY}. The regeneration outlet state (12^*) becomes drier because the desiccant moisture content at the end of the dehumidification period is drier (eq (4.2.5)), $W_{WET} = W(t_{14}, w_8)$). State 12* is affected more, so $(\dot{m}_R/\dot{m}_D)^*$ increases with ambient temperature. Increasing ambient humidity ratio produces an additional effect on 12^* and W_{DRY} by raising the regeneration humidity, along with raising the sink temperature.

The consequences of operating the dehumidifier at flow ratios other than $(\dot{m}_R/\dot{m}_D)^*$ were presented in section 4.2.4. Operation with a flow ratio less than $(\dot{m}_R/\dot{m}_D)^*$ results in an idealized dehumidifier outlet state given by eq (4.2.22),

$$w_2^+ = w_8 - \frac{(\dot{m}_R/\dot{m}_D)}{(\dot{m}_R/\dot{m}_D)^*} (w_8 - w_2^*)$$

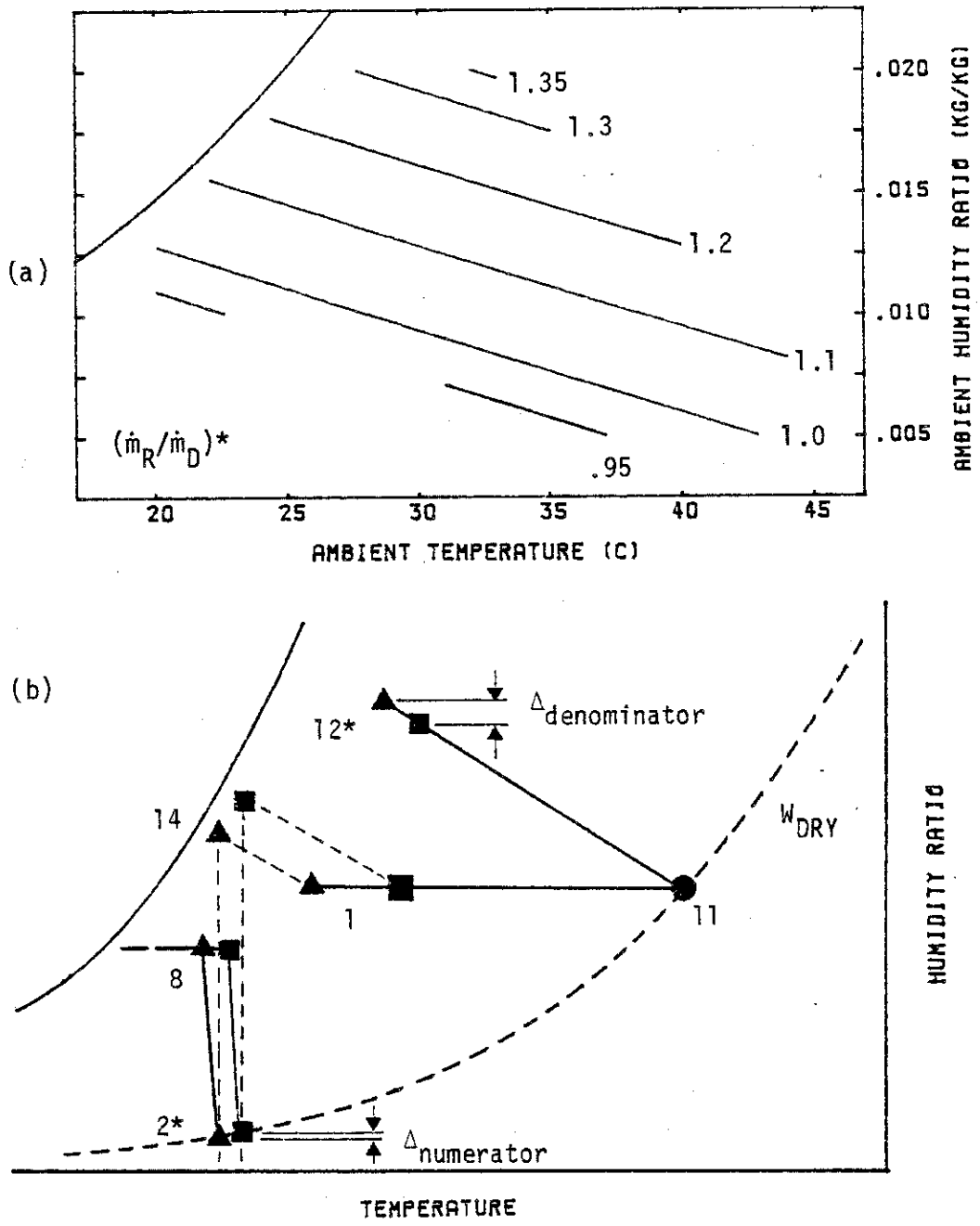

Figure 5.2.3 (a) Variation of $(\dot{m}_R/\dot{m}_D)^*$ with ambient condition for cooled Dunkle cycle (t_{RM} = 25°C w_{RM} = .010 T_{REG} = 60°C).

(b) Effect of ambient temperature on ideal outlet states that influence $(\dot{m}_R/\dot{m}_D)^*$.

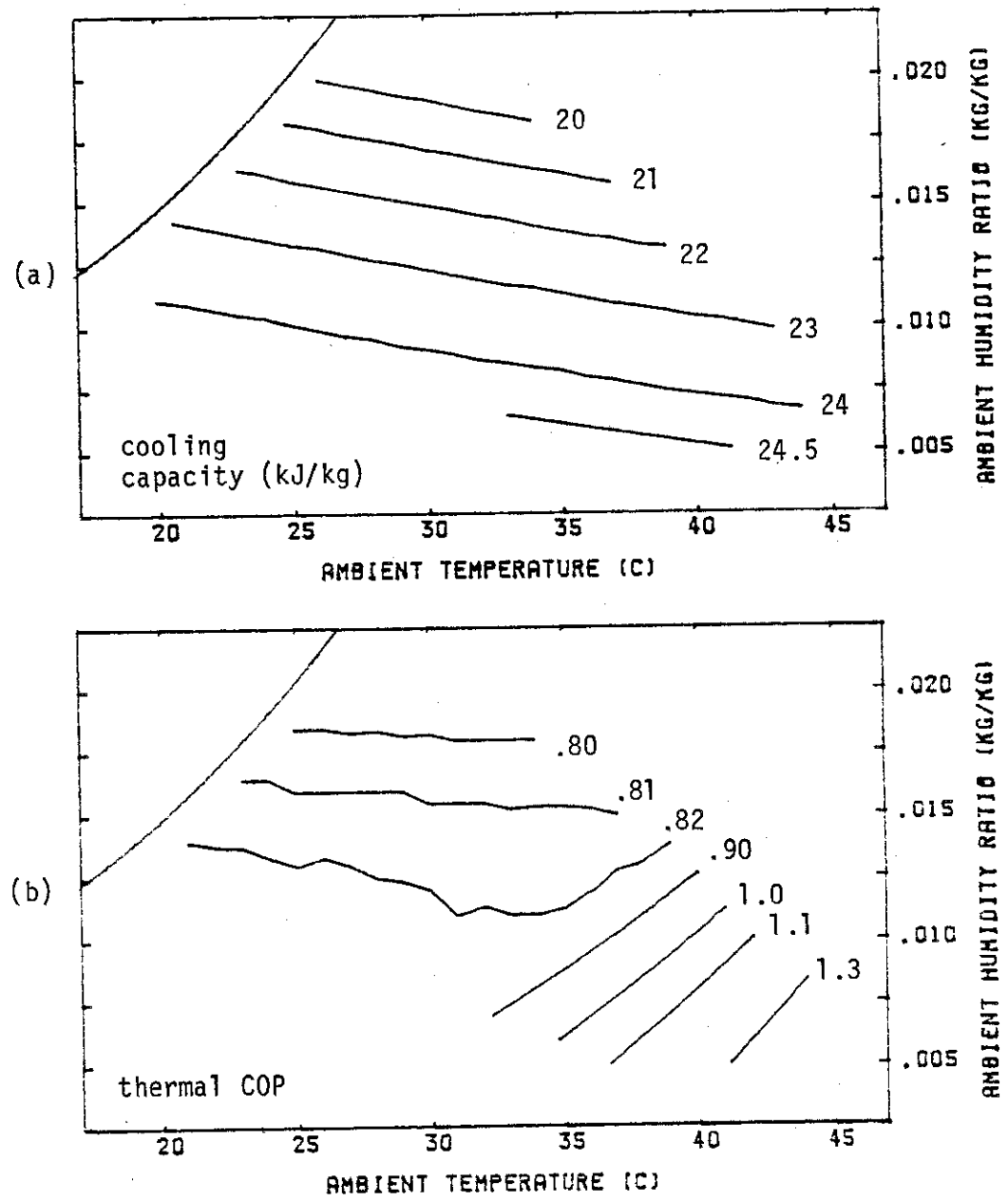

Figure 5.2.4 Performance of cooled Dunkle cycle operated with a flow ratio of $(\dot{m}_R/\dot{m}_D)^*$. (a) specific cooling capacity. (b) thermal COP.

This is the case over most of the range of ambient conditions in figure 5.2.1 ($\dot{m}_R/\dot{m}_D = 1$). The cooling capacities are affected by ambient conditions directly through 2^* and also indirectly through the variation of $(\dot{m}_R/\dot{m}_D)^*$. This causes cooling capacity to decrease more rapidly with ambient condition for a fixed flow ratio than if the flow ratio at each point were adjusted for optimum performance. This can be seen by comparing figures 5.2.4a and 5.2.1a.

Operation at flow ratios less than $(\dot{m}_R/\dot{m}_D)^*$ has little effect on COP as can be seen by comparing figures 5.2.4b and 5.2.1b. The gain in capacity by operating at $(\dot{m}_R/\dot{m}_D)^*$ over a flow ratio less than that is offset by the increased thermal energy requirement due to the higher regeneration flowrate (eq (5.1.1)).

For situations where $(\dot{m}_R/\dot{m}_D)^*$ is less than $\dot{m}_R/\dot{m}_D$, cooling capacity is not affected by the flow ratio because w_2^+ is equal to w_2^* (eq (4.2.21)). Less thermal energy is required, though, because of the lower flow rate in the regenerating stream and so COP is improved. This can be seen by comparing the lower regions of figures 5.2.1b and 5.2.4b.

5.2.3 Effect of Regeneration Temperature

Increasing the regeneration temperature results in increased cooling capacity for the cooled Dunkle cycle as can be seen by comparing figures 5.2.5a and 5.2.1a. As the regeneration temperature is increased, the desiccant is regenerated to a lower moisture content and therefore a drier outlet state can be obtained from the

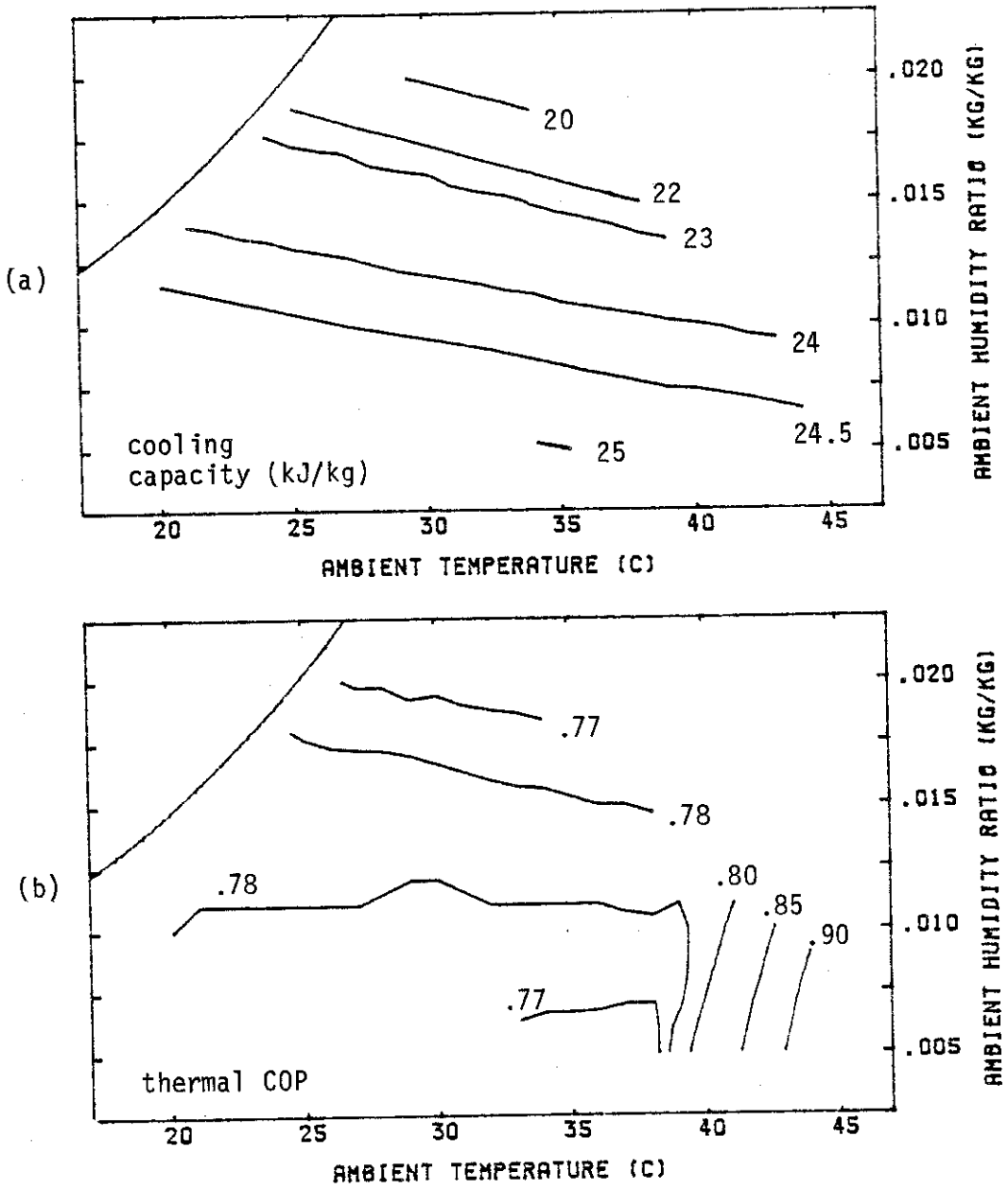

Figure 5.2.5 Performance of cooled Dunkle cycle at a regeneration temperature of 70°C (same operating parameters as figure 5.2.1). (a) specific cooling capacity. (b) thermal COP.

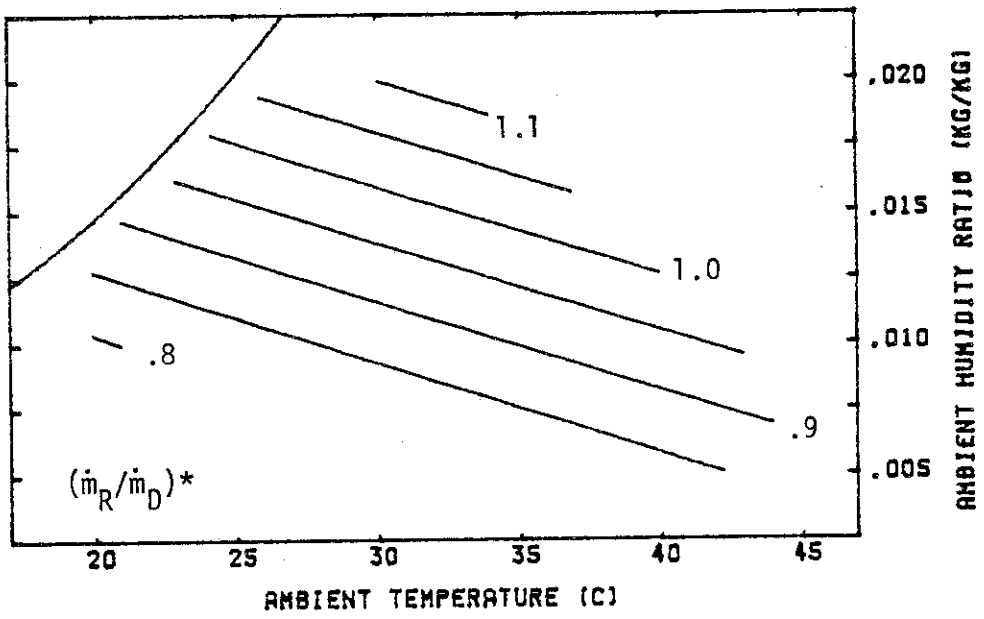

Figure 5.2.6 Cooled Dunkle cycle ideal flow ratio $(m_R/m_D)^*$ at a regeneration temperature of 70°C.

dehumidifier. Because of the shape and spacing of the lines of constant W (figure 2.6.1), larger increments in regeneration temperature are required to provide equal increments in cooling capacity. On the other hand, cooling capacity does not drop rapidly as regeneration temperature is lowered. Finite cooling capacities can be obtained even when regenerating the desiccant with unheated ambient air (infinite thermal COP).

Higher regeneration temperatures require the addition of more thermal energy. Again, because of the shape of the W lines, the increment in thermal energy is larger than the increase in capacity so COP falls with increasing regeneration temperature. This is seen by comparing figures 5.2.5b and 5.2.1b. The range of ambient conditions under which HX_2 is useful is extended because the regeneration outlet state increases. The energy reclaimed by HX_2 helps offset the increased thermal energy requirement in this region, so COP is decreased only slightly.

The effect on $(\dot{m}_R/\dot{m}_D)^*$ of increasing regeneration temperature can be seen by comparing figures 5.2.6 and 5.2.3. The optimum flow ratio is reduced as regeneration temperature increases. Operation with balanced flow is near optimum for the situation in figure 5.2.5. The effects of operation away from $(\dot{m}_R/\dot{m}_D)^*$ are therefore diminished.

5.2.4 Effect of Room State

The effect of the room humidity level on the performance of the cooled Dunkle cycle is shown in figure 5.2.7a. Even though

the drier room state (6) produces a lower dehumidifier outlet humidity (2), the decrease is less than the drop in room humidity and therefore total and maximum latent cooling capacity decrease. The loss in cooling capacity is offset by requiring less thermal energy to reach the regeneration temperature, but COP is decreased slightly. In contrast, the maximum sensible capacity increases as room humidity drops. A lower sink temperature (7) for the heat exchanger and the lower dehumidifier outlet humidity (2) combine to produce a cooler room inlet state (4). This trade-off on sensible capacity and COP will be important in hot and dry climates.

A cooler room state produces the same effects on the cycle state points as does a drier room state as shown in figure 5.2.7b. Again, total cooling capacity and COP are decreased, but sensible capacity decreases and latent capacity increases instead.

The points selected for figure 5.2.7 are representative of those in figure 5.2.1. Table 5.2.1 quantifies the effects of room state on results shown in those figures. The results are influenced by changes in $(\dot{m}_R/\dot{m}_D)^*$ caused by the change in room state. The differences given in table 5.2.1 are fairly constant in the regions where

$$\dot{m}_R/\dot{m}_D > (\dot{m}_R/\dot{m}_D)^*_{RM1} \quad \text{and} \quad (\dot{m}_R/\dot{m}_D)^*_{RM2}$$

$$\dot{m}_R/\dot{m}_D < (\dot{m}_R/\dot{m}_D)^*_{RM1} \quad \text{and} \quad (\dot{m}_R/\dot{m}_D)^*_{RM2}$$

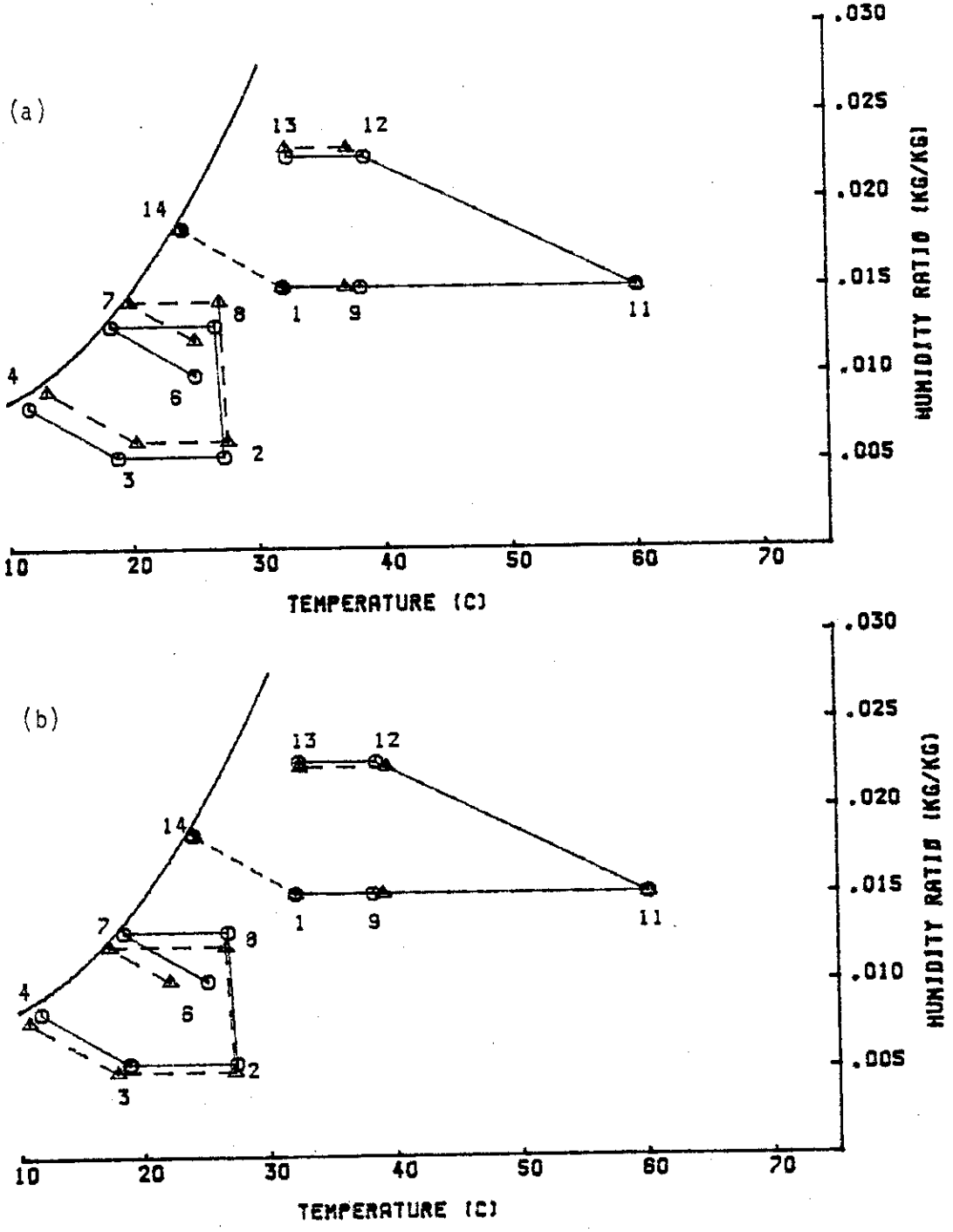

Figure 5.2.7 Effect of (a) room humidity level and (b) room temperature on the performance of the cooled Dunkle cycle.

Table 5.2.1

Change in Performance of the Cooled Dunkle Cycle Shown in Figure 5.2.1 as a Function of Room State

room state	A	B	C
t(°C)	25	25	22
w(kg/kg)	.010	.008	.010

$\Delta X = X_{B \text{ or } C} - X_A$

effect of room humidity (B - A)

	$(\dot{m}_R/\dot{m}_D)^*_A < 1.00$	$(\dot{m}_R/\dot{m}_D)^*_A > 1.06$
$\Delta(\dot{m}_R/\dot{m}_D)^*$	- .06	- .06
$\Delta q_{cap,T}$(kJ/kg)	-2.5	-1.5
$\Delta q_{cap,S,max}$(kJ/kg)	+1.0	+1.5
$\Delta q_{cap,L,max}$(kJ/kg)	-4.5	-3.0
$\Delta COP(HX_2)$	--	- .02
$\Delta COP(\text{no } HX_2)$	-1.2	- .08

effect of room temperature (C - A)

	$(\dot{m}_R/\dot{m}_D)^*_A < 1.00$	$(\dot{m}_R/\dot{m}_D)^*_A > 1.04$
$\Delta(\dot{m}_R/\dot{m}_D)^*$	- .04	- .04
$\Delta q_{cap,T}$(kJ/kg)	-1.6	- .8
$\Delta q_{cap,S,max}$(kJ/kg)	-2.4	-2.1
$\Delta q_{cap,L,max}$(kJ/kg)	+ .4	+1.2
$\Delta COP(HX_2)$	--	- .01
$\Delta COP(\text{no } HX_2)$	- .07	- .04

In the region where

$$(\dot{m}_R/\dot{m}_D)^*_{RM2} < \dot{m}_R/\dot{m}_D < (\dot{m}_R/\dot{m}_D)^*_{RM1}$$

the results vary between the two values given.

5.2.5 Effect of Individual Component Performance on Overall System Performance

A two level, five parameter factorial analysis was performed to examine the effect of the performance of the individual components on the overall system performance. Table 5.2.2 gives the values of the component effectivenesses used. The total cooling capacity and COP at four ambient conditions were determined for each combination of components. The results are given in table 5.2.3.

The inlet evaporative cooler (EC_1) does not have any effect on the total cooling capacity or COP of the cooled Dunkle cycle because the adiabatic saturation process is nearly isenthalpic. Therefore, this component was not included in the analysis. The load outlet evaporative cooler (EC_2) was found to have a negligible effect on overall system performance for the range of effectivenesses used in the analysis. In this range, gains due to lowering the sink temperature for HX_1 by improving EC_2 are offset by the increase in humidity of the process air stream sent to the dehumidifier. For values of ε_{EC_2} less than 0.80, little effect is seen on COP, but cooling capacity decreases significantly.

Table 5.2.3 shows the overall system performance to be most sensitive to the level of performance of the dehumidifier.

Table 5.2.2

Component Effectivenesses Used in Factorial Analysis

	Low	High
Heat Exchangers	.80	.95
Evaporative Coolers	.80	.96
Dehumidifier, ε_w	.70	.80
ε_t	.80	.85
r_c	1.13	1.10

Table 5.2.3

Sensitivity of Cooled Dunkle Cycle Performance

to Individual Component Performance

(The room state was set at 25°C and .010 kg/kg and T_{REG} = 60°C.)

Ambient Temperature (°C)	28	28	33	38
Humidity (kg/kg)	.008	.013	.013	.008
Average Percent Increase in COOLING CAPACITY by Improving Component				
HX_1	4	12	10	8
EC_3	2	4	9	14
DH	17	18	18	18
Average Percent Increase in COP by Improving Component				
HX_1	3	11	8	9
HX_2	3	12	4	-
EC_3	2	2	4	14
DH	7	9	8	18

Cooling capacity is affected largely by the humidity of the dehumidifier outlet state and is therefore linked directly to dehumidifier performance. Clearly, development of a high effectiveness cooled dehumidifier is essential for good system performance.

The influence of the other components varies with ambient condition. As ambient temperature increases, EC_3 can produce a larger cooling effect. As the difference in inlet dry-bulb and wet-bulb temperature increases, the outlet temperature becomes more sensitive to EC_3 performance. As ambient condition increases and the dehumidifier sink temperature rises, so does the dehumidifier outlet temperature. This results in a larger temperature difference across HX_1, the potential for greater heat exchange, and a greater sensitivity to HX_1 performance. The same situation exists in the adiabatic vent and Dunkle cycles. In these systems, large temperature differences exist across the heat exchanger and therefore overall system performance is very sensitive to HX_1 performance, possibly even more so than to dehumidifier performance.

Heat exchanger HX_2 does not affect cooling capacity, only the amount of thermal energy input required. The potential for reclaiming energy from the regeneration outlet state is greater at warm, humid conditions and so HX_2 is more important in this region. For hot, dry ambient conditions where the ambient temperature is greater than the regeneration outlet temperature, HX_2 is not useful. The energy reclaimed by HX_2 provides about

35% of the total thermal energy required at (28°C, 0.18) for a system of high level components, but only 13% at (33°C, 0.13) and 9% at (28°C, .008) which are near the region where HX_2 is not useful (see figure 5.2.1).

5.2.6 Summary of the Characteristics of the Cooled Dunkle Cycle

The effects of the operating conditons on the performance of the cooled Dunkle cycle are as follows:

i) Total, maximum sensible, and maximum latent capacities all decrease with increasing ambient conditions. This is the opposite of how the cooling loads vary with ambient condition. COP tends to decrease with increasing ambient condition except in the region where the ambient temperature is greater than the regeneration outlet temperature (HX_2 not useful). Here, COP increases with ambient temperature.

ii) Cooling capacities can be increased in several ways. The process stream mass flowrate can be increased (eq. 5.1.2). While the thermal performance of the system scales with $\dot{m}_D$, the energy required to push the air through the system (parasitic power) increases. Cooling capacity can be increased without affecting the parasitic power consumption by raising the regeneration temperature, but the thermal COP decreases. For conditions where the operating flow

ratio is less than the optimum $(\dot{m}_R/\dot{m}_D)^*$, capacity can be increased by raising the flow ratio toward $(\dot{m}_R/\dot{m}_D)^*$, but this again entails an increase in parasitic power consumption with little effect on thermal COP. The trade-offs between increasing either the thermal energy input or parasitic power consumption in order to obtain the required cooling capacity will be investigated further in chapter 6.

iii) The thermal COP of the cooled Dunkle cycle improves as the room state is allowed to become warmer and more humid. Total cooling capacity also increases, but sensible capacity decreases as room humidity increases and latent capacity decreases as room temperature increases. The trade-off between sensible capacity and COP as affected by room humidity will be investigated further in chapter 6.

iv) Overall system performance is significantly affected by individual component performance. The performance of the cooled Dunkle cycle is very sensitive to dehumidifier performance. This is in contrast to the adiabatic cycles where heat exchanger performance can be of equal or greater importance.

v) Other effects, such as load-system interaction and the control strategy and a time-varying regeneration temperature (solar system) need also to be accounted

for in determining overall system performance.

5.3 Characteristics of the Cooled Recirculation Cycle

The cooled recirculation cycle is similar in layout to the cooled Dunkle cycle. The only major difference is the placement of evaporative cooler EC_1 and heat exchanger HX_1 (compare figures 2.4.1 and A.2). In the cooled recirc system, they have been removed from the process stream ahead of the dehumidifier inlet and a stream of ambient air is passed through them instead. The result is that the cooled recirc system sends drier air to the dehumidifier which should produce a higher latent capacity. A potential loss in sensible capacity due to using the ambient wet-bulb temperature as the sink for HX_1 rather than the room wet-bulb is a consequence of this however.

The performance of the cooled recirc cycle as a function of ambient condition is shown in figure B.1. The characteristics of the cooled Dunkle and cooled recirc cycles are very similar. The cooled recirc performance varies somewhat more strongly with ambient condition. This is because of the additional effect of ambient condition on the sink for HX_1, along with the effects of changing the sink for the dehumidifier cooling stream and the regeneration humidity as in the cooled Dunkle cycle.

Comparing the total and sensible cooling capacities of the two systems shows the cooled Dunkle cycle to have the advantage over a fairly large range including harsher ambient

conditions where the cooling loads are expected to be high. The cooled recirc cycle has a higher latent cooling capacity because of the drier dehumidifier inlet state, but in chapter 6 a modification to the operation of the cooled Dunkle cycle will be discussed which will increase the latent capacity by sacrificing some of its excess sensible capacity under warm, humid conditions. The higher capacity of the Dunkle cycle would allow the system to meet a larger load than the cooled recirc cycle, or to use a lower regeneration temperature (higher COP) or lower flow rate (lower parasitic power consumption) to meet the same load.

The cooled recirc cycle has a slight advantage in COP over a fairly wide range of conditions, but the largest differences are in regions of mild ambient conditions with small cooling loads. The higher COP of the cooled recirc cycle does not appear to be great enough to significantly offset the potential benefits of the larger cooling capacity available from the cooled Dunkle cycle.

In order to investigate system performance thoroughly, only one of the systems will be investigated. The cooled Dunkle cycle was chosen for the following reasons:

i) similarity in the performance of the cooled Dunkle and cooled recirc cycles with neither showing a clear-cut advantage over the other.

ii) cooled Dunkle cycle cooling capacity advantage at higher ambient conditions where cooling loads will

be higher.

iii) cooled Dunkle cycle performance shows less variation with ambient conditions.

iv) The cooled recirculation cycle has already been investigated to some extent through work at the Illinois Institute of Technology, while the cooled Dunkle cycle has not been looked at.

The general results of the performance of the cooled Dunkle cycle to be presented in chapter 6 should be applicable to the cooled recirc cycle because of the similarities between the two systems shown here. A complete comparison of the total performance of the two systems would require a detailed investigation of the cooled recirc system though.

5.4 Characteristics of the Cooled Ventilation Cycle

The effect of ambient condition on the cooling capacity and COP of the cooled ventilation cycle are shown in figure B.2. The characteristics are somewhat different than for the other two cycles. The cooled vent cycle performance varies more strongly with ambient humidity while being less dependent on ambient temperature. As with the other two cycles, performance is affected by the variation of the sink temperature for the dehumidification process with ambient condition. The strong variation of performance with humidity is due to having ambient air as the input directly to the dehumidifier and the resultant strong variation

of $(\dot{m}_R/\dot{m}_D)^*$. If the system were operated at $(\dot{m}_R/\dot{m}_D)^*$, it is suspected that capacity could be improved significantly at higher humidities, but at the expense of higher parasitic power consumption. Ambient temperature is seen to have relatively little effect on performance because the dehumidifier cooling process is fairly efficient ($\varepsilon_t = .85$) and the dehumidifier outlet state is always near the sink temperature.

Because of the strong variation in performance with ambient condition and the problem of deciding which air stream to use for the regeneration process, the cooled ventilation cycle was not investigated in any more detail. This system does not appear to have any advantage over the other two.

5.5 Comparison of the Characteristics of the Cooled Dunkle with the Adiabatic Dunkle and Ventilation Cycles

Figure B.3 shows the cooling capacity and COP of the Dunkle cycle as a function of ambient condition. The behavior is somewhat similar to the cooled Dunkle cycle, but cooling capacity is significantly lower when operated at the same regeneration temperature. This agrees with the arguments made in sections 2.3 and 2.4.

Figure 5.5.1 presents a comparison of the performance of the cooled and adiabatic Dunkle cycles. The regeneration temperature of each system was chosen to provide a specific cooling capacity of 15.5 kJ/kg[5] at an ambient condition of 35°C

[5] 15.5 kJ/kg = 6.67 Btu/lbm = (400 cfm/ton)$^{-1}$

and 40% rh[6]. The temperatures required were 55°C for the cooled cycle and 70°C for the adiabatic cycle, a difference of 15°C. The room state was set at 25°C and .010 kg/kg. The cooled Dunkle cycle has a larger specific cooling capacity in the region of hot, dry ambient conditions, implying the potential for meeting larger loads or operating at a lower flow rate and less parasitic power consumption. On the other hand, the adiabatic cycle has an advantage in thermal COP.

While figure 5.5.1 is helpful in showing the general trends of the two systems compared, it does not provide the complete picture. The position of the lines dividing the two systems depends on the design conditions chosen. Other effects, such as interactions with a load and/or a solar system are not accounted for either. A more complete comparison, in the form of estimates of long term performance of these systems, is made in chapter 6.

The characteristics of the adiabatic ventilation cycle are shown in figure B.4. Cooling capacity varies with ambient condition in a manner similar to the cooled Dunkle cycle, but, as with the adiabatic Dunkle cycle, capacity is lower when operated at the same regeneration temperature as for the cooled Dunkle cycle.

Figure 5.5.2 shows a comparison between the performance of the cooled Dunkle and adiabatic ventilation cycles. The

---

[6]ARI outdoor design point

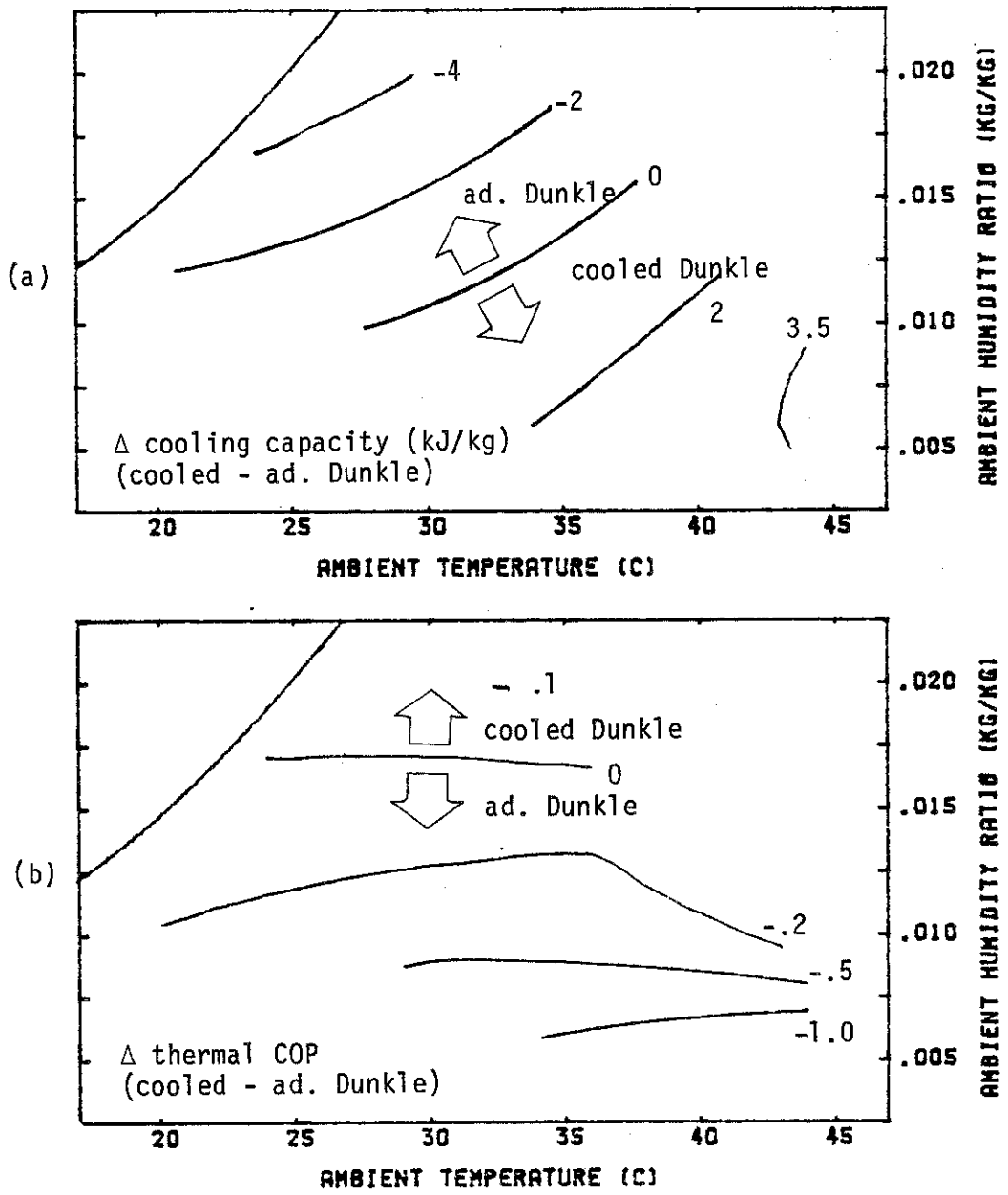

Figure 5.5.1 Difference between performance of cooled Dunkle (T_{REG} = 55°C) and adiabatic Dunkle (T_{REG} = 70°C) cycles. (a) cooling capacity. (b) thermal COP.

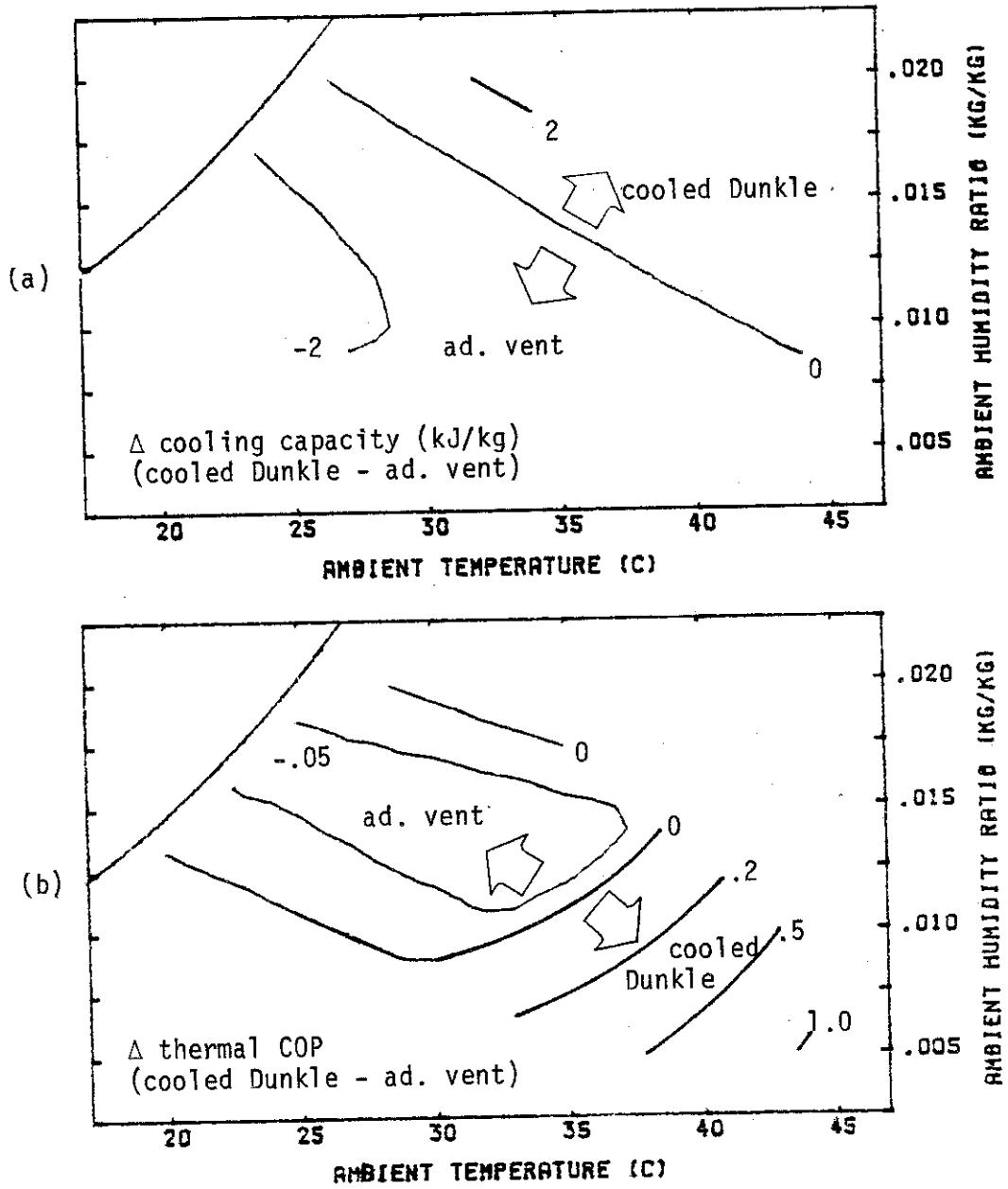

Figure 5.5.2 Difference between performance of cooled Dunkle (T_{REG} = 55°C) and adiabatic vent (T_{REG} = 76°C) cycles. (a) cooling capacity. (b) thermal COP.

results are rather different from the cooled and adiabatic Dunkle comparison. Again, the results are dependent on the design point chosen. A complete comparison accounting for load and solar system interactions is made in chapter 6.

CHAPTER 6

ESTIMATES OF LONG TERM PERFORMANCE OF THE COOLED DUNKLE CYCLE AND COMPARISON WITH ADIABATIC SYSTEMS

A full assessment of the cooled Dunkle cycle requires estimates of long term system performance. These estimates are presented in this chapter. Complete system performance depends on the interaction of the cooling system with the load. A steady state cooling load model is used and a control strategy for the cooled Dunkle cycle operation that attempts to minimize thermal energy consumption is presented. The electrical energy consumed (parasitic power) to move the air stream through the system is estimated. Natural gas and/or solar energy are considered as sources of thermal energy for the regeneration process. With solar energy as a source, the interaction of the desiccant air-conditioning system and the solar energy collection system must be taken into account. The results for the cooled Dunkle cycle are compared with estimates of performance of the adiabatic ventilation and Dunkle cycles obtained from models by Jurinak [6,22].

6.1 Additional Component Models

6.1.1 Cooling Load Model

The cooling load model used in this work is the same as

that used by Jurinak [6] in his investigation of the adiabatic desiccant air-conditioning systems. The load is assumed to have zero thermal and moisture capacitance and is therefore only a function of ambient condition and room state. The room state is maintained at a fixed set point.

With zero thermal capacitance, the sensible portion of the cooling load is given by

$$\dot{Q}_{load,S} = UA(t_{amb} - t_{rm}) + \dot{m}_{inf} c_{air}(t_{amb} - t_{rm}) + \dot{Q}_{gen} \qquad (6.1.1)$$

where the first term represents the heat gains through the building shell, the second is due to infiltration, and the third is the gain from energy sources within the room. The latent load is calculated from

$$\dot{Q}_{load,L} = (\dot{m}_{inf}(w_{amb} - w_{rm}) + \dot{M}_{gen})h_v \qquad (6.1.2)$$

where the first term is the moisture gain due to infiltration and the second is the water vapor generated within the space. The energy contained in the vapor is the enthalpy of the vapor, h_v, referenced to water at 0°C. The total cooling load is the sum of the sensible and latent parts,

$$\dot{Q}_{load,T} = \dot{Q}_{load,S} + \dot{Q}_{load,L} \qquad (6.1.3)$$

The control strategy employed does not allow for heating or humidification. If either the sensible or latent load is negative when calculated at the set room condition, the appropriate room condition is found to make that part of the load zero, and the room state is reset.

The values of the load parameters used in this work and the design point loads that result are shown in table 6.1.1.

The ratio of latent load to sensible load can be represented on a psychrometric chart by a line through the room state with a slope given by

$$\frac{\Delta w}{\Delta t} = \frac{c_{air}}{h_v} \frac{\dot{Q}_{load,L}}{\dot{Q}_{load,S}}$$

This is called the load line. In order to meet the load exactly and maintain the set room state, the conditioned inlet state must lie somewhere along the load line. The mass flowrate of conditioned air required to meet the cooling load is given by

$$\dot{m}_L = \frac{\dot{Q}_{load,T}}{h_{rm} - h_{in}} \qquad (6.1.4)$$

Several potential combinations of load lines and inlet states are shown in figure 6.1.1b for the cooled Dunkle cycle (see figure 2.4.2 for complete system). It was noted in section 5.1 that the ratio of latent to sensible capacity can be controlled by varying the effectiveness of the inlet evaporative cooler (EC_1). This is how the inlet state for case A is obtained.

Table 6.1.1

Load Parameter Values and Design Loads

Load Parameters

$UA = 1000$ watts/°C

$\dot{m}_{inf} = .0766$ kg/sec $= 275$ kg/hr

$\dot{Q}_{gen} = 750$ watts

$\dot{M}_{gen} = 0.0014$ kg/sec $= 0.5$ kg/hr

Design Loads at 5% Design Point (room state: 25°C, .010 kg/kg)

Location	Miami, FL	Phoeniz, AZ	Columbia, MO
t_{amb}(°C)	31.	40.5	33
w_{amb}(kg/kg)	.0176	.0084	.0134
$\dot{Q}_{load,T}$(watts)	9130	17,460	10,400
$\dot{Q}_{load,S}$(watts)	7290	17,460	9,380
$\dot{Q}_{load,L}$(watts)	1840	~0	1,020
$\dot{Q}_{load,L}/\dot{Q}_{load,S}$	.25	~0	.11
$\dot{Q}_{load,T}$(tons)	2.6	5.0	3.0

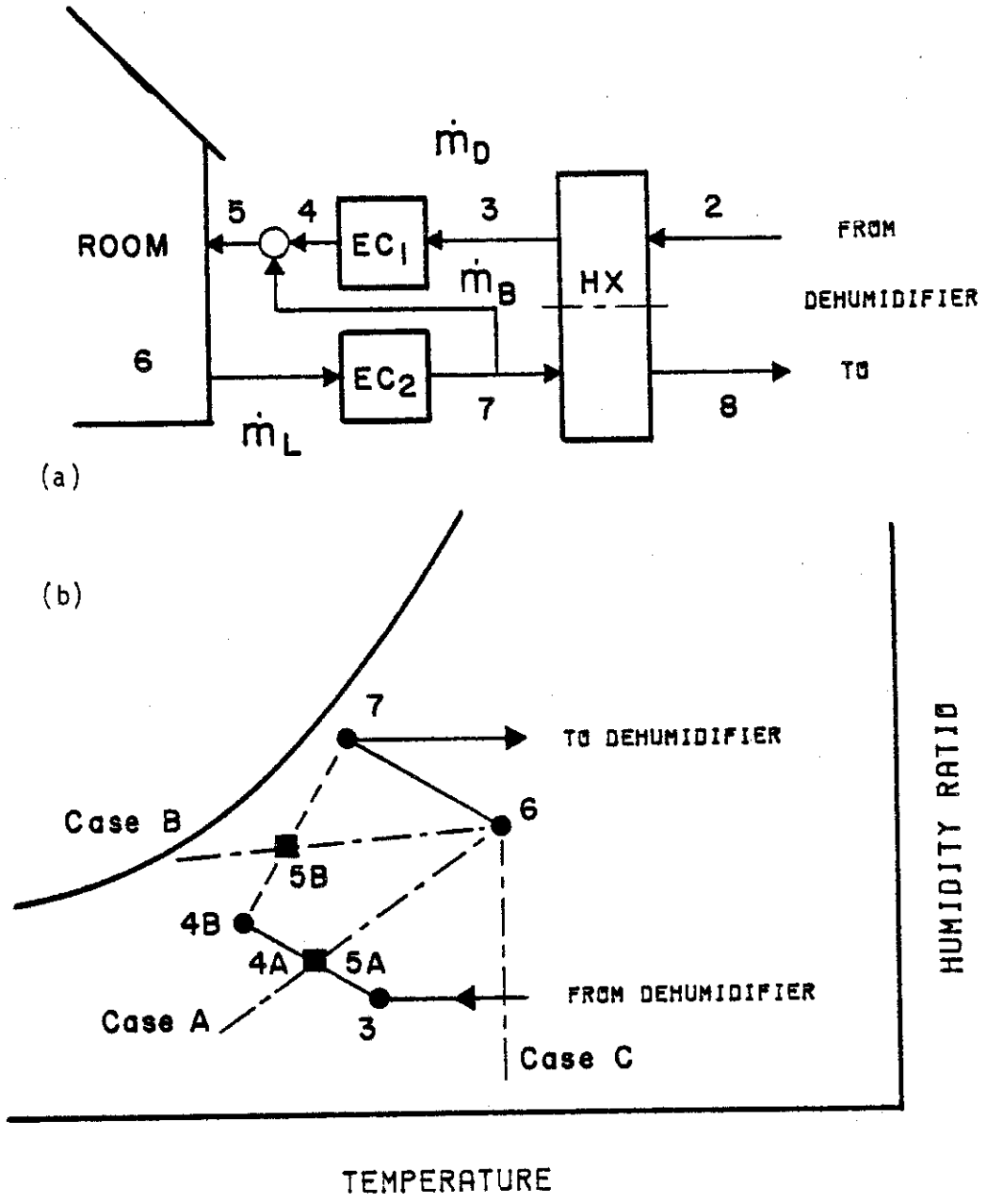

Figure 6.1.1 Load line -- inlet state combinations. (a) system diagram showing by-pass mixing and flow-rates. (b) psychrometric diagram for three cases.

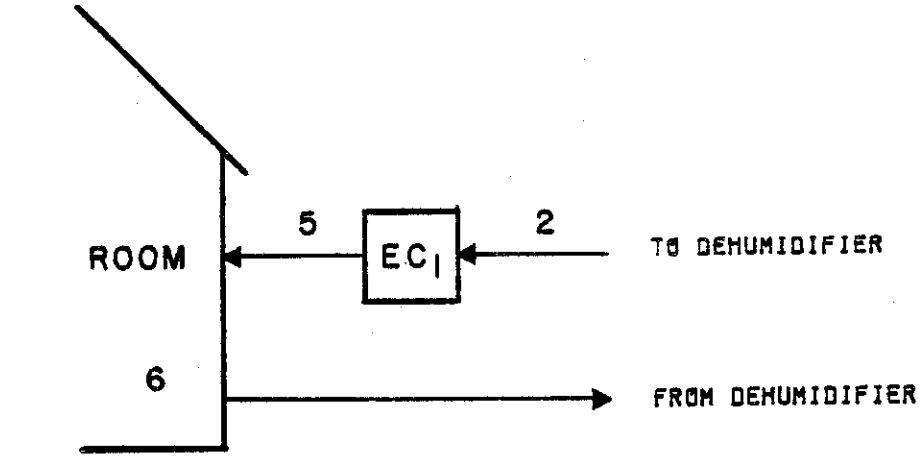

(c)

(d)

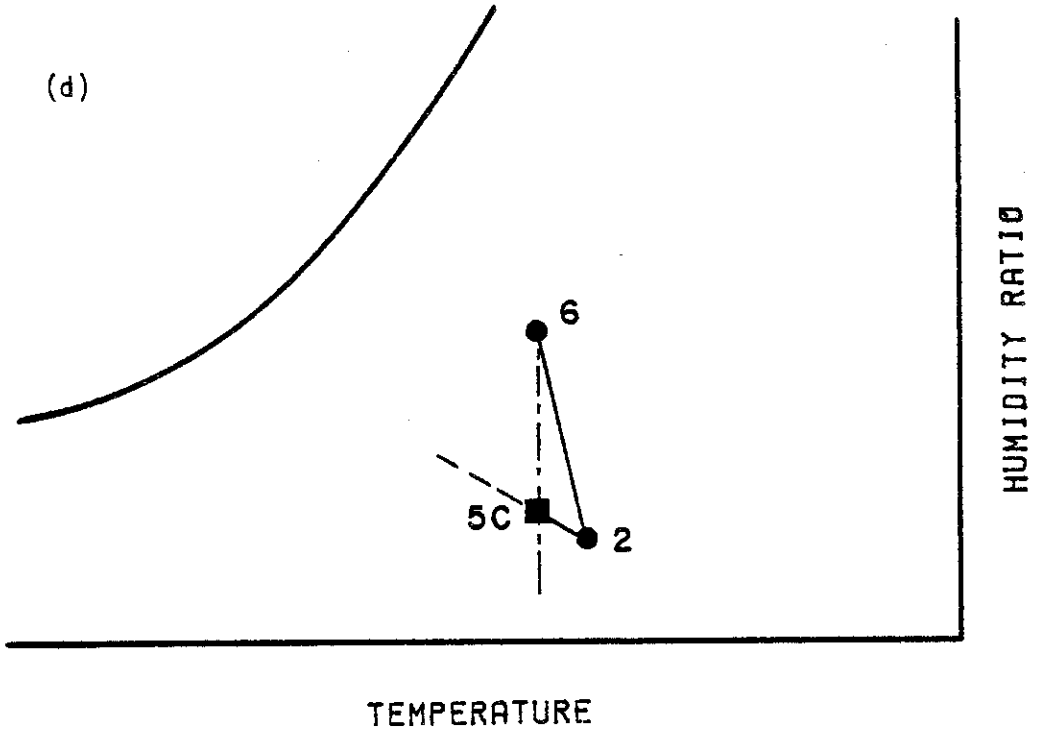

Figure 6.1.1 (cont) (c) system diagram for case C. (d) psychrometric diagram for case C.

In this case, $\dot{m}_D$ is equal to $\dot{m}_L$.

In case B, the outlet state of EC_1 (4B) has excess latent capacity. By mixing air from state 4B and state 7, an inlet state (5B) with the proper proportion of latent to sensible capacity can be obtained. The flowrates shown in figure 6.1.1 are given by

$$\frac{\dot{m}_B}{\dot{m}_L} = \frac{h_{5B} - h_{4B}}{h_7 - h_{4B}} \quad \text{and} \quad \frac{\dot{m}_D}{\dot{m}_L} = 1 - \frac{\dot{m}_B}{\dot{m}_L}$$

where $\dot{m}_L$ is found from eq (6.1.4). This by-pass mixing has several advantages. It allows the room inlet state to be controlled in order to maintain a set room state. It does not affect the thermal COP of the system (a result of the evaporative cooling process being nearly isenthalpic). It can result in a lower flowrate ($\dot{m}_D$) through the rest of the system and therefore less parasitic power consumption. A serious disadvantage to by-pass mixing is that significant sensible cooling capacity can be destroyed.

In case C, the system has excess sensible capacity which is generated by EC_2 and HX_1. The excess sensible capacity can be eliminated by by-passing EC_2 and HX_1, sending room air directly to the dehumidifier as shown in figure 6.1.1c-d. The effectiveness of EC_1 is controlled to obtain state 5 as in case A above. An added benefit is the potential for increased latent capacity by sending drier air to the dehumidifier.

Similar cases occur for the other desiccant dehumidifier air-conditioning systems, both cooled and adiabatic. Controlling

the conditioned inlet state is essential to maintaining a comfortable room state.

6.1.2 Solar Energy Collection and Storage System Model

Silica-gel dehumidifier air-conditioning systems can use thermal energy at temperatures ranging from 50-90°C. Temperatures in this range can be obtained from flat plate type solar collectors. The collector/storage model used in this work is the same as that used by Jurinak [6]. The describing parameters are given in table 6.1.2. They are representative of an air based collector with two covers and a selective surface with pebble bed storage. The collector array is rather large (50 m^2) and may not be the economically optimum size, but it is used in an attempt to provide as much of the thermal energy required by the desiccant system as possible.

The collector/storage system is coupled directly to the desiccant system in series with the auxiliary energy source, a natural gas furnace. The system operates whenever there is useful solar radiation available. The air delivered from the solar system to the desiccant system is used as the regenerating air stream if the temperature is high enough so that the cooling load can be met. If not, auxiliary energy is added.

6.1.3 Component Pressure Drops and Parasitic Power Consumption

Estimates of the pressure drops through the components

Table 6.1.2

Solar Energy Collection And Storage System

Collector	
area (m^2)	50
$F_R(\tau\alpha)$	0.49
$F_R U_L$ (watts/m^2 - °C)	2.85
flowrate	$\dot{m}_{L,max}$
slope	latitude
Storage	
volume (m^3)	12.5
apparent pebble density (kJ/m^3)	1600
thermal capacitance (kJ/kg - °C)	0.84
losses	0
nodes	5

were taken from Jurinak [7] and are shown in table 6.1.3. The design flowrates are not the same as in ref [7], but the values used result in good agreement between estimates of ventilation cycle performance arrived at here and in ref [7].

In order to reduce parasitic power consumption, it is assumed that the components are designed for laminar flow. The pressure drop through a component i at a flowrate other than the design value is given by

$$\Delta P_i = \frac{\dot{m}_i}{\dot{m}_{i,design}} \Delta P_{i,design}$$

The fan power required to blow the air through the component is then

$$\dot{Q}_{fan,i} = \dot{m}_i \frac{\Delta P_i}{\rho \eta_{fan}} = \frac{\Delta P_{i,design}}{\rho \eta_{fan} \dot{m}_{i,design}} \cdot \dot{m}_i^2 \qquad (6.1.5)$$

6.1.4 Control Strategy for Desiccant System Operation

The control strategy for desiccant system operation used in this work attempts to minimize the amount of purchased thermal energy that is consumed. As noted in section 2.1, under certain ambient conditions simple regenerative evaporative cooling can be used to meet the cooling load. This mode of operation does not require any thermal energy input and so is preferable to desiccant system operation if sufficient cooling capacity is available. In section 5.2.3, it was noted that finite cooling capacities can

Table 6.1.3

Component Pressure Drops and Parasitic Power Consumption

Component	Design Pressure Drop (Pa)	Design Flowrate (kg/sec)
Heat Exchangers (both sides)	125	0.50
Evaporative Coolers	100	0.50
Dehumidifiers		
process side[7]	125	0.50
regeneration side[7]	125	0.50
cooling stream[8]	100	0.50
purge stream[8]	62.5	0.50
Duct Losses	100	0.50
Collector	200	1.00
Pebble Bed	62.5	1.00
Fan Efficiency	50%	
Other Losses	100 watts	

[7] split to allow for unbalanced flow calculations

[8] cooled dehumidifier only

be produced by the cooled Dunkle cycle while regenerating with unheated ambient air, again preferable if sufficient capacity is available.

Table 6.1.4 gives the hierachy of desiccant system operating modes used to meet the cooling load. The lowest mode of operation in which the cooling load can be met completely is used. If the cooling load can not be met completely by the desiccant system, the remainder is assumed to be met by some auxiliary cooling source. Modes 5 and 6 are necessary because the load model requires that the room state be maintained at the set point. In an actual system, this back up would not be present and the room state would tend to float. The effect of modes 5 and 6 will be reduced here by considering only systems and system operation in which more than 95% of the cooling load is met by the desiccant system.

Figure 6.1.2 shows the operating mode of the cooled Dunkle cycle as a function of ambient condition for a particular set of operating parameters. The ranges of modes 1,2, and 4 are limited by the cooling capacity that can be produced. As discussed in chapter 5, cooling capacity can be increased by increasing the flowrate of air through the system. This would extend the ranges of modes 1,2, and 4. The range of mode 4 can also be extended by raising the regeneration temperature as noted in section 5.2.3.

This control strategy, while attempting to minimize the consumption of purchased thermal energy, may not minimize total

Table 6.1.4

Modes of Operation of Desiccant Air-Conditioning Systems

Mode of Operation	Description
0	no cooling load, system off
1	regenerative evaporative cooling
2	desiccant cooling, regenerate with ambient air
3	desiccant cooling, regenerate with solar (if available)
4	mode 3 plus auxiliary thermal energy
5	mode 4 plus auxiliary cooling (desiccant system can not meet all of the load)
6	desiccant system can meet none of cooling load, all met by auxiliary cooling

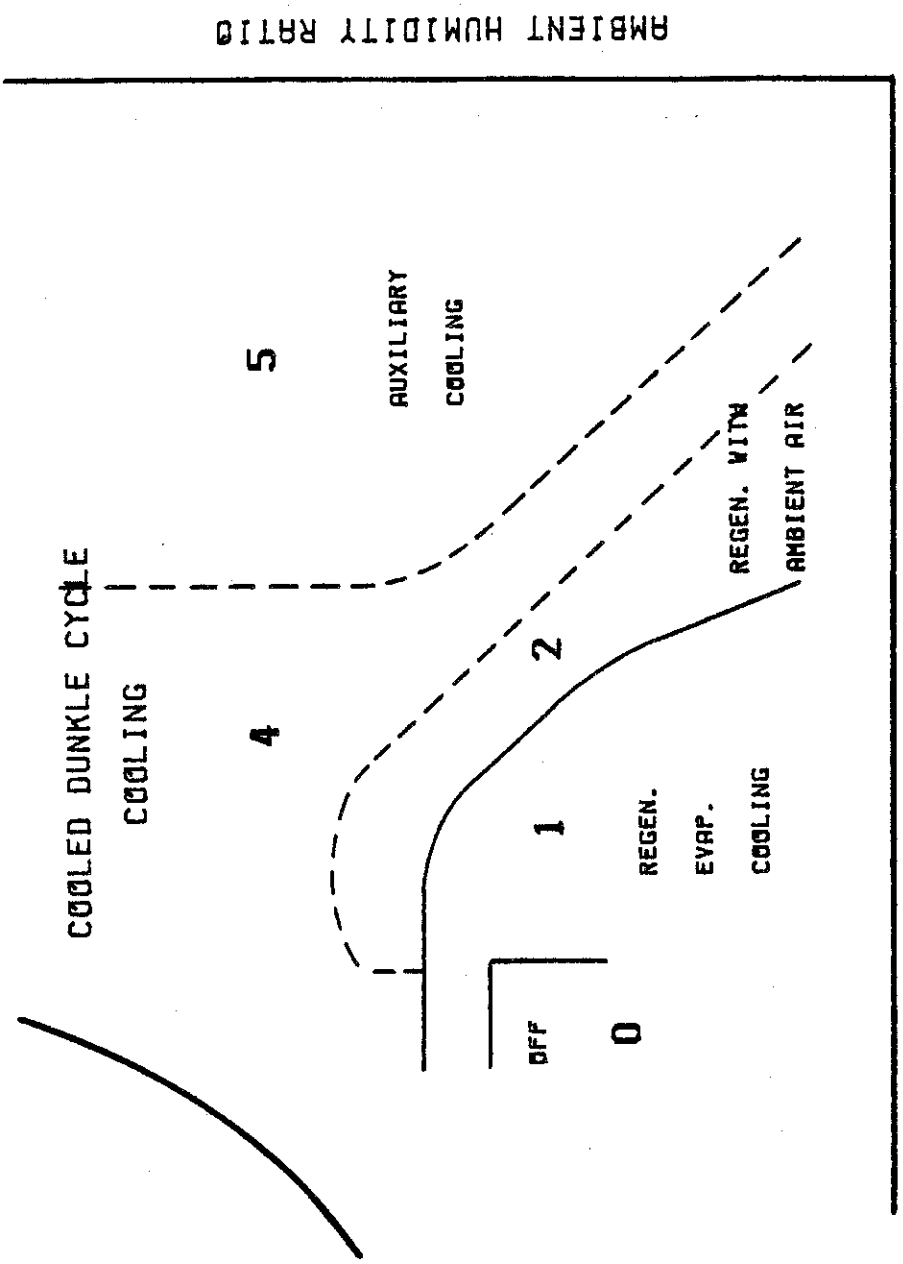

Figure 6.1.2 Effects of ambient condition on mode of operation of the cooled Dunkle cycle.

energy consumption or operating costs because the trade-off's between thermal performance and parasitic power consumption have not been accounted for. More sophisticated control strategies can be developed, but these would be difficult to implement in an actual system.

6.2 Methods of Obtaining Estimates of System Performance

Two methods will be used in this work to obtain estimates of the long term performance of the cooled Dunkle cycle from computer models. For gas-fired operation, the bin data method will be used. For solar-fired operation, performance will be estimated from hour-by-hour simulations of system operation.

6.2.1 Bin Data Method

For gas-fired operation, all of the component models involved are based on steady state operation. Desiccant system performance is then a function of only ambient condition for a set of fixed operating parameters.

In the bin method, the range of ambient conditions encountered at a particular location is divided into a set of bins of a certain temperature and humidity size and the number of hours of occurence of conditions within each bin is found. Long term system performance estimates are then obtained by calculating the performance at each of the bin centers and weighting the results by the number of hours in each bin.

where the fraction of the thermal energy input that is supplied by the solar system is given as

$$f_{SOL} = \frac{\text{thermal energy from solar}}{\text{total thermal energy input}} \qquad (6.2.6)$$

The electric COP (COP_e) is defined as in eq (6.2.3). These measures are also applicable to the step by step performance calculations.

6.3 Economic Considerations

The performance measures defined in section 6.2 have all dealt with the comparison of energy quantities. For example, comparing COP_{th} and COP_e provides a measure of the relative consumption of thermal and electrical energy consumed by the system. A comparison of this sort may not be entirely meaningful because the costs of the two energy types can be very different and the operating costs of the system are more important to the owner than the relative energy quantities.

To provide a measure of the operating energy costs of the desiccant systems, a cost ratio is defined,

$$CR = \frac{Q_a P_a + Q_e P_e}{Q_{vc} P_e} \qquad (6.3.1)$$

The numerator represents the operating cost of the desiccant system where

Q_a = total purchased thermal energy input

Q_e = total electric energy consumed

P_a = price of a unit of thermal auxiliary energy

P_e = price of a unit of electrical energy

The desiccant system operating cost has been normalized by dividing by the cost of operating a standard vapor compression cooling system where Q_{vc} is the electrical energy consumed by the vapor compression system. Eq (6.3.1) can be rearranged to

$$CR = \frac{Q_e + \frac{Q_a}{(P_e/P_a)}}{Q_{vc}} \qquad (6.3.2)$$

where CR is seen to be a function of the ratio of the costs of electrical to thermal energy. Two values of this ratio will be considered in this work:

i) $P_e/P_a = 3.5$ This is representative of the prices charged to residential customers in Madison, WI by Madison Gas and Electric Company for the summer of 1982. (4.75 \$/GJ for gas and 0.06 \$/kW-hr for electricity)

ii) $P_e/P_a = 7.0$ This might correspond to the price of "new" electricity relative to gas which would include the costs of building new power plants to generate electricity for a whole bunch of new (not replacement) air-conditioning systems.

The reference vapor compression system was assumed to have a seasonal COP_{vc} of 2.5, representative of current technology (for example, ref [27]). The cost ratio CR, while providing a

convenient measure by which to compare desiccant system operating costs, also provides a measure of how well the desiccant systems compare with a standard vapor compression system.

6.4 Cooled Dunkle Cycle Performance[9]

In this section, estimates of long term cooled Dunkle cycle performance for both gas- and solar-fired operation are reported and compared with adiabatic system performance. Table 6.4.1 summarizes the system operating parameters used. Two levels of cooled dehumidifier performance are considered along with unbalanced flow in the cooled Dunkle cycle. Adiabatic system performance is included for comparison.

The levels of dehumidifier development represented by the parameters in Table 6.4.1 are better than currently available in practice. Based on equal time scales for development, cooled Dunkle cycle B can be considered equivalent to the adiabatic systems considered. Further development of a flow controller for the dehumidifier would lead to system B* or further improvements in cooled dehumidifier performance would lead to system A.

Performance is determined for these locations representing a wide range of climates:

i) Miami, FL (warm and humid)

ii) Phoenix, AZ (hot and dry)

---

[9] Finally!

Table 6.4.1

Summary of the Operating Parameters for the

Desiccant Cooling Systems

Cooled Dunkle Cycle Parameters

System	ε_{HX}	ε_{EC}	ε_{w}	ε_{t}	r_c	$\dot{m}_R/\dot{m}_D$
B	.95	.96	.80	.85	1.10	1.0
B*	.95	.96	.80	.85	1.10	$(\dot{m}_R/\dot{m}_D)^*$
A	.95	.96	.90	.95	1.05	1.0

Adiabatic Cycle Parameters

$\varepsilon_{HX} = .95$ $\varepsilon_{EC} = .96$ $\varepsilon_{F1} = .05$ $\varepsilon_{F2} = .95$

Load Parameters -- See Table 6.1.1

Collector/Storage System Parameters -- See Table 6.1.2

Pressure Drop Parameters -- See Table 6.1.3

iii) Columbia, MO (moderate cooling loads with a significant winter heating load)

6.4.1 Miami Performance

The Miami climate is characterized by its high humidity and relatively high latent loads. In section 5.2.4, it was noted that total cooling capacity, maximum latent capacity, and thermal COP all increase as the room state is allowed to become more humid. For this reason, a room state of 25°C and .012 kg/kg is used for Miami. This state is at the extreme corner of the comfort region defined by ASHRAE [23]. The maximum flowrate of air to the load is taken as 0.75 kg/sec. This flowrate provides a fair compromise between maximum cooling capacity and parasitic power consumption.

The performance of the gas-fired cooled Dunkle cycle as a function of regeneration temperature is shown in figure 6.4.1. The cooling loads are summarized in table 6.4.2.

The thermal COP of the cooled Dunkle cycle in Miami is not greatly affected by either regeneration temperature, dehumidifier performance, or flow ratio. In section 5.2.3, it was noted that COP_{th} is only slightly decreased in the region of warm and humid ambient conditions as regeneration temperature is raised. The improved dehumidifier (system A) increases COP_{th} by about 8% which agrees with the factorial analysis results in section 5.2.5.

The potential for increased cooling capacity with unbalanced flow operation (B^*) results in the system being able to meet the cooling load while regenerating with ambient air (mode 2

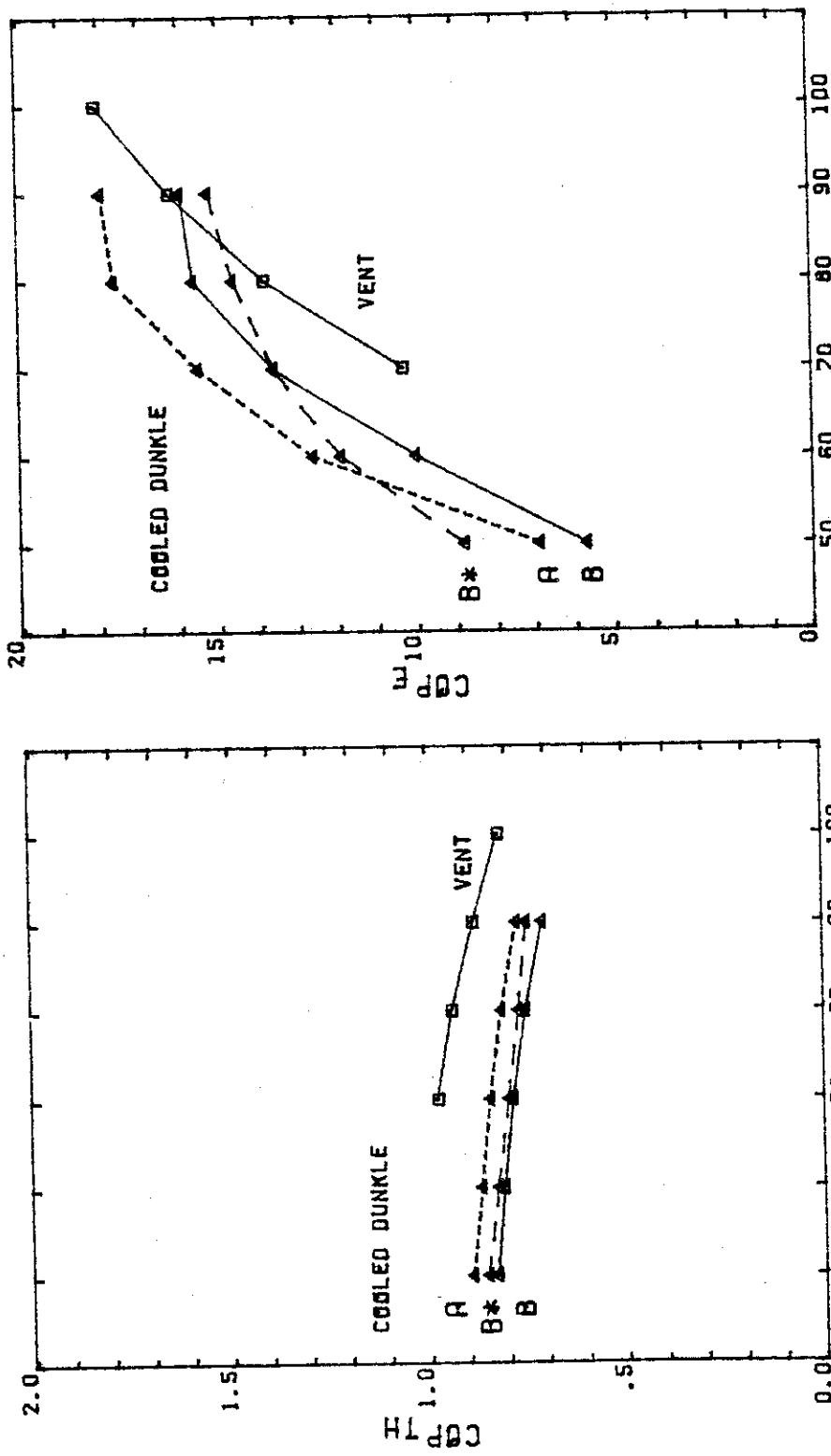

Figure 6.4.1 Performance of the gas-fired cooled Dunkle cycle in Miami, FL, for the months of June, July, and August. (a) thermal COP. (b) electric COP.

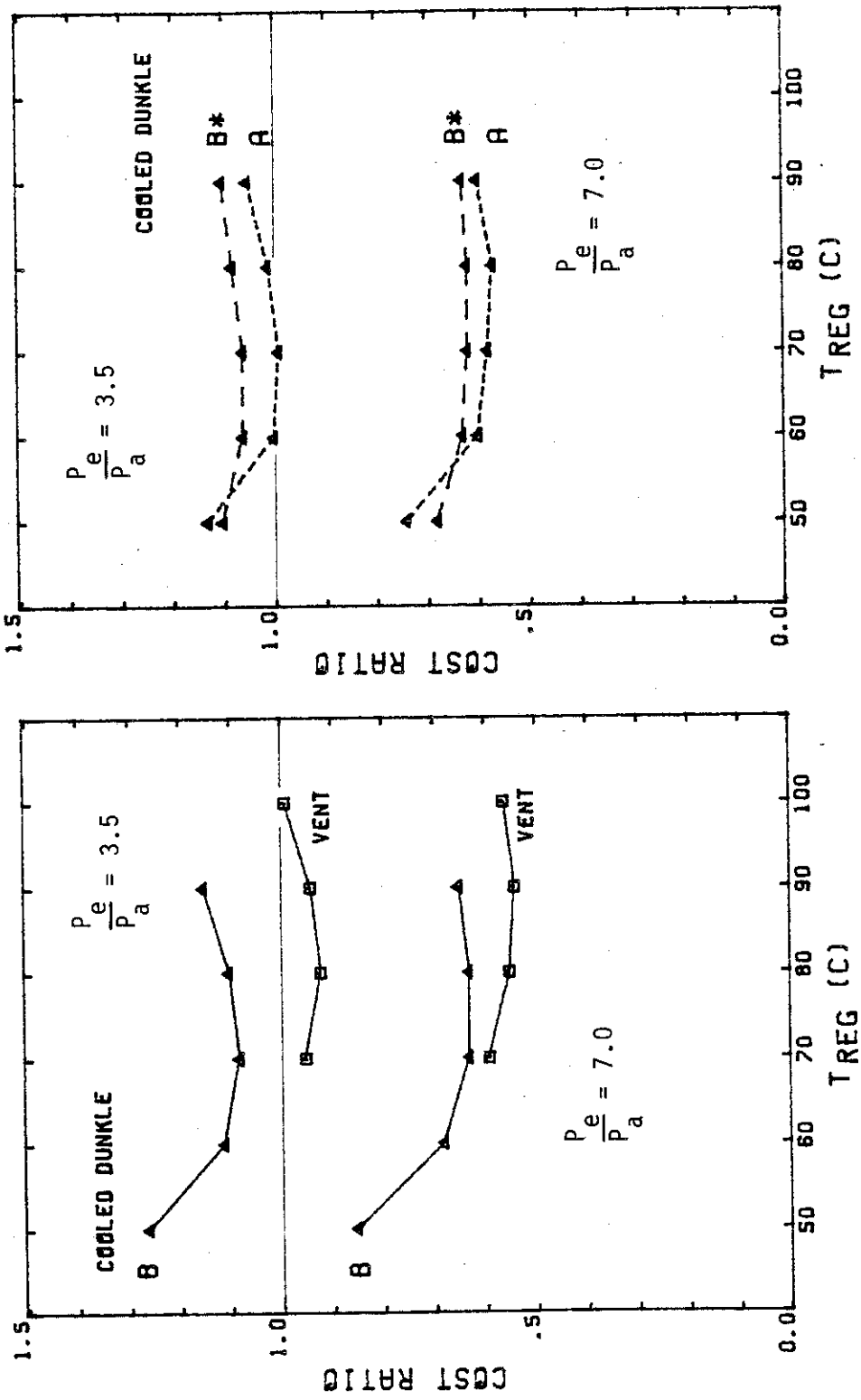

Figure 6.4.1 (cont) Miami, gas-fired. (c) & (d) cost ratios.

operation) and therefore requiring no thermal energy input. Although this situation occurred only 22 of 2200 hours, it accounts for the majority of the small increase in COP_{th}. For regeneration temperatures less than 80°C, $(\dot{m}_R/\dot{m}_D)^*$ is greater than unity for much of the Miami weather. Section 5.2.2 explains that gains in cooling capacity by operating with unbalanced flow are offset by requiring more thermal energy and so COP_{th} is essentially unaffected.

In contrast to thermal COP, figure 6.4.1b shows that electric COP is sensitive to regeneration temperature. Specific cooling capacity primarily depends on the humidity level of the dehumidifier outlet state. Higher regeneration temperatures produce drier outlet humidity levels and increased specific cooling capacity. This larger enthalpy difference between room state and conditioned air stream allows a lower airflow rate to be used to meet the cooling load and therefore lowering parasitic power consumption. Improved dehumidifier performance (A) also results in a drier dehumidifier outlet state and higher specific cooling capacity.

The higher specific cooling capacity due to unbalanced flow operation results in reduced process stream flowrates and parasitic power consumption for regeneration temperatures less that 70°C even though higher regeneration side flowrates are required. During the times of mode 2 operation, high flowrates and a large flow unbalance are required to meet the load and

therefore parasitic power consumption is very high. This is why COP_e for system B^* is less than for B for regeneration temperatures greater than 70°C. If mode 2 operation is inhibited, operating with unbalanced flow results in better electric performance than balanced flow at all regeneration temperatures.

The performance of the adiabatic ventilation cycle is included for comparison. Jurinak [6] has shown that the vent cycle performs the best of the adiabatic cycles in Miami. The vent cycle is seen to have a significantly higher thermal COP than any of the cooled Dunkle cycles. The electric COP behavior of the two cycles is similar with vent cycle shifted to higher regeneration temperatures as expected from the discussion in sections 2.3 and 5.5.

The relative importance of thermal and electric performance is shown by figure 6.4.1c-d. The cost ratio CR represents the operating costs of desiccant systems relative to a vapor compression system ($COP_{vc} = 2.5$). The minimum of each curve determines the optimum regeneration temperature for the lowest operating cost. The optimum regeneration temperature is a function of the fuel price ratio. When the price of electricity increases relative to natural gas, the importance of the electrical performance increases and the optimum regeneration temperature is shifted in the direction of better electrical performance.

Figure 6.4.1c-d shows that the adiabatic vent system has a lower operating cost than any of the cooled Dunkle systems.

Table 6.4.2

Miami Cooling and Heating Loads

room state: 25°C .012 kg/kg

max load air flowrate: 0.75 kg/sec

(a)	June, July, August (gas-fired operation)	
	Total Cooling Load	37.9 GJ
	Sensible	26.5
	Latent	11.4
(b)	July (solar-fired operation)	
	Total Cooling Load	12.5 GJ
	Sensible	8.6
	Latent	3.9
(c)	Estimates for Year (Economics)	
	Cooling Load (5 x July)	62.7 GJ
	Heating Load (500 watts/°C)	4.9
	by solar (FCHART)	4.9
	Domestic Hot Water (300 l/day)	24.7
	by solar (FCHART)	14.4

(The effect of mode 2 operation in system B* on CR is small.) At the lower fuel price ratio, only the vent system can be operated more inexpensively than the vapor compression system. At the higher fuel price ratio, the desiccant systems can be operated at about 60% of the cost of the vapor compression system. This comparison will become less favorable if, in the time it takes to develop the desiccant systems with the levels of performance investigated here, the cooling performance of vapor compression systems can be improved.

The performance of the cooled Dunkle cycle in solar-fired operation with gas auxiliary backup is shown in figure 6.4.2. The abscissa represents the temperature at which the auxiliary energy is available. The cooling load information is given in table 6.4.2. Solar only operation is not considered here because cooled Dunkle system B and the vent system met less than 80% of the cooling load and cooled Dunkle system A met only 85% of the load. Unbalanced flow was also not considered mainly because high regeneration side flowrates were involved which created problems in the numerical stability of the storage model. The high flowrates encountered also tend to destroy the temperature stratification in the pebble bed. This results in higher collector inlet temperatures (increased collector losses) and lower return temperatures to the desiccant system (lower regeneration temperature and less cooling capacity).

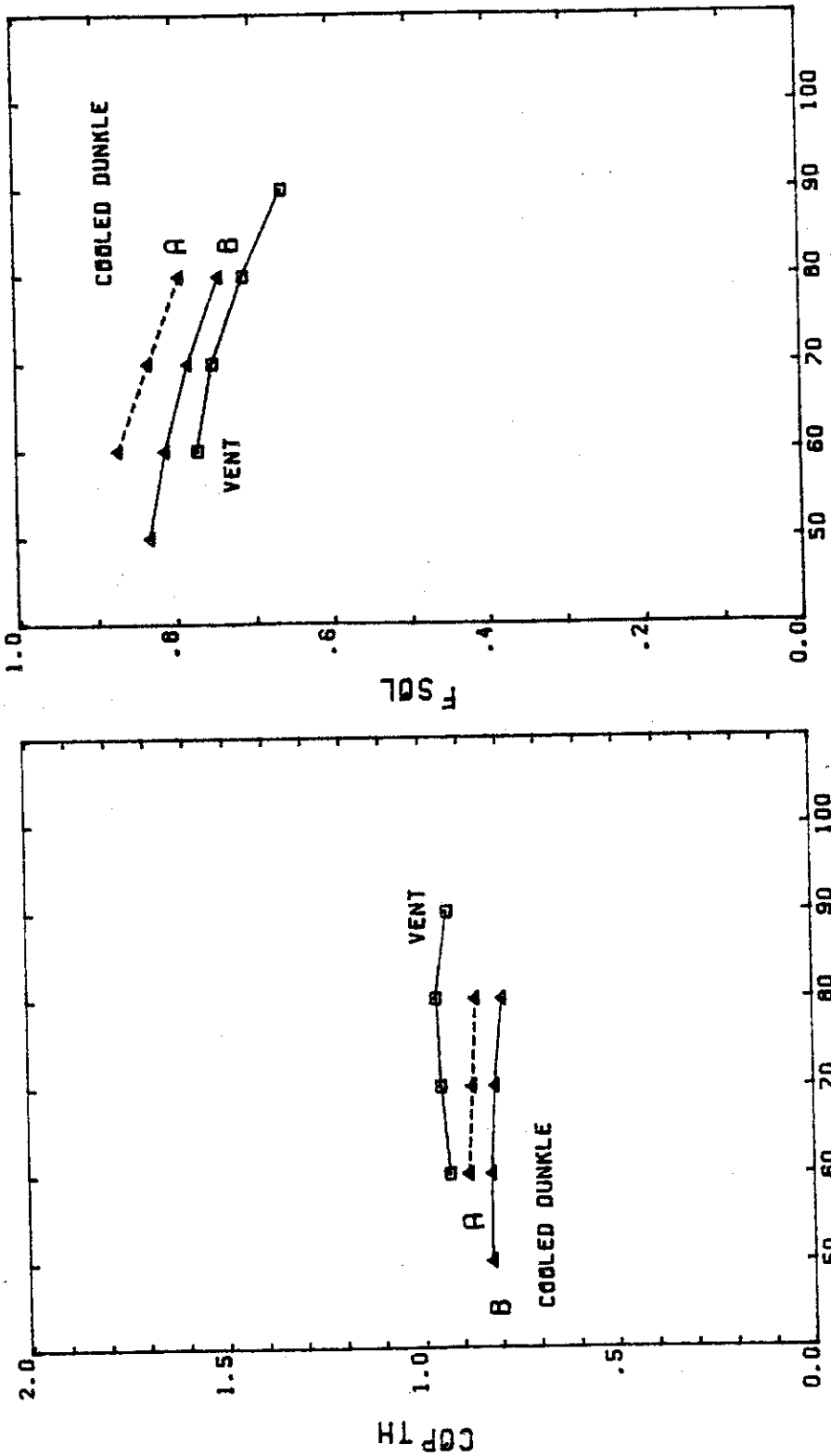

Figure 6.4.2 Performance of solar-fired cooled Dunkle cycle in Miami, FL for month of July. (a) thermal COP. (b) fraction of thermal energy supplied by solar.

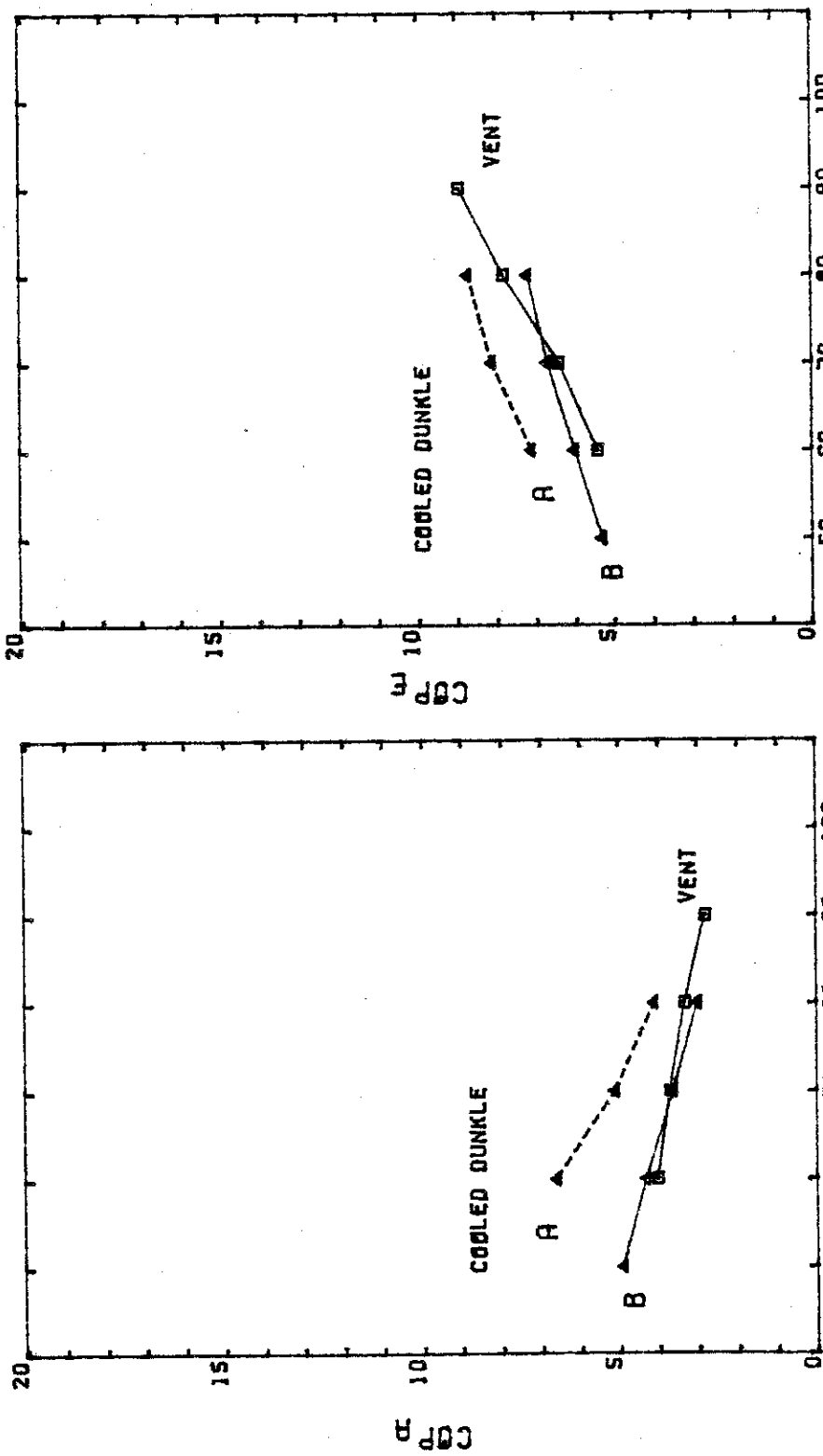

Figure 6.4.2 (cont) Miami, solar-fired. (c) purchased thermal energy COP. (d) electric COP.

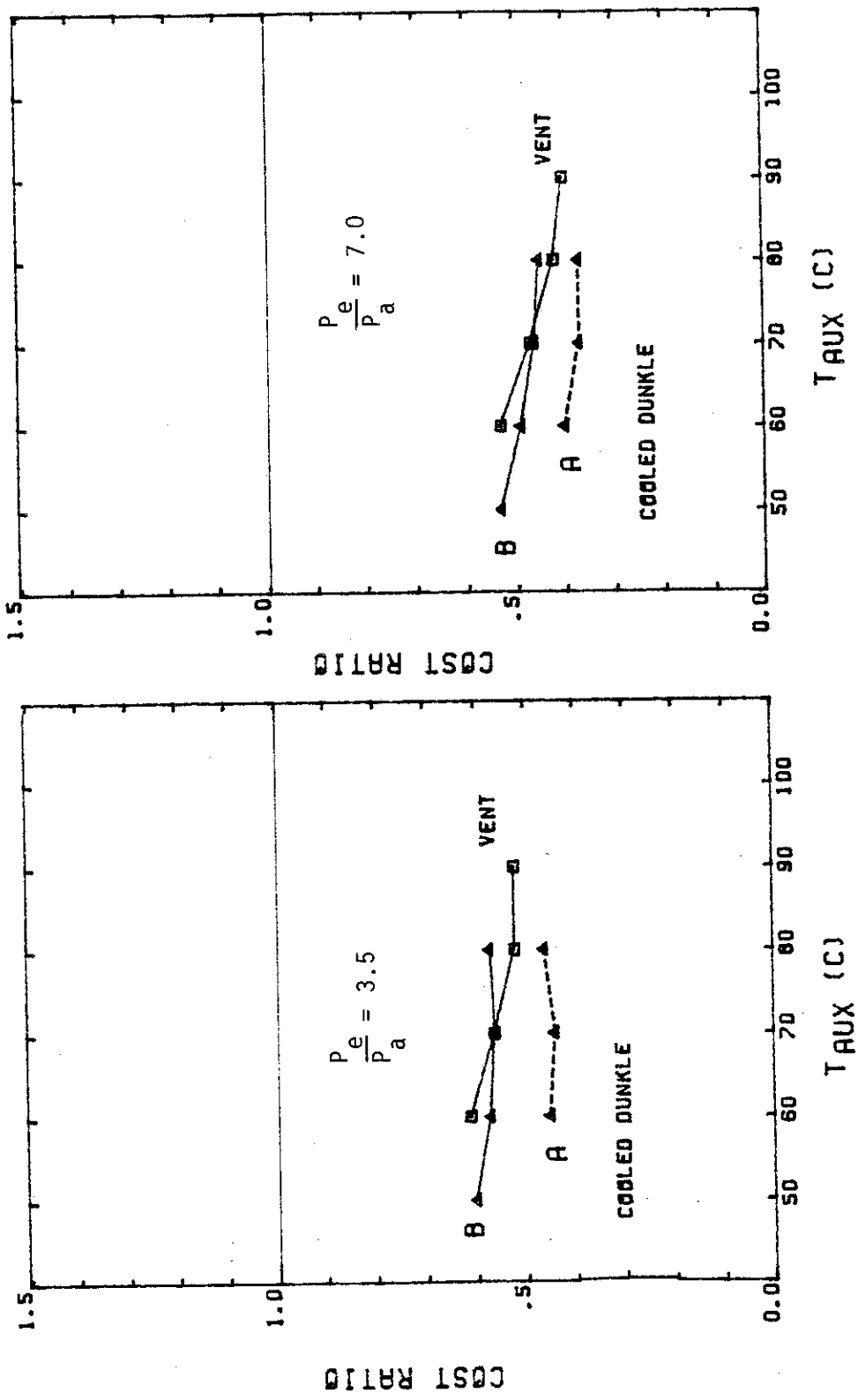

Figure 6.4.2 (cont) Miami, solar-fired. (e) & (f) cost ratios.

Because thermal COP is only slightly affected by regeneration temperature in the region of warm and humid ambient conditions, COP_{th} is not changed much from the gas-fired results by the addition of the solar system and subsequent range of regeneration temperatures that occur (figure 6.4.2a). Figure 6.4.2b shows the fraction of the total required thermal energy that is supplied by the solar system. As the auxiliary energy temperature is raised, it causes the average collector inlet temperature to increase. Losses from the collector increase and less useful energy can be collected. Cooled Dunkle systems A and B obtain essentially the same amount of energy from the solar system, but A requires less thermal energy (higher COP_{th}) and so the fraction by solar is higher.

Figure 6.4.3 shows the distribution of temperatures sent to the solar system and returned to the desiccant system for cooled Dunkle system B and the vent system with an auxiliary energy temperature of 70°C. The vent system operates at much higher temperatures and therefore the collector losses are much higher. The losses are of such magnitude that even though the vent system requires less thermal energy, the fraction by solar is less than that of cooled Dunkle system B.

The COP based on purchased energy is shown in figure 6.4.2c. The poorer thermal performance of the cooled Dunkle systems is compensated for by being able to operate with lower regeneration temperatures and obtaining more useful energy from the

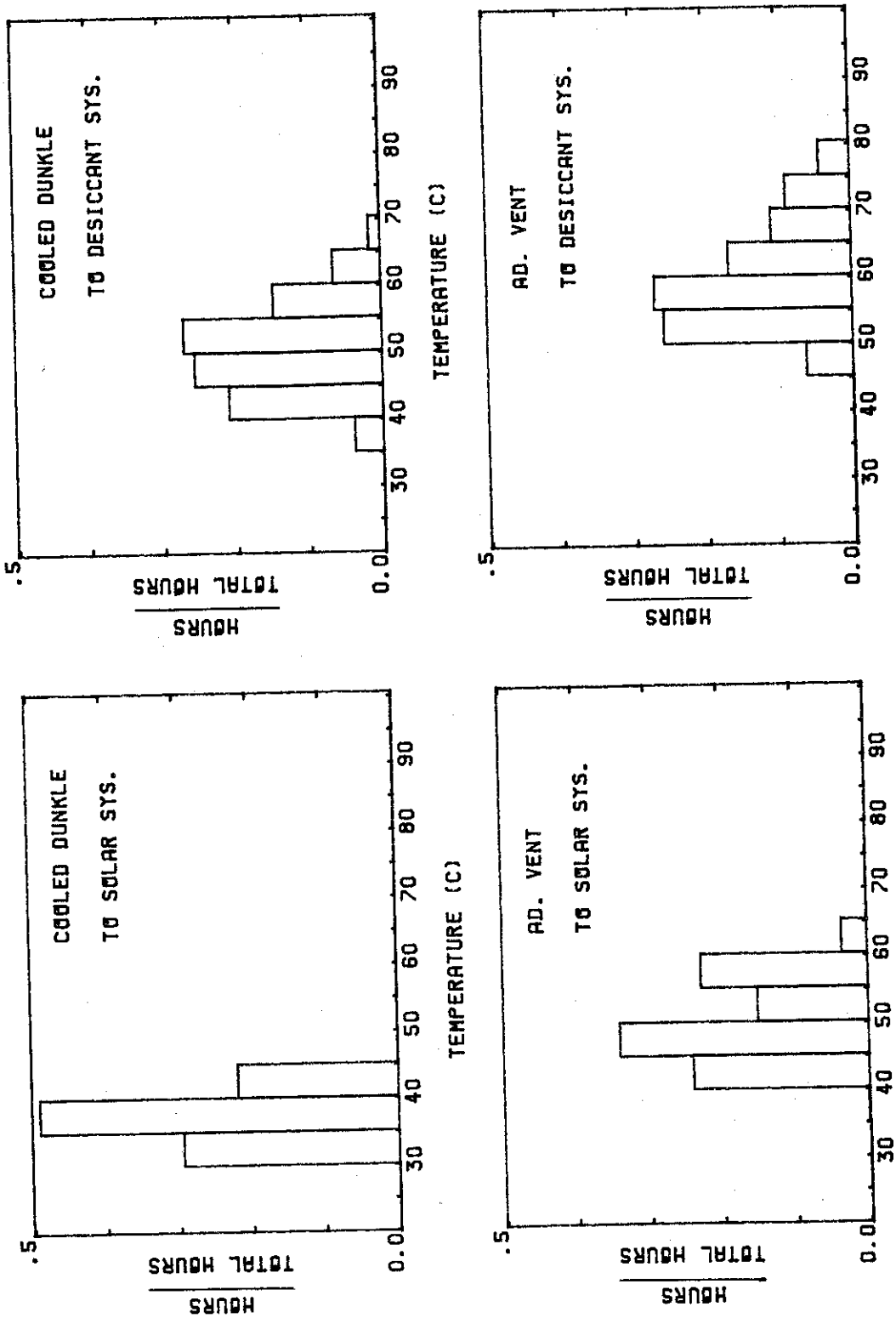

Figure 6.4.3 Distribution of temperatures sent to the solar system and returned to the desiccant system for the cooled Dunkle and adiabatic vent cycles.

solar system. The electric COP is shown in figure 6.4.2d. The effects on energy storage of raising the auxiliary energy temperature tend to shift the distributions in figure 6.4.3 to higher temperatures which means higher specific capacities and lower flowrates.

The operating costs of the solar-fired desiccant systems are shown in figure 6.4.2e-f. The vent sytem has slightly lower operating costs than cooled Dunkle cycle B. If the higher performance dehumidifier in system A can be developed, the solar-fired cooled Dunkle system will be more economical to operate. As for the gas-fired systems, the optimum temperature of auxiliary energy increases as the relative price of electricity goes up.

Table 6.4.3 contains estimates of the yearly operating costs of the desiccant systems for fuel prices of $5/GJ for gas and $25/GJ for electricity. The estimated space and domestic hot water (DHW) heating loads are given in table 6.4.2. The performance of the solar system for space and DHW heating was determined by using FCHART [28]. At this fuel price ratio, all of the systems have lower operating costs than the vapor compression system.

The savings by displacing gas with solar energy are 40-50% of the no solar operating costs with 70-75% of the savings attributable to the desiccant systems. For solar savings on the order of $300/yr and assuming collector costs of $200/m^2 [29] and a reasonable set of economic parameters (see appendix C), positive

Table 6.4.3

Estimates of Miami Yearly Heating and Cooling Costs for Natural Gas @$5/GJ and Electricity @$25/GJ

	Cooled Dunkle System B	Dunkle System A	Vent System	Vapor Compression
$T_{aux,opt.}$ (°C)	70	70	80	
gas-fired				
COP_{th}	.78	.84	.94	
COP_e	13.6	15.5	13.8	2.5
solar-fired				
COP_{th}	.81	.87	.95	
f_{SOL}	.78	.83	.71	
COP_e	6.72	8.13	7.80	
costs ($)				
gas-fired				
cooling	517	475	448	627
htng & DHW	148	148	148	148
total	665	622	596	776
solar-fired				
cooling	318	254	297	
htng & DHW	52	52	52	
total	370	306	349	
solar savings	295	316	247	

life cycle savings [29] cannot be generated over a period of 20 years without the benefit of tax credits. Tax credits of approximately 50% of the purchase price would be required for the solar system to be economically viable.

No attempt was made to optimize the collector area. Smaller solar systems, while not providing as large a fraction of the thermal energy for the desiccant system, may be more economical. Higher fuel prices relative to collector costs would increase the solar savings available and make the solar-desiccant systems look more attractive. If electricity prices increase relative to gas prices, solar savings will decrease because the solar-desiccant systems have a larger parasitic power consumption.

In summary for Miami: Solar-fired desiccant system operation does not appear to be an economic alternative for large collectors and no tax credits. Gas-fired desiccant system operation appears to be economically viable compared with vapor compression cooling at higher fuel price ratios. The adiabatic vent cycle can be operated at less cost than the comparable cooled Dunkle cycle (system B). Cooled Dunkle cycle performance can approach that of the vent cycle if unbalanced flow is used or cooled dehumidifier performance is improved.

6.4.2 Phoenix Performance

The summer weather in Phoenix is hot and dry. Large cooling loads result with most of the load being sensible. Sensible cooling capacity can be increased by maintaining a drier room

state (section 5.2.4). This also reduces the excess latent capacity available and lessens the effects of by-pass mixing (section 6.1.1). A room state of 25°C and .008 kg/kg is used. (In a system without by-pass mixing, the excess latent capacity would tend to keep the room on the dry side anyway.) A maximum flowrate to the load of 1.0 kg/sec is allowed in order to meet the high cooling loads.

The performance of the gas-fired cooled Dunkle systems is shown in figure 6.4.4. The cooling loads are summarized in table 6.4.4. The thermal COP of the cooled Dunkle systems is seen to be effected more strongly by regeneration temperature in Phoenix than in Miami. This is because Phoenix weather lies in the regions where HX_2 is not very useful and COP_{th} is a strong function of ambient condition and regeneration temperature (sections 5.2.1 and 5.2.3).

The thermal COP in Phoenix is also considerably higher than in Miami. There are several reasons for this. First, cooled Dunkle cycle COP_{th} is higher for hot and dry ambient conditions, especially at lower regeneration temperatures. Second, 15% of the cooling load is met by regenerative evaporative cooling with no thermal energy input. Third, significant fractions of the cooling load are met by mode 2 operation (regeneration with ambient air) because of the high ambient temperatures encountered. System B^* is the most dramatic. The thermal COP of B^* with modes 1 and 2 inhibited is 0.88 compared with 1.60 at a regeneration temperature

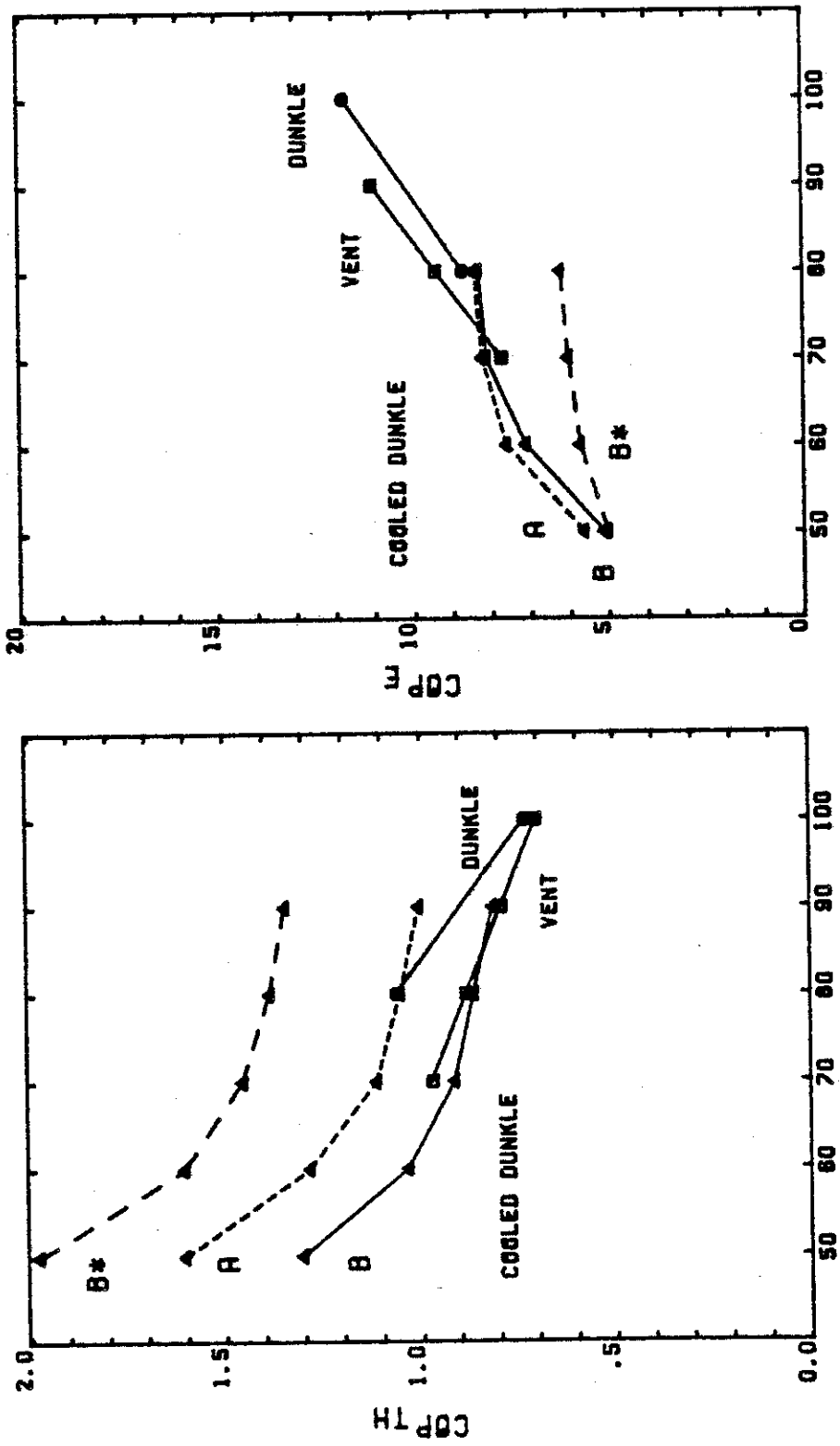

Figure 6.4.4 Performance of gas-fired cooled Dunkle cycle in Phoenizx, AZ, for the months of June, July, and August. (a) thermal COP. (b) electric COP.

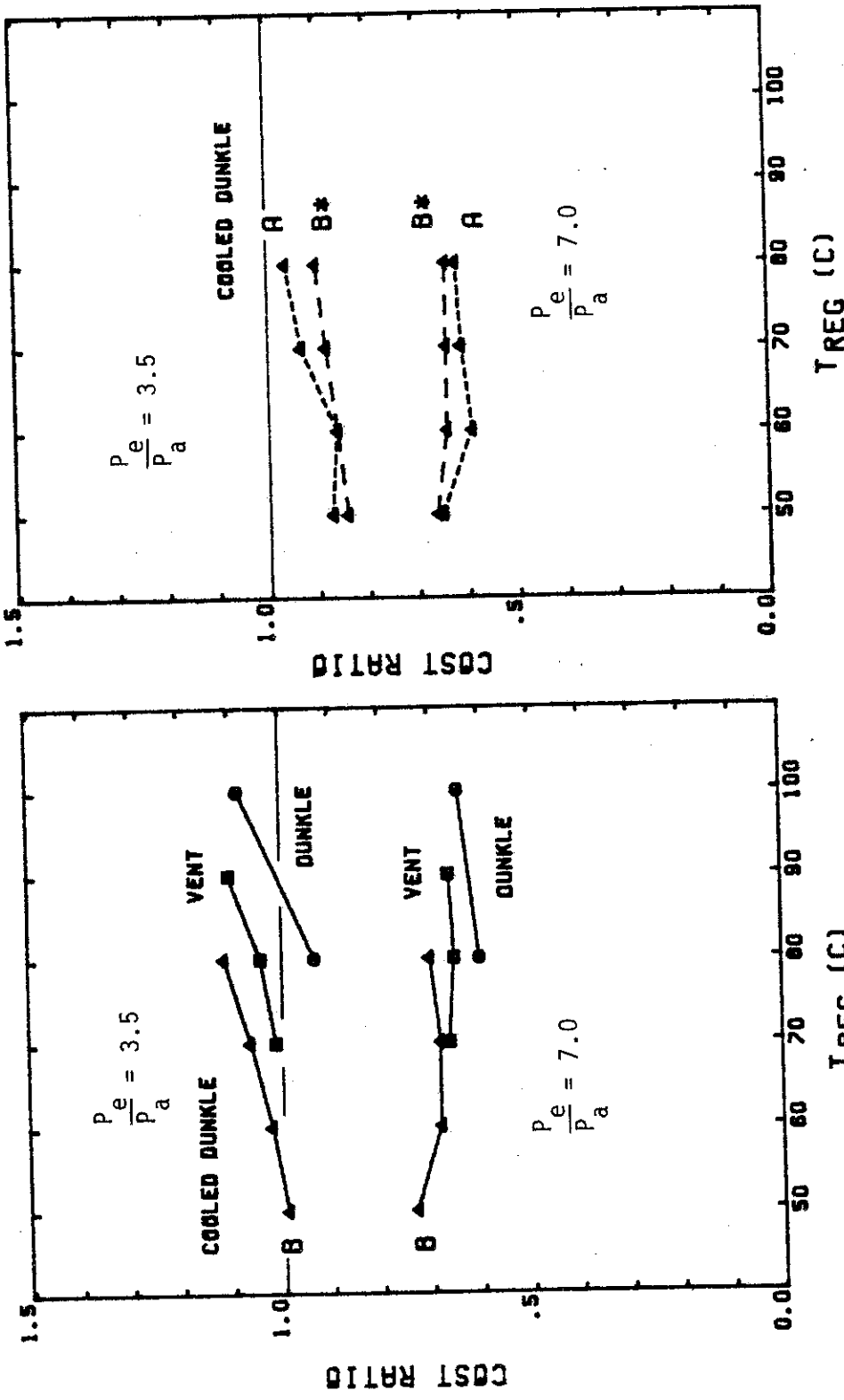

Figure 6.4.4 (cont) Phoenix, gas-fired. (c) & (d) cost ratios.

of 60°C. The increased specific cooling capacity at low regeneration temperatures allows system B^* to operate in mode 2 586 of 2058 hours (28%). Without mode 2 operation, the thermal COP of the cooled Dunkle systems would be significantly lower, about the same levels as the adiabatic systems shown. (Dunkle cycle performance was estimated from data obtained from Jurinak [22].)

The electric COP is shown in figure 6.4.4b. The higher flowrates required during mode 2 operation do hurt electric performance, especially system B^* with unbalanced flow. In contrast to Miami, though, the operating costs in Phoenix are less when mode 1 and mode 2 operation are allowed. The thermal energy saved more than makes up for the additional parasitic power consumption.

The operating cost ratios are shown in figure 6.4.4c-d. An adiabatic system, in this case the Dunkle cycle, still has an advantage over the comparable cooled Dunkle system (B). Improved dehumidifier performance (if obtainable) can give the edge to the cooled Dunkle cycle, but only at lower fuel price ratios.

The thermal COP of the solar-fired systems is shown in figure 6.4.5a. Again, the abscissa represents the temperature at which auxiliary thermal energy is available. This is not necessarily the regeneration temperature. The cooled Dunkle cycle COP_{th} for solar-fired operation appears to be lower than gas-fired operation for a given auxiliary temperature. This is because the average regeneration temperature obtained from the solar system is higher than the auxiliary temperature and higher regeneration temperatures result in a lower COP_{th}. Also, the solar performance

Table 6.4.4

Phoenix Cooling and Heating Loads

room state: 25°C .008 kg/kg

max load air flowrate: 1.0 kg/sec

(a)	June, July, August (gas-fired operation)	
	Total Cooling Load	73.6 GJ
	Sensible	68.9
	Latent	4.7
(b)	July (solar-fired operation)	
	Total Cooling Load	29.9 GJ
	Sensible	27.6
	Latent	2.3
(c)	Estimates for Year (Economics)	
	Cooling Load (1.8 x June-August)	132 GJ
	Heating Load (500 watts/°C)	37.2
	by solar (FCHART)	30.2
	Domestic Hot Water (300 l/day)	24.7
	by solar (FCHART)	12.8

was obtained for only the month of July, which is much warmer than June or August in Phoenix. A much smaller proportion of the July cooling load can be met by regenerative evaporative cooling or the desiccant system while regenerating with ambient air.

The fraction of the thermal energy supplied by the solar system is shown in figure 6.4.5b. Phoenix has about 37% more solar radiation available than in Miami. Also, a higher collector flowrate is used (equal to $\dot{m}_{L,max}$) and so lower collector temperatures occur. This reduces losses and increases collector efficiency. Yet, the solar fraction is lower in Phoenix because the cooling loads are so much larger. Again, the cooled Dunkle systems operate with lower collector temperatures than the adiabatic systems and so show better solar system performance.

The performance based on purchased thermal energy and electric power consumption is shown in figures 6.4.5c-d. The higher COP_e for the adiabatic systems is due to lower flowrates and less pressure drop (fewer components).

Operating costs relative to a vapor compression system are shown in figure 6.4.5e-f. Again, the adiabatic Dunkle system appears to have lower operating costs than cooled Dunkle system B. Improved cooled dehumidifier performance can result in a significant reduction in cooled Dunkle cycle operating costs, though.

As in Miami, the addition of the solar system appears to result in a significant reduction in operating costs. Estimates of the yearly heating and cooling costs are given in table 6.4.5

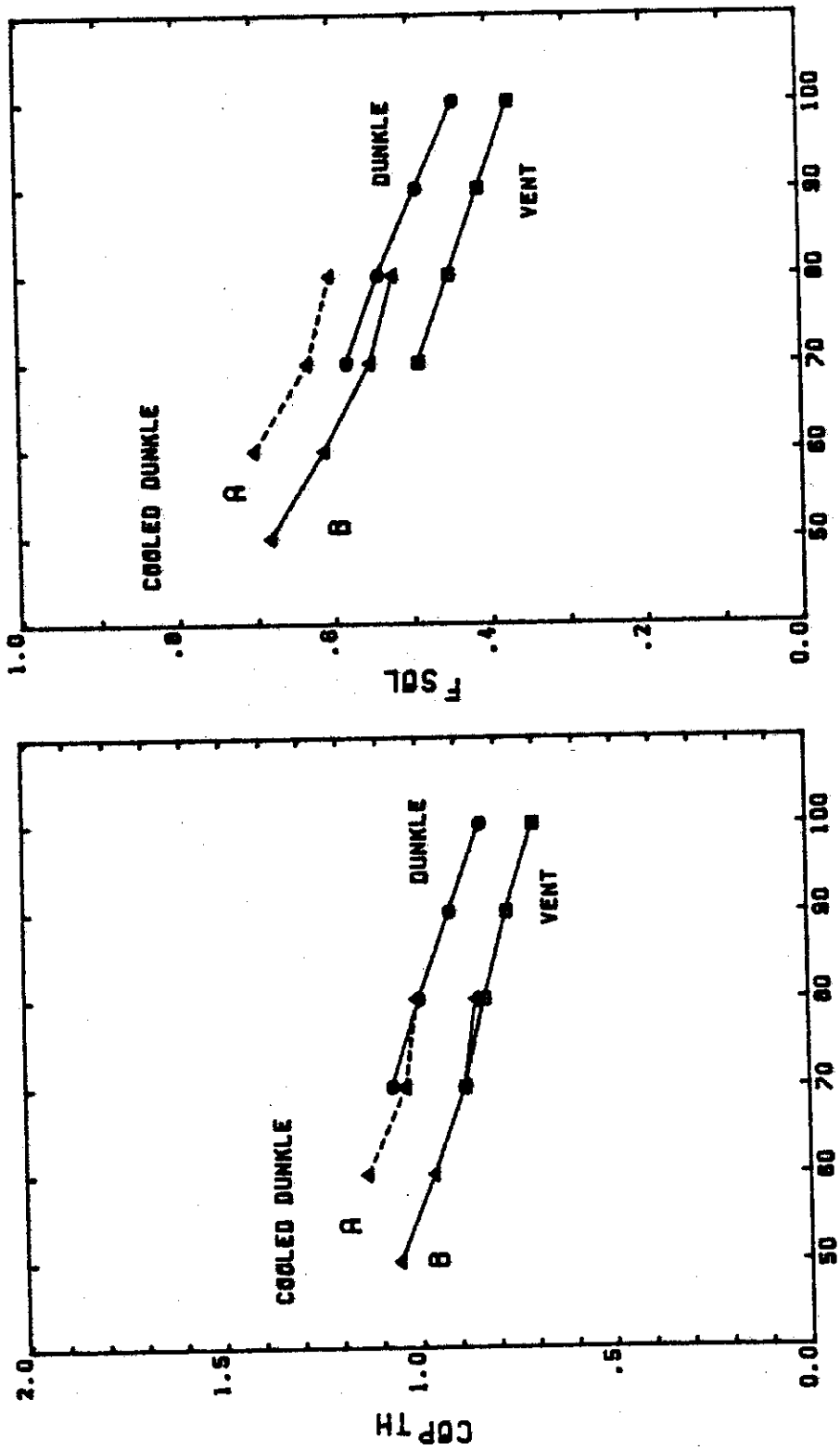

Figure 6.4.5 Performance of solar-fired cooled Dunkle cycle in Phoenix, AZ for the month of July. (a) thermal COP. (b) fraction of thermal energy supplied by solar.

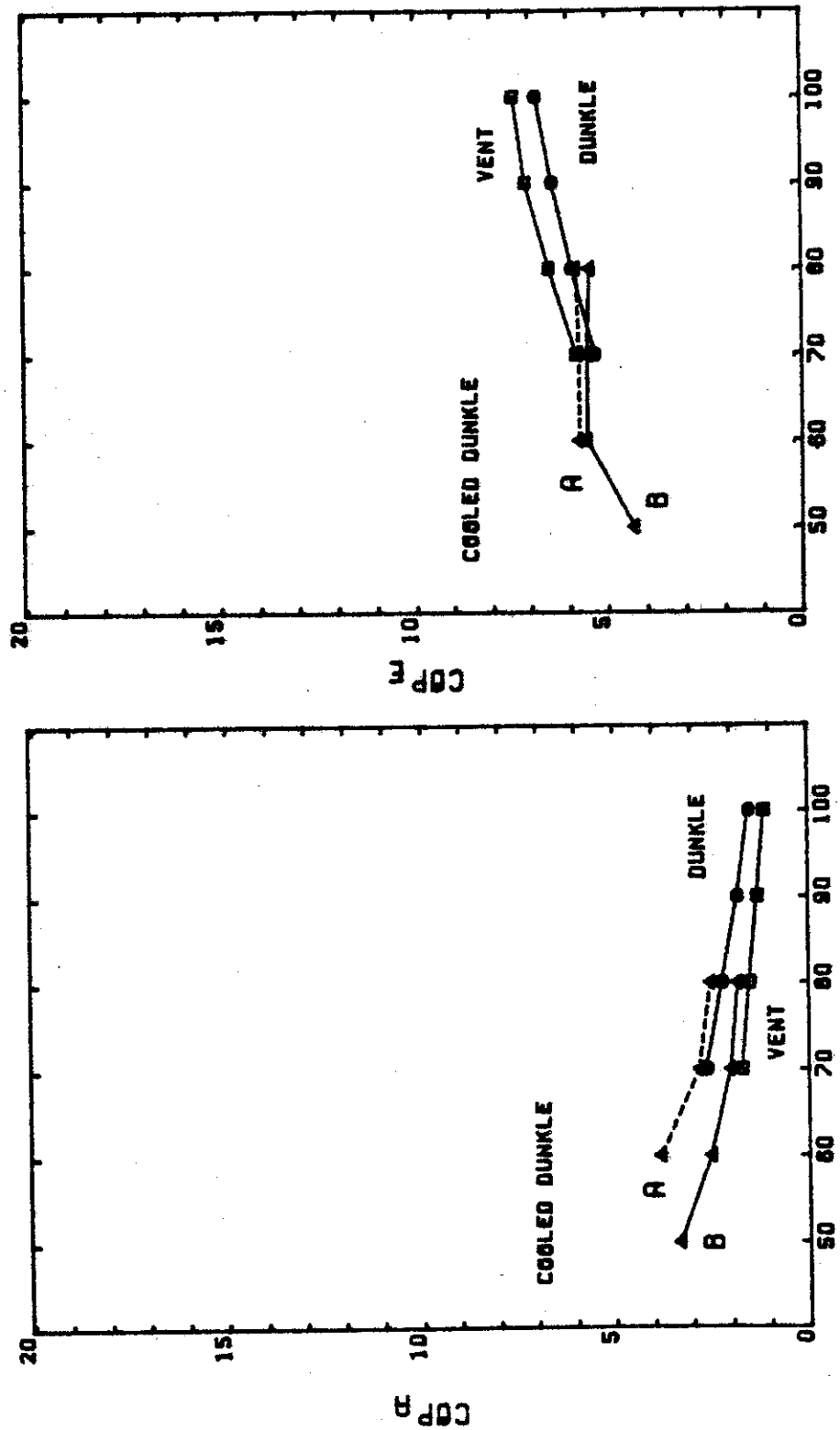

Figure 6.4.5 (cont) Phoenix, solar-fired. (c) purchased thermal energy COP.
(d) electric COP.

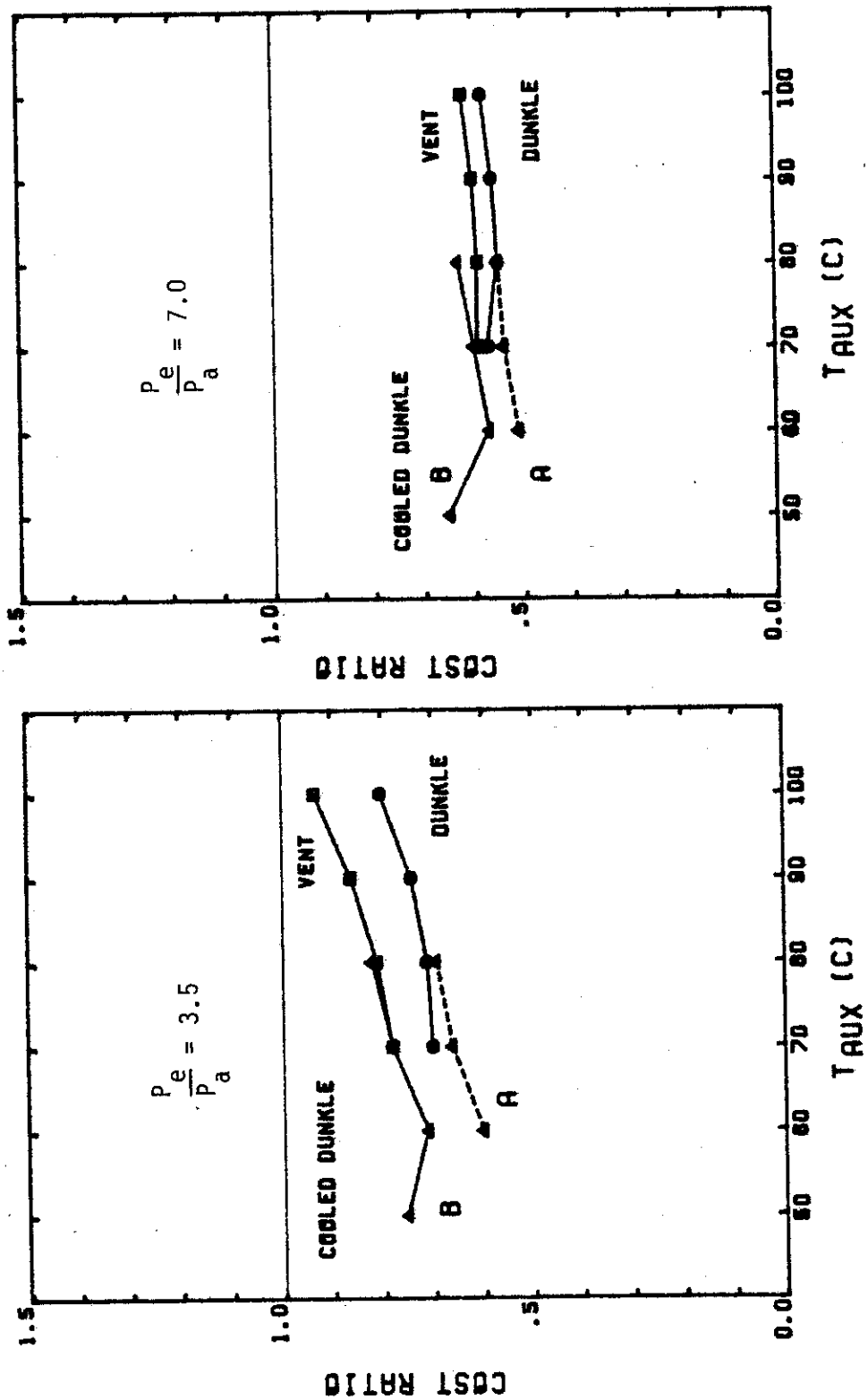

Figure 6.4.5 (cont) Phoenix, solar-fired. (e) & (f) cost ratios.

Table 6.4.5

Estimates of Phoenix Yearly Heating and Cooling Costs for Natural Gas @$5/GJ and Electricity @$25/GJ

	Cooled Dunkle System B	Dunkle System A	Dunkle System	Vapor Compression
$T_{aux,opt}$(°C)	60	60	80	
gas-fired				
COP_{th}	1.03	1.28	1.06	
COP_e	7.1	7.6	8.7	2.5
solar-fired				
COP_{th}	1.05	1.25	1.11	
f_{SOL}	.61	.77	.58	
COP_e	5.5	6.2	6.5	
costs ($)				
gas-fired				
cooling	1106	951	999	1320
htng & DHW	310	310	310	310
total	1416	1261	1309	1630
solar-fired				
cooling	845	650	758	
htng & DHW	95	95	95	
total	940	745	853	
solar savings	476	516	456	

for gas at $5/GJ and electricity at $25/GJ. The heating and cooling loads are given in table 6.4.4. Solar-fired operation produces a 35-40% reduction in operating costs over gas-fired operation, but approximately 45% of the solar savings is due to solar displacing gas in space and domestic water heating.

The solar savings from the desiccant system alone are not enough to make the solar system worth the investment. Solar savings (~ $475/yr), including space heating and DHW, are still not enough to produce positive life cycle savings without the benefit of tax credits. Tax credits amounting to approximately 25% of the initial investment in collectors would be needed. Again, no attempt was made to optimize collector area and this may have an impact on the analysis.

In summary for Phoenix: Solar-fired desiccant system operation again does not appear to be economical for large collectors and no tax credits, but the prospects are better than in Miami. Gas-fired desiccant systems do appear to be economically viable compared with vapor compression cooling at higher fuel price ratios. An adiabatic system, in this case the Dunkle cycle, performs better than the comparable cooled Dunkle cycle. Improvements in cooled Dunkle cycle operation could make it competitive with the adiabatic cycle.

6.4.3 Columbia Performance

The Phoenix and Miami results have shown that adding a solar system just to supply thermal energy to a desiccant system for

summer cooling is not economical. In order to make the large investment in a solar system worthwhile, the collector must be fully utilized. Columbia, MO, has a significant winter heating load along with a moderate summer cooling load and so the solar system can be used to a fuller extent all year long than in Phoenix or Miami.

A room state of 25°C and .010 kg/kg and a maximum load air flowrate of 0.75 kg/sec are assumed. The cooling and heating loads for the various periods of analysis are shown in table 6.4.6.

The thermal and electric performance of the gas-fired cooled Dunkle systems are shown in figure 6.4.6a-b. The increase in COP_{th} due to unbalanced flow operation (B^*) is because of the increased cooling capacity at low regeneration temperatures and the potential for meeting the cooling load while regenerating with ambient air. The higher flowrates required result in a lower COP_e, though. The increase in COP_{th} and COP_e of system A is due mainly to the improvement in dehumidifier performance.

Figure 6.4.6c-d show the operating costs of the systems relative to a vapor compression system. Again, the adiabatic system appears to have an advantage over the comparable cooled Dunkle system, but it is not as large as in the other two locations. Improvements in cooled Dunkle cycle operation can increase performance so that it is competitive with the vent cycle. Also, somewhat higher fuel price ratios are required for the desiccant systems to show an advantage over a vapor compression system.

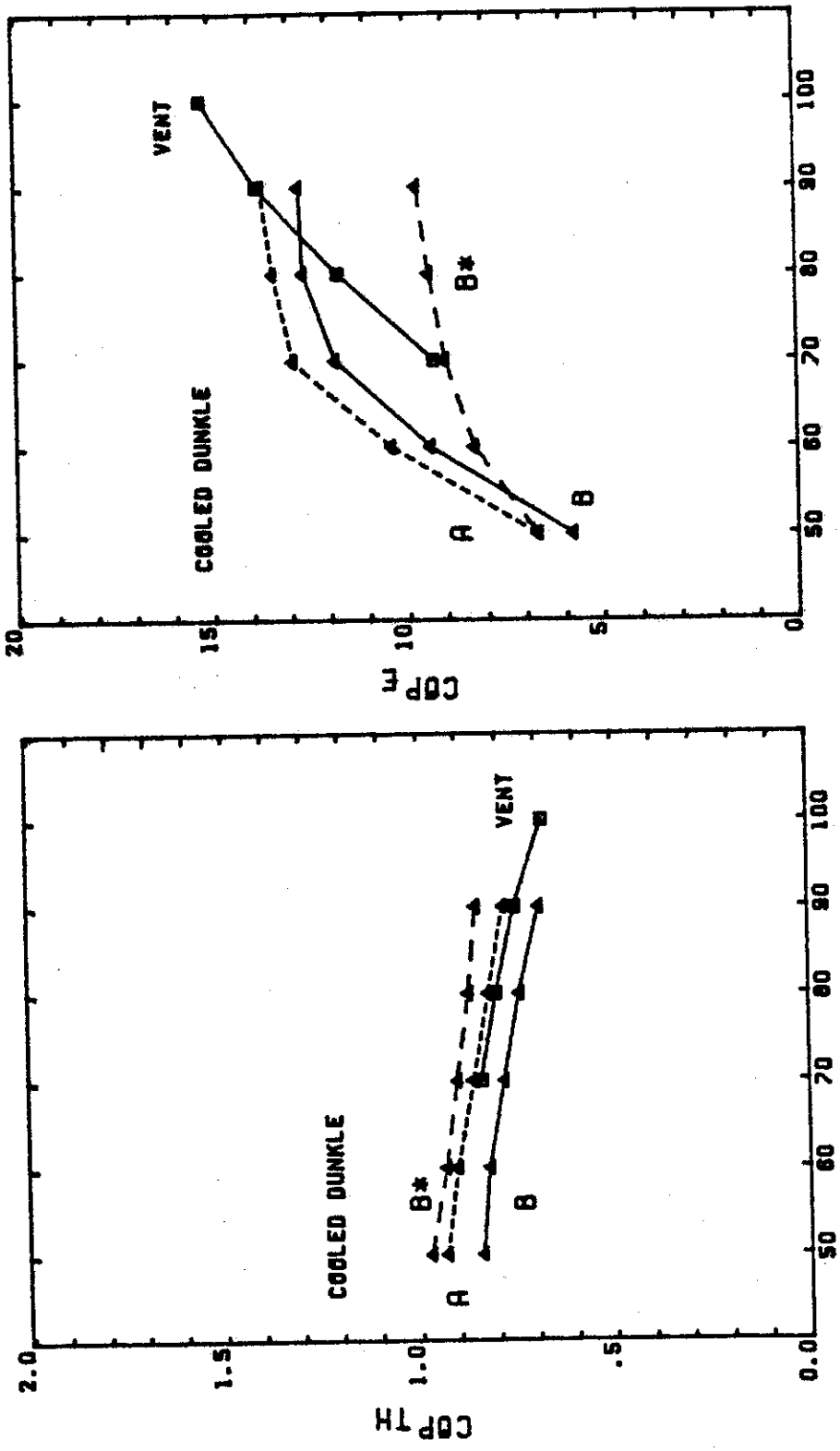

Figure 6.4.6 Performance of gas-fired cooled Dunkle cycle in Columbia, MO, for the months of June, July, and August. (a) thermal COP. (b) electric COP.

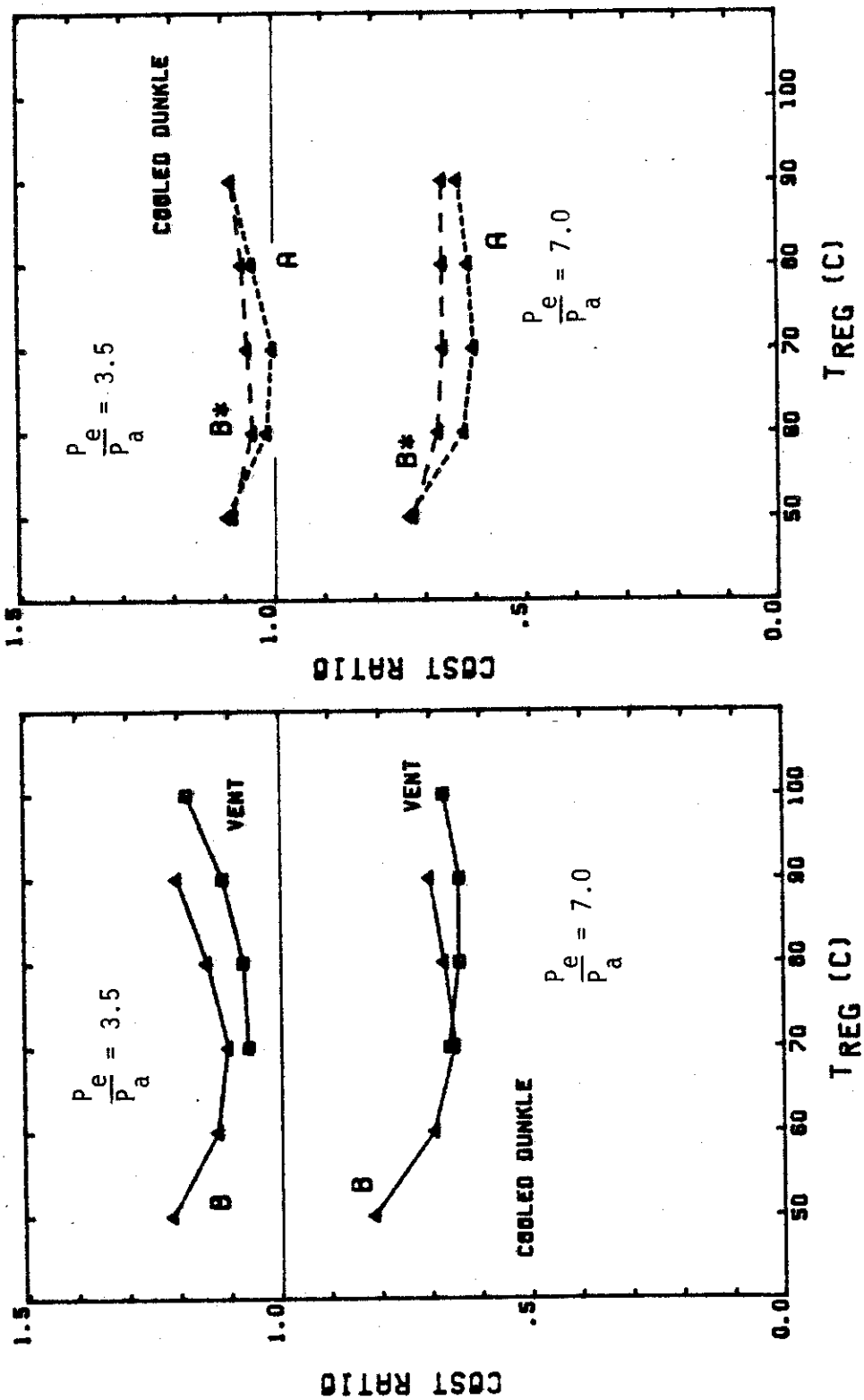

Figure 6.4.6 (cont) Columbia, gas-fired. (c) & (d) cost ratios.

Table 6.4.6

Columbia, MO, Cooling and Heating Loads

room state: 25°C .010 kg/kg

max load air flowrate: .075 kg/sec

(a)	June, July, August (gas-fired operation)	
	Total Cooling Load	24.0 GJ
	Sensible	16.1
	Latent	7.9
(b)	July (solar-fired operation)	
	Total Cooling Load	9.5 GJ
	Sensible	6.5
	Latent	3.0
(c)	Estimates for Year (Economics)	
	Cooling Load (1.7 x June-August)	40.8 GJ
	Heating Load (500 watts/°C)	118
	by solar (FCHART)	35.2
	Domestic Hot Water (300 l/day)	24.7
	by solar (FCHART)	6.1

The performance of the solar-desiccant systems is shown in figure 6.4.7. The thermal COP is somewhat decreased from the gas-fired case for a given auxiliary temperature because the solar system is supplying temperatures higher than the auxiliary. The fraction by solar is very high, especially for the cooled Dunkle systems which operate at lower collector temperatures than the vent system and so have lower losses. This results in very good performance with respect to purchased thermal energy.

The high fractions by solar result in low operating costs relative to a vapor compression system as shown in figure 6.4.7e-f. Because of the high solar performance, the cooled Dunkle cycle can be less expensive to operate than the vent system, especially at higher fuel price ratios. Improvements in the cooled Dunkle cycle performance would extend this advantage.

Table 6.4.7 gives estimates of the yearly heating and cooling costs for the loads shown in table 6.4.6 for a gas price of $5/GJ and electricity price of $25/GJ. The solar system reduces the no solar costs by about 40%, but again 50% of the reduction comes from displacing gas for space and domestic hot water heating.

The magnitude of the solar savings is somewhat low to provide any economic benefit to solar operation without tax credits (about 35% tax credits would be required). The high solar fractions obtained for the cooling season indicate that the collectors may be somewhat oversized for economical desiccant system operation. It is somewhat disappointing that only 30% of the heating load is

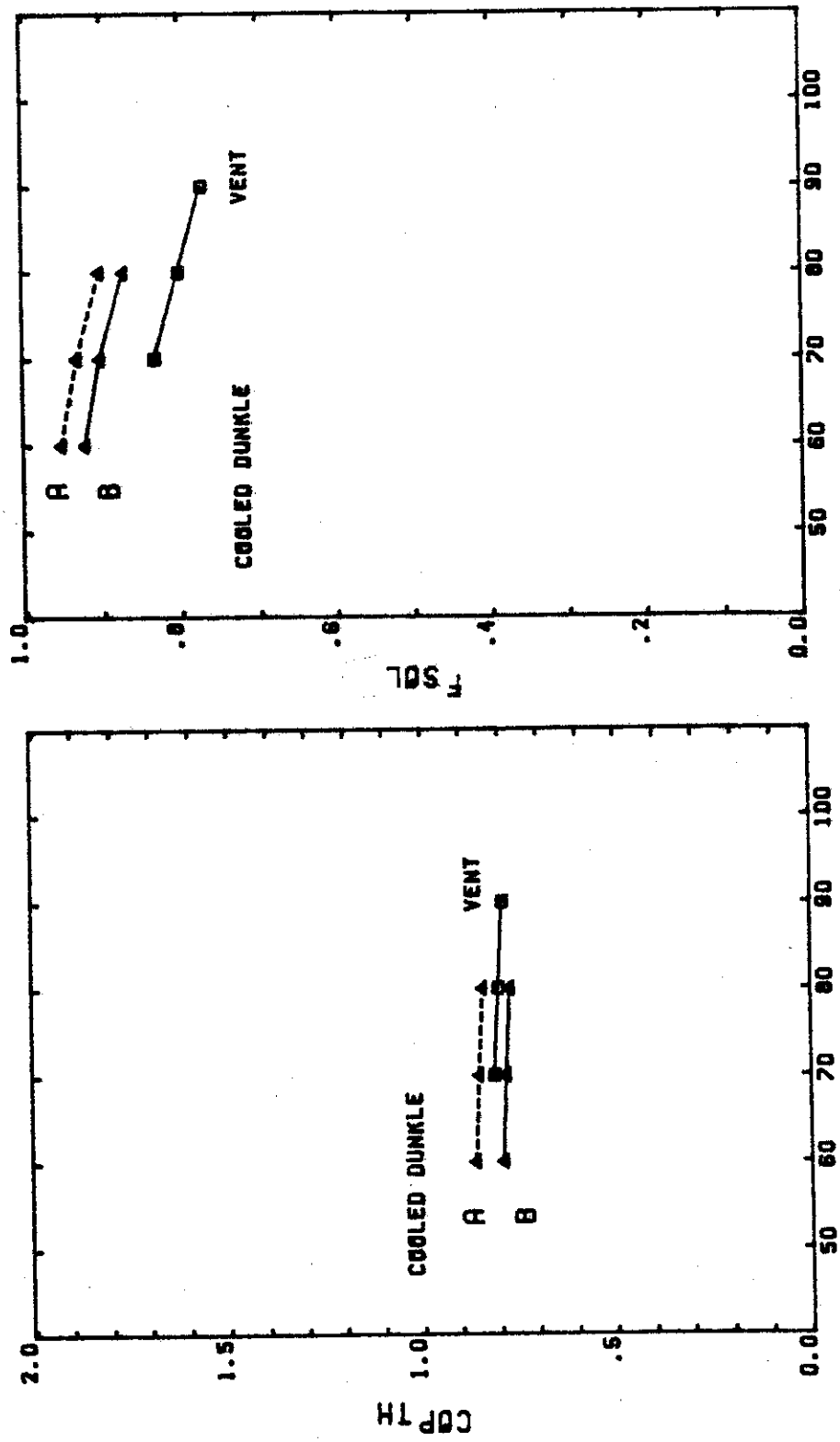

Figure 6.4.7 Performance of solar-fired cooled Dunkle cycle in Columbia, MO, for the month of July. (a) thermal COP. (b) fraction of thermal energy supplied by solar.

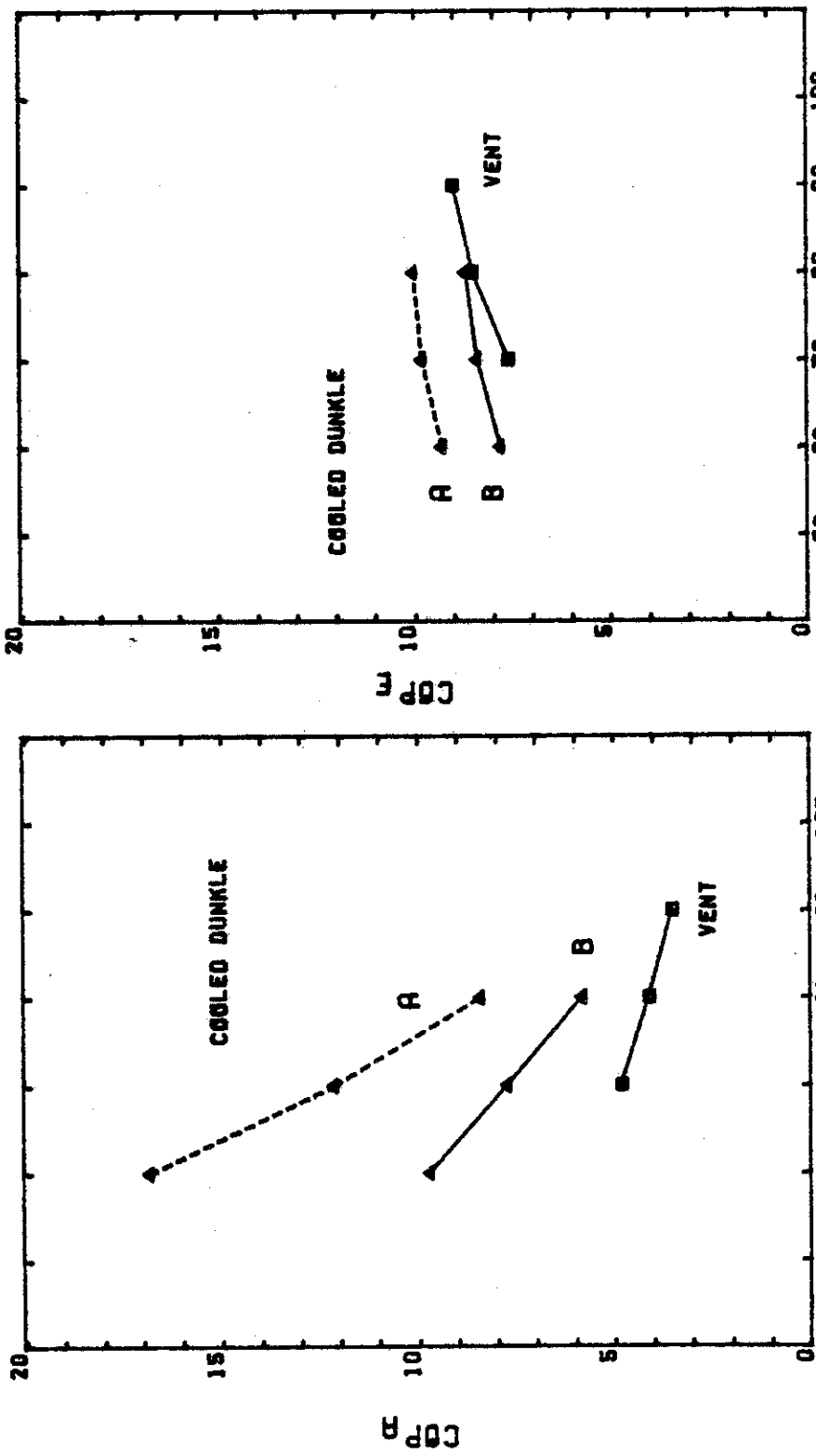

Figure 6.4.7 (cont) Columbia, solar-fired. (c) purchased thermal energy COP.
(d) electric COP.

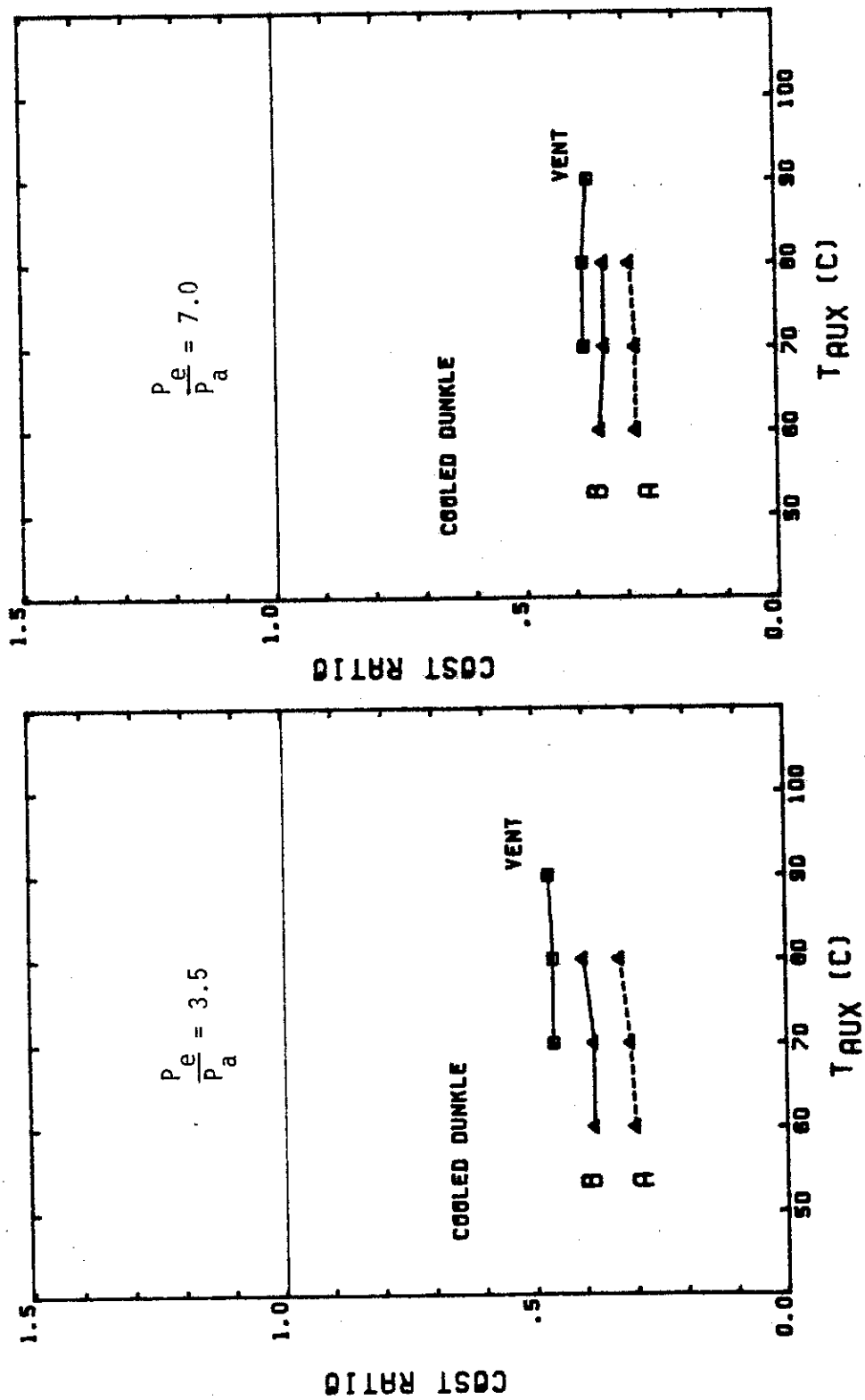

Figure 6.4.7 (cont) Columbia, solar-fired. (e) & (f) cost ratios.

Table 6.4.7

Estimates of Columbia Yearly Heating and Cooling Costs for Natural Gas @$5/GJ and Electricity @$25/GJ

	Cooled Dunkle System B	System A	Vent System	Vapor Compression
$T_{aux,opt}$(°C)	70	70	80	
gas-fired				
COP_{th}	.78	.86	.80	
COP_e	11.9	12.9	11.7	2.5
solar-fired				
COP_{th}	.78	.85	.80	
f_{SOL}	.90	.93	.81	
COP_e	8.4	9.8	8.5	
costs ($)				
gas-fired				
cooling	348	316	342	408
htng & DHW	714	714	714	714
total	1062	1030	1056	1122
solar-fired				
cooling	147	121	168	
htng & DHW	507	507	507	
total	654	628	675	
solar savings	408	402	381	

met by the large solar system. If the heating load could be reduced by other means (the house heat loss used may be somewhat high), a smaller collector may be able to still contribute during the heating season while being more economical for use with the desiccant system.

In summary, then, for Columbia: Economical solar-desiccant system operation appears to be somewhat doubtful unless smaller collector areas can be used without reducing solar savings proportionately. Gas-fired desiccant system operation in Columbia compares somewhat less favorably to vapor compression cooling than in Miami or Phoenix. The cooled Dunkle cycle can be operated at costs equal to or less than the adiabatic vent cycle, but the margin is not very large.

CHAPTER 7

CONCLUSIONS AND RECOMMENDATIONS

The performance of the cooled Dunkle cycle desiccant air-conditioning system has been shown to depend on a number of factors. These include the level of individual component performance, regeneration temperature, relative energy costs, thermal energy source, and climate. The conclusions that can be drawn from the results presented in chapters 5 and 6 are summarized below.

- In general, gas-fired desiccant cooling systems with well engineered components can be competitive with vapor compression cooling systems. The economic advantage of the desiccant systems increases as the price of electricity rises in relation to natural gas.
- Optimum desiccant system operation involves trade-offs in thermal and electrical performance with regeneration temperature. The optimum regeneration temperature depends on the cycle and the climate.
- Solar-fired operation of desiccant systems can significantly reduce operating costs. Solar only (no auxiliary energy source) operation does not appear

feasible because of the large collector arrays required (greater than 50 m^2). The optimum collector size depends on the solar savings available from space and domestic hot water heating and on the tax credits available to offset the initial costs of the solar system.

- Solar-fired operation appears to have the greatest potential for success in locations with moderate climates where smaller solar systems supply a significant fraction of the required thermal energy. An increase in natural gas prices would also enhance the economic benefits of a solar system.

- The long term performance results show that a gas-fired cooled Dunkle system with reasonable levels of component performance (system B, table 6.4.1) can meet the cooling loads in a variety of climates with a thermal COP near 0.8 and an electric COP in the range of 8-14. A significant increase in seasonal thermal COP can be obtained in hot and dry climates by making use of regenerative evaporative cooling.

- It appears that the gas-fired cooled Dunkle system has slightly higher operating costs than a comparable adiabatic system. The margin is fairly large in

climates with large cooling loads. In mild climates, the difference is small.

- The cooled Dunkle cycle can operate at lower regeneration temperatures than can the adiabatic cycles. Therefore more useful energy can be obtained from the solar system by the cooled Dunkle cycle. In mild climates, this can give a small operating cost advantage to the cooled Dunkle cycle.

- The cooled Dunkle cycle can be more competitive with adiabatic cycles if improvements are made in the cooled dehumidifier performance. The use of unbalanced flow in the dehumidifier at low regeneration temperatures results in an increase in cooling capacity and enables the system to meet the cooling load while regenerating with ambient air. This situation occurs most frequently in hot, dry climates and results in a large rise in seasonal thermal COP. A more efficient dehumidifier (better heat and mass transfer) can also increase cooled Dunkle cycle performance.

- The other cooled dehumidifier cycle of interest, the cooled recirculation cycle, shows performance characteristics similar to the cooled Dunkle cycle. No particularly significant advantages over the cooled Dunkle cycle are apparent. Long term estimates of

cooled recirc performance are not expected to show any significant increase over cooled Dunkle performance.

- o The cooled dehumidifiers modeled in this work represent significant improvements over what is currently available (table 4.3.1). The physical construction of the cooled dehumidifier is necessarily more complex than an adiabatic dehumidifier because of the cooling stream. It may be difficult to manufacture a high effectiveness cross- or counter-cooled dehumidifier as compactly as an adiabatic unit. The development of the adiabatic dehumidifier is well under way with high performance units on the drawing board [3] and prospects for further improvement ([3], unbalanced flow [7]). It may be difficult for the cooled dehumidifier systems to overcome these challenges.

Based on these conclusions, the following recommendations are made.

- oo It is recommended that the development of desiccant dehumidifier air-conditioning systems for residential scale applications continue to be pursued. Improvements in both electrical as well as thermal performance should be considered. Continued development of accurate, easily computed models of dehumidifier and system performance is also important.

oo Solar-fired operation of desiccant systems should continue to be investigated. In particular, economical collector array sizes should be determined.

oo It is recommended that emphasis be placed on adiabatic dehumidifier systems because of extensive past efforts, current level of development, and apparent operating cost advantage. Consideration of cooled dehumidifier systems is warranted because of the potential for efficient solar-fired operation in mild climates.

oo Appropriate control strategies and systems need to be developed which will maximize system performance. Optimum load/system interaction may require control over system flowrate and load inlet evaporative cooler performance to match system cooling capacity to the load in proper proportion of latent and sensible parts. Control over regeneration temperature may be required to optimize electric and thermal performance. For this reason also, more sophisticated solar system controls may be needed to control the air temperature returned to the desiccant system and to match collector flowrate with system flowrate.

oo If further investigation of cooled dehumidifier systems is continued, it is recommended that efforts be

made to improve dehumidifier performance. In particular, the potential benefits of operation with unbalanced flow at low regeneration temperatures should be considered. Development of an easily computed model in which the performance parameters can be determined from the design of the dehumidifier is desirable.

REFERENCES

1. American Gas Association Monthly, Vol. 64, No. 5, May 1982.

2. Mr. Glenn Chinery, Tennessee Valley Authority, personal communication.

3. Macriss, R.A., and Zawacki, T.S., "High COP Rotating Wheel Solid Desiccant System," Proc. 9th Energy Technology Conference, Washington, D.C., February (1982).

4. Dunkle, R.V., "A Method of Solar Air-Conditioning," Mech. and Chem. Trans. Inst. Engs. Australia, MC1, 73 (1965).

5. Nelson, J.S., Beckman, W.A., Mitchell, J.W., and Close, D.J., "Open Cycle Desiccant Systems Using Solar Energy," Solar Energy, 21, 273-278 (1978).

6. Jurinak, J.J., and Beckman, W.A., "A Comparison of the Performance of Open Cycle Air Conditioners Utilizing Rotary Desiccant Dehumidifiers," Proc. 1980 Annual Meeting of AS/ISES, 215-219 (1980).

7. Jurinak, J.J., "Open Cycle Desiccant Cooling -- Component Models and System Simulations," Ph.D. thesis, Solar Energy Laboratory, University of Wisconsin-Madison (August 1982).

8. Maclaine-cross, I.L., and Banks, P.J., "Coupled Heat and Mass Transfer in Regenerators -- Prediction Using an Analogy With Heat Transfer," Int'l Jrnl. Heat and Mass Transfer, 15, 1225-1242 (1972).

9. Lunde, P., "Solar Desiccant Air Conditioning with Silica Gel," Proc. 2nd Workshop on the Use of Solar Energy for Cooling of Buildings, SAN/1122-76/2, 280 (1976).

10. Pryor, T., "Heat and Mass Transfer in a Cooled Packed Bed," Ph.D. Thesis, University of Melbourne, Australiz (1982).

11. Gidaspow, D., Lavan, Z., Onishak, M., and Perkari, S., "Development of a Solar Desiccant Dehumidifier," Proc. 13th Intersociety Energy Conversion Engineering Conf., 1623-1627 (1978).

12. Mei, V., and Lavan, Z., "Performance of Cross-Cooled Desiccant Dehumidifiers," ASME paper 80-WA/SOL-34, ASME Winter Annual Meeting, Chicago, Illinois, November (1980).

13. Worek, W.M., and Lavan, Z., "Performance of a Cross-Cooled Desiccant Dehumidifier Prototype," DOE-CS/31589-T9, (DE82003366), August (1980).

14. Roy, D., and Gidaspow, D., "Nonlinear Coupled Heat and Mass Exchange in a Cross-Flow Regenerator," Chem. Engr. Sci., 29, 2101-2114 (1974).

15. Majumdar, P., Worek, W.M., and Lavan, Z., "Simulation of a Cooled Bed Solar Powered Desiccant Air-Conditioning System," Proc. 1982 Annual Meeting of AS/ISES, 567-572 (1982).

16. Banks, P.J., "Coupled Equilibrium Heat and Single Adsorbate Transfer in Fluid Flow Through a Porous Medium: 1. Characteristic Potentials and Specific Capacity Ratios," Chem. Engr. Sci., 74, 1143-1155 (1972).

17. Close, D.J., and Banks, P.J., "Coupled Equilibrium Heat and Single Adsorbate Transfer in Fluid Flow Through a Porous Medium: 2. Predictions for a Silica-Gel Air-Drying Using Characteristic Charts," Chem. Engr. Sci., 27, 1157-1169 (1972).

18. Kays, W.M., and London, A.L., Compact Heat Exhangers, 2nd Ed., McGraw-Hill, New York, 1964.

19. Banks, P.J., "Predictions of Heat and Water Vapour Exchanger Performance from that of a Similar Heat Exchanger," Compact Heat Exchangers -- History, Technological Advancement, and Mechanical Design Problems (ASME 1980 Winter Annual Meeting), HTD-10, 57-74, November (1980).

20. Worek, W.M., "Experimental Performance of a Cross-Cooled Desiccant Dehumidifier Prototype," Ph.D. Thesis, Illinois Institute of Technology, Chicago, IL (1980).

21. Mathiprakasam, B., "Performance Predictions of Silica Gel Desiccant Cooling Systems," Ph.D. thesis, Illinois Institute of Technology, Chicago, IL (1980).

22. Dr. J. Jurinak, personal communication (plot of F_i characteristics for silica gel on mylar).

23. ASHRAE, ASHRAE Handbook 1977 Fundamentals, American Society of Heating, Refrigerating, and Air-Conditioning Engineers, New York (1977).

24. Brandemuehl, M.J., "Analysis of Heat and Mass Transfer Regenerators with Time Varying or Spatially Nonuniform Inlet Conditions," Ph.D. thesis, Dept. of Mech. Engr., University of Wisconsin-Madison (1982).

25. Available from the National Oceanic and Atmospheric Administration.

26. Klein, S.A., et al., TRNSYS, A Transient System Simulation Program, Engineering Experiment Station Report 38-11, Solar Energy Laboratory, University of Wisconsin-Madison, Madison, WI (April 1981).

27. Product literature, "Carrier Weathermaster III Heat Pump System," form 38HQ-5P, Carrier Corp., Syracuse, NY.

28. FCHART, A Design Program for Solar Heating Systems, Engineering Experiment Station Report 50, Solar Energy Laboratory, University of Wisconsin-Madison (September 1980).

29. Duffie, J.A., and Beckman, W.A., Solar Engineering of Thermal Processes, Wiley-Interscience, New York, 1980.

APPENDIX A

CONFIGURATIONS OF OTHER DESICCANT AIR-CONDITIONING SYSTEMS

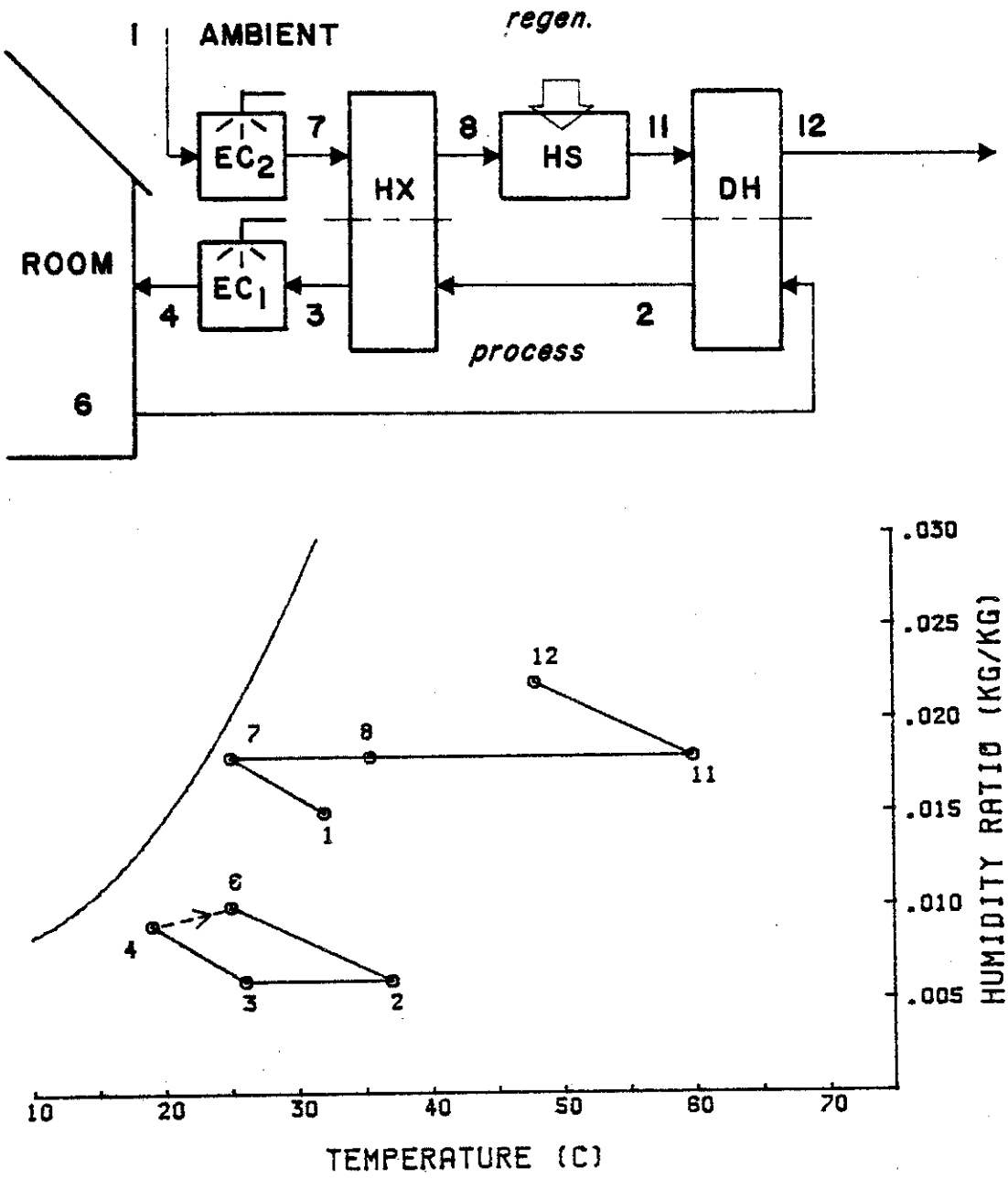

Figure A.1 Recirculation cycle desiccant dehumidifier cooling system.

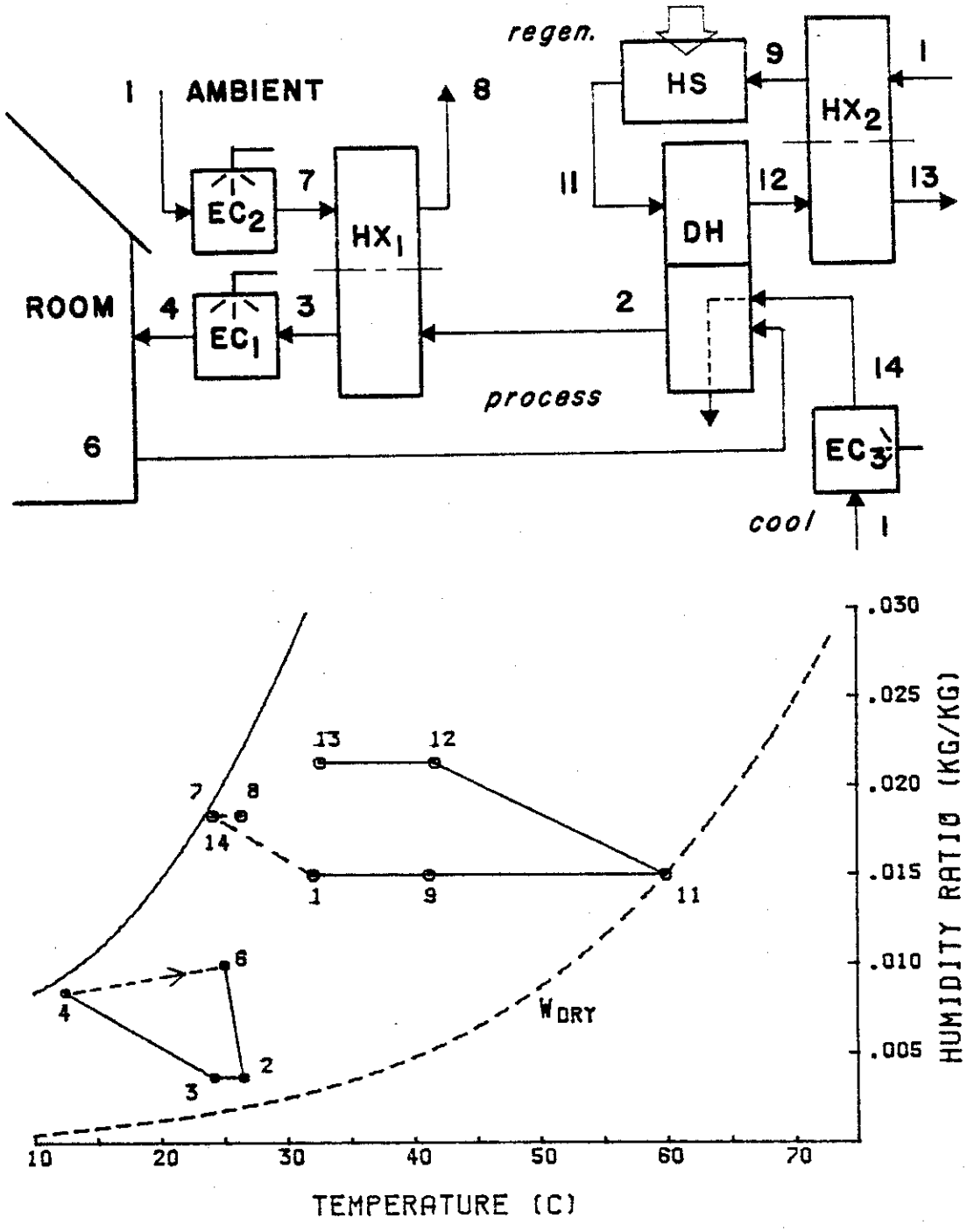

Figure A.2 Cooled recirculation cycle desiccant dehumidifier cooling system.

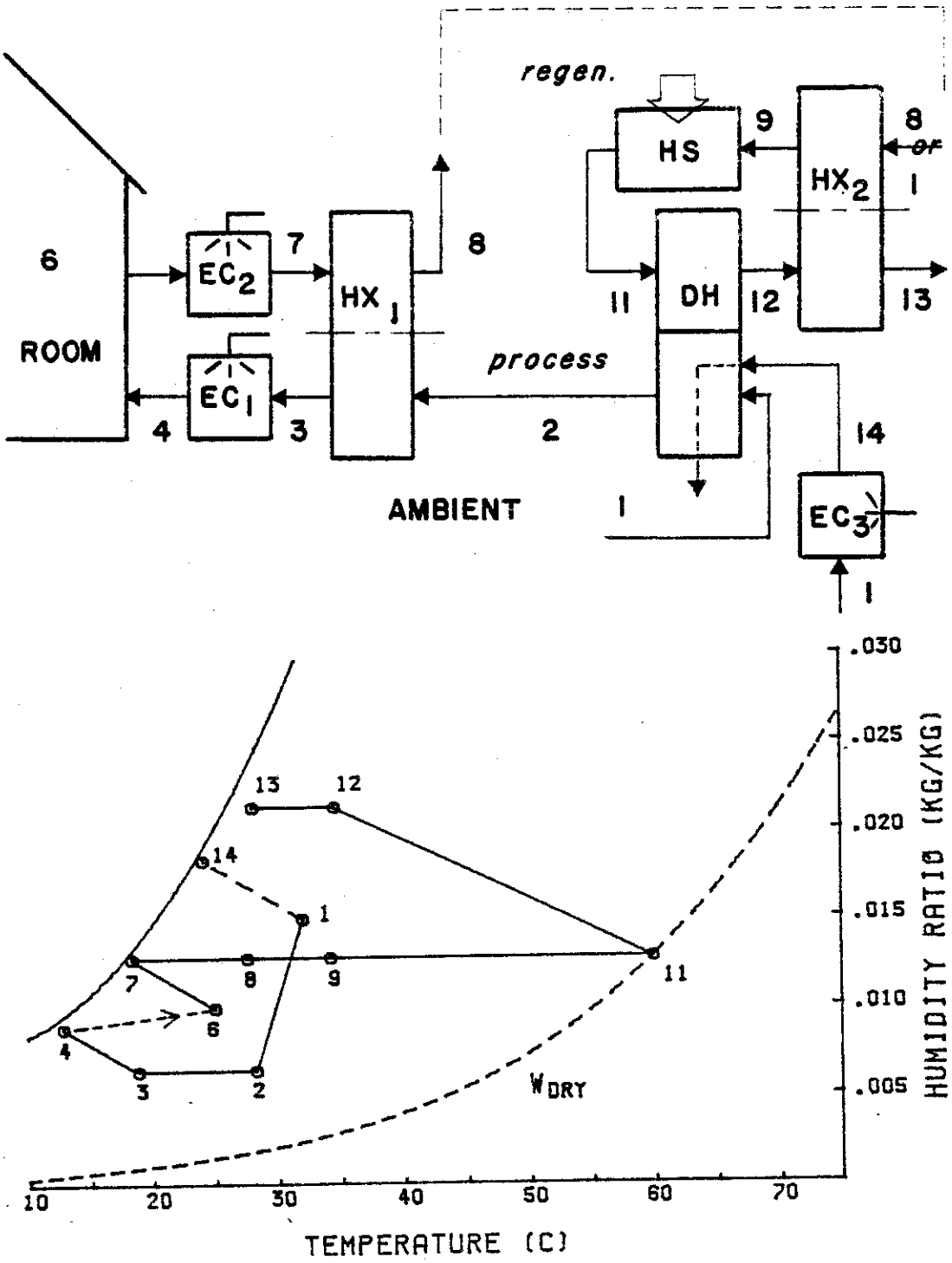

Figure A.3 Cooled ventilation cycle desiccant dehumidifier cooling system.

APPENDIX B

CHARACTERISTICS OF OTHER DESICCANT AIR-CONDITIONING SYSTEMS

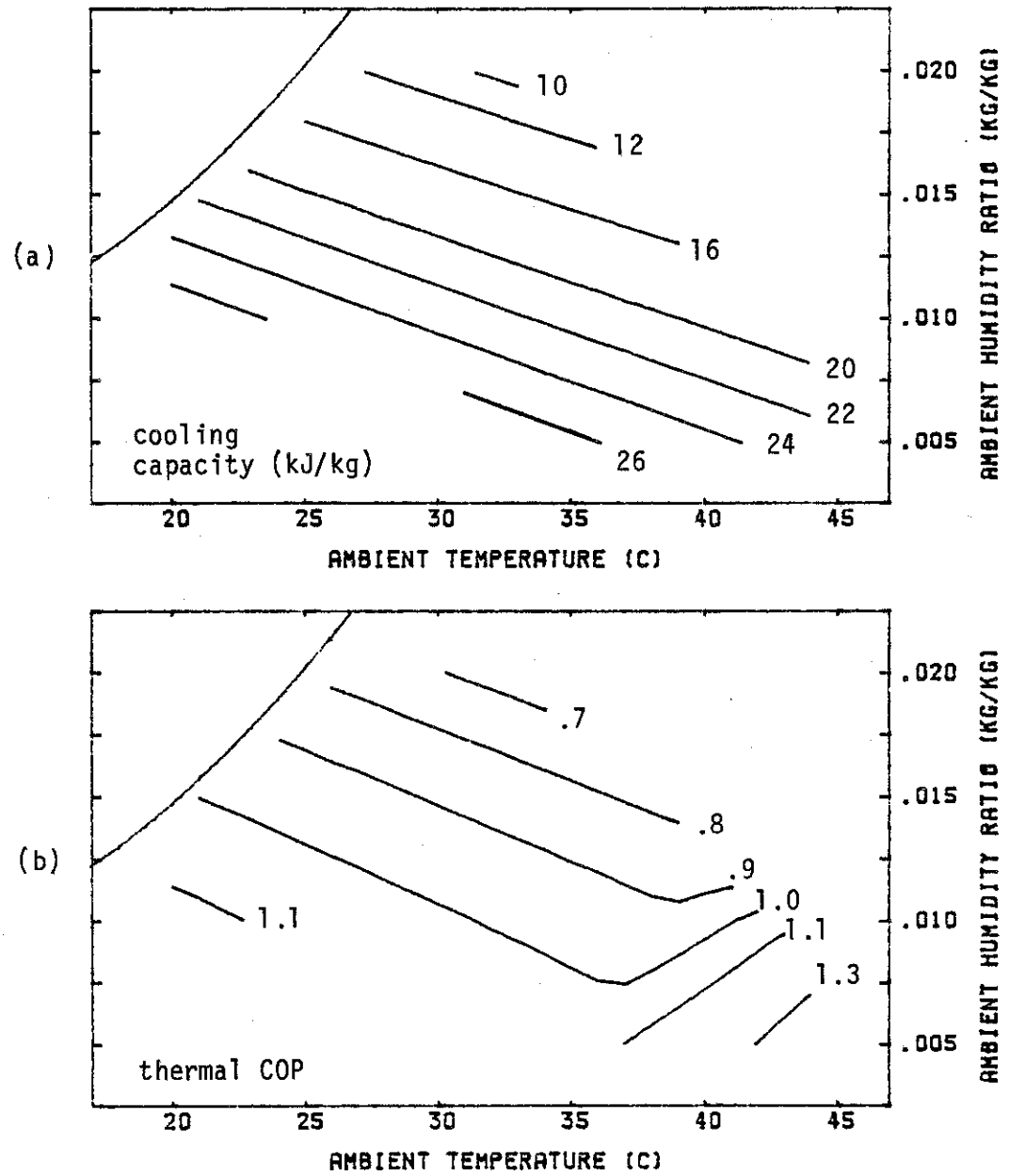

Figure B.1 Cooled recirculation cycle system performance maps.
$\varepsilon_w = .80$ $\varepsilon_t = .85$ $r_c = 1.10$ $\varepsilon_{HX} = .95$ $\varepsilon_{EC} = .96$
$t_{RM} = 25°C$ $w_{RM} = 0.10$ $T_{REG} = 60°C$ $\dot{m}_R/\dot{m}_D = 1.0$
(a) total cooling capacity. (b) thermal COP.

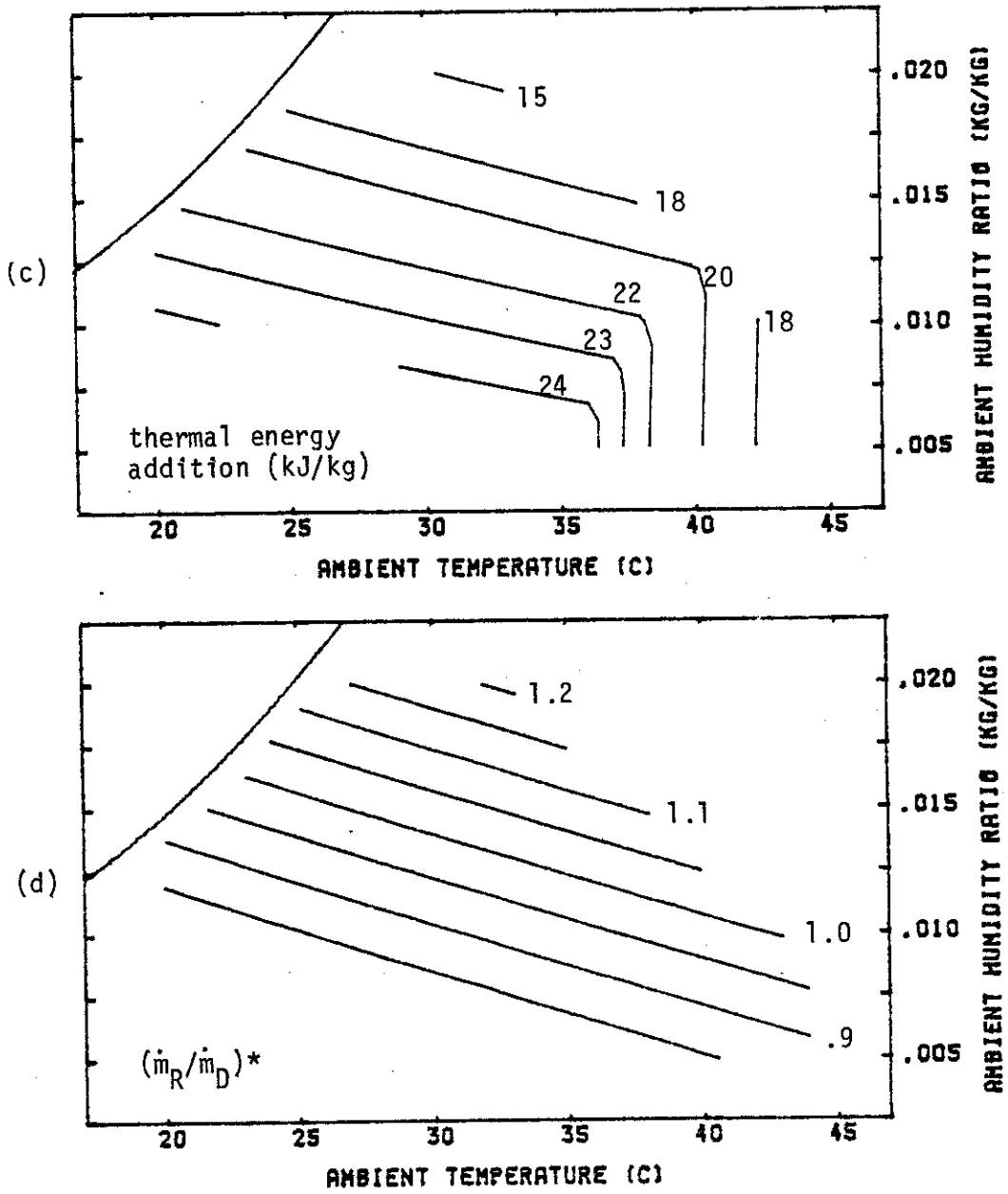

Figure B.1 (cont) (c) required thermal energy addition.
(d) ideal flow ratio, $(\dot{m}_R/\dot{m}_D)^*$.

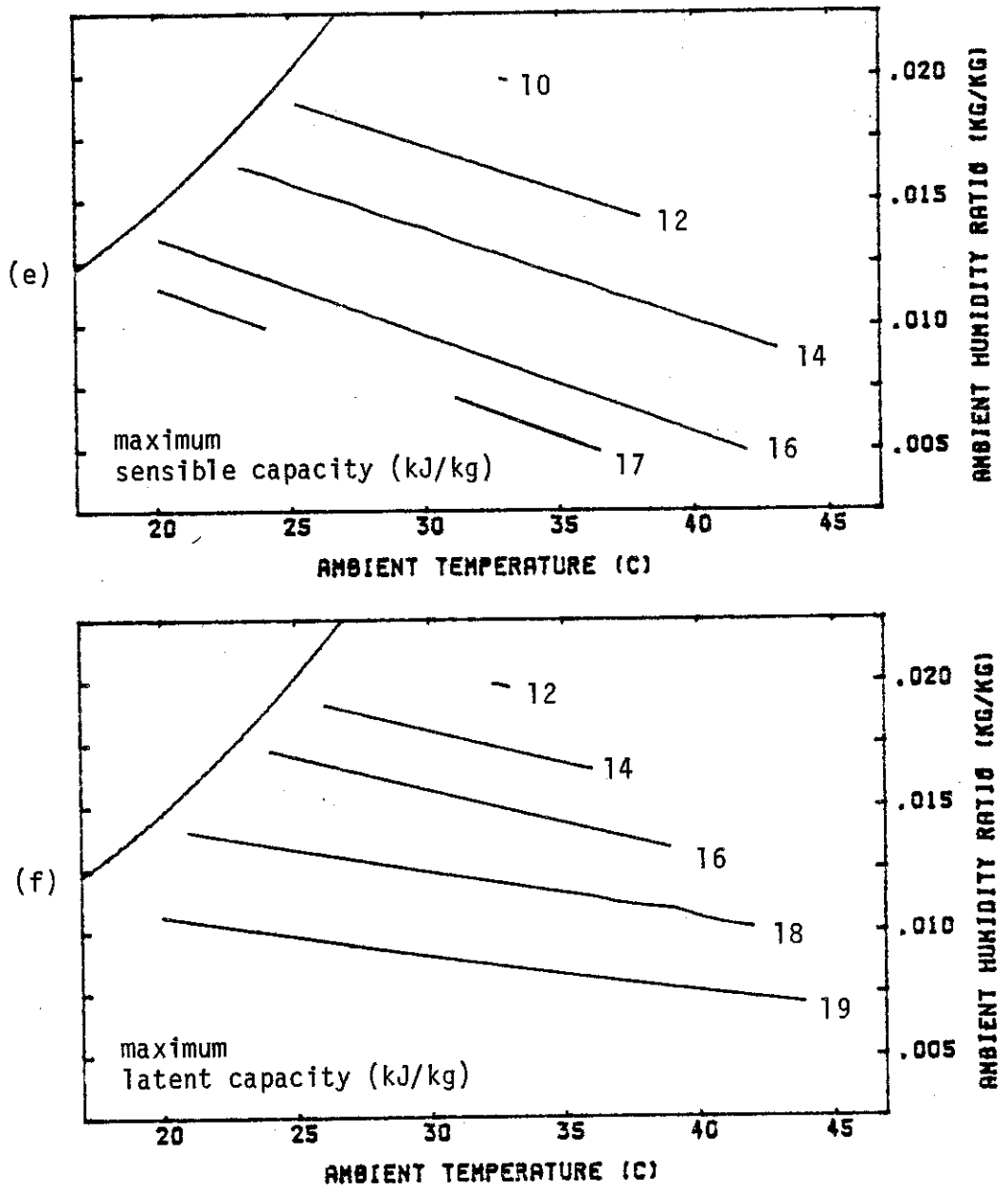

Figure B.1 (cont) (e) maximum sensible cooling capacity.
(f) maximum latent cooling capacity.

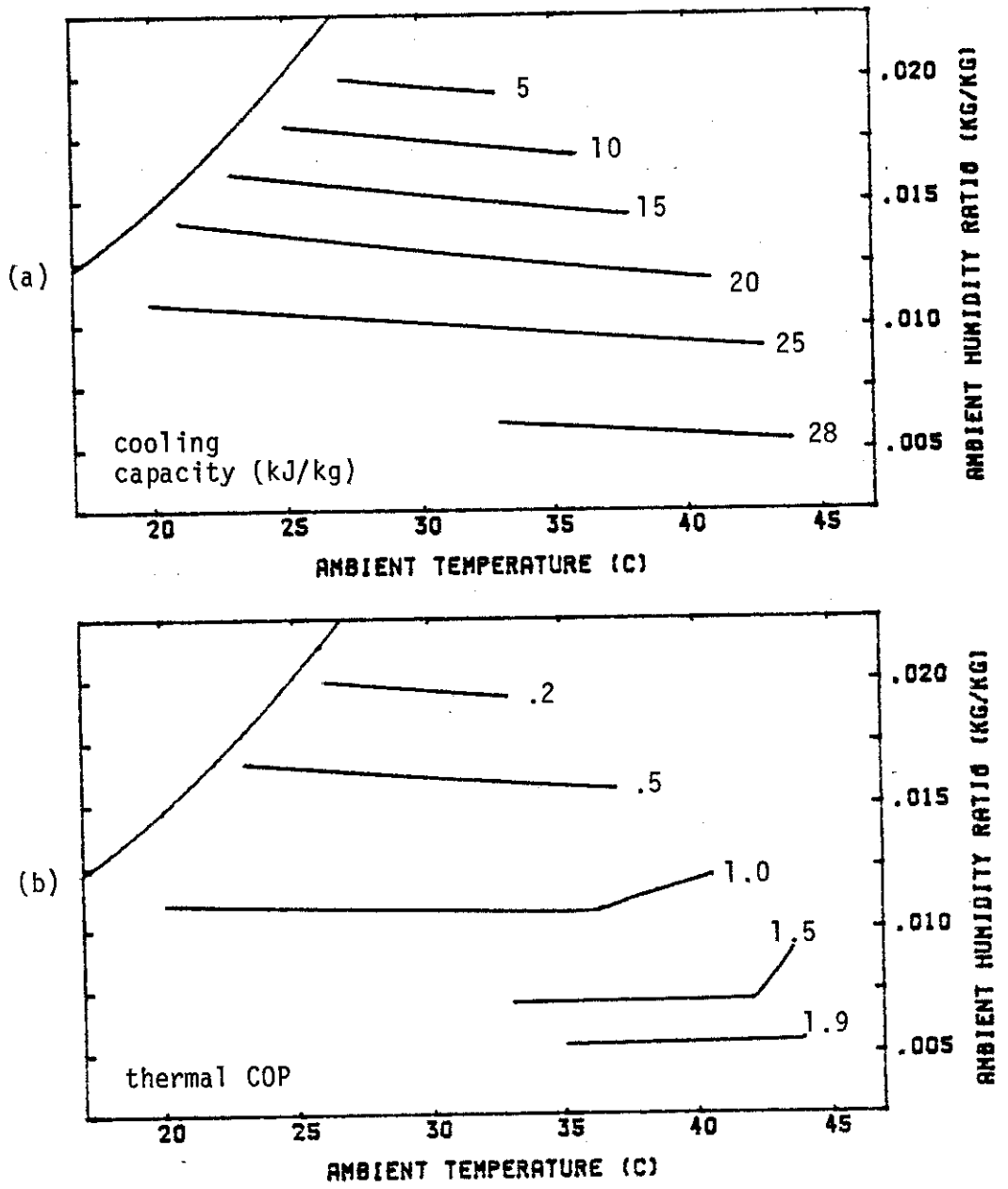

Figure B.2 Cooled ventilation cycle system performance maps.

$\varepsilon_w = .80$ $\varepsilon_t = .85$ $r_c = 1.10$ $\varepsilon_{HX} = .95$ $\varepsilon_{EC} = .96$

$t_{RM} = 25°C$ $w_{RM} = .010$ $T_{REG} = 60°C$ $\dot{m}_R/\dot{m}_D = 1.0$

(a) total cooling capacity. (b) thermal COP.

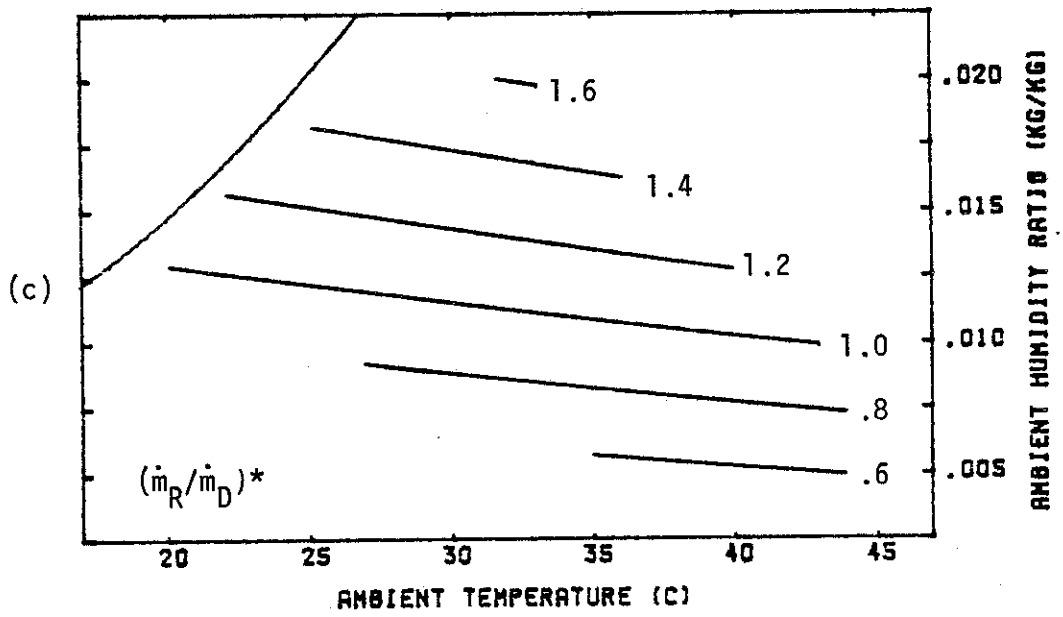

Figure B.2 (cont) (c) ideal flow ratio. $(\dot{m}_R/\dot{m}_D)^*$.

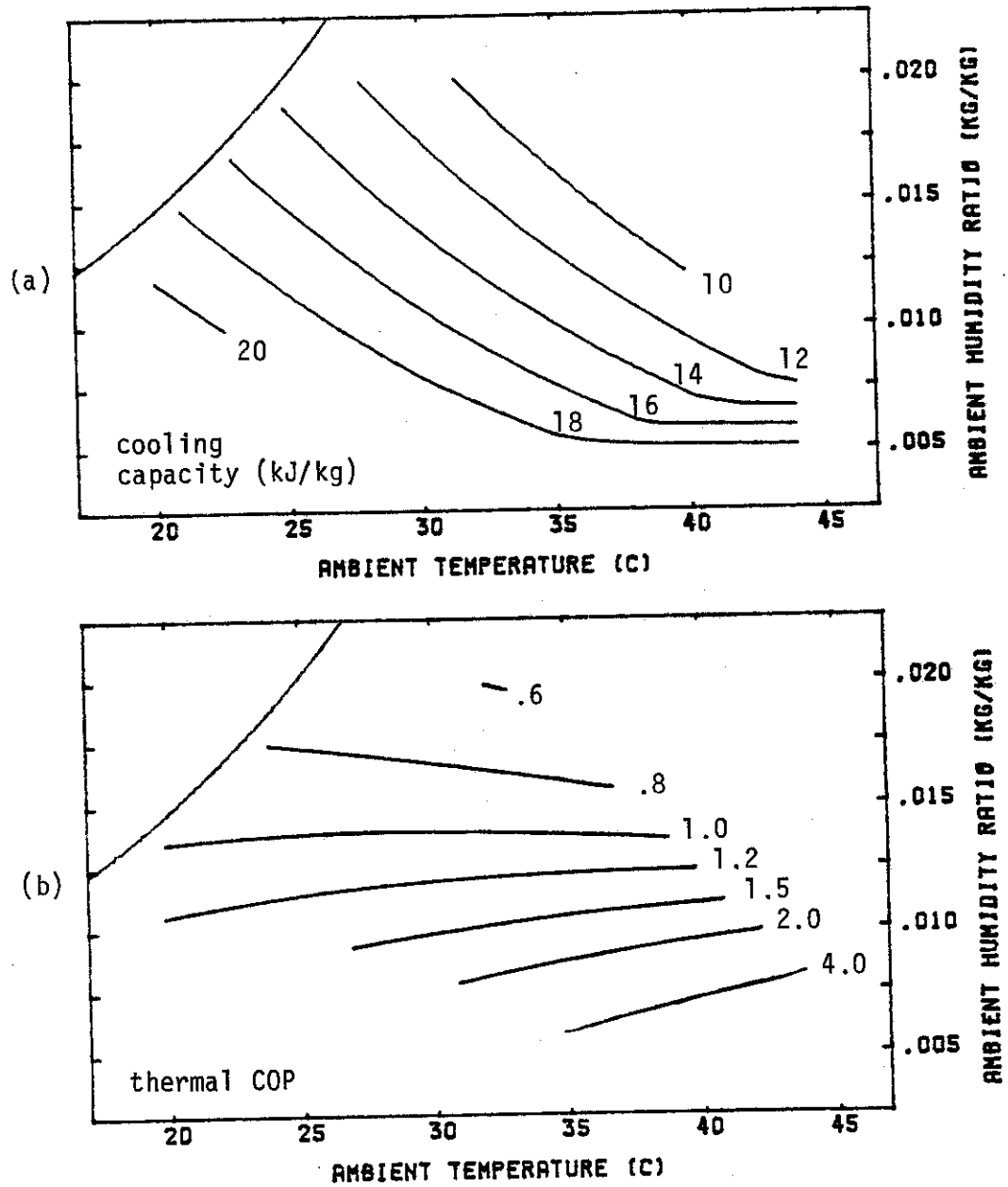

Figure B.3 Adiabatic Dunkle cycle system performance maps.

$\varepsilon_{F_1} = .05$ $\varepsilon_{F_2} = .95$ $\varepsilon_{HX} = .95$ $\varepsilon_{EC} = .96$

$t_{RM} = 25°C$ $w_{RM} = .010$ $T_{REG} = 60°C$

(a) total cooling capacity. (b) thermal COP.

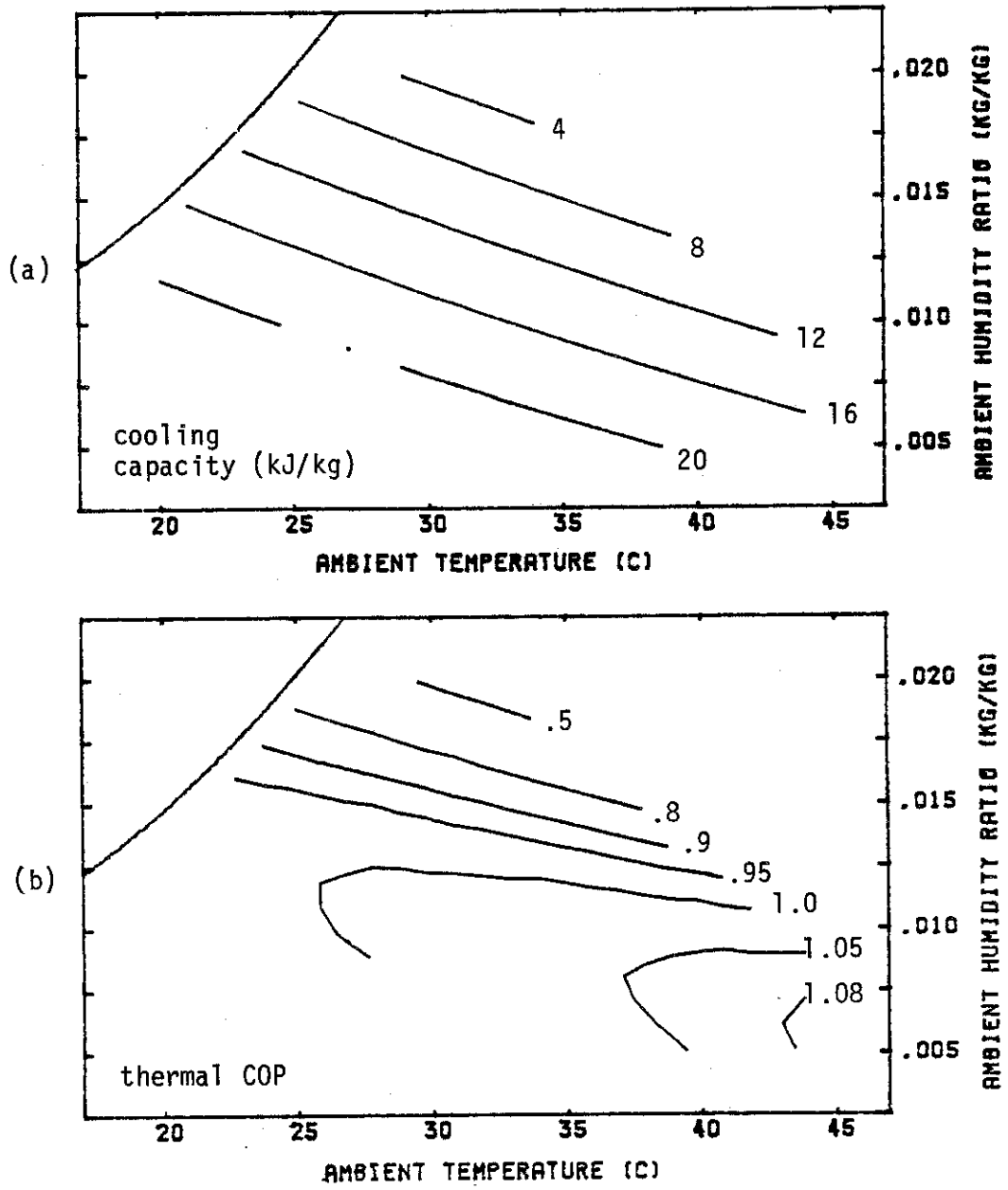

Figure B.4 Adiabatic ventilation cycle performance maps.

$\varepsilon_{F_1} = .05$ $\varepsilon_{F_2} = .95$ $\varepsilon_{HX} = .95$ $\varepsilon_{EC} = .96$

$t_{RM} = 25°C$ $w_{RM} = .010$ $T_{REG} = 60°C$

(a) total cooling capacity. (b) thermal COP.

APPENDIX C

ASSUMED PARAMETERS FOR LIFE CYCLE SAVINGS ANALYSIS BY THE P1, P2 METHOD [29]

N_e	period of analysis	20 yrs
i_f	fuel inflation rate	10%
d	market discount rate	15%
m	mortgage interest rate	12%
D	ratio of downpayment to initial investment	0.2
$\bar{t}$	effective income tax rate	18%
R_v	ratio of resale value to initial investment	1.0

maintenance costs and property taxes were neglected

APPENDIX D

COOLED DUNKLE CYCLE MODEL

TRNSYS SUBROUTINE LISTING

AND

LISTING OF A TYPICAL TRNSYS DECK

```
@PRT,S  KS*TRNSYS,CDKLSYS
FURFUR 28R3 U01 SLIB82 01/06/83 19:52:39

KS*TRNSYS(1),CDKLSYS(0)
     1            SUBROUTINE TYPE32(TIME,XIN,OUT,TD,DTDT,PAR,INFO)
     2      C  MODEL OF COOLED DUNKLE CYCLE DESICCANT AIR-CONDITIONING SYSTEM
     3      C  CONFIGURATION  CC-A/B
     4            DIMENSION  XIN(4),OUT(60),PAR(22),INFO(10)
     5            DIMENSION  TN(21),WN(21),HN(21),TO(21),WO(21)
     6            REAL  MDOTM,MDOTB,MDOTS,MDOTR,MDOTI,LATENT
     7            REAL  MRMD,MRMDS,MRS,MRD,MDOTSR
     8            INTEGER  PC,PX
     9      C
    10            DATA A,B,C/1005.,1859.,2.5014E+6/
    11            DATA A1,A2,A3/2865.,4.344,.8624/
    12            DATA B1,B2,B3/6360.,1.127,.07969/
    13            DATA EX/1.490/
    14            DATA C1,C2,C3/3.2438,5.8683E-3,1.1702E-8/
    15            DATA C4,C5,C6/2.1878E-3,218.17,2.3026/
    16            DATA CM,CL,DC/.921,4.187,.06445/
    17            DATA TMIN,WMIN,EXCMAX/100.,1.,0./
    18            DATA CLDMAX,QAUXM/0.,0./
    19            DATA IOPT,NI,NP,ND,NO/1,4,22,0,60/
    20      C
    21      C   UNITS: TEMPERATURE    T = DEG C
    22      C          SP HUMIDITY    W = KG-WATER/KG-AIR
    23      C          MATRIX WATER   X = KG-WATER/KG-MATRIX
    24      C          AIR ENTHALPY   H = J/KG
    25      C
    26      C  FUNCTIONS:
    27      C   MOIST AIR ENTHALPY  (TREF = 0 C)
    28            ENTH(I) = A*TN(I) + WN(I)*(B*TN(I) + C)
    29      C   TEMPERATURE OF THE MOIST AIR STREAM
    30            TEMP(I) = (HN(I) - C*WN(I))/(A + B*WN(I))
    31      C   SATURATION PRESSURE  (ATM)
    32            BT(T) = 374.12 - T
    33            PSAT(T) = C5*EXP(-C6*BT(T)*(C1 + C2*BT(T) + C3*(BT(T)**3))/
    34           -           ((T+273.15)*(1. + C4*BT(T))))
    35      C   SATURATION SPECIFIC HUMIDITY
    36            WSAT(T) = .62198*PSAT(T)/(1.- PSAT(T))
    37      C   FOR EVAP COOLER CALCULATIONS
```

```
      WW(T,TSTAR,WSTAR) = (A*(TSTAR-T) + WSTAR*(C-2331.*TSTAR))
     -                        /(C + B*T - 4190.*TSTAR)
C     DESICCANT ANALOGY FI CHARACTERISTICS FOR ADIABATIC CASE (5-PAR)
      FONE(I) = -A1/((TN(I)+273.15)**EX) + A2*(WN(I)**A3)
      FTWO(I) = ((TN(I)+273.15)**EX)/B1 - B2*(WN(I)**B3)
C     EQUILIBRIUM RELATIONSHIP FUNCTIONS
      WMAT(X,T) = .0208*(GX(X,T) **HSHV(X))
      GX(X,T) = 60.09*X*PSAT(T)
      DGX(T) = 60.09*PSAT(T)
      HSHV(X) = 1. + .2843*EXP(-10.28*X)
      DHSHV(X) = -2.9226*EXP(-10.28*X)
C     MATRIX PURGE CAPACITY RATES
      CR(X) = CM + CL*X + DC*(1.- EXP(-10.28*X))
C
C     MODES:  0   NO LOAD, MACHINE OFF
C             1   REGENERATIVE EVAPORATIVE COOLING
C             2   DESICCANT COOLING, REGENERATE AT AMBIENT TEMPERATURE
C             3   DESICCANT COOLING, REGENERATE WITH SOLAR
C             4   MODE 3 PLUS AUXILIARY THERMAL
C             5   MODE 4 PLUS AUXILIARY COOLING
C             6   DESICCANT SYSTEM CAN NOT MEET ANY OF LOAD
C
C     NCASE -- INTERSECTION OF LOAD LINE AND SYSTEM PROCESS LINE
C               1     BY-PASS MIXING
C               2     INLET EVAP COOLER PROCESS LINE
C               3     2, BUT WITH EC#2 & HX#1 BY-PASSED
C               4     2, BUT WITH EC#3 BY-PASSED  (NOT USED)
C               5     2, BUT WITH EC#3, EC#2, & HX#1 BY-PASSED
C               6     L-L TO RT OF T2 (EC#3, EC#2, & HX#1 BY-PASSED)
C
C     FLAGS: ICN = -1     AUXILIARY THERMAL ONLY
C                   0     SOLAR IF AVAILABLE, AUX OTHERWISE
C                   1     SOLAR ONLY
C
C            ISOLAR = 0     NO SOLAR AVAILABLE/SOLAR NOT NEEDED
C                     1     SOLAR AVAILABLE/SOLAR USED
C
C            ION = 0    DEHUMIDIFIER NOT IN USE
C                  1    DEHUMIDIFIER IN USE
C
C            NM = 0     ALL MODES AVAILABLE
C                 1     INHIBIT MODE 1
C                 2     INHIBIT MODE 2
C                 3     INHIBIT BOTH MODES 1 AND 2
C
C     INPUT DEFINITIONS:  XIN(1) = AMBIENT TEMPERATURE (C)
C                         XIN(2) = AMBIENT HUMIDITY RATIO (KG/KG)
C                         XIN(3) = TEMP FROM SOLAR SYSTEM (C)
C                         XIN(4) = EXTERNAL HEAT GAIN TO LOAD (WATTS)
C
```

```
C   SET SYSTEM PARAMETERS ON INITIAL CALL OF SIMULATION
      IF(INFO(7).EQ.-1)  THEN
        TREG   = PAR(3)
        MDOTM  = PAR(4)
        ICN    = IFIX(PAR(5))
        ETAH1T = PAR(6)
        ETAH1W = PAR(7)
        ETAH2T = PAR(8)
        ETAH2W = PAR(9)
        ETAEC1 = PAR(10)
        ETAEC2 = PAR(11)
        ETAEC3 = PAR(12)
        EW     = PAR(13)
        ET     = PAR(14)
        RCC    = PAR(15)
        MRD    = PAR(16)
        UA     = PAR(17)
        QDOT   = PAR(18)
        MDOTI  = PAR(19)
        WDOT   = PAR(20)
        ISTK   = IFIX(PAR(21))
        NM = IFIX(PAR(22))
        INFO(6) = 20
        CALL TYPECK(IOPT,INFO,NI,NP,ND)
      ENDIF
C   SET AMBIENT STATE ON INITIAL CALL OF TIMESTEP
      IF(INFO(7).LE.0)  THEN
        TN(1) = XIN(1)
        WN(1) = XIN(2)
          WSN = WSAT(TN(1))
          IF(WN(1).GT.WSN)  THEN
            WRITE(*,601)  TIME,TN(1),WN(1),WSN
 601         FORMAT(6X,'*** ERROR IN INPUT WEATHER DATA:  W > WSAT *
**',
     -             5X,'TIME:',F10.3,5X,'T1=',F6.2,5X,'W1=',F6.4,
     -             5X,'WSAT=',F6.4)
            WN(1) = WSN
          ENDIF
        HN(1) = ENTH(1)
      ENDIF
C   SET REQUIRED VARIABLES TO INITIAL VALUES FOR SYSTEM CALCULATIONS
      IF(INFO(7).GT.0 .AND. MODE.LE.2)  RETURN
        TSOL = XIN(3)
        ISAT = 0
        NCASE = 0
        EXCOOL = 0.
         EXSENS = 0.
         EXLAT = 0.
        QHX1 = 0.
        QHX2 = 0.
```

```
137             J23 = 0
138             JR2 = 0
139             IJK = 0
140            IF(INFO(7).GT.0)  GO TO 202
141             QIN = XIN(4)
142             TN(6) = PAR(1)
143             WN(6) = PAR(2)
144             ICOOL = 0
145             IDRY = 0
146             RMEC = 0.
147             ECCOOL = 0.
148             COOLM2 = 0.
149             MRMDS = 0.
150      C
151      C  LOAD CALCULATIONS  (JEFF'S UA*(DELTA T) MODEL)
152           SENSBL = (UA + MDOTI*(A+B*WN(1)) )*(TN(1)-TN(6)) + QDOT + QIN
153           IF (SENSBL.LE.0.)  THEN
154             TN(6) = TN(1) + (QDOT+QIN)/(UA + MDOTI*(A + B*WN(1)))
155             SENSBL = 0.
156             ICOOL = 1
157             SLOAD = 1.E+20
158             TMAX = TN(6)
159             WSN = WSAT(TN(6))
160             IF(WN(6).GT.WSN)  WN(6) = WSN
161           ENDIF
162           LATENT = (MDOTI*(WN(1)-WN(6)) + WDOT)*(B*TN(6) + C)
163           IF (LATENT.LE.0.)  THEN
164             WN(6) = WN(1) + WDOT/MDOTI
165             LATENT = 0.
166             IDRY = 1
167             SLOAD = 0.
168             WMAX = WN(6)
169           ENDIF
170           CLOAD = SENSBL + LATENT
171              IF(CLOAD.GT.CLDMAX)  CLDMAX = CLOAD
172             HN(6) = ENTH(6)
173             HMAX = HN(6) - CLOAD/MDOTM
174             IF (ICOOL.EQ.1 .AND. IDRY.EQ.1)  THEN
175               MODE = 0
176               RMDOT = 0.
177               GO TO 550
178             ENDIF
179             IF(IDRY.NE.1)  WMAX = WN(6) - (MDOTI*(WN(1)-WN(6)) + WDOT)/M
DOTM
180             IF(ICOOL.NE.1)  TMAX = (HMAX - C*WMAX)/(A + B*WMAX)
181           IF (ICOOL.NE.1 .AND. IDRY.NE.1)
182          :  SLOAD = ((A + B*WMAX)*(MDOTI*(WN(1)-WN(6)) + WDOT))/SENSBL
183           IF (TN(6).LT.TMIN)  TMIN = TN(6)
184           IF (WN(6).LT.WMIN)  WMIN = WN(6)
185      C
```

```
C  EVAPORATIVE COOLER 2 CALCULATION
      ETA = ETAEC2
      L = 6
      J = 7
      ASSIGN 102 TO PC
      GO TO 700
102   CONTINUE
      HN(7) = ENTH(7)
C
C  TRY REGENERATIVE EVAPORATIVE COOLING
      IF (WN(1).LT.WMAX .AND. NM.NE.1 .AND. NM.NE.3)  THEN
        MODE = 1
         ION = 0
         ISOLAR = 0
        TN(2) = TN(1)
        WN(2) = WN(1)
        HN(2) = HN(1)
        TN(3) = TN(2) + ETAH1T*(TN(7) - TN(2))
        WN(3) = WN(2) + ETAH1W*(WN(7) - WN(2))
        HN(3) = ENTH(3)
        WN(8) = WN(2) - WN(3) + WN(7)
        HN(8) = HN(2) - HN(3) + HN(7)
        TN(8) = TEMP(8)
        GO TO 300
      ENDIF
C
C  DEHUMIDIFICATION REQUIRED
C
C   DETERMINE REGENERATION TEMPERATURE
C    IF SOLAR AVAILABLE, USE TEMPERATURE FROM SOLAR SYSTEM
C    IF NOT, OR NOT HOT ENOUGH, USE FIXED AUXILIARY TEMPERATURE
C   REGENERATE WITH AMBIENT?
201   IF(TN(1).LT.25. .OR. NM.EQ.2 .OR. NM.EQ.3)  GO TO 202
      MODE = 2
       ION = 1
       ISOLAR = 0
       J23 = 0
       JR2 = 0
      TN(11) = TN(1)
      GO TO 206
C   SOLAR ALONE ?
202   IF(ICN.GE.0)  THEN
        TN(11) = TSOL
         IF(INFO(7).GT.ISTK .OR. (TN(1).GT.TSOL .AND. NM.NE.2 .AND.
     -                                NM.NE.3))  THEN
           IF(TN(1).GT.TSOL)  TN(11) = TN(1)
           IJK = 1
           IF(ICN.EQ.0)  GO TO 203
           IF(ICN.EQ.1)  GO TO 505
         ENDIF
```

```
236              MODE = 3
237               ION = 1
238               ISOLAR = 1
239               J23 = 0
240               JR2 = 0
241              GO TO 206
242            ENDIF
243      C   ADD/USE AUXILIARY THERMAL ?
244       203  MODE = 4
245             ION = 1
246             IF(ICN.EQ.0)  ISOLAR = 1
247              IF(INFO(7).GT. ISTK+4)  ISOLAR = 0
248             IF(ICN.EQ.1)  GO TO 300
249             IF (TREG.LT.TSOL .OR. TREG.LT.TN(1))  THEN
250               IF(IJK.EQ.0)  GO TO 300
251               IF(IJK.EQ.1)  GO TO 205
252             ENDIF
253            TN(11) = TREG
254             J23 = 0
255             JR2 = 0
256      C
257       205     IJK = 0
258      C  EVAPORATIVE COOLER 2 CALCULATION
259       206  IF(TN(7).EQ.TN(6))  THEN
260              ETA = ETAEC2
261              L = 6
262              J = 7
263              ASSIGN 207 TO PC
264              GO TO 700
265       207  CONTINUE
266              HN(7) = ENTH(7)
267            ENDIF
268      C
269      C  EVAPORATIVE COOLER 3 CALCULATION
270              ETA = ETAEC3
271              L = 1
272              J = 14
273              ASSIGN 210 TO PC
274              GO TO 700
275       210  CONTINUE
276              HN(14) = ENTH(14)
277       212    TN(16) = TN(14)
278      C
279      C  DEHUMIDIFIER-HEAT EXCHANGER CALCULATIONS
280       213  DO 250 M=1,10
281               IF(M.EQ.1)  THEN
282                 WN(9) = WN(1)
283                 WN(8) = WN(7)
284                 TN(8) = TN(14)
285                   IF(J23.EQ.1)  TN(8) = TN(7)
```

```
286               ENDIF
287             WN(11) = WN(9)
288             WN(10) = WN(9)
289             HN(11) = ENTH(11)
290             HN(8) = ENTH(8)
291             DO 215 N=1,21
292               WO(N) = WN(N)
293               TO(N) = TN(N)
294      215    CONTINUE
295     C   FIND STATES  2A(20)  AND  12A(21)
296             F1 = FONE(8)
297             F2 = FTWO(11)
298             WOLD = .01
299             DO 217 I=1,15
300               FF = B1*(F2 + B2*(WOLD**B3)) + A1/(F1 - A2*(WOLD**A3))
301               DFF = B1*B2*B3*(WOLD**(B3-1.)) + A1*A2*A3*(WOLD**(A3-1.))/
302          -                                        ((F1 - A2*(WOLD**A3))**2)
303               WNEW = WOLD - FF/DFF
304                 IF (WNEW.LT.0.)  WNEW = 0.1*WOLD
305                 IF (ABS((WNEW-WOLD)/WOLD).LT..01)  GO TO 218
306               WOLD = WNEW
307      217    CONTINUE
308               WRITE(*,661)  F1,F2,WOLD
309      661       FORMAT(1X/5X,'*** ANALOGY FOR  2A,12A  DID NOT CONVERGE *
**'/
310          -              10X,'F1=',E11.5,5X,'F2=',E11.5,5X,'WOLD=',E11.5/
/)
311               GO TO 991
312      218    WN(20) = WNEW
313             TN(20) = (B1*(F2 + B2*(WN(20)**B3)))**(1/EX) - 273.15
314             HN(20) = ENTH(20)
315             WN(21) = WN(8) - WN(20) + WN(11)
316             HN(21) = HN(8) - HN(20) + HN(11)
317             TN(21) = TEMP(21)
318     C   FIND IDEAL DEHUMIDIFIER STATES  2*(16)  AND  12*(17)
319     C     DESORBED MATRIX WATER CONTENT
320               T = TN(11)
321               W = WN(11)
322               ASSIGN 220 TO PX
323               GO TO 800
324      220    CONTINUE
325               XD = XX
326               WN(16) = WMAT(XD,TN(16))
327               HN(16) = ENTH(16)
328     C     SORBED MATRIX WATER CONTENT
329               T = TN(14)
330               W = WN(8)
331               ASSIGN 225 TO PX
332               GO TO 800
333      225    CONTINUE
```

```
334               XW = XX
335       C     MATRIX STATE AS LEAVES PREHEAT PURGE
336               CRR = CR(XD)/CR(XW)
337               TN(18) = (1. - CRR)*TN(14) + CRR*TN(11)
338               WN(18) = WMAT(XW,TN(18))
339               HN(18) = ENTH(18)
340       C     REGENERATION SIDE ANALOGY CALCULATIONS
341               F1 = FONE(11)
342               F2 = FTWO(18)
343               WOLD = .015
344               DO 230 I=1,15
345                 FF = B1*(F2 + B2*(WOLD**B3)) + A1/(F1 - A2*(WOLD**A3))
346                 DFF = B1*B2*B3*(WOLD**(B3-1.)) + A1*A2*A3*(WOLD**(A3-1.))/
347              -                                        ((F1 - A2*(WOLD**A3))**2)
348                 WNEW = WOLD - FF/DFF
349                   IF (WNEW.LT.0.)  WNEW = 0.1*WOLD
350                   IF (ABS((WNEW-WOLD)/WOLD).LT..01)  GO TO 233
351                 WOLD = WNEW
352        230    CONTINUE
353                 WRITE(*,662)  F1,F2,WOLD
354        662       FORMAT(1X/5X,'*** ANALOGY FOR  2*,12*  DID NOT CONVERGE *
**'/
355              -              10X,'F1=',E11.5,5X,'F2=',E11.5,5X,'WOLD=',E11.5/
/)
356                 GO TO 991
357        233    WN(17) = WNEW
358               TN(17) = (B1*(F2 + B2*(WN(17)**B3)))**(1/EX) - 273.15
359               HN(17) = ENTH(17)
360               WN(19) = WN(11) + WN(18) - WN(17)
361               HN(19) = HN(11) + HN(18) - HN(17)
362               TN(19) = TEMP(19)
363       C
364               MRMDS = (WN(8)-WN(16))/(WN(17)-WN(11))
365       C   REAL OUTLET STATES
366               TN(2) = TN(20) - ET*(TN(20) - TN(14))
367                 IF(MRD.LT.0.)  MRMD = MRMDS
368                 IF(MRD.GT.0.)  MRMD = MRD
369                MRS = MRMD/MRMDS
370               IF(MRS.LE.1.)  WN(2) = WN(8) - EW*MRS*(WN(8) - WN(16))
371               IF(MRS.GT.1.)  WN(2) = WN(8) - EW*(WN(8) - WN(16))
372                 IF(MODE.EQ.2 .AND. WN(2).GT.WN(6))  GO TO 202
373               HN(2) = ENTH(2)
374               WN(12) = WN(11) + (WN(8) - WN(2))/MRMD
375               HN(12) = HN(21) + (1. - RCC)*(HN(20) - HN(2))/MRMD
376               TN(12) = TEMP(12)
377       C     HEAT EXCHANGER 1 CALCULATIONS
378                 IF(TN(7).LT.TN(2) .AND. J23.EQ.0)  THEN
379                   TN(3) = TN(2) - ETAH1T*(TN(2) - TN(7))
380                   WN(3) = WN(2) - ETAH1W*(WN(2) - WN(7))
381                   HN(3) = ENTH(3)
```

```
382               WN(8) = WN(2) - WN(3) + WN(7)
383               HN(8) = HN(2) - HN(3) + HN(7)
384               TN(8) = TEMP(8)
385             ELSE
386               IF(J23.EQ.0)  THEN
387                 TN(7) = TN(6)
388                 WN(7) = WN(6)
389                 HN(7) = HN(6)
390                 J23 = 1
391                 GO TO 212
392               ENDIF
393               TN(3) = TN(2)
394               WN(3) = WN(2)
395               HN(3) = HN(2)
396             ENDIF
397       C     HEAT EXCHANGER 2 CALCULATIONS
398             IF(TN(12).GT.TN(1))  THEN
399               TN(9) = TN(1) + ETAH2T*(TN(12) - TN(1))
400               WN(9) = WN(1) + ETAH2W*(WN(12) - WN(1))
401               HN(9) = ENTH(9)
402               HN(13) = HN(1) - HN(9) + HN(12)
403               WN(13) = WN(1) - WN(9) + WN(12)
404               TN(13) = TEMP(13)
405                IF(WN(13).GT.WSAT(TN(13)))  ISAT = 1
406             ELSE
407               TN(9) = TN(1)
408               WN(9) = WN(1)
409               HN(9) = HN(1)
410               TN(13) = TN(12)
411               WN(13) = WN(12)
412               HN(13) = HN(12)
413             ENDIF
414       C
415             IF(ABS((WN(9)-WO(9))/WO(9)).LT..001 .AND.
416          -     ABS(TN(9)-TO(9)).LT..03  .AND.
417          -     ABS((WN(8)-WO(8))/WO(8)).LT..001 .AND.
418          -     ABS(TN(8)-TO(8)).LT..03)  GO TO 300
419        250  CONTINUE
420               WRITE(*,663)
421        663    FORMAT(1X/5X,'*** DH-HX CALC DID NOT CONVERGE ***'//)
422               GO TO 991
423       C
424        300  IF(JR2.EQ.1 .AND. SLOAD.GT..99E+20 .AND. TN(2).LE.TN(6))  THEN
425        301    TINT = TN(2)
426               WINT = WN(2)
427       C       EEC = 0.   EHX = 0.   ESK = 0.
428               TN(3) = TN(2)
429               WN(3) = WN(2)
430               HN(3) = HN(2)
431               TN(4) = TN(2)
```

```
      WN(4) = WN(2)
      HN(4) = HN(2)
      NCASE = 6
      GO TO 440
    ENDIF
C
C  CALCULATION OF DELIVERED AIR STATE (WITH POSSIBLE BY-PASS MIXING)
 310  IF (WN(2).GT.WN(6) .OR. HN(3).GT.HN(6))  GO TO 501
    IF (MODE.LE.3)  THEN
      IF (WN(2).GT.WMAX .OR. HN(3).GT.HMAX)  GO TO 502
    ENDIF
C
C  EVAPORATIVE COOLER 1 CALCULATIONS
      ETA = ETAEC1
      L = 3
      J = 4
      ASSIGN 330 TO PC
      GO TO 700
 330  CONTINUE
      HN(4) = ENTH(4)
C
C     EEC = ETAEC1
C     EHX = ETAH1T
C       IF(J23.EQ.1)  EHX = 0.
C     ESK = ETAEC3
C       IF(JR2.EQ.1)  ESK = 0.
C   LOAD LINE INTERSECT LINE 4-7 ?
       IF(J23.EQ.1)  GO TO 420
      IF (WN(4).GT.WN(7))  GO TO  420
      S74 = (WN(7) - WN(4))/(TN(7) - TN(4))
        IF (ABS(TN(7)-TN(4)).LT.1.E-6)  S74 = 1.E+20
        IF (ABS(SLOAD-S74).LT.1.E-4)  GO TO 420
      IF (S74.LT..99E+20)  THEN
        TINT = (WN(6) - WN(4) + S74*TN(4) - SLOAD*TN(6))/(S74 - SLOA
D)
          IF (SLOAD.GT..99E+20)  TINT = TN(6)
        WINT = WN(4) + S74*(TINT - TN(4))
          IF(SLOAD.EQ.0.)  WINT = WN(6)
        IF (WINT.GT.WN(7))  GO TO 420
       IF (WINT.GT.WN(4))  THEN
         NCASE = 1
         GO TO 440
       ENDIF
      ELSE
        TINT = TN(4)
        WINT = WN(6) - SLOAD*(TN(6) - TINT)
       IF (WINT.GT.WN(4))  THEN
         NCASE = 1
         GO TO 440
       ENDIF
```

```
481           ENDIF
482       C   LOAD LINE INTERSECT LINE 3-4 ?
483        420  S43 = (WN(4) - WN(3))/(TN(4) - TN(3))
484             TINT = (WN(6) - WN(3) + S43*TN(3) - SLOAD*TN(6))/(S43 - SLOAD)
485               IF (SLOAD.GT.,99E+20)  TINT = TN(6)
486             IF (TINT.LE.TN(3))  THEN
487               WINT = WN(3) + S43*(TINT - TN(3))
488                 IF(SLOAD.EQ.0.)  WINT = WN(6)
489       C         EEC = ETAEC1*(TN(3) - TINT)/(TN(3) - TN(4))
490               TN(4) = TINT
491               WN(4) = WINT
492               HN(4) = ENTH(4)
493               NCASE = 2
494                 IF(J23.EQ.1)  NCASE = 3
495       C         IF(JR2.EQ.1)  NCASE = 4
496                 IF(J23.EQ.1 .AND. JR2.EQ.1)  NCASE = 5
497               GO TO 440
498             ENDIF
499       C   LOAD LINE INTERSECT LINE 2-3 ?
500               IF(J23.EQ.1)  GO TO 435
501             S32 = (WN(3) - WN(2))/(TN(3) - TN(2))
502             TINT = (WN(6) - WN(2) + S32*TN(2) - SLOAD*TN(6))/(S32 - SLOAD)
503               IF (SLOAD.GT.,99E+20)  TINT = TN(6)
504             IF (TINT.LE.TN(2))  THEN
505               J23 = 1
506       C       EEC2 = 0.
507       C       EHX1 = 0.
508               IF(MODE.EQ.1)  THEN
509                 TN(3) = TN(2)
510                 WN(3) = WN(2)
511                 HN(3) = HN(2)
512                 GO TO 300
513               ENDIF
514               WN(7) = WN(6)
515               TN(7) = TN(6)
516               HN(7) = HN(6)
517               GO TO 213
518             ENDIF
519        C   LOAD LINE LIES TO RIGHT OF TN(2),  USE AMBIENT AS SINK
520        C    AND BY-PASS HX1 & EC2, AS NCASE=4 PROBABLY WOULD NOT OCCUR
521         435    IF(JR2.EQ.1)  GO TO 301
522                JR2 = 1
523        C       EEC3 = 0.
524                J23 = 1
525        C       EEC2 = 0.
526        C       EHX1 = 0.
527                IF(MODE.EQ.1)  THEN
528                  TN(3) = TN(2)
529                  WN(3) = WN(2)
530                  HN(3) = HN(2)
```

```
531               GO TO 300
532             ENDIF
533             TN(7) = TN(6)
534             WN(7) = WN(6)
535             HN(7) = HN(6)
536             TN(14) = TN(1)
537             WN(14) = WN(1)
538             HN(14) = HN(1)
539             GO TO 212
540       C
541        440  TN(5) = TINT
542             WN(5) = WINT
543             HN(5) = ENTH(5)
544       C   CHECK TO SEE IF CAN MEET LOAD WITH THIS STATE
545               IF(MODE.EQ.1)  RMEC = CLOAD/(HN(6) - HN(5))
546             IF (TN(5).GT.TMAX .OR. WN(5).GT.WMAX)  GO TO 303
547             MDOTB = CLOAD/(HN(6) - HN(5))
548              RMDOT = MDOTB
549             COOL = CLOAD
550               IF(MODE.EQ.1)  ECCOOL = CLOAD
551               IF(MODE.EQ.2)  COOLM2 = CLOAD
552             IF (NCASE.EQ.1)  THEN
553               MDOTS = MDOTB*(HN(5) - HN(7))/(HN(4) - HN(7))
554               BPR = 1. - MDOTS/MDOTB
555             ELSE
556               MDOTS = MDOTB
557               BPR = 0.
558             ENDIF
559       C
560        460  IF(ION.EQ.1)  THEN
561               MDOTSR = MDOTS
562               MDOTR = MRMD*MDOTS
563               QTHERM = MDOTR*(HN(11)-HN(9))
564               QCC = MDOTS*(HN(2) - HN(8)) + MDOTR*(HN(12) - HN(11))
565             ELSE
566               MDOTSR = 0.
567               MDOTR = 0.
568               QTHERM = 0.
569               QCC = 0.
570             ENDIF
571             IF(ISOLAR.EQ.1 .AND. TN(9).LT.TSOL)  THEN
572               TN(10) = TSOL
573               HN(10) = ENTH(10)
574               QSOL = MDOTR*(HN(10) - HN(9))
575             ELSE
576               ISOLAR = 0
577               TN(10) = TN(9)
578               HN(10) = HN(9)
579               QSOL = 0.
580             ENDIF
```

```
581             QAUX = QTHERM - QSOL
582               IF(QAUX.GT.QAUXM)  QAUXM = QAUX
583             FLOAD = COOL/CLOAD
584               IF(CLOAD.EQ.0.)  FLOAD = 1.
585             FSOL = QSOL/QTHERM
586             COP = COOL/QTHERM
587               IF(QTHERM.EQ.0. .AND. COOL.NE.0.)  COP = 99.
588             COPA = COOL/QAUX
589                IF(QAUX.EQ.0. .AND. COOL.NE.0.)  COPA = 99.
590             QHX1 = MDOTS*(HN(2)-HN(3))
591             QHX2 = MDOTR*(HN(9)-HN(1))
592          C
593          C  OUTPUT OF INFORMATION
594           480  OUT(1) = FLOAT(MODE)
595                OUT(2) = FLOAT(NCASE)
596                OUT(3) = CLOAD*3600.
597                OUT(4) = COOL*3600.
598                OUT(5) = EXCOOL*3600.
599                OUT(6) = MDOTR*3600.
600                OUT(7) = MDOTS*3600.
601                OUT(8) = MDOTR*3600.
602                OUT(9) = QTHERM*3600.
603                OUT(10) = QAUX*3600.
604                OUT(11) = QSOL*3600.
605                OUT(12) = QCC*3600.
606                OUT(13) = COP
607                OUT(14) = COPA
608                OUT(15) = FLOAD
609                OUT(16) = FSOL
610                OUT(17) = TN(9)*FLOAT(ION)
611                OUT(18) = WN(9)*FLOAT(ION)
612                OUT(19) = FLOAT(INFO(7)) + 1.
613                OUT(20) = MDOTR*3600.*FLOAT(ISOLAR)
614           C
615                OUT(21) = SENSBL*3600.
616                OUT(22) = LATENT*3600.
617                OUT(23) = TN(6)
618                OUT(24) = WN(6)
619                OUT(25) = ICOOL
620                OUT(26) = IDRY
621                OUT(27) = TMIN
622                OUT(28) = WMIN
623                OUT(29) = EXCMAX
624                OUT(30) = COOLM2*3600.
625                OUT(31) = MDOTSR*3600.
626                OUT(32) = MDOTSR/MDOTM
627                OUT(33) = QHX1*3600.
628                OUT(34) = QHX2*3600.
629                OUT(35) = FLOAT(ISAT)
630                OUT(36) = TMAX
```

```
      OUT(37) = WMAX
      OUT(38) = HMAX
      OUT(39) = SLOAD
      OUT(40) = ECCOOL*3600.
C
      OUT(41) = MDOTM
      OUT(42) = QAUXM
      OUT(43) = MDOTB/MDOTM
      OUT(44) = MDOTS/MDOTM
      OUT(45) = MDOTR/MDOTM
      OUT(46) = CLDMAX
      OUT(47) = RMDOT/MDOTM
      OUT(48) = RMEC*3600.
      OUT(49) = RMEC/MDOTM
      OUT(50) = MRMDS
      OUT(51) = MRMD
      OUT(52) = BPR
      OUT(53) = EXSENS*3600.
      OUT(54) = EXLAT*3600.
      OUT(55) = TN(10)*FLOAT(ION)
      OUT(56) = TN(11)*FLOAT(ION)
      OUT(57) = (TN(10) - TN(9))*FLOAT(ION)
      OUT(58) = FLOAT(ISOLAR)
      OUT(59) = TN(10) * FLOAT(ISOLAR)
      OUT(60) = CLOAD/1000.
C
      IF(IOPT.EQ.-1)  GO TO 992
      IF(COOL.GT.CLOAD .OR. MDOTS.GT.MDOTB .OR. MDOTB.GT.MDOTM .OR.
     -   MDOTB.LT.0. .OR. QAUX.LT.0. .OR. QSOL.LT.0. .OR.
     -   COOL.LT.0.)  THEN
        WRITE(*,665)
 665    FORMAT(1X/5X,'*** NONSENSE VALUE IN AN OUTPUT ***'/)
        IOPT = -1
        GO TO 992
      ENDIF
C
      RETURN
C
C  CAN NOT MEET LOAD IN PRESENT MODE, GO TO NEXT MODE
 501  GO TO (201,202,203,505),MODE
 502  GO TO (201,202,203),MODE
 503  GO TO (201,202,203,504),MODE
C
C  SYSTEM CAN NOT MEET ALL OF THE LOAD.  FIND AUXILIARY COOLING REQU
IRED
 504  IF (HN(5).GE.HN(6) .OR. WN(5).GT.WN(6))  GO TO 505
        MODE = 5
        MDOTB = MDOTM
        RMDOT = CLOAD/(HN(6) - HN(5))
        MDOTS = MDOTB*(HN(5)-HN(7))/(HN(4)-HN(7))
```

```
      TN(J) = TIN + ETA*(TSTAR - TIN)
      WN(J) = WIN + ETA*(WSTAR - WIN)
     GO TO PC,(102,207,210,330)
704  WRITE(*,671)  L,J,MODE,TN(L),WN(L),WSIN
671    FORMAT(1X/3X,'INPUT ERROR TO EVAP COOLER'/
     -         10X,'L=',I2,5X,'J=',I2,5X,'MODE=',I2,5X,'TL=',F6.2,5X
,
     -         'WL=',F8.6,5X,'WLS=',F8.6/)
      GO TO 991
706  WRITE(*,672)  L,J
672   FORMAT(1X/5X,'*** EVAP COOLER DID NOT CONVERGE ***'/
     -         10X,'L=',I2,7X,'J=',I2//)
      GO TO 991
C
C  EQUILIBRIUM SUBROUTINE
800  XLST = .10
     DO 810 IX=1,15
       GXK = GX(XLST,T)
       DGXK = DGX(T)
       HSHVK = HSHV(XLST)
       DHSHVK = DHSHV(XLST)
       FX = .0208*(GXK**HSHVK) - W
       DFX = .0208*(HSHVK*(GXK**(HSHVK-1.))*DGXK
     -         + (ALOG(GXK))*(GXK**HSHVK)*DHSHVK)
       XNXT = XLST - FX/DFX
         IF(XNXT.LT.0.)  XNXT = 0.1*XLST
         IF (ABS((XNXT-XLST)/XLST).LT..01) GO TO 820
       XLST = XNXT
810  CONTINUE
       WRITE(*,681)  T,W
681     FORMAT(1X/5X,'*** EQUILIBRIUM SUBROUTINE DID NOT CONVERGE *
**'/
     -      10X,'T= ',F5.2,5X,'W= ',F6.5//)
      GO TO 991
820  XX = XNXT
     GO TO PX,(220,225)
C
991  IOPT = -1
     GO TO 480
992  WRITE(*,692)  TIME,MODE,NCASE,TN(1),WN(1)
692   FORMAT(1X/' ***ERROR IN COOLSYS -- EXECUTION TERMINATED***'/
     -         10X,'TIME:',F10.3,5X,'MODE:',I3,5X,'NCASE:',I3,
     -         5X,'TAMB=',F6.2,5X,'WAMB=',F6.4//)
     WRITE(*,693)
693   FORMAT(16X,'TEMP (C)',10X,'SP HUMIDITY',10X,'ENTHALPY',
     -         13X,'TO',16X,'WO'/)
     WRITE(*,694)  (I,TN(I),WN(I),HN(I),TO(I),WO(I), I=1,21)
694   FORMAT(6X,I2,8X,F6.2,12X,F8.6,12X,E10.4,10X,F6.2,10X,F8.6)
     WRITE(*,695)  (PAR(I), I=1,NP)
695   FORMAT(1X/5X,'PARAMETERS'/4(1X,10(E12.4)/) )
```

```
680              BPR = 1.- MDOTS/MDOTB
681              COOL = MDOTB*(HN(6) - HN(5))
682               IF(NCASE.EQ.6 .AND. COOL.GT.CLOAD)  COOL = CLOAD
683              EXCOOL = CLOAD - COOL
684               EXSENS = SENSBL - MDOTB*(A + B*WN(5))*(TN(6) - TN(5))
685               EXLAT = LATENT - MDOTB*(B*TN(6) + C)*(WN(6) - WN(5))
686               IF (EXCOOL.GT.EXCMAX)  EXCMAX = EXCOOL
687              GO TO 460
688      C
689      C  SYSTEM OVERLOAD
690       505  MODE = 6
691            EXCOOL = CLOAD
692             EXSENS = SENSBL
693             EXLAT = LATENT
694             IF (EXCOOL.GT.EXCMAX)  EXCMAX = EXCOOL
695            RMDOT = -1.
696      C
697      C  TURN SYSTEM OFF  (MODE 0 OR 6)
698       550   ION = 0
699            NCASE = 0
700            ISOLAR = 0
701            BPR = 0.
702      C     EEC = 0.   EHX = 0.   ESK = 0.
703            MDOTB = 0.
704            MDOTS = 0.
705            COOL = 0.
706            GO TO 460
707      C
708      C  EVAPORATIVE COOLER SUBROUTINE
709       700  WIN = WN(L)
710            TIN = TN(L)
711            WOLD = WIN
712            TSTAR = TIN
713              IC = 0
714              TLOW = -10.
715            WSIN = WSAT(TIN)
716              IF (WIN.GT.WSIN) GO TO 704
717       701    IC = IC + 1
718                IF (IC.GT.100)  GO TO 706
719              WSTAR = WSAT(TSTAR)
720            WNEW = WW(TIN,TSTAR,WSTAR)
721              IF (ABS(WNEW-WOLD).LT..00001)  GO TO 703
722              IF ((WNEW-WOLD).GT.0.)  TSAVE = TSTAR
723              IF ((WNEW-WOLD).LT.0.)  GO TO 702
724                TSTAR = AMAX1(TLOW,TSTAR-5.)
725                GO TO 701
726       702    TLOW = TSTAR
727              TSTAR = (TSTAR+TSAVE)/2.
728              GO TO 701
729       703  WSTAR = WSAT(TSTAR)
```

```
  778            WRITE(*,696)  (XIN(I), I=1,NI)
  779       696   FORMAT(5X,'INPUTS'/1X,10(E12.4) )
  780            WRITE(*,697)  (OUT(I), I=1,NO)
  781       697   FORMAT(5X,'OUTPUTS'/6(1X,10(E12.4)/) )
  782            CALL TYPECK(IOPT,INFO,NI,NP,ND)
  783            RETURN
  784            END
------>EXIT PRT
```

```
@PRT,S  KS*TRNSYS.MVV60X

KS*TRNSYS(1).MVV60X(1)
     1      * COOLED DUNKLE CYCLE DESICCANT COOLING SYSTEM TRNSYS SIMULATION
     2      *
     3      *  MIAMI    JULY     SOLAR + AUX @ 60C
     4      *  ALL MODES AVAILABLE
     5      *  VERY GOOD HX & EC, VERY GOOD DH     MAX FLOW RATE = .75 KG/SEC
     6      *  COLLECTOR SET FLOW RATE = .75 KG/SEC  --  .015 KG/SEC-M2
     7      *  COLLECTOR STORAGE VOLUME = 12.5 M3  --  .25 M3/M2
     8      *
     9      *  LABELS FOR KS*HISTOGRAM:
    10      *     1 - MODE     2 - NCASE    3 - COP      4 - FLOAD    5 - FSOL
    11      *     6 - RMDOT    7 - MDOTS    8 - MDOTR    9 - MRMDS   10 - MCOLL
    12      *    11 - MDOTSR  12 - COOL    13 - EXCOOL  14 - QAUX    15 - QSOL
    13      *    16 - QTHERM  17 - ECCOOL  18 - INF7/3  19 - INF7/6  20 - MROOK
    14      *
    15       CONSTANTS  36
    16         DTM = .50     NM  =  0
    17         GO  = 4345    STP = 5089    DAY = 182     PRT =   -1     LAT = 25
.5
    18         SLP = 25.5    TRM = 25.     WRM = .012    TREG= 60.      MDM = .7
5
    19         ICN = 0       H1T = .95     H1W = 0.      H2T = .95      H2W = 0.
    20         EC1 = .96     EC2 = .96     EC3 = .96
    21         EW  = .90     ET  = .95     RCC = 1.05    MRD = 1.0      TRC = 1
    22         UA  = 1000.   QDT = 750.    MDI = .0766   WDT = .00014   STK = 5
    23         SP1 = STP - 1   AC = 50.         FLC = 2700.     VOL = 12.5
    24         FRT = .49       FUL = 1.026E+4
```

```
@PRT,S  KS*TRNSYS.CDKLDECK

KS*TRNSYS(1).CDKLDECK(0)
     1      *TRNSYS DECK FOR SYSTEM COOLED DUNKLE SYSTEM + SOLAR
     2       SIMULATION    GO  STP  DTM
     3       TOLERANCES    -.05  -.05
     4       LIMITS       35  20  32
     5       WIDTH         120
     6       NOLIST
     7      *
     8       UNIT 1  TYPE 9     CARD READER
     9        PARAMETERS  16
    10         4  1,  -1  1000  0,  -2  1000  0,  3  0.1  0,  4  .0001  0,  -1
1
    11      (T20,F4.0,1X,F4.0,T30,F4.0,T53,F4.0)
    12      *
    13       UNIT 2  TYPE 16     RADIATION PROCESSOR
    14        PARAMETERS  7
    15         5  1  DAY  LAT  4.871E+6  0  -1
    16        INPUTS  7
    17         1,2  1,1  1,19  1,20  0,0  0,0  0,0
    18          0.   0.   0.    1.    .2  SLP   0.
    19      *
    20       UNIT 3  TYPE 32     DESICCANT SYSTEM  CC-A
    21        PARAMETERS  22
    22         TRM  WRM  TREG  MDM  ICN  H1T  H1W  H2T  H2W  EC1  EC2  EC3
    23         EW   ET   RCC   MRD  UA   QDT  MDI  WDT  STK  NM
    24        INPUTS  4
    25         1,3  1,4  6,1  0,0
    26         25.  .012  0.   0.
    27      *
    28       UNIT 4  TYPE 38     EXTRA OUTPUT #1 FOR TYPE 32
    29        PARAMETERS  1
    30         TRC
    31        INPUTS  1
    32         3,19
    33          10
    34      *
    35       UNIT 5  TYPE 38     EXTRA OUTPUT #2 FOR TYPE 32
    36        PARAMETERS  1
    37         TRC
    38        INPUTS  1
    39         3,19
```

```
40          10
41       *
42        UNIT 6  TYPE 22     SOLAR AIR COLLECTOR AND STORAGE
43         PARAMETERS  11
44          AC  FLC  -1.  FRT  FUL  3.  VOL  1600.  840.  0.  20.
45         INPUTS  6
46          2,6  1,3  3,17  3,18  3,20  0,0
47           0.  25.  25.   .012   0.   25.
48         DERIVATIVES  5
49          40.  40.  40.  40.  40.
50       *
51        UNIT 7  TYPE 25     PRINTER
52         PARAMETERS  4
53          PRT  GO  SP1  -1
54         INPUTS  5
55          4,7   4,8   4,9     5,2    5,6
56          TMIN  WMIN  EXCMAX  QAUXM  CLDMAX
57       *
58        UNIT 8   TYPE 37     KS*HISTOGRAM
59         PARAMETERS  63
60          PRT  GO  STP, -1  6  7, -1  6  7, -.1  2.0  21, -.05  1.0  21,
61          -.05  1.0  21, -.1  2.0  21, -.1  1.0  11, -.1  2.0  21,
62          .4  2.5  21, -.2  4.0  21,
63          -.1  2.0  21, -3600000  72000000  21,
64          -3600000  72000000  21, -3600000  72000000  21,
65          -3600000  72000000  21, -3600000  72000000  21,
66          -1  20  21, -1  20  21, -1  20  21, -360.  7200.  21
67         INPUTS  20
68          -3,1  -3,2  -3,13  -3,15  -3,16  -5,7  -5,4  -5,5  -5,10   -6,4
69          -4,12  -3,4  -3,5  -3,10  -3,11  -3,9  -16,8  3,19  6,11  -6,20
70            0.   0.   0.   0.   0.   0.   0.   0.   0.   0.
71            0.   0.   0.   0.   0.   0.   0.   0.   0.   0.
72       * LABELS    1 - MODE    2 - NCASE   3 - COP     4 - FLOAD   5 - FSOL
73       *           6 - RMDOT   7 - MDOTS   8 - MDOTR   9 - MRMDS  10 - MCOL
L
74       *          11 - MDOTSR 12 - COOL   13 - EXCOOL 14 - QAUX   15 - QSOL
75       *          16 - QTHERM 17 - COPE   18 - INF7/3 19 - INF7/6 20 - MROC
K
76       *
77        UNIT  9  TYPE 27     HISTOGRAM  #1
78         PARAMETERS  35
79          1  PRT  -1  GO  SP1, 27  90  21, 21  84  21, 27  90  21, -2  40
21,
80          21  84  21, 27  90  21, -2  40  21, 21  84  21, 21  84  21,
81          21  84  21   .
82         INPUTS  10
83          5,16  3,17  5,15   5,17    6,18   6,19    6,3     6,7    6,5   6,
6
84          TREG  TN-9  TN-10  T10-T9  TC-IN  TC-OUT  OUT-IN  TBARS  TS-1  TS
-N
```

```
*
 UNIT 10  TYPE 27     HISTOGRAM  #2
  PARAMETERS  35
   2  PRT  -1  GO  SP1, 0  24  24, 0  24  24, 0  24  24, 0  24  24,
   0  24  24, 0  24  24, 0  24  24, 0  24  24, 0  24  24, 0  24  24
  INPUTS  10
   3,4   3,3    3,5    6,8  3,10  3,11  3,6  3,7  3,8  6,14
   COOL  CLOAD  XCOOL  QU   QAUX  QSOL  MB   MS   MR   MCOLL
*
 UNIT 11  TYPE 28     SIMULATION SUMMARY #1
  PARAMETERS  34
   PRT  GO  SP1  -1, 0  -4, 0  -4, 0  -4, 0  -4, 0  -4, 0  -4,
   -12  -11  2  -4,  -16  -11  2  -4, -12  -14  -15  3  2  -4,
   -12  -14  2  -4
  INPUTS  6
   3,3  3,4  3,5  3,10  3,11  4,20
  LABELS  10
   CLOAD  COOL  EXCOOL  QAUX  QSOL  ECCOOL  FLOAD  FEC  COP  COPA
*
 UNIT 12  TYPE 28     SIMULATION SUMMARY #2
  PARAMETERS  34
   PRT  GO  SP1  -1, 1   0  -4, 0  -4, 0  -4, 0  -4, 0  -4, 0  -4,
   0  -4, -13  -13  -18  3  2  -4, -12 -17 -1 AC 1 2 -4, -19  -4
  INPUTS  9
   6,13  6,8  3,11  6,12  6,9  6,10  2,6  3,10  5,18
  LABELS  10
   DE  QU  QSOL  QENV  Q1N  QOUT  HT   FSOL   ETACOL   ISOLAR
  CHECK  .20    2,-1,-3,-4
  CHECK  .20    5,-6,-1
*
 UNIT 13 TYPE 28     SIMULATION SUMMARY #3
  PARAMETERS  24
   PRT  GO  SP1  -1, 0  -4, 0  -4, 0  -4, 0  -4, 0  -4, 0  -4
   0  -4, 0  -4, 0  -4, 0  -4
  INPUTS  10
   4,13  4,14  3,6  3,7  3,8  6,14  6,20  6,16  4,5  4,6
  LABELS  10
   QHX1  QHX2  MB  MS  MR  MCOLL  MROCK  C-XON  ICOOL  IDRY
*
 UNIT 14  TYPE 28     SIMULATION SUMMARY  #4
  PARAMETERS  22
   PRT  GO  SP1  -1, 0  -4, 0  -4, 0  -4, 0  -4, 0  -4, 0  -4, 0  -4
,
   -18  -19  2  -4
  INPUTS  9
   3,9     3,12  4,1     4,2     5,13    5,14   4,15   3,4   3,6
  LABELS  8
   QTHERM  QCC  SENSBL  LATENT  EXSENS  EXLAT  ISAT   DELHIN
*
 UNIT 15   TYPE 28     SIMULATION SUMMARY #5
```

```
 134        PARAMETERS  26
 135         PRT  GO  SP1  -1,  0  -4, 0  -4, 0  -4, 0  -4, 0  -4, 0  -4,
 136         0  -4, 0  -11  2  -4, 0  -4, 0  -4
 137        INPUTS  10
 138         16,1  16,2  16,3  16,4  16,5  16,6  16,7  3,4  4,10  4,11
 139        LABELS  10
 140         ETOT  MB2  MS2  MSR2  MR2  MCOLL3  MROCK3  COPE  COOLM2  MSR
 141       *
 142        UNIT 16   TYPE 36     PARASITICS
 143         PARAMETERS  1
 144          DTM
 145         INPUTS  8
 146          3,6  3,7  4,11  3,8  6,14  6,20  3,1  3,4
 147           0.   0.   0.    0.   0.    0.    0.   0.
 148       *
 149        END
------>EXIT PRT
```